ANTIMICROBIAL PEPTIDES FROM MARINE CRUSTACEANS: MOLECULAR CHARACTERIZATION AND EVALUATION OF BIOACTIVE POTENTIAL

Thesis submitted to

Cochin University of Science and Technology

in Partial Fulfilment of the Requirements for

the Award of the Degree of

Doctor of Philosophy

in

Marine Biotechnology

Under the Faculty of Marine Sciences

By

SRUTHY K. S.
Reg. No. 4392

DEPARTMENT OF MARINE BIOLOGY, MICROBIOLOGY AND BIOCHEMISTRY
SCHOOL OF MARINE SCIENCES
COCHIN UNIVERSITY OF SCIENCE AND TECHNOLOGY
KOCHI –682 016, INDIA

May 2017

Antimicrobial Peptides from Marine Crustaceans: Molecular Characterization and Evaluation of Bioactive Potential

Ph.D. Thesis in Marine Biotechnology under the Faculty of Marine Sciences

Author

Sruthy K. S.
Research Scholar
Department of Marine Biology, Microbiology and Biochemistry
School of Marine Sciences
Cochin University of Science and Technology
Kochi – 682 016

Supervising Guide

Dr. Rosamma Philip
Professor
Department of Marine Biology, Microbiology and Biochemistry
School of Marine Sciences
Cochin University of Science and Technology
Kochi – 682 016

Department of Marine Biology, Microbiology and Biochemistry
School of Marine Sciences
Cochin University of Science and Technology
Kochi – 682 016

May 2017

Dedicated to...

My family.....

Department of Marine Biology, Microbiology and Biochemistry
School of Marine Sciences
Cochin University of Science and Technology
Kochi – 682 016

Dr. Rosamma Philip
Professor

Certificate

This is to certify that the thesis entitled **"Antimicrobial Peptides from Marine Crustaceans: Molecular Characterization and Evaluation of Bioactive Potential"** is an authentic record of research work carried out by **Ms. Sruthy K. S.** under my supervision and guidance in the Department of the Marine Biology, Microbiology and Biochemistry, School of Marine Sciences, Cochin University of Science and Technology, in partial fulfilment of the requirements of the degree of **Doctor of Philosophy** in **Marine Biotechnology** under the Faculty of Marine Sciences of Cochin University of Science and Technology, and no part thereof has been presented for the award of any other degree, diploma or associateship in any University or Institution. All the relevant corrections and modifications suggested by the audience during the pre-synopsis seminar and recommended by the Doctoral Committee have been incorporated in the thesis.

Kochi - 682 016
May 2017

Prof. (Dr.) Rosamma Philip
(Supervising Guide)

Declaration

I hereby declare that the thesis entitled **"Antimicrobial Peptides from Marine Crustaceans: Molecular Characterization and Evaluation of Bioactive Potential"** is a genuine record of research work done by me under the supervision and guidance of **Dr. Rosamma Philip**, Professor, Department of Marine Biology, Microbiology and Biochemistry, Cochin University of Science and Technology and no part thereof has been presented for the award of any other degree, diploma or associateship in any University or Institution earlier.

Kochi - 682 016
May 2017

Sruthy K. S.

Acknowledgement

This thesis is the accomplishment of a long cherished vision and culmination of my voyage of Ph.D which was just like mountaineering convoyed with inspiration, hardship, faith, and frustration. When I found myself at highest experiencing the sensation of fulfillment, I recognized my name alone appears on the cover page of this thesis, a great many people including my family members, my teachers, well-wishers, my friends, colleagues and several institutions have contributed to achieve this enormous task.

First and foremost I would like to express my special appreciation and thanks to my advisor Prof. Dr. Rosamma Philip, you have been an incredible mentor for me. It has been an honor to be her Ph.D. student. She has introduced and educated me, both consciously and un-consciously, about the basics and techniques of Molecular Biology. I really appreciate her assistances of time, ideas, brain storming discussions and funding to make my Ph.D. experience creative and inspiring. The dedication, ecstasy and eagerness she has for her research was infectious and motivational for me, during Ph.D. pursuit. I am a big fan of her thousand volt smile and the power blow-outs always cheered up me. I am also thankful for the admirable example she has delivered as a successful scientist and professor. For all these, I sincerely thank her from bottom of my heart and will be truly indebted to her throughout my life time.

I am extremely obliged to. Dr I. S. Bright Singh, UGC-BSR- Faculty and Former Coordinator, , National Centre for Aquatic Animal Health for his constant support, guidance, and for providing all the amenities throughout my research period. Above all this, I am profoundly influenced with your easiness, dedication towards research and polite nature. Discussions with you was always inspiring and a great experience for me.

I gratefully acknowledge Dr. R. Damodaran, Professor (Retd)., Department of Marine Biology, Microbiology and Biochemistry, for the enough kindness offered and providing me all the help, support and encouragement.

I am extremely indebted to Kerala State Council for Science Technology and Environment, Govt. of Kerala and Cochin University of Science and Technology for providing me research fellowship during the tenure of my Ph.D.

I would like to express my honest thanks to The Head, Department of Marine Biology, Microbiology and Biochemistry, for all the assistance and support extended all over the period of Ph. D. work. I also extend my deep felt gratefulness to the Dean, Faculty of Marine Sciences and Director, CUSAT for all the service and facilities delivered for research.

I am always grateful to all my beloved teachers in the Dept. for their care and encouragement. I thank (Prof.) Dr. Babu Philip (Rtd.), (Prof.) Dr. A.V.Saramma, (Prof.) Dr. A. A. Mohamed Hatha, (Prof.) Dr. Aneykutty Joseph and (Prof.) and Dr. S. Bijoy Nandan for their valuable advice, suggestion and support.

I acknowledge library staff, all lab assistants and technical staff of Dept. of Marine Biology, Microbiology and Biochemistry especially all Section officers, Santhosh Sir, Jismon Chettan, Laly chechi, Saify Chettan and Lakshmi Chechi for their generous support and apt help during the tenure of my work. I am always grateful to the electric wing staff and security staff for providing necessary facilities.

It's my fortune to gratefully acknowledge the support of and generous care of RP research group members including Dr. Swapna P. Antony, Dr. Naveen Sathyan, Chaithanya E. R. Dr. Afsal V. V., Anilkumar P.R., Jini Jacob, Dr. Jayesh P., Solly Solomon, Aishwarya Ajith, Archana K., Neema Job, Divya T. Babu, Jayanath G., Wilsy Munna, Deepthi Augustine, Dr. Reema Kuriakose, Sephy Rose Sebastian, Bhavya K., Manomi S., Jimly C. J. and Ramya K. D. I would like to also express my gratitude to new members including Dr. Smitha C. K., Dr. Preetha Shenoy, Dr. Anju Antony, Anju M. V. and Dhanya Keshavan.

Very special thanks to the 'AMP family' senior members, Swapna Chechi, Naveen chettan, Anil Chettan, Chaithu Chechi, and Afsal Chettan for introducing me to the world of "Antimicrobial peptides". It would have been impossible for me to even start my study without all of your support. Ph.D. students often talk about loneliness and depression throughout the course of their study but this is something which I certainly not experienced at CUSAT and this is only because of your companionship and support.

A big thanks also goes to Dr. Jayesh P. for his support during cancer cell lines work and Real-time PCR analysis. Interesting discussion with J.P. and Rosamma

Ma'am always ended in some innovative and thought-provoking ideas. His constant motivation really helped a lot in the frame-work and completion of my thesis within a period of four years.

Special cheers to Dr. Lijo John, for learning me the basics and techniques of 'Western blotting'. It was really a great experience to interact and share information regarding molecular biology techniques with him.

Also I would like to owe special thanks to my dear and dearest, Chaithu Chechi, Deborah Chechi (Dr. A. Deborah Gnanaselvam), Jini Chechi, and Aishwarya Chechi for always beside me during the happy and hard moments and to drive me and motivate me during my Ph. D. pursuit.

I would also like to thank all of my friends especially my M.Sc. colleagues Sulfath, Remya, Neelima, Ajitha, Anjali, Honey, Aswathy, Santu, Bhavya, Thasneem, Barsana, Varsha, Smruthu, Nashad, Solly, Vincent and Ajin who supported me to strive towards my goal. Special thanks are extended to my seniors, Sini Itha, Sreelakshmi Chechi, Lekshmi Chechi and Jabir Ikka for their support throughout the research tenure.

I am also indebted to my best friends Devika, Renu, Praveena and Archana not only for their unconditional support but also for being there to listen when I needed an ear.

I would like to acknowledge all research scholars of Marine Biology department especially for their co-operation and support. Also like to extend my gratitude to research scholars of NCAAH, especially to Dr. Shalini, Dr. Vrinda S., Ramya Chechi, Dhaneesha M., Anoop Chettan and Soumya Chechi for their support.

Special thanks are extended to Swapna chechi for helping in my thesis correction and Chaithanya chechi for the cover design and all the technical support offered. Also I would like to acknowledge Sephy Chechi and Neema Chechi for providing accommodation and all support rendered during Pre-synopsis presentation and Ph.D. thesis submission. Thanks are due to Mr. Binoop Kumar, Indu Photos, for the thesis outlay and his excellent professional work.

Words cannot express the feelings I have for my parents for their love and encouragement. I especially thank my Acha and Amma, Mr Sreekumar K. P. and

Mrs Sathy Sreekumar, and my younger brother, Shambhu for their support in all my pursuits. My hard-working parents have sacrificed their lives for my brother and myself and provided unconditional love and care. I love them so much, and I would not have made it this far without them. Also grateful to all of my Kalappurackal family members, especially to my Ottan kochachan, Unni kochachan, Jaya Appachi and my wonderful cousins for their constant affection, moral support and blessings. I also thank my beloved grand parents Mr Prabhakaran Nair and Mrs Sarojini who have both passed on. I still miss them, especially for their prayers, unconditional love and care. I wished they could have lived for another few years for my wedding and for my Ph.D. convocation. I know I always have my family to count on when times are rough and it would be impossible to achieve this without their support.

I am also grateful to my in-laws Mr Vijayakumar, Mrs Shailaja and Arun Chettan. I am so blessed to being part of this supportive, caring and wonderful family. Finally, I would like to acknowledge the most important person in my life, my loving, supportive and encouraging friend and husband Mr. Anand Vijayan, whose faithful support during the writing and final stages of this Ph.D. is so appreciated.

I don't know how to thank my little one, who has been with me in my womb throughout my thesis writing. I was very lucky to have quite an easy first and second trimester of my pregnancy and thus helped a lot in my writing period. I constantly talked to my baby in belly regarding my thesis and he responded accordingly with his small kicks and movements.

I thank the Almighty for giving me the power and perseverance to work through all these years and fulfill my dream.

Sruthy K. S.

Contents

List of Tables

List of Figures

.....ஜ۞ஜ.....

Chapter 1

GENERAL INTRODUCTION

Contents

1.1 Introduction

Antimicrobial peptides (AMPs) are evolutionarily ancient, gene-encoded, ribosome-synthesized peptides, less than 10 kDa, have an overall net positive charge, hydrophobic and are membrane active (Boman, 2003; Yeaman & Yount, 2003). Their wide spread distribution throughout the animal and plant kingdoms suggests that antimicrobial peptides have served a fundamental role in the successful evolution of complex multicellular organisms. Among the main effector molecules of innate immunity, antimicrobial peptides (AMPs) are of prime importance. Since most living organisms are constantly exposed to potentially harmful pathogens through contact, ingestion and inhalation, survival of such organisms in a microbe thriving environment depends on a network of host defence mechanisms involving various components. In contrast to the acquired immune

mechanisms, endogenous peptides, which are constitutively expressed or induced, provide a fast and effective means of defence against the pathogens.

All AMPs are derived from proteolytic processing of larger precursors, including a signal sequence. Post-translational modifications occur commonly, and include C-terminal amidation and, in some instances, amino-acid isomerisation. Most of these gene-encoded peptides are mobilized shortly after microbial infection and act rapidly to neutralize a broad range of microbes and share several common properties. Among the larger class of cationic AMPs, the principal structural feature common to all is their ability to adopt an amphipathic configuration in which clusters of hydrophobic and cationic amino acids are spatially organized such that the molecule possesses discrete hydrophobic and hydrophilic faces (Oren and Shai, 1998). The net positive charge of antimicrobial peptides causes their preferential binding to negatively charged target on bacteria, which may account for the selectivity of antimicrobial peptides (Hancock and Diamond, 2000).

1.2 Characteristics of AMP

Polypeptides that exert antimicrobial activity have been isolated from basically every tissue in which they have been sought. A pivotal consideration in this regard is the degree to which an antimicrobial peptide distinguishes between microbial and host cells in terms of potential toxicity. Antimicrobial peptides have amphipathic features that mirror phospholipids, thus allowing them to interact with and exploit vulnerabilities inherent in essential microbial structures such as cell membrane. Structural parameters

include conformation, charge (Q), hydrophobicity (H), hydrophobic moment (MH), amphipathicity (A), and polar angle.

1.2.1 Conformation (χ).

Though antimicrobial peptides vary extensively in sequence and source, several themes in their three-dimensional topology appear principal, and peptides have been categorized consequently. The two largest groups are the α-helical and β-sheet peptides.

1.2.2 Charge (Q).

Many of the antimicrobial peptides characterized to date display a net positive charge, ranging from +2 to +9 (Giangaspero et al., 2001; Yeaman and Yount, 2003), and may contain highly defined cationic domain(s). Cationicity is undoubtedly important for the initial electrostatic attraction of antimicrobial peptides to negatively charged phospholipid membranes of bacteria and other microorganisms, and the mutual electroaffinity confers selective antimicrobial targeting relative to host tissues.

1.2.3 Amphipathicity (A) and hydrophobic moment (MH).

Nearly all antimicrobial peptides form amphipathic structures upon interaction with target membranes. Amphipathicity can be achieved via a multitude of protein conformations; however, one of the simplest and perhaps most elegant is the amphipathic helix. The amphipathic α-helix has a periodicity of three to four residues and is optimal for interaction with amphipathic biomembranes. While the extent of amphipathic helicity influences peptide activity against negatively charged membranes, it may have an even more pronounced effect in rendering peptides haemolytic

against zwitterionic or neutral membranes. Thus, a high degree of helicity and/or amphipathicity yielding a segregated hydrophobic domain is correlated with increased toxicity towards cells composed of neutral phospholipids.

1.2.4 Hydrophobicity (H)

Peptide hydrophobicity, defined as the percentage of hydrophobic residues within a peptide, is approximately 50% for most antimicrobial peptides. Hydrophobicity is an essential feature for antimicrobial peptide membrane interactions, as it governs the extent to which a peptide can partition into the lipid bilayer. Many antimicrobial peptides are moderately hydrophobic, such that they optimize the activity against microbial cell membranes.

1.2.5 Polar Angle (θ)

Polar angle is a measurement of the relative proportion of polar versus nonpolar facets of a peptide conformed to an amphipathic helix. For example, in a hypothetical α-helical peptide, in which one facet is exclusively composed of hydrophobic residues and the other solely composed of charged residues, the polar angle would be 180˚. A smaller polar angle (and therefore a greater hydrophobic surface) is associated with increased capacity to permeabilize membranes. The polar angle has also been shown to correlate with the overall stability and half-life of peptide-induced membrane pores.

1.3 Classification of AMPs

The AMPs discovered so far have been divided into several groups based on their length, secondary and tertiary structure and presence or

absence of disulfide bridges. These peptides exhibit bactericidal, fungicidal, virucidal and tumouricidal activities and the fact that they have potential to overcome bacterial resistance make them promising candidates for therapeutic drugs. AMPs can be characterized into many subtypes based on different standards: origin, size, charge, length, structure, amino acid sequence, biological action and mechanism of action but secondary structure was found to be the only meaningful criterion to sort and classify them (van't Hof et al., 2001). The three dimensional structure analysis using nuclear magnetic resonance spectroscopy has led to better understanding of the function of AMPs. Based on the NMR structure and sequence analysis, Hancock & Lehrer (1998) proposed four classes of AMPs, which are α-helical, β-sheeted, loop and extended peptides.

1.3.1 Antimicrobial peptides with α-Helical Structures

This is one of the largest and widely studied antimicrobial peptides. Majority of this class of peptides are cationic and the formation of a helix gives a highly amphipathic structure suitable for interaction with the negatively charged microbial membrane. Peptides of the α-helical class are characterized by their α-helical conformation, and frequently contain a small bend in the middle of the molecule (Tossi et al., 2000). Also this hinge is found to be critical for selectivity by suppressing the haemolytic activity. Helical AMPs are involved in stimulation of autolytic enzymes, interference with the synthesis of proteins, inhibition of DNA synthesis leading to filamentation and inhibition of cellular functions by binding to nucleic acids. The α-helical magainins are typical example for this structural class identified from the skin of the African clawed frog

Xenopus laevis. The antimicrobial action of magainin has been anticipated to involve selective permeabilisation of bacterial membranes leading to disruption of the membrane potential (Matsuzaki. 1999).

1.3.2 Antimicrobial Peptides with β-Sheet Structure

This group of peptides are categorized by the occurrence of cysteine residues and comprised of several antiparallel β-sheets generally stabilised by disulfide bonds. (Yount et al., 2006). Larger peptides in this family also comprise minor helical regions. Most of the β-sheeted peptides disturb the lipid organization and traverse the bilayer, but do not form enduring pores or channels. Representatives of this group includes defensins (García et al., 2001); hepcidins (Lee et al., 2012), protegrins (Ishitsuka et al., 2006), tachyplesins (Kushibiki et al*.,* 2014) and polyphemusin II (Tamamura et al., 1993).

1.3.4 Antimicrobial peptides with a looped structure

This group of is characterized by their looped structure because of the incidence of a single bond (disulfide or amide or isopeptide bond). Thanatin, a 21-residue peptide from the spined soldier bug, *Podisus maculiventris* (Fehlbaum et al., 1996) is a representative of looped peptides consisting of an anti-parallel β- sheet, stabilized by a single disulfide bond.

1.3.5 Antimicrobial peptides with linear extended structure

This class of AMP is devoid of a classical secondary structure, due to the overexpression of proline and/or glycine or tryptophan or histidine residues. These peptides form their structures by hydrogen bond and Van der Waals interactions with membrane lipids. Histatin, an AMP from

human saliva is rich in histidine residues and found active against *Candida albicans* (Xu et al., 1991). Whereas cathelicidins are proline rich peptides and have irregular structures, indolicidins and tripticin (Lawyer et al., 1996) are AMPs rich in tryptophan. This class of peptides form aggregate channels in the membranes and are translocated into cytoplasm where they prevent DNA from replicating (Falla et al., 1996; Subbalakshmi & Sitaram, 1998).

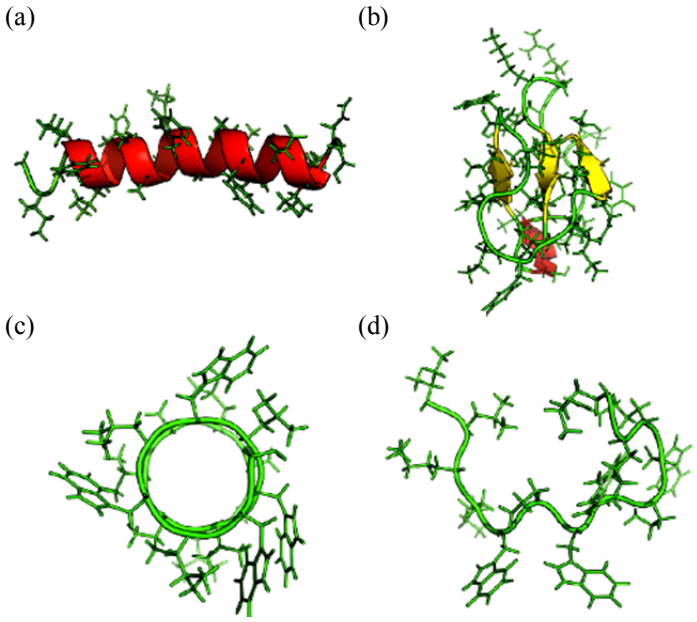

Fig. 1.1 Three dimensional model structures demonstrating the differences between the four classes of cationic peptides; (a) α-helical peptide, (b) β-defensin, (c) Loop structure and (d) Extended peptide (Adopted from Cézard et al. 2011).

1.4 Mode of action of AMPs

Even though the exact mechanism of action of AMPs remains a matter of discussion, there is consent that these peptides selectively disturb the cell membranes. AMPs are basic and thus easily recognize the acidic phospholipids of the bacterial membrane. In mammalian cells, anionic

lipids are present along the cytoplasmic side of the membrane and this feature account for their better activity against bacteria but not against eukaryotic cells. The amino acid sequence, membrane lipids, peptide concentration and amphipathic structural arrangement of the peptides are alleged to play an imperative role in this mechanism. It has been mostly recognized that AMP intervened killing of microorganisms normally occurs through membrane disruptive (Fig. 1.2) and non-membrane disruptive mechanism and can hinder most of the cellular processes (Fig. 1.3).

1.4.1 Membrane disruptive mechanism of AMPs

1.4.1.1 *Barrel-stave model*

The barrel-stave model was the first mechanism proposed to explain bacterial killing by AMPs (Ehrenstein and Lecar, 1977). This model involves the perpendicular insertion and aggregation of a relatively small number of individual peptides (or peptide complexes) also referred as staves in a barrel-like ring inside the membrane leading to a transmembrane pore or channel with a cylindrical structure. In this mechanism, the hydrophobic surfaces of α-helical or β-sheet peptides face outward, towards the acyl chains of the membrane, whereas the hydrophilic surfaces form the pore lining. The initial step in a barrel-stave pore formation involves peptide binding at the membrane surface; most likely as monomers and after a conformational phase transition, the hydrophobic portion of the peptide is inserted into the membrane to an extent corresponding to the hydrophobicity of the membrane, while electrostatic interaction facilitates this process. When bound peptide reaches a threshold concentration, peptide monomers self-aggregate and insert deeper into the hydrophobic membrane core.

1.4.1.2 *Carpet model*

Membrane disruptive 'carpet model' was projected by Pouny et al. (1992). The carpet mechanism involves initial peptide binding to the membrane surface to form high density clusters that cover the surface. The peptides ultimately cover the bacterial surface in a carpet-like way. It is generally accepted that peptide activity is not detergent-like and occurring by phospholipid displacement that changes membrane fluidity and / or reductions in membrane barrier properties that subsequently lead to membrane disruption.

1.4.1.3 *Toroidal pore model*

The toroidal pore model (the wormhole mechanism) which combines the actions of the barrel-stave and carpet models was the third model to be proposed (Hancock and Chapple, 1999). This model is an extension of the transmembrane helical bundle in which the pores are lined with peptides and lipids. The model postulates that peptide and lipid together form well-defined pores, with the membrane also curving inward to form a hole with the head groups facing towards the core of the pore, while the peptides line this hole.

1.4.1.4 *Aggregate channel model*

The aggregate channel model was projected by Hancock and Chapple (1999). After binding to the phospholipid head groups, the peptides introduce into the membrane and then gather into unstructured aggregates allowing the vigorous creation of pores that span the membrane for short periods. AMPs can also move in to the intracellular space through this mechanism.

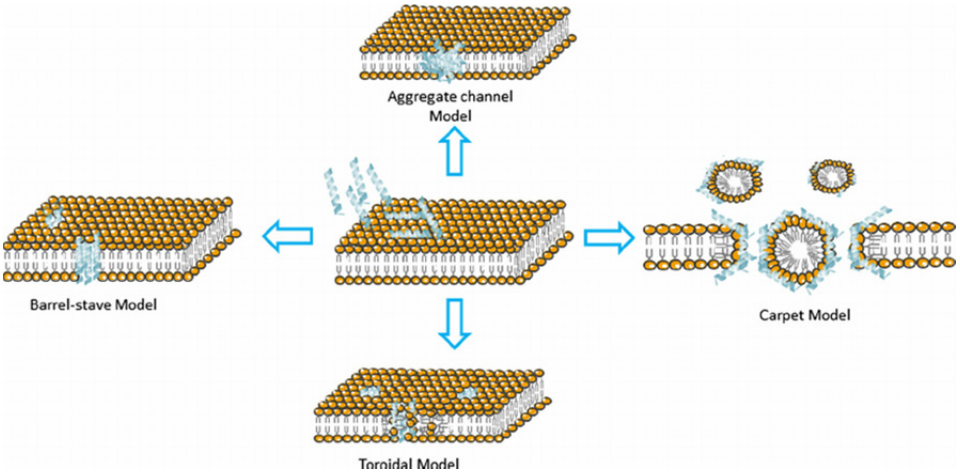

Fig. 1.2 Membrane disruptive mode of action representing models subsequent to initial adsorption of AMPs (Adapted from Nguyen et al., 2011).

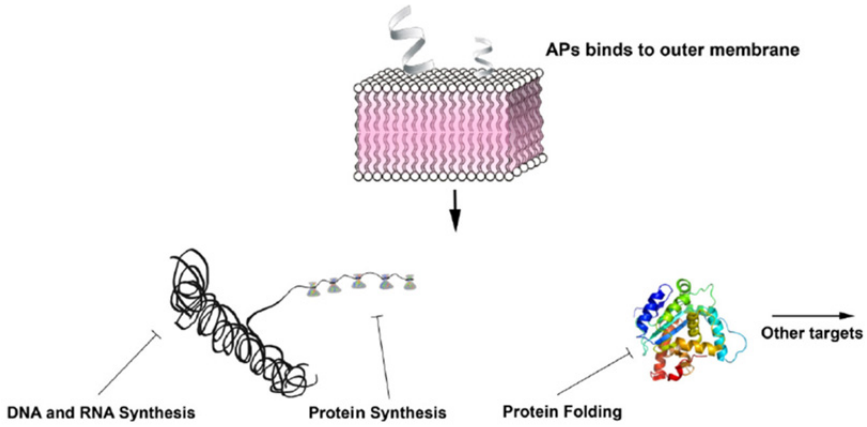

Fig. 1.3 Net consequences after AMP entry to the bacterial cytoplasm it can bind to cellular polyanions such as DNA and RNA, hinder enzymatic activity including protein synthesis or chaperone assisted protein folding (Modified from Brandenburg et al., 2012).

1.4.2 Non-membrane disruptive mechanism of AMP

Studies have shown that cell killing may proceed with relatively little membrane disruption suggesting that AMPs may interact with

putative key intracellular targets (Yeaman & Yount, 2003). There are reports of bacterial killing by AMPs with very little or no membrane disruption. AMP like buforin II, penetrates the bacterial outer membrane, and accumulates in the cytoplasm interacting with nucleic acids and exerting cytotoxic activity (Park et al., 2000). Once translocated in the cytoplasm, AMPs are able to act on many levels including inhibition of cell-wall synthesis, enzymatic activity, DNA/ RNA/ protein synthesis, altering cytoplasmic membrane and/or activation of autolysin.

1.5 Multidimensional properties of AMPs

Antimicrobial peptides display a broad spectrum of activity. Many antimicrobial peptides not only kill bacteria, but also are cytotoxic to fungi (Fehlbaum et al., 1996; Kieffer et al., 2003), protozoa (Arrighi et al., 2002), malignant cells (Cruciani et al., 1991; Baker et al., 1993; Lindholm et al., 2002), and even enveloped viruses like HIV, herpes simplex virus.

1.5.1 Antibacterial activity

AMPs retain broad-spectrum activity against Gram-negative bacteria and Gram-positive bacteria (Miyasaki and Lehrer, 1998). Antibacterial activity of AMPs is explained using previously described models for mode of action. Majority of the AMPs exhibits antibacterial activity even at micromolar concentrations and act within a short time (less than 20 mins). The most active AMPs present a minimum inhibitory concentration (MIC) of 1 to 4 μg/ml, at this concentration AMPs completely prevent bacterial growth (Hancock, 2001).

Biological fluids including human saliva, urine, sweat, frog and fish skin mucus, arthropod haemolymph, mollusc mucus and several vertebrate tissues are rich source of antibacterial peptides (Bachère et al., 1995; Saito et al., 2005). In some cases, certain AMPs show activity against several multi drug resistant bacteria such as *Staphyloccocus aureus, Pseudomonas aeruginosa* and *Escherichia coli* (van't Hof et al., 2001). AMPs such as drosocin, apidaecin, pyrrhocoricin and buforin II act on their intracellular target (Park et al., 1998a; Otvos et al., 2000; Kragol et al., 2001).

1.5.2 Antifungal activity

Rise in mycoses, expansion of resistance to existing drugs among fungal pathogens, as well as adverse side effects of drugs have led to better efforts to discover the antifungal activity of AMPs and to isolate new candidates for treatment. Comparable to bacterial cell wall/membrane, fungal cell wall is rich in negatively charged moieties and chitin (Narayana and Chen, 2015). Antifungal property is exhibited by several AMPs which kill fungi by binding to chitin of the cell wall or intracellular components (Pushpanathan et al., 2012). Most of the plant and animal defensins (Rogozhin et al., 2011), insect- cecropin, drosomycin (De Lucca et al., 1997; Michaut et al., 1996), frog peptides- magainin (Bechinger and Salnikov 2012), brevinin (Pal et al., 2006), fish derived peptides- epinecidin (Pan et al., 2010), crustacean AMP- anti-lipopolysaccharide factors (Zhang et al., 2010), human secretory peptides- lactoferirin and histatin are examples for potential antifungal peptides (Brandenburg et al., 2012). Many of antifungal peptides exhibit activity against pathogenic yeast and fungal species like *Candida albicans, C. tropicalis, C. krusae,*

C. parapsilopsis, Fusarium graminearum, F. oxysporum, Cryptococcus neoformans, Saccharomyces cerevisiae, Pichia membranifaciens, Aspergillus sp. etc (Ajesh and Sreejith, 2009).

1.5.3 Antiviral activity

Generally accepted mechanism of antiviral action is a direct interaction of these peptides with the envelope of the virus, leading to permeation of the envelope and, interaction with virus proteins and ultimately, lysis of the virus particle, analogous to the pore-formation model suggested for antibacterial activity. The α-defensin HNP-1 impedes the replication of human immunodeficiency virus (HIV) and influenza virus subsequent to viral entry into target cells (Zhang et al., 2004). Similarly, HNP-1 can inactivate papillomavirus, herpes simplex virus, cytomegalovirus, vesicular stomatitis virus and adenovirus (Daher et al., 1986). Insect AMPs like melittins and cecropins also showed anti-HIV activity by suppression of the long-terminal repeat gene (Wachinger et al., 1998). Crustacean AMPs including ALF from *Fenneropenaeus chinensis* (Guo et al., 2014) and Type-I crustin, CrustinPm-4 from *Penaeus monodon* (Donpudsa et al., 2014) exhibited activity against crustacean virus, white spot syndrome virus (WSSV). The principal mechanisms of virus inhibition by AMPs need further investigations.

1.5.4 Antiparasitic activity

Since the identification of antiparasitic activity of magainin against *Paramecium caudatum* (Zasloff, 1987), many AMPs with antiparasitic activities have been identified. It includes defensins and cathelicidins exhibiting activity against the African trypanosome *Trypanosoma brucei*,

the cause of sleeping sickness, by disrupting their cell membrane integrity (McGwire et al., 2003). Also a truncated form of the bovine myeloid antimicrobial peptide-27 (BMAP-27), displayed robust action against several parasites, including trypanosomes and *Leishmania* spp. (Haines et al., 2009). BMAP-18 found to upset the mitochondrial potential at lower concentrations without plasma membrane alteration, and at higher concentrations, the peptide disrupted the membrane (Haines et al., 2009). Whereas the cathelicidin-derived AMP, porcine myeloid antimicrobial peptide-23 (PMAP-23) exerts anti-nematodal activity by disturbing the cell membrane through pore development (Park et al., 2004).

1.5.5 Anticancer activity

Worldwide, human cancer remains as foremost cause of high illness and mortality, an urgent requirement for novel, more efficient drugs is evident. Increased vulnerability of cancer cells to cationic membrane active AMPs is mainly due to the occurrence of high content of anionic phosphatidylserine molecules and O-glycosylated mucins on their membranes making it an exciting candidate to use AMPs as antitumour/ anticancer agents (Gaspar et al., 2013). The increased membrane fluidity and negative membrane potential of cancer cells could also subsidize the selective cytotoxic activity of AMPs or anticancer peptides (ACPs). In normal healthy cells, a net neutral charge is conferred by the zwitter ionic nature of their major membrane constituents such as phosphatidylethanolamine (PE), phosphatidylcholine (PC), and sphingomyelin (SM). Another possible mechanism is the initiation of apoptosis in cancer cells by mitochondrial membrane disruption following ACP uptake (Hoskin and Ramamoorthy, 2008). Many ACPs from various sources including crustaceans have

exhibited promising anticancer activity against various cancer cell lines. The skin secretions of amphibians are a rich source of AMPs, including temporin and magainins, selectively cytotoxic to human cancer cells (Cruciani et al., 1991; Park et al., 1994) AMPs including shrimp anti-lipopolysaccharide factor (Lin et al., 2010), molluscan peptides (Chi et al., 2015), fish AMPs - Tilapia hepcidin TH1-5 (Hsieh et al., 2010), epinecidin (Chen et al., 2009; Chang et al., 2011) and human salivary peptides (da Costa et al*.,* 2015) reveal *in vitro* cytotoxic activity against many cancer cell lines, including leukemia cells, fibrosarcoma cells, and neuroblastoma cells.

1.5.6 Immunomodulatory activities of AMP

AMPs could act as adjuvants encouraging innate immunity by improving recruitment of immune cells to the site of inflammation, endorsing the stimulation and polarising the response of T helper cells. Finally results in the upsurge of innate and adaptive immunity in response to infections. Cationic AMPs, like the human cathelicidin LL-37, perform many activities relating to innate immunity, including the induction or modulation of chemokine and cytokine production, alteration of gene expression in host cells, and inhibition of pro-inflammatory responses of host cells to bacterial components such as lipopolysaccharide (LPS) *in vitro* and *in vivo*, promoting wound healing and modulating the responses of dendritic cells and cells of the adaptive immune response**.** Defensins comprising α-defensins (e.g., HNP1-3) and β-defensins (human β-defensin 3 and 4; HBD3 and 4) induce the migration of phagocytes, neutrophil granulocytes and monocytes to the inflamed site (Brandenburg et al., 2012).

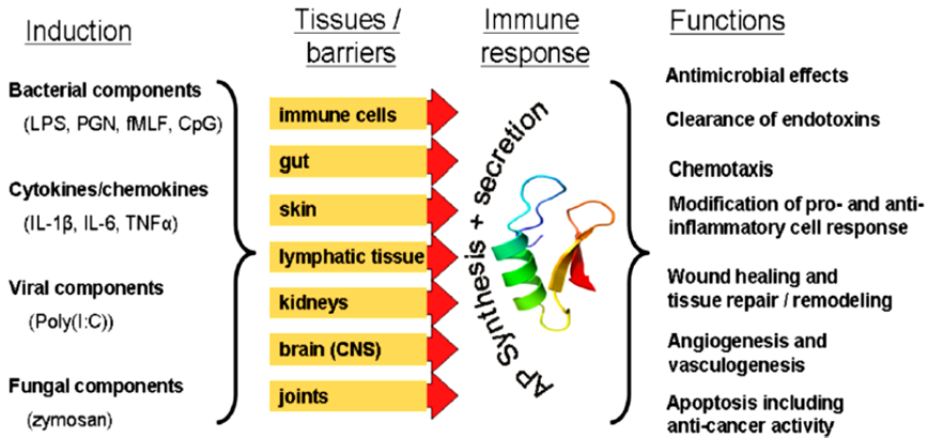

Fig. 1.4 Diagrammatic representation of induction and potential biological roles of antimicrobial peptides (Adopted from Brandenburg et al., 2012).

1.6 AMPs as potential therapeutics and its role in drug development

Broad spectrum activity of AMPs including the drug-resistant pathogens, rapid onset of activity, and relatively low possibility of resistance emergence makes AMPs as attractive candidate as unique antibiotics. Some limitations imposed by AMPs in drug development includes, their unstable nature in the presence of protease and pH change; possible toxicity of AMPs in oral application and increased cost of peptide production (Silva et al., 2013). Several approaches have been projected to overcome the limitations and it includes incorporation of unusual amino acids (D-form of amino acids), end modifications (acetylation or amidation) and delivery of AMPs as encapsulated liposomes (Samad et al., 2007; John et al., 2008). Therapeutic efforts are mainly dedicated to the development of topical agents mainly because of the safety behinds topical therapy (Zasloff 2001). Eventhough the therapeutic potential of AMPs are recognized well, pharmacology and pharmacokinetics of AMPs are still at infancy.

1.7 Production strategies of AMPs

With the intention to better characterize a novel AMP, such as to determine the mechanism of action, to report the structure and function, or its potential use as a pharmaceutical drug, a reasonable amount of purified compound is needed. In general, there are three different approaches that can be employed to obtain enough AMPs: direct isolation from natural sources, chemical synthesis, or recombinant expression (Li and Chen, 2008). However, very low concentrations of AMPs are present in most organisms. For this reason, the isolation of peptides directly from natural sources sometimes is time consuming, environmental unfriendly and a high-cost strategy (Li et al., 2008). In addition, peptide expression in the original host can be extremely low or affected by unknown environmental factors resulting in problems when scaling up (Li et al., 2010).

The chemical synthesis of peptides allows the production of both natural and synthetic AMPs. Nevertheless, a high cost for large-scale peptide synthesis has been observed. Moreover, these costs can be considerably high in the synthesis of peptides that have disulfide bonds, which hampers the production of such molecules (Li, 2011). If the sequence of a peptide contains one or more disulfide bridges, this is likely to result in difficulties during synthesis, and therefore production costs will increase substantially. Thus the recombinant expression system would be the most cost-efficient method for large-scale production of AMPs (Parachin et al., 2012). For these reasons, chemical synthesis of AMPs is also considered, in some cases, ineffective for large-scale production, and is therefore restricted to smaller AMPs lacking post-translational modifications and low cysteine content.

The expression host and vector system for recombinant production should be selected on the basis of features of AMPs and its size, intracellular localization or secretion, proper folding, and glycosylation pattern. Majority of the hosts used for AMP production are bacteria and yeasts, representing 97.4% of heterologous-expressed AMPs (Li and Chen, 2008). More recently, plants have emerged as a promising host for AMP production since transgenic plants can be directly used for microbial control by simply expressing the peptide in the desired crop without need for purifying the peptide (Desai et al., 2010.). Therefore, bacteria, yeast, and plants are the systems chosen here as promising candidates for peptide production.

1.8 AMPs recognized from marine crustaceans and its significance

Crustaceans represent one of the most abundant animals inhabiting both aquatic and terrestrial habitats. By virtue of their diversity and abundance they have earned consideration as a potential source of bioactive compounds. The lack of an adaptive immune system has led to the evolution of potent compounds including AMPs used in self-defense against pathogens. Different families of AMPs have been identified and characterized from crustaceans. At the present, 15 AMP families or single peptides sharing common molecular features with the currently known AMP families have been recognized in crustaceans (Rosa and Barracco, 2010). Considering the amino acid composition, peptide structure and multi-functionality, Rosa and Barracco (2010) clustered the families of AMPs in crustacean species into four main groups. Details

regarding the characteristics and first description of crustacean AMPs are listed in Table 1.1.

1.8.1 Single-domain linear α-helical AMPs and peptides enriched in certain amino acids

This group of peptides lack cysteine residues engaged in disulfide bonds and most of them are enriched with a high proportion of amino acids such as arginine, proline, glycine, tryptophan or histidine (Tossi and Sandri, 2002). These peptides are usually unstructured in solution, but in the presence of lipid bilayers it can assume an amphipathic α-helical structure (Brogden, 2005) and are found active against bacteria, fungi and protozoa. Till date, five linear AMPs have been defined from crustaceans, including three proline/arginine-rich peptides: Bac-like peptide (Schnapp et al., 1996), callinectin (Khoo et al., 1999) and astacidin (Jiravanichpaisal et al., 2007a); glycine rich armadillidin (Herbinière et al., 2005) and homarin (Battison et al. 2008).

1.8.2 Single-domain peptides containing cysteine residues engaged in disulfide bonds

This group is characterized by the presence of pair of cysteine residues engaged in disulfide bond and result in the formation of cyclic or open-ended cyclic stabilized peptides. The number of cysteine residues usually varies from 2-12. Only three families of AMPs containing cysteine residues have been characterized from decapods which comprises of defensins (6 Cys residues) (Pisuttharachai et al., 2009), anti-lipopolysaccharide factors (2 Cys residues) (Gross et al., 2001) and anionic peptide, scygonadin (2 Cys residues) (Huang et al., 2006).

1.8.3 Multi-domain or chimeric AMPs

AMPs with at least two distinctive domains exhibiting specific features of classical single-domain AMPs, such as PRP- or cysteine-rich peptides are included in this group. The multi-domain structure is crucial for creating cationicity and amphipathicity of peptides. Cationic domain is involved in electrostatic interactions with anionic microbial membranes and the hydrophobic domain for membrane destabilization. AMPs in this group include penaeidins with N-terminal PRP-rich domain and a C-terminal region containing six cysteine residues that are engaged in three intramolecular disulfide bridges (Destoumieux et al., 1997), crustins with glycine/ cysteine/ PRP rich domain and one whey acidic protein (WAP) domain at the C-terminus (Smith et al., 2008), hyastatin with N-terminal glycine-rich domain, a short PRP-containing portion and a C-terminal cysteine rich domain(Sperstad et al., 2009a), arasins with PRP-rich N-terminal region and four cysteine containing C-terminus (Stensvag et al., 2008) and anionic AMP, stylicins with proline-rich N-terminus and a 13 cysteine residues comprising C-terminus (Rolland et al., 2010).

1.8.4 Unconventional AMPs

Unconventional AMPs possess molecular elements that are found in the structure of classical AMPs, including charge, hydrophobicity and/or amphipathicity (Smith et al., 2010). These AMPs are multifunctional proteins that principally assist other functions and post proteolytic cleavage; the protein fragments display antimicrobial activity. This group includes histone-derived AMPs (Patat et al., 2004) and haemocyanin-derived AMPs (Destoumieux-Garzón et al., 2001).

Table 1.1 Details regarding reported crustacean AMPs.

AMP	Mol. Wt. (kDa)	Peptide Characteristics	Crustacean order	Details about first description
Bac-like	6.5	Cationic, PRP rich	Decapoda	*Carcinus maenas*-Schnapp et al. 1996.
Penaeidin	5.5-6.6	Cationic, N-terminal PRP-rich domain and a C-terminal region with six cysteine	Decapoda	*Litopenaeus vannamei*-Destoumieux et al. 1997
Callinectin	3.7	Cationic, PRP rich	Decapoda	*Callinectes sapidus*- Khoo et al. 1999.
Crustin	7-14	Cationic, N-terminal WAP domain	Decapoda Amphipoda	*C. maenas* - Relf et al. 1999
ALF	7-11	Cationic, cysteine containing	Decapoda Stomatopoda	*L. setiferus*- Gross et al. 2001; *P. monodon*- Supungul et al. 2002; *Miyakea nepa* - Sruthy et al. 2015.
Haemocyanin- derived peptides	1.9-8.3	Anionic, Cationic	Decapoda	*L. vannamei* Destoumieux-Garzon et al. 2001
Histone derived peptides	11-15	Cationic	Decapoda	*L. vannamei*- Patat et al. 2004
Armadillidin	5.2	Cationic	Isopoda	*Armadillidium vulgare*- Herbiniere et al. 2005
Scygonadn	10.8-11.4	Anionic, cysteine containing	Decapoda	*Scylla serrata*- Huang et al. 2006
Astacidin 2	1.8	Cationic, PRP rich	Decapoda	*Pacifastacus leniusculus*- Jiravanichpaisal et al. 2007
Arasin	4.3-4.8	Cationic, N-term PRP: C- term 4 cysteine	Decapoda	*Hyas araneus*- Stensvag et al. 2008
Homarin	4-6	Cationic, Glycine rich	Decapoda	*Homarus americanus*- Battison et al. 2008
Hyastatin	11.7	Cationic, N- term Gly: PRP : C term- 6Cys	Decapoda	*Hyas araneus*- Sperstad et al. 2009
Defensin	6.7-7.1	Cationic, cysteine containing	Decapoda	*Panulirus japonicus*- Pisuttharachai et al. 2009
Stylicin	8.9	Anionic, N-term P rich : C-term 13 cysteine	Decapoda	*L. stylirostris*- Rolland et al. 2010

1.9 Importance and objectives of the study

Marine organisms are constantly exposed to potentially harmful pathogens through contact, ingestion, inhalation etc. Their survival in a microbe thriving environment depends on a network of host defence mechanisms involving various components. In the milieu of emergence of multi-drug resistant pathogens and restrictions on antibiotic therapy in aquaculture and medicine, AMPs, the endogenous antibiotics can be considered as a potential therapeutic agent. The low propensity of resistance development, decreased toxicity to eukaryotic cell and broad spectrum activity of AMPs increase the demand for identification and production of new potent AMPs.

Crustaceans constitute the most abundant animals inhabiting the world oceans. The evolutionary success of crustaceans and lack of an adaptive immune system make them a potential source for novel AMPs. Among the crustaceans, most of the AMPs are characterized from marine decapods such as prawns, lobsters and crabs and it includes major AMP families namely, anti-lipopolysaccharide factors (ALF), crustin, penaedin and unconventional peptides derived from histone proteins and haemocyanin.

With the above mentioned perceptions, present study was commenced with the following objectives:

- Bio-prospecting for novel AMPs from marine crustaceans using gene based approach
- Molecular and phylogenetic characterization of AMPs with the aid of bioinformatics tools.

- Recombinant production of AMPs and its functional characterization.
- Functional characterization of synthetic AMPs.

The thesis is included of six chapters. A general introduction of the research subject is given in Chapter 1. Molecular and functional characterization of AMP, crustin from the Indian white shrimp, *Fenneropenaeus indicus* is presented in Chapter 2 and ALF, from crucifix crab, *Charybdis feriatus* is included in Chapter 3. The Chapter 4 deals with the molecular characterization of ALF isoform from mantis shrimp, *Miyakea nepa* and its functional analysis using the synthetic peptide. Chapter 5 illustrates the molecular characterization of histone H2A derived AMP from the Indian white shrimp, *F. indicus* and finally the functional analysis using the synthetic peptide. The work is summarized and discussed in Chapter 6, followed by references, GenBank accessions and publications.

Chapter 2

MOLECULAR AND FUNCTIONAL CHARACTERIZATION OF AN ANTIMICROBIAL PEPTIDE CRUSTIN FROM THE INDIAN WHITE SHRIMP, *FENNEROPENAEUS INDICUS*

Contents

2.1 Introduction

Antimicrobial peptides (AMPs) comprise of molecules that involve in the defense mechanism of various organisms towards pathogens such as bacteria, fungi, parasites and viruses. To date, over 800 AMPs from eukaryotic organisms have been described in literature, the majority being identified from mammals, insects or amphibians. Only less than 10 % of all known AMPs are from crustaceans, with nearly all of these being reported from decapods. Numerous AMPs have been identified in crustaceans, including the penaeidins (Destoumieux et al., 1997), anti-lipopolysaccharide factors (ALFs) (Gross et al., 2001), histone derived AMPs (Patat et al., 2004) and hemocyanin derived AMPs (Destoumieux-Garzon et al., 2001). Crustin is a multi-domain cationic AMP with a molecular weight of 7-14 kDa, and *p*I in the range of 7.0-8.7 comprising one whey acidic protein (WAP) domain at the C-terminus (Smith et al.,

2008). Crustin had been evidenced to be an imperative AMP in the plasma and haemocyte granules of crustaceans and are described as a constituent of the innate immune system (Vargas-Albores et al., 2004). The WAP domain consists of 8 Cys residues engaged in disulfide bonds and form the four disulfide core (4DSC).

The first recognized crustin isoform is an 11.5-kDa protein purified from the granular haemocytes of the shore crab *Carcinus maenas* which shows precise activity to Gram-positive salt-tolerant bacteria (Relf et al., 1999). Till this date more than 60 crustins and crustin-like sequences have been recognized using EST-based approaches from decapod crustacean species including crayfishes, shrimps, freshwater prawns, crabs, lobsters as well as non-decapod crustacean species such as amphipods (Bartlett et al., 2002; Hauton et al., 2006; Zhang et al., 2007; Smith et al., 2008; Supungul et al., 2008). The term crustin was later proposed by Bartlett and co-workers (2002) to describe transcripts found in two penaeid shrimp species (*L. vannamei* and *L. setiferus*) with high sequence similarity to the crab 11.5-kDa protein, which was later designated as carcinin by Brockton et al. (2007). Based on the structural features, Smith et al., (2008) characterized crustins into three main types (Type I, II and III). Type I crustin members are mainly found in crabs, lobsters, crayfishes, shrimps and freshwater prawns and have a Cys-rich region of variable length between the signal peptide sequence and the WAP domain (Imjongjirak et al., 2009). Whereas, Type II crustins hold a signal sequence trailed by a long Gly-rich region, a Cys-rich region and the WAP domain and are found in penaeid shrimps and crayfishes (Amparyup et al., 2008a, 2008b). Type III crustins retain a short proline-rich peptide (PRP) region between

the signal peptide region and the single WAP domain and are confined to shrimps (Supungul et al., 2004).

The genomic organization of crustin was found to be distinct among different groups. The genomic organization of Type-I and Type-III crustins were studied; Type I crustins are found to be encoded by four exons traversed by three introns (Brockton et al., 2007; Imjongjirak et al., 2009), and Type III crustins are found to possess three exons and two introns (Amparyup et al., 2008a). Two crustin isoforms from the *P. monodon* were encoded by different genes; crustin*Pm*5 contained four exons separated by three introns, and crustin-like*Pm* contained only two exons and one intron (Amparyup et al., 2008b; Vatanavicharn et al., 2009). As determined by RT-PCR, expression of crustin-encoding genes has primarily been identified in haemocytes, and in other tissues such as heart, ovary and intestines (Smith et al., 2008). Remarkably, transcripts of crustin isoforms, such as crustin *Pm*5, Plcrustin2 and Fc-crus3 were found in the epipodite, hematopoietic tissue, ovary and olfactory organ (Stoss et al., 2003; Jiravanichpaisal et al., 2007; Vatanavicharn et al., 2009; Sun et al., 2010).

Biological activity of crustin was characterized mainly using peptide isolated from natural sources and also by recombinant production of the peptide. Challenges encountered in the production of crustin by synthetic approach include the large size and four disulfide bond which forms the active domain of the peptide. Thus for functional characterization, the crustins were first produced by recombinant expression in a prokaryotic system. Biological activities exhibited by crustin include protease inhibition and antibacterial activities which could be correlated to a specific structure

of the WAP domain. The anti-protease activities have only been reported for Type III crustins (Amparyup et al., 2008a; Jia et al., 2008), and found to be generally related with the incidence of a methionine residue contiguous to the second cysteine in the 4DSC. In the case of WAP domain containing peptides with anti-bacterial activity, the Met residue is replaced by cationic or hydrophobic amino acids (Hagiwara et al., 2003). Type III crustins are found to be multifaceted immune proteins that possess both antimicrobial and anti-protease properties (Amparyup et al., 2008a; Jia et al., 2008). This anti-protease ability is necessary to disable microbial proteases during infection and/or control endogenous protease cascades, such as the pro-phenol oxidase system.

In vitro antimicrobial studies have showed that all crustin groups are mainly active against Gram-positive bacteria with an MIC <8 μM and it include *Micrococcus, Aerococcus, Planococcus, Staphylococcus, Streptococcus, Corynebacterium* and *Bacillus* (Relf et al., 1999; Zhang et al., 2007; Supungul et al., 2008; Imjongjirak et al., 2009; Sperstad et al., 2009b; Mu et al., 2010; Suthianthong et al., 2012). On the contrary, a Type II crustin from *P. monodon*, crustin-like *Pm* (Amparyup et al., 2008b) and crustin *Pm*7 (Krusong et al., 2012) showed strong antibacterial activity against both Gram-positive and Gram-negative bacteria (MIC < 5 μM), including the *E. coli* and crustacean opportunist pathogen, *V. harveyi.* Krusong et al. (2012) found that the isoforms crustinPm1 and crustinPm7 from *P. monodon* exhibited binding activity with cell wall components, lipoteichoic acid (LTA) and lipopolysaccharide (LPS). The antimicrobial activity of crustins seems to be correlated to the tertiary structure of the

4DSC which is tightly constrained by three disulfide bonds and containing a small α-helix (Smith et al., 2008).

For characterizing a novel AMP, it is imperative to understand the mechanism of action, to elucidate the structure and function, or its prospective usage as a pharmaceutical drug. For that, a reasonable quantity of purified and active AMP molecule is desired. Overall, there are three different methodologies employed to obtain enough AMPs: direct isolation from natural sources, chemical synthesis and recombinant expression (Parachin et al., 2012). Direct extraction requires sacrificing large number of animals and the yield also is generally low necessitating the adoption of alternate methods. The large size and the disulphide bond within functional WAP domain of crustin hampers it production by solid-phase synthesis approach and thus researchers mainly rely on recombinant technology for large scale production of the peptides. Crustin was produced by recombinant method using both eukaryotic, yeast *Pichia pastoris* expression system (Arayamethakorn et al., 2013; Liu et al., 2016) and prokaryotic *E. coli* based system (Zhang et al., 2007; Amparyup et al., 2008; Mu et al., 2010; Jiang et al., 2015a).

Even though the gene expression (Vargas-Albores et al., 2004; Hauton et al., 2006) and molecular characterization of crustins from crustaceans were done (Brockton et al., 2007), the functional characterization of crustin using recombinant product was done by Zhang et al. (2007). Identification, molecular characterization and recombinant production of a crustin-like gene (Cru*Fc*) from the haemocytes of Chinese shrimp, *Fenneropenaeus chinensis* was accomplished using pCR® T7/NT TOPO® TA vector in

BL21(DE3) pLysS *E. coli* cells. Refolded rCru*Fc* inhibited the growth of gram-positive bacteria with MIC values of 2–8 μM. Amparyup et al. (2008a) identified Crus-like*Pm* from haemocytes of *P. monodon* and cloned into the pET-28b with an N-terminal hexa-histidine tag fused in-frame, and expressed in *E. coli* BL21-Codon Plus (DE3)-RIL. The recombinant peptide, rCrus-like*Pm* was found in both inclusion bodies and soluble fraction and the purified rCrus-like*Pm* showed strong antimicrobial activity against both Gram-positive and Gram-negative bacteria including *V. harveyi* with MIC values ranging from 0.312 to 20 μM.

The most abundant antibacterial peptide, Crustin*Pm*1 from *P. monodon,* was overexpressed using *E. coli* expression vector, pET-28a (Novagen) in *E. coli* BL21-(DE3) (Supungul et al., 2008). The rcrustin*Pm*1 exhibited bactericidal activity only against Gram-positive bacteria with strong inhibition against *Staphylococcus aureus* and *Streptococcus iniae* with an MIC of 3.13–6.25 μM. Later in the year 2010, Donpudsa and co-workers identified two Type-I crustins, *Pl*crustin1 and *Pl*crustin2 from *Pacifastacus leniusculus* and recombinantly produced in the *E. coli* Rosettagami B (DE3) with pVR500 vector. Antimicrobial assays showed that the growth of Gram-positive bacterium, *Micrococcus luteus* was inhibited by the recombinant *Pl*crustin1 and *Pl*crustin2 with MIC of about 0.07–0.27 μM and 3.5–8 μM, respectively.

In the same year Mu et al. (2010) using RACE approaches identified Type-I crustin-like peptide (CrusEs) from the Chinese mitten crab, *Eriocheir sinensis*. The recombinant CrusEs was cloned into pET-21a(+) with a C-terminal hexa-histidine tag and expressed in *E. coli* Origami

(DE3) and the rCrusEs inhibited the growth of Gram-positive bacteria with a lower MIC of 0.11– 0.46 μM. Also, Cui et al. (2010) recognised two Type-I crustins (PtCrustin2 and PtCrustin3) from swimming crab *Portunus trituberculatus.* Two crustin isoforms were produced using recombinant approach in *E. coli* BL21 (DE3)-pLysS using pET-32a(+) vector. Unlike most crustins, both recombinant PtCrustin2 and PtCrustin3 exhibit antibacterial activity against Gram-positive bacteria, *M. luteus* and *S. aureus* and Gram-negative bacterium, *P. aeruginosa.* In addition, rPtCrustin2 was moderately active against yeast, *P. pastoris* and rPtCrustin3 showed significant activity against Gram-negative bacterium, *V. alginolyticus*.

Two crustin isoforms from *P. monodon* crustin*Pm*1 and crustin*Pm*7 genes in pET-28b were expressed in *E. coli* strain Rosetta (DE3) (Krusong et al., 2012). Both recombinant crustins exhibited bacterial agglutination and caused inner membrane permeabilization in *E. coli*. Scanning electron microscopic (SEM) analysis revealed the remarkable changes on the cell surface of *S. aureus*, *V. harveyi* and *E. coli* after the bacteria were treated with the recombinant crustin*Pm*7 with an MIC ranging from 3.13- 12.5 μM. In the same year Suthianthong et al. (2012) studied about the antibacterial and anti-proteinase activities of various mutants of recombinant crustin*Pm*1 and found that antibacterial activity of crustin*Pm*1 is exerted from the N-terminus part and that the numerous mutations in the WAP domain cannot render the crustin*Pm*1 active in anti-proteinase. Also found that the incidence or lack of Met residue in the WAP domain is not the discriminating factor for anti-proteinase and antibacterial activities of crustin*Pm*1.

In 2013, Arayamethakorn and co-workers identified another isoform of crustin, Crustin*Pm*7 from *P. monodon* and produced recombinant peptide in eukaryotic *P. pastoris* yeast expression system using pPIC9K vector. The rCrustin*Pm*7 demonstrated antimicrobial activity against both Gram-positive and Gram-negative bacteria including *S. aureus*, *M. luteus*, *E. coli* 363 and *V. harveyi* with MIC values ranging from 2 to 10 μM. Arockiaraj et al. (2013a) identified crustin isoform (*Mr*Crs) from a freshwater prawn *M. rosenbergii* and was found to be up-regulated following viral challenge by infectious hypodermal and hematopoietic necrosis virus (IHHNV) and white spot syndrome virus (WSSV) besides bacteria, *A. hydrophila* and *E. faecium*. The recombinant *Mr*Crs was expressed in *E. coli* BL21 (DE3) and r*Mr*Crs protein exhibited bactericidal activity against *A. hydrophila* with an MIC of 25 μg/ml.

In order to study the biological potential of Type-I crustin, Donpudsa et al. (2014) prepared the recombinant protein of Crustin-*Pm*4-1 isoform from *P. monodon* in *E. coli* expression system and tested for its antimicrobial and antiviral activity. The rcrustinPm4-1 was able to inhibit the growth of *B. megaterium* and also affect the WSSV infection by down-regulating the early gene ie-1 in WSSV-infected shrimp haemocyte cell culture. In the same year, Banerjee et al. (2015) also performed the recombinant production of another crustin isoform from *P. monodon,* rCrustin in *E. coli* SG 13009 and exhibited a MIC of 0.5 μg/ml against the pathogenic vibrios in shrimps.

Jiang et al. (2015) identified four isoforms of crustin *Mj*Crus I-2, 3, 4 and 5 from *Marsupenaeus japonicus,* and the gene expression of these

isoforms were found to be upregulated by bacterial or WSSV challenge. All the isoforms were recombinantly produced in *E. coli* BL21-DE3 using pET-30a(+). The r*Mj*Crus I-2 and 3 were found to possess different inhibitory abilities to bacterial proteases. However, MjCrus 4 was not able to inhibit bacterial proteases and revealed scavenging activity against *V. anguillarum* infection. In the same year Yu et al. (2015) isolated and characterized a novel Type-I crustin, *Cq*Crs from the red claw crayfish *Cherax quadricarinatus.* Gene expression of *Cq*Crs was identified in all tissues, post-stimulation with β-1,3-glucan, lipopolysaccharides and peptidoglycans. Recombinant *Cq*Crs produced in *E. coli* BL21-DE3 exhibited diverse binding and antibacterial activity in response to different bacteria including *E. coli, P. pastoris* and *S. aureus* with an MIC of 200 µg/ml. In 2016, Liu and his co-workers identified a novel crustin isoform from red swamp cray fish, *Procambarus clarkia, Pc*Cru. Recombinant *Pc*Cru was produced using both prokaryotic system with pET-30a (+) vector and *E. coli* BL21 (DE3) cells and eukaryotic system with pPIC9k vector and *P. pastoris* KM71 cells. Both recombinant peptides were found to have broad-spectrum anti-microbial activity to many pathogenic bacteria including *V. anguillarum* and *B. subtilis* with an MIC of 1.5 and 0.75 µM.

The Indian white shrimp, *F. indicus* is the most prevailing shrimp species in the shrimp fishery along the west and east coast of India and forms an important shrimp species which is cultured in pokkali paddy fields (paddy-cum-prawn farming). Even though a huge number of AMPs have been described in various shrimp species, only a few AMPs have been reported including isoforms of crustin, Fi-crustin (Antony et al., 2011a);

penaeidins, Fi-penaeidin (Antony et al., 2011) and Fi-penaeidin2 (Afsal et al., 2016). The present chapter is focused at the molecular cloning and phylogenetic characterization of second Type-I crustin AMP isoform from the Indian white shrimp, *Fenneropenaeus indicus* (*Fi*-crustin2) and its recombinant production, purification and functional characterization.

2.2 Materials and Methods

2.2.1 Experimental organism

Live and healthy shrimp, *Fenneropenaeus indicus* was collected from Cochin estuary along Fort Kochi, Kerala, India. By providing aeration, the samples were taken to the laboratory in live condition.

Fig. 2.1 Experimental organism used for the study, Indian white shrimp *Fenneropenaeus indicus*.

2.2.2 Precautions for RNA preparation

While working with RNA because of the chemical instability of the RNA and the ubiquitous presence of RNases, general precautions for RNA extraction includes: (i) Diethyl pyrocarbonate (DEPC) treatment of Milli-Q water, glass wares, homogenizers, scissors and forceps with 0.1 % DEPC at room temperature overnight. In order to remove the residual DEPC, after incubation all the required items were autoclaved at 15 lb

pressure for 1 hour. This is followed by autoclaving at 15 lb pressure for 15 min for ensuring sterile condition. (ii) Work bench, pipettes, micro tip boxes and MCT racks were wiped with RNase Away before the experiment (iii) Wearing gloves and mask throughout the experiments to prevent contamination from RNases from saliva and sweat (iv) Always maintained a set of pipettes and plastic wares that are used solely for RNA work (v) Usage of RNase-free chemicals, reagents, barrier tips and tubes.

2.2.3 Haemolymph collection

Haemolymph was collected from rostral sinus of *F. indicus* carefully using DEPC treated RNase-free capillary tubes rinsed using pre-cooled anticoagulant solution (RNase free 10 % sodium citrate, pH 7.0 in DEPC treated water). Haemolymph was homogenised in TRI reagent (Sigma) using RNase free micro-pestle and kept at -20˚C for total RNA isolation.

2.2.4 Total RNA isolation

Total RNA was isolated from haemocytes using TRI reagent (Sigma) following manufacturer's instructions. This includes three main steps including sample preparation, phase separation and RNA isolation.

For sample preparation about 0.5 ml of haemolymph was homogenized in 0.3 ml of TRI Reagent in RNase free micro-centrifuge tubes (MCTs) using sterile micro pestle and finally 0.7 ml of TRI Reagent was added and mixed well by vigorous shaking. In order to ensure complete dissociation of nucleoprotein complexes, the samples were allowed to stand for 5 min at room temperature. For phase separation, 0.2 ml of chloroform was added and vigorously shaken for 30 sec, and allowed to stand for 15 min at room temperature. The resultant mixture was centrifuged at 12000

x g for 15 min at 4 °C. Centrifugation separates the mixture into 3 phases: a red organic phase (containing protein), an interphase (containing DNA), and a colourless upper aqueous phase (containing RNA).

Aqueous phase with RNA was then carefully transferred to a fresh MCT with 0.5 ml ice cold isopropanol, mixed slowly by inversion and kept for 5-10 min at room temperature. Precipitated RNA was further pelletized by centrifugation at 12000 x g for 10 min at 4 °C. RNA pellet was washed twice using 1 ml 75 % ethanol. Followed by a mild vortexing, samples were centrifuged at 7500 x g for 5 min each at 4 °C. Washed RNA pellet were kept for drying in a laminar air flow chamber by keeping the MCTs in an inverted position over tissue paper towel. RNA pellets were dried for 10 min and dissolved in 35 µl of RNase free water (volume varies and depends on the size of the pellet) by repeated pipetting with a micropipette, for complete dissolution kept at 55 °C for 5 min.

2.2.5 Quality assessment and quantification of RNA

In the present work RNA was quantified and qualified by measuring optical density (O.D.) at 260 and 280 nm in a UV spectrophotometer. The ratio of absorbance at 260 nm and 280 nm is an indication of RNA quality. Only RNAs with absorbance ratio (A260: A280) ≥1.7 were used for cDNA synthesis (Hitachi U-2900). 1 $O.D_{260}$ of RNA = 40 µg/ml, and hence, RNA concentration was calculated as:

RNA concentration (µg/ml) = O.D at 260 nm × dilution factor × 40

2.2.6 Reverse transcription

Single stranded cDNA was synthesized from total RNA using specific oligo-d(T20) primers targeting the mRNA, which contains a

poly-A tail. First strand synthesis of cDNA requires a 20 μl reaction mix containing 5 μg total RNA, 1x RT buffer, 2 mM dNTP, 2 mM oligo d(T20), 20 U of RNase inhibitor, and 100 U of MMLV reverse transcriptase (New England Biolabs, USA). The reaction was conducted at 42 ˚C for 1 h followed by an inactivation step at 85 ˚C for 15 min.

2.2.7 PCR amplification

Reverse transcription was confirmed and ensured by using PCR amplification of the constitutively expressed gene, beta-actin using the single stranded cDNA as the template. Amplification of the AMP, crustin was done using the primers Crustin F and Crustin R (Antony et al., 2010) with the cDNA as template. Sequences of primers are given in the Table. 2.1. PCR was performed in a 25 µl reaction volume containing 1x standard Taq buffer (10 mM Tris HCl, 50mM KCl, pH 8.3), 3.5mM MgCl2, 200 µM dNTPs, 0.4 µM each primer and 1U Taq DNA polymerase (New England Biolabs). The thermal profile used was 95 ˚C for 2 min followed by 35 cycles of 94 ˚C for 15 s, 57 ˚C for 30 s and 72 ˚C for 30 s and a final extension at 72 ˚C for 10 min.

2.2.8 Agarose gel electrophoresis

For analysis of PCR products, 1.5 % agarose gel was prepared in 1 X TBE buffer (Tris-base -10.8 g, 0.5 M EDTA- 4 ml, Boric acid- 5.5 g, double distilled water- 100 ml, pH- 8.0). Ethidium bromide (2 µl /100 ml of agarose gel (stock concentration 1mg/ml)) was added to the melted agarose. After cooling to ear bearing temperature, the agarose was poured on to gel tray and was allowed to solidify. The solidified gel with the casting tray was submerged in a buffer tank of electrophoresis unit

containing 1X TBE buffer. 5 µl of PCR product was mixed with 2 µl of 6 x gel loading buffer (1 % Bromophenol blue- 250 µl, 1 % xylene cyanol-250 µl, glycerol–300 µl, double distilled water–200 µl) and loaded into the well. Electrophoresis was performed at constant voltage of 3-5 volt/cm till the bromophenol blue dye front migrated to the middle of the gel. The gel was visualized on a UV transilluminator using the Gel-DOC^{TM} XR+ imaging system (BioRad, USA).

2.2.9 TA cloning of amplicons

Purified PCR products were cloned into pGEM®-T Easy cloning vector (Promega) based on TA-cloning strategy. System facilitates the cloning of PCR products by providing linear vectors that have a single thymidine extension at the 3´-ends. These terminal thymidines are complementary to the non-template derived 3´ adenosine residues that are added to double-stranded DNA products by many non-proof reading DNA polymerase.

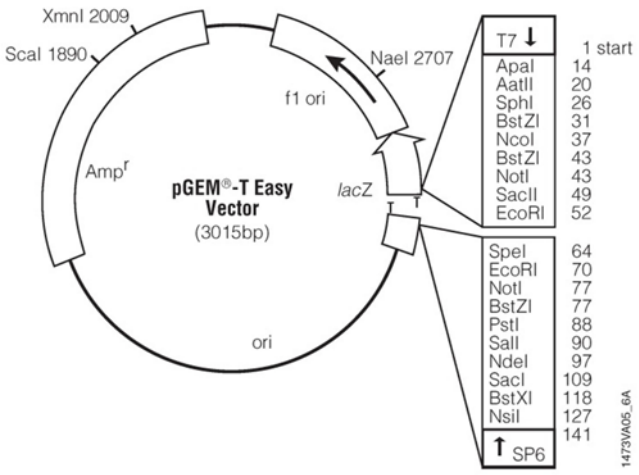

Fig. 2.2 Vector map of TA cloning vector, pGEM®-T Easy cloning vector (Promega)

2.2.9.1 *Ligation*

The ligation reaction (10 µl) consisted of 5 µl ligation buffer (2x), 0.5 µl of the vector (50 ng/ µl), 3.5 µl PCR product (600 ng/ µl) and 1 µl of T4 DNA ligase (3 U/ µl). The ligation mix was mixed well by pipetting and incubated in a cooling water bath at 4 °C for 12 hr.

2.2.9.2 *Competent cell preparation of E. coli DH5α*

Competent cells of *E. coli* DH5α for transformation of pGEM®-T Easy vector with the insert were prepared as follows. Briefly, a single colony of *E. coli* DH5α was inoculated to 10 ml Luria Bertani (LB) broth and cultured overnight at 37 °C at 150 rpm. An aliquot of 5 ml of overnight culture was inoculated into 50 ml of LB broth and incubated at 37 °C for 2 hrs at 250 rpm in order to collect the cells in their log phase. Culture was centrifuged at 6000 rpm for 20 min at 4 °C in a refrigerated centrifuge (Hitachi). The pellet was collected and then re-suspended in 50 ml of sterile ice-cold 100 mM $CaCl_2$ with gentle vortexing. Centrifuge tubes with cells were placed on ice for 1 hr with intermittent gentle swirling and mixing. The cells were then centrifuged at 6000 rpm for 20 min at 4 °C. The supernatant was decanted and cell pellet was again re-suspended using 1 ml of 100 mM $CaCl_2$. From the competent cells suspension, 80 µl each was transferred to 1.5 ml MCT and mixed slowly with 20 µl of sterile 60 % glycerol and then stored at -80 °C for further use.

2.2.9.3 *Transformation into E. coli DH5α*

Frozen competent *E. coli* DH5α, was taken from deep freezer (-80 °C) and thawed in ice for 5 min. Gently spin down the ligation reaction mix and 5 µl was taken carefully from the top and added to the competent

cells. Gently flicked the tubes and kept in ice for 30 min. The cells were then given a heat-shock for 60 sec in a water-bath at exactly 42 °C without shaking. Immediately the tubes were returned to ice for 3 min. To the transformed cells, 500 µl of LB broth was added gently by pipetting without any bubbles and incubated for 1.5 h at 37 °C with shaking (~150 rpm). Transformed cells were spread plated on to LB agar plates supplemented with ampicillin (100 µg/ml), Isopropyl-β-d-thiogalactoside (IPTG) (100 mM) and 5-bromo-4-chloroindolyl-β-D-galactopyranoside (X-gal) (80 µg/ml) and, incubated at 37 °C for 16 h. The recombinant clones with the inserts were selected by blue white screening.

2.2.9.4 *Confirmation of gene insert by colony PCR.*

The white colonies were selected and patched on to fresh LB/ampicillin/IPTG/X-Gal plates and colonies were screened by colony PCR with vector specific (T7 F and SP6 R) and gene specific (Crustin F and R) primers in a 25 µl reaction volume containing 1x standard Taq buffer (10 mM Tris-HCl, 50 mM KCl, pH 8.3), 3.5 mM $MgCl_2$, 200 µM dNTPs, 0.4 µM each primer, 1U Taq DNA polymerase (Fermentas, Inc.) and a pinch of colony as template. The PCR condition involved an initial denaturation of 95 °C for 5 min followed by 35 cycles of 94 °C for 15 seconds, annealing temperature of 57 °C for 30 seconds and 72 °C for 30 seconds and a final extension at 72 °C for 10 minutes. The PCR products were analysed by electrophoresis in 1.5 % agarose gel as explained in section 2.2.8. Positive clones were selected for plasmid isolation and thus single colony was inoculated in LB broth supplemented with ampicillin (100 µg/ml).

2.2.9.5 *Plasmid extraction*

Plasmid with the insert was then isolated and purified using GenElute HP plasmid MiniPrep kit (Sigma) following manufacturer's protocol with minor modifications. During purification, the spin columns were kept open during the whole steps and were done at room temperature. Briefly, cells were harvested by centrifugation of 7 ml overnight recombinant *E. coli* culture at 12000 x g for 1 min. The pellet was then re-suspended in 200 µl resuspension solution supplemented with RNase. The cells were then lysed by adding 200 µl of the lysis buffer in order to release the cell contents including the plasmids. The contents were then mixed gently by inversion until the mixture becomes clear and viscous.

In order to precipitate the cell debris from plasmid, 350 µl of the neutralization buffer was added and pelletized by centrifugation at 12000 x g for 10 min. GenElute HP MiniPrep binding column were activated by the addition of 500 µl of the column preparation solution and centrifuged at 12000 x g for 1 min. Cleared lysate from neutralization step was transferred to the prepared column and proceeded to washing steps twice with wash solution I and II respectively by centrifugation at 12000 x g for 1 min and flow through was discarded. Another centrifugation at 12000 x g for 1 min was done to remove the residual ethanol (from wash buffer-II) in the column. Concentrated plasmid DNA was then eluted from the column with 100 µl of elution solution (10 mM Tris-HCl) by centrifuging at 12000 x g for 1 min and stored at -20 °C. Plasmid DNA obtained was analysed for quality and confirmed by agarose gel electrophoresis.

2.2.10 Sequencing of plasmids

Extracted plasmid with insert having an O.D. greater than 1.7 were sequenced using vector specific primers T7 F and Sp6 R, with an ABI Prism Sequencing kit (Big-Dye Terminator Cycle) at SciGenom sequencing facility, Kakkanad, Kochi, Kerala, India.

Table 2.1 List of primers used.

Target gene	Sequence (5'-3')	Product Size (bp)	Annealing Temp. (°C)	$MgCl_2$ Conc. (mM)
Crustin	F: CGCACAGCCGAGAGAAACA CTATCAAGAT R: GGCCTATCCCTCAGAACCCA GCACG	354	55	1.5
β-actin	F: CTTGTGGTTGACAATGGCTC CG R: TGGTGAAGGAGTAGCCACG CTC	520	60	1.5
T7	F: TGTAATACGACTCACTATAG GG R: CTAGTTATTGCTCAGCGGTG	--	57	1.5
SP6	R: GATTTAGGTGACACTATAG	--	57	1.5

2.2.11 Sequence characterization and phylogenetic analysis

Nucleotide sequence was analysed, and assembled using GeneTool software. The cDNA sequences obtained were translated using Expert Protein Analysis System (ExPASy) translate tool (http://au.expasy.org/translate) to obtain amino acid sequence. Homology searches of nucleotide and deduced

amino acid sequences were performed using BLASTn and BLASTp algorithm of the NCBI (http://www.ncbi.nlm.nih.gov/blast). Signal peptide (SP) region was identified using the online programme SignalP (http://www.cbs.dtu.dk/ services/SignalP). Domains and motifs in peptide sequence were analysed on PROSITE Database (http://prosite.expasy.org/ scanprosite/). The N-terminal trans-membrane sequence of the mature peptide was determined by DAS transmembrane prediction program (http://www.sbc.su.se/~miklos/DAS). Physico-chemical parameters of the full length peptide and mature peptide were predicted separately using the online protein parameters analysis tool, ExPASy PROTPARAM bioinformatics resource portal (http://web.expasy. org/protparam) and Protein calculator (http://protcalc.sourceforge.net/).

The helical property was predicted using Heliquest online tool (http://heliquest.ipmc.cnrs.fr/cgi-bin/ComputParamsV2.py) to analyse the segregation of hydrophobic and hydrophilic amino acid residues. Hydrophobic nature of the peptide was also analysed by Kytee-Doolittle plot using the ProtScale tool of ExPASy bioinformatics resource portal (http://web.expasy.org/protscale/) The cDNA sequence of peptide was converted to the corresponding RNA sequence (http://www.attotron.com/) and submitted to RNA Fold Server Program (http://rna.tbi.univie.ac.at/ cgi-bin/RNAfold.cgi) to envisage the RNA structure with minimum free energy (MFE) to observe the stability of mRNA structure. The antimicrobial activity was predicted using Antimicrobial peptide database – calculation and prediction tool (http://aps.unmc.edu/). The amphipathicity and antimicrobial activity of LPS domain was interpreted using Heliquest online tool (http://heliquest.ipmc.cnrs.fr/cgi-bin/ComputParamsV2.py).

Multiple sequence alignment of deduced amino acid sequence was performed on ClustalW in BioEdit software for the comparison and alignment with other crustacean crustin encoding sequences. The phylogenetic tree was constructed using Neighbor-Joining method using MEGA version 7. The spatial structure was established with PyMOL, using the SWISS-MODEL prediction algorithm based on homology modelling (Guex and Peitsch, 1997; Schwede et al., 2003; Arnold et al., 2006). The secondary structure prediction of the peptide was also analysed and confirmed using PSIPRED protein sequence analysis work bench (http://bioinf.cs.ucl.ac.uk/psipred/).

2.2.12 Selection of active peptide region for recombinant expression

Functional characterization of an AMP is an inevitable tool in the screening for novel and potent antimicrobials. In order to study the bioactive potential of peptides, we chose the active peptide region for recombinant production using pET-32a(+) and *E. coli* Rosettagami™B (DE3) pLysS expression system.

2.2.13 Details of expression vector: pET-32a(+)

The pET-32a(+) is one of the efficient translational vectors of pET series vectors, which are intended for cloning and the high-level production of recombinant peptide sequences as fusion protein containing the thioredoxin (Trx•Tag™), cleavable His•Tag® and S•Tag™ sequences for detection and purification. The Trx•Tag expressed from pET-32a(+) vector enhances the solubility of expressed protein and catalyzes the disulphide bond formation in the cytoplasm of trx/gor mutants of expression hosts i.e., the mutant strains of *E. coli:* Origami™, Origami B

and Rosetta-gami™ strains (Stewart and Aslund, 1998). Multiple cloning site of pET-32a-c(+) vector series is shown in the Fig. 2.3.

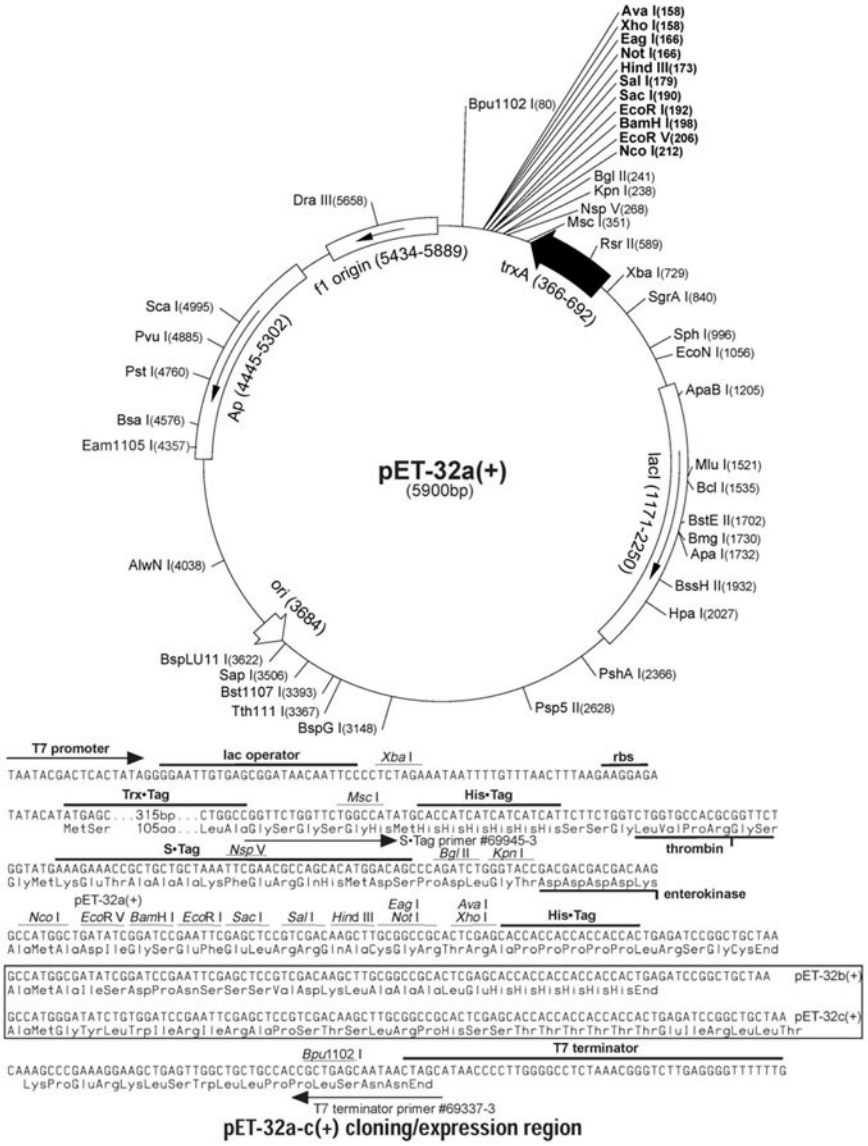

Fig. 2.3 Vector map of pET-32a(+) expression vector and its multiple cloning site.

2.2.14 Primer designing for restriction cloning into expression vector

Selected mature peptide region of *Fi*-crustin2 was amplified using primers with suitable restriction enzyme sites for directional cloning into the expression vector pET-32a(+) (Novagen, UK). Restriction sites from multiple cloning site (MCS) of vector was selected in such a way that it should be absent within the target gene.

Table 2.2 Sequence of restriction primer designed for *Fi*-crustin2

Target gene	Sequence (5'-3')
pET ***Fi*-crustin2** F	TAAGCACCATGGGTCAAGAAGATACTCGCTTC
pET ***Fi*-crustin2** R	TAAGCAAAGCTTTTACTATCCCTCAGAACCCAG

* Colour definitions

Nucleotide bases included to ensure enzyme digestion.

Nucleotide bases added to make the frame correct

Restriction enzyme site NcoI in F and HindIII in R primer

Target gene sequence

Stop codon

2.2.15 PCR amplification of mature peptide

In order to amplify the active peptide region with restriction primers pET-*Fi*-crustin2 F and R, pGEMT-*Fi*-crustin2 was used as the template. PCR was performed in a 25 µl reaction volume containing 1x standard Taq buffer (10 mM Tris HCl, 50mM KCl, pH 8.3), 3.5mM $MgCl_2$, 200 µM dNTPs, 0.4 µM each primer and 1U Taq DNA polymerase (New England Biolabs). The thermal profile used was 95 ˚C for 2 min followed by 35 cycles of 94 ˚C for 15 s, 60 ˚C for 30 s and 72 ˚C for 30 s and a final extension at 72 ˚C for 10 min. Amplicons were analysed by electrophoresis

in 1.5 % agarose gel in TBE buffer, stained with ethidium bromide and visualized under UV light.

2.2.16 Restriction digestion

Expression vector pET-32a(+) (Novagen, UK) and the PCR products flanking the restriction sites for insertion into vector were proceeded to restriction digestion using the restriction enzymes NcoI and HindIII (FastDigest restriction enzymes, Thermo). Double RE digestion of insert and vector was done in separate reactions. For performing restriction digestion, 50 µl of PCR product was incubated with 5 µl of 10X reaction buffer and 0.5 unit each of NcoI and HindIII and kept for 1 h at 37 °C followed by an inactivation at 65 °C for 20 min. Vector was also treated the same way for ligation. Restriction digestion was confirmed by agarose gel electrophoresis.

2.2.17 Purification of restriction digested insert and expression vector by gel elution

Gel purification of the restriction enzyme digested insert and vector, pET-32a(+) were done using GenJET™ Gel Extraction Kit (Thermo Scientific, USA) as per manufacturer's instructions with slight modifications. Using the kit, DNA fragments of interest can be extracted from slices of an agarose gel by solubilizing the gel. While doing the agarose gel electrophoresis, fresh electrophoresis running buffer was used since the electrophoresis buffer, which has been used repeatedly, will reduce the DNA recovery efficiency from the gel. Ethidium bromide-stained agarose gels were observed under UV transilluminator equipped with a long-wavelength (302 nm) UV light source to minimize the damaging effects of UV light on DNA.

In brief, the DNA fragment of interest was excised from the agarose gel with a sterile, sharp scalpel. Gel slice was collected and weighed in a tared 1.5 ml MCT. In order to solubilize the gel 3 gel volumes of the gel solubilisation solution (binding buffer) was added to the gel slice and incubated at 55 °C for 10 minutes with intermittent vortexing to aid dissolution. In order to maximize the binding of DNA to column, it was pre-treated with 500 µl of Column Preparation Solution and subjected to centrifugation at 12000 x g for 1 min. To the dissolved gel, 1 gel volume of 100% isopropanol was added and mixed until it became homogenous. Gel solution was then added on to a prepared binding column and centrifuged at 12000 x g for 1 min. After the sample loading step, the column was washed two times with 700 µl of wash solution followed by centrifugation at 12000 x g for 1 min. Flow through was discarded in all of the above steps. Residual wash solution was removed further by another centrifugation at 12000 x g for 1 min. Finally the purified insert and vector was eluted from the column with 25 µl of elution buffer in a fresh collection tube by centrifugation at 12000 x g for 1 min and stored at -20 °C for further use. Concentration of nucleic acid in the eluate was measured spectrophotometrically at 260/280 nm in a UV-VIS Spectrophotometer (U2800, Hitachi, Japan).

2.2.18 Construction of recombinant expression vector and transformation into *E. coli* DH5α

Restriction digested insert and vector were ligated using T4 DNA ligase (Company) as per manufacturer's instruction.

Concisely, ligation mixture of volume 10 µl containing 1 µl pET-32a(+) vector (50 ng/µl), 4 µl of insert, 1 µl ligation buffer (10x), 1 µl T4 DNA ligase (1U/µl) and 3 µl MilliQ water were incubated at 4 °C

overnight. Transformation of ligated products to *E. coli* DH5α competent cells were performed as discussed in section 2.2.9.3. Recombinant clones were selected and streaked on to LB/ampicillin (50 µg/µl) plates to confirm the presence of vector with insert. Followed by overnight incubation, most of the colonies were selected for colony PCR using the insert specific primer (Table 2.2) and vector specific T7 Forward and T7 Reverse primers (Table 2.1). Colonies were picked using micro tips and mixed well in PCR reaction mix (25 µl) containing 1x standard Taq buffer (10 Mm Tris-HCl, 50 mM KCl, pH 8.3), 200 µM dNTPs, 0.4 µM each primer (T7 forward and T7 reverse) and 1U Taq DNA polymerase. The thermal profile used was an initial denaturation at 95 °C for 5 min followed by 35 cycles of denaturation at 94 °C for 15 sec, annealing at 60 °C for 30 sec and extension at 72 °C for 1 min and a final extension at 72 °C for 10 min. The amplicons were examined by electrophoresis in 1.5 % agarose gel as explained in section 2.2.8. Recombinant clones were selected for plasmid isolation and for that a single colony was inoculated in 10 ml LB broth supplemented with ampicillin (50 µg/ml) and kept at 37 °C, with shaking at 250 rpm for 16 hours.

2.2.19 Plasmid extraction and sequencing

Plasmid isolation of pET-*Fi*-crustin2 was carried out from the overnight culture of recombinant clone as discussed in section 2.2.9.5. Recombinant plasmids were sequenced at SciGenom, Kochi, India using both T7 F and T7 R sequence and the sequences obtained were analyzed using GeneTool software to ensure whether the sequence is in correct frame with respect to that of expression unit.

2.2.20 Expression host transformation

2.2.20.1 *Selection and features of expression host*

E. coli Rosettagami™B (DE3) pLysS strain is a high stringency expression host, combine the key features of BL21 (and its Tuner™ derivative), Origami™, and Rosetta™ to enhance the expression of eukaryotic proteins and the formation of target protein disulfide bonds in the bacterial cytoplasm. Enhanced disulfide bond formation resulting from glutathione reductase (gor) and thioredoxin reductase (trxB) mutations with enhanced expression of eukaryotic proteins that contain codons rarely used in *E. coli.* These strains supply tRNAs for AGG, AGA, AUA, CUA, CCC, GGA on a compatible chloramphenicol resistant plasmid.

The rare tRNA genes are present on the same plasmids that carry the T7 lysozyme and lac repressor genes. Also this strain is deficient in the lon protease and the ompT outer membrane protease that can degrade proteins during purification. Since the target peptide contains disulphide bond and of eukaryotic origin, the *E. coli* host Rosettagami™B (DE3) pLysS would be ideal for recombinant expression while combined with the features of pET-32a(+) expression vector.

2.2.20.2 *Transformation to expression host*

Competent cells of *E. coli* Rosettagami™ B (DE3) pLysS were purchased from Novagen, UK and stored at -80 °C until use. Recombinant pET-32a(+) plasmids with *Fi*-crustin2 insert and control vector pET-32a(+) without insert were transformed to competent cells using heat shock method as described in section 2.2.9.3. The transformation mixture (300 µl) was plated on to LB agar plates,

containing the antibiotics ampicillin (50 µg/µl), kanamycin (15 µg/ µl) chloramphenicol (125 µg/µl) and tetracycline (340 µg/µl). The plates were then incubated overnight at 37 °C and observed for colonies. Positive clones were identified by colony PCR with vector specific as well as gene specific primers.

2.2.21 Induction and optimization of target protein expression

Single colony of positive transformants, and parent vector pET-32a(+) transformed host (negative control), were inoculated to 100 ml LB broth supplemented with antibiotics viz. ampicillin (50 µg/µl), kanamycin (15 µg/µl), chloramphenicol (12.5 µg/µl) and tetracycline (34 µg/ µl) and incubated at 37 °C with shaking at 250 rpm till OD_{600nm} of 0.5–0.7 was attained. The inducer IPTG was then added to the medium to a final concentration of 0.1 mM to induce expression. An un-induced culture was also sustained to know the basal level expression. Both the cultures were incubated further for 5-7 h at 37 °C with shaking at 250 rpm. At every 1 h interval post-induction, 2 ml of culture was collected and centrifuged, the cell pellet was stored at -20 °C for SDS-PAGE analysis.

2.2.22 Target protein detection by Sodium Dodecyl Sulphate Polyacrylamide Gel Electrophoresis (SDS- PAGE)

Recombinant protein expression of *Fi*-crustin2 (r*Fi*-crustin2) and control, thioredoxin (Trx) was analyzed by SDS- PAGE analysis. Bacterial pellet from 2 ml of un-induced control, negative control and hour-wise samples of induced cultures were boiled in 100 µl sample buffer [150 mM Tris-Cl (pH 7), 12 % SDS, 30 % glycerol, 6 % mercaptoethanol, 5 % coomassie brilliant blue R-250 (CBB)] for 10 min. The supernatant from

the boiled samples were subjected to SDS-PAGE on a 4 % stacking and 16 % resolving (running) gel using 4-gel Mini-PROTEAN® Tetra cell protein electrophoresis unit, BioRad, USA. Electrophoresis was accomplished using 1X Tris (pH 8.9) as the anode buffer and 1X Tris-tricine (pH 8.3) as the cathode buffer at a voltage of 60 V in stacking gel and 120 V in resolving gel respectively. After the completion of separation, plates were de-assembled and the stacking gel alone was taken out carefully, stained in staining solution (0.5 % CBB R-250, 40 % methanol and 10 % acetic acid in distilled water), de-stained using de-staining solution (10 % methanol and 10 % acetic acid in distilled water) and photographed using Gel-DOC^{TM} XR+ imaging system (BioRad, USA).

2.2.23 Western blotting

SDS-PAGE of recombinant peptide, r*Fi*-crustin2 was done as explained in the previous section. After electrophoresis, the gel was trans-blotted onto a 0.2 mm PVDF membrane at 100 V for 1 h (Mini-PROTEAN® Tetra cell protein electro blotting unit, BioRad, USA). The PVDF membrane was then incubated in blocking buffer (5 % non-fat dry milk with 1X tris-buffered saline and 0.1 % Tween 20) on a shaker for 1 h at room temperature followed by overnight incubation with gentle shaking at 4 °C in His-Tag (27E8) Mouse mAb (HRP conjugate) horseradish peroxidase-labelled anti-His tag antibody (Cell Signaling Technology® Inc.) at 1:1000 dilution in blocking buffer. Membranes were then rinsed in Tris-buffered-saline with Tween 20 on a shaker at room temperature for 30 min. The 1–Step™ Chloronaphthol reagent (Thermo Scientific, USA) was added to the membrane and incubated for 30 min at

RT with gentle shaking. The blue coloured substrate developed was photographed using Gel-DOC^{TM} XR+ imaging system (BioRad, USA).

2.2.24 Scale-up production of recombinant *Fi*-crustin2

In order to study the bioactive potential of r*Fi*-crustin2, the production was done in 2l culture medium as explained earlier (see section 2.2.21). Cell pellet with r*Fi*-crustin2 was harvested and stored at -20 °C for SDS-PAGE analysis and purification.

2.2.25 Extraction and affinity purification of recombinant *Fi*-crustin2

Purification of the 6x-histidine tagged recombinant *Fi*-crustin2 and Trx from bacterial pellet was carried out employing Ni-NTA spin column (Qiagen®) according to the manufacturer's protocol.

Concisely, the cell pellet from 5 ml culture was allowed to thaw for 15 min at room temperature and re-suspended in 700 µl of buffer B (7 M Urea, 100 mM Na_2HPO_4, pH 8.0), which aids in the cell lysis and extraction. Crude cell lysate in buffer B was kept at room temperature for 15 min with continuous agitation. When the lysate became translucent, it was centrifuged at 12000 x g for 30 min at room temperature; supernatant was collected for further purification. Briefly, the Ni-NTA spin columns were equilibrated with 600 µl of buffer B and centrifuged at 2900 rpm for 2 min with lid open to ensure complete removal of the buffer. Pre-equilibrated columns were loaded with 600 µl of cleared lysate containing fusion protein with 6x-Histidine tags loaded and centrifuged at 1600 rpm at room temperature for 5-10 min. The column was washed two times with 600 µl buffer C (8 M Urea, 100 mM NaH_2PO_4, pH 6.3) and centrifuged at 2900 rpm

for 2 min at room temperature to remove unbound proteins and untagged proteins.

The flow through was collected and saved after each step for SDS-PAGE analysis to test the efficiency of binding. Finally, the recombinant protein with 6x-Histidine tags was eluted twice with 200 µl of buffer E (8 M urea, 100 mM NaH_2PO_4, and pH 4.5) by centrifugation at 2900 rpm for 2 min at room temperature. The purification steps were repeated to obtain sufficient amounts of protein to perform experiments. The eluted purified protein was stored at -20 °C for further use.

2.2.26 Re-folding of the recombinant protein

Amicon ultra centrifugal filters with 3 kDa cut-off membranes (Millipore) were used to concentrate the Ni-NTA column eluted recombinant protein. An initial centrifugation of 5000 x g for 30 min was performed to get the sample concentrated. Then the concentrated samples were reconstituted to the original volume using the refolding buffer (50 mM Tris-Cl (pH 8)) to remove the urea from the eluted protein and centrifuged at 5000 x g for 30 min. Repeated washing of peptides for 10-15 times with the refolding buffer aids the removal of urea. After complete removal of urea from the sample, the concentrated sample was diluted to a desired volume in refolding buffer.

2.2.27 Protein quantification of recombinant *Fi*-crustin2

Quant-iT^{TM} protein assay kit using Qubit fluorometer (Invitrogen, UK) was used to quantify the concentration of purified r*Fi*-crustin2. Briefly, the Quant-iT working solution was prepared by diluting the

Quant-iT protein reagent in Quant-iT protein buffer (1:200) and mixed well by vortexing without any air bubbles. From the working solution, 190 µl was aliquoted into a fresh clean 0.5 ml tube to which 10 µl of the protein to be quantified was added, mixed by vortexing and incubated at room temperature for 15 min and using the Quant-iT protein programme the protein was quantified. The sample concentration was calculated using the following equation:

Concentration of sample = QF value x (200/X)

Where,

QF value = the value given by the Qubit fluorometer,

X = volume of sample (in microliters) added to the assay tube

2.2.28 Haemolytic activity

Haemolytic activity of the peptides was determined using human red blood cells (hRBCs) with a modified protocol of Onuma et al. (1999). The hRBCs were centrifuged for 15 min at 3000 x g to remove the serum part and washed with equal volume of phosphate buffer saline (35 mM phosphate buffer, 150 mM NaCl (pH 7.2)) until the colour of the supernatant turned clear. One hundred microliters of the hRBC 4 % (v/v) suspended in PBS added to 0.5 ml MCTs and then 100 µl peptide solution (serial two fold dilution in PBS) was added to each tubes. The tubes were incubated for 1 h at 37 °C without agitation and centrifuged at 5000 x g for 5 min. The supernatant was transferred to 96 well plates, to monitor the haemoglobin release using ELISA plate reader (Tecan, USA) by measuring the absorbance at 405 nm. The assay was performed in triplicate. Haemolysis reference (positive control) was 100 µl of the cell suspension with 100 µl of 1 %

(v/v) Triton X-100 and 100 µl of the PBS was used as the negative control.

Percentage haemolysis was calculated by the following formula:

$$\text{Percentage haemolysis} = 100\ [(A_s - A_0) / (A_t - A_0)]$$

where A_s represents absorbance of peptide sample at 405 nm and A_0 and A_t represent zero % and hundred % haemolysis determined in PBS and 1% Triton X-100, respectively.

2.2.29 *In vitro* cytotoxicity assay

Human cancer cells NCI-H460 was used to assess the inhibitory effect of peptide on cellular metabolism. About, 1×10^6 human lung cancer cells NCI-H460 were inoculated into each well of a 96 well tissue culture plate containing minimal essential medium (MEM) and incubated for 12 h at 37 °C. After incubation, the cells were washed twice with phosphate buffered saline (PBS), and the medium was exchanged with fresh MEM containing desired concentrations of the peptide (two fold serial dilutions). Cytotoxic AMP, mellitin was used as the positive control and media without peptide was employed as the negative control. All the experiments were done in triplicates.

The cells were incubated with peptide for 24 h at 37 °C, and observed for morphological changes under Inverted phase contrast microscope (Leica, Germany). The medium was changed and 50 µl of 2, 3-bis [2-methyloxy-4-nitro-5-sulfophenyl]-2H-tetrazolium-5-carboxanilide (XTT) solution (1 mg/ ml in RPMI 1640 medium with 25 µL PMS solution (3 mg PMS into 1 mL PBS)) was added and incubated for 2 h at 37 °C in

a CO_2 incubator (Scudiero et al., 1988). After incubation the absorbance was measured at 450 nm with a reference at 690 nm in a microplate reader (TECAN Infinite Tm, Austria) and calculated the difference. Succinate-tetrazolium reductase system which belongs to the mitochondrial respiratory chain reduces XTT to water soluble formazan yielding a purple-colored solution, which is directly proportional to the viability of cells. The results are expressed as a percentage of the inhibition rate for viable cells. The IC_{50} value was calculated as the concentration of peptide that induced 50 % growth inhibition related to the untreated control

2.2.30 Antimicrobial activity

2.2.30.1 *Microorganisms used*

Antimicrobial activity of the peptide was tested against two Gram positive strains viz. *B. cereus* (MCCB 101) and *S. aureus* (MTCC 3061) and Gram negative bacterial strains including *E. tarda* (MTCC 2400), *P. aeruginosa* (MCCB 119), *A. hydrophila* (MCCB 113), *E. coli* (MTCC 483), *V. cholera* (MCCB 129), *V. vulnificus* (WV13), *V. proteolyticus* (M10W1), *V. alginolyticus* (VKF44) and *V. parahaemolyticus* (MCCB 133).

2.2.30.2 *Broth microdilution assay*

The antimicrobial activity of the peptide was determined using the broth microdilution assay as described by Park et al. (2004) with slight modifications. Concisely, mid-logarithmic-phase bacteria were diluted to 10^4 cfu/ml in 50 mM 4-(2-hydroxyethyl)-1-piperazine ethane sulfonic acid (HEPES) buffer pH 7.4. Each well of 96 well propylene microtitre plates (Costar, Cambridge, MA, USA) was filled with 10 µl of the diluted

cell suspension and 10 µl of serially two fold diluted peptide samples and incubated at room temperature for 2 h to minimize interference with the peptide's biological activity.

Then fresh medium (Muller Hinton broth) was added to the mixture and incubated for an additional 16 h at 37 °C with shaking at 100 rpm. HEPES buffer was served as the blank group and fusion protein thioredoxin was maintained as the negative control. The inhibition of growth was determined by measuring absorbance at 600 nm.

Inhibition percentage was calculated as

Inhibition % = 100 – Growth percentage.

Where, Growth % = (OD of Test / OD of Control) × 100.

The inhibition percentage was calculated as the average of three independent experiments performed in triplicate.

2.2.30.3 ***Bactericidal activity assay***

The bactericidal effect of the peptide was determined according to Andra et al. (2007) with minor modifications. After 16 h incubation of peptide and pathogen as explained in the previous section, aliquot of 50 µl was taken, adequately diluted and plated on to MH agar plates. Plates were incubated overnight at 37 °C and the colonies were counted. The MBC (minimal bactericidal concentration) of peptide for a given bacterial strain was regarded as the minimal concentration of the peptide that kills 99.9 % of the cfu present in the final inoculum.

2.2.30.4 *Propidium iodide staining and epi-fluorescence microscopy*

Pathogens which were found sensitive against the peptide were selected for observation using an epi-fluorescence microscope followed by propidium iodide (PI) staining to detect the dead cells. As described in the previous sections, microbial inoculum was prepared and treated with peptide concentration at the minimum inhibitory concentration (MIC) value obtained for each pathogen. After incubation at 37 °C for 2 h, cells were pelleted by centrifugation at 5000 rpm for 5 min, re-suspended and washed in PBS. For dead cell staining, propidium iodide of concentration 50 µg/mL (in PBS) was employed. Bacterial pellet was re-suspended in 200 µl of PI solution, mixed well by vortexing and incubated at room temperature in dark for 5 min; washed the cells two times in PBS, smear was prepared in a glass slide and covered with coverslip for observation. Images were acquired within 30 min and examined by fluorescence microscopy (Leica DMRA, Heidelberg, Germany) and photographed with a Leica DMDL digital camera. Fluorescence of PI was perceived using a filter with excitation wavelength of 540 - 580 nm and an emission filter of 600 - 660 nm.

2.2.30.5 *Morphological observation by scanning electron microscopy*

Scanning electron microscopy (SEM) was conducted to evaluate the antimicrobial mechanism of the recombinant peptide. The microbial suspension was treated with higher concentration of the peptide (2 times of MIC) to ensure the killing of higher number of microbes. Controls were run without peptides. After incubation of pathogens with peptide at 37 °C for 1 h, the cells were pelleted by centrifugation at 5000 rpm for

5 min, re-suspended and washed twice with 0.1 M sodium phosphate buffer. Followed by this the cells were fixed in 2.5 % glutaraldehyde at room temperature for 2 h, post-fixed in 1 % osmium tetroxide at 4 °C for 2 h and dehydrated using graded ethanol solutions. After dehydration, the cells were air dried after immersion in hexamethyldisilazane (Sigma) for 20 min, sputter coated with gold in an ion coater, and examined by scanning electron microscopy with a VEGA3 TESCAN scanning electron microscope.

2.2.31 DNA binding assay

The DNA binding activity of the peptides were examined by a gel retardation assay with slight modification as described by Park et al. 1998. Briefly, 50 ng of pUC-18 plasmid DNA was incubated at room temperature with increasing concentrations of peptides in a peptide to DNA ratio of 0:1, 2.5:1, 5:1, 10:1, 20:1 and 50:1 in 20 µl of binding buffer (5 % glycerol, 10 mM Tris–HCl (pH 8.0), 1 mM EDTA, 1 mM DTT, 20 mM KCl and 50 µg/ml BSA) for 1h. DNA bands were analyzed by electrophoresis in 1.5 % agarose gel in TBE buffer, stained with ethidium bromide and visualized under UV light.

2.3 Results

2.3.1 Molecular characterization of crustin from *F. indicus.*

Gene based screening of AMPs from *F. indicus* led to the identification of the second isoform of a Type I crustin isoform, herein after named as *Fi*-crustin2**.** This section deals with the molecular and phylogenetic characterization of *Fi*-crustin2 by various bioinformatics tools.

2.3.1.1 *PCR amplification, TA cloning and sequencing of Fi*-crustin2

A 354 bp fragment cDNA encoding 117 amino acids was obtained from the mRNA of *F. indicus* haemocyte by RT-PCR (Fig. 2.4). Amplicons were then cloned into pGEM®-T Easy cloning vector and insert was confirmed using gene specific and vector-specific primers by colony PCR. The plasmid pGEMT-*Fi*-crustin2 was extracted from positive colonies; purity analysis was done by AGE (Fig. 2.5) and sequenced. The *Fi*-crustin2 nucleotide and deduced amino acid sequences are shown in Fig. 2.6 and the sequence data has been submitted to the GenBank under the accession number, **KX622789.**

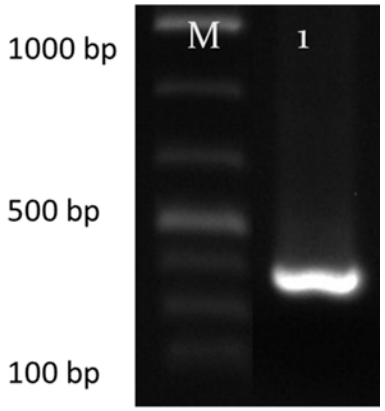

Fig. 2.4 Agarose gel electrophoretogram of PCR amplification of *Fi*-crustin2. Lane M: 100 bp marker, Lane 1: *Fi*-crustin2 amplicons of 354 bp.

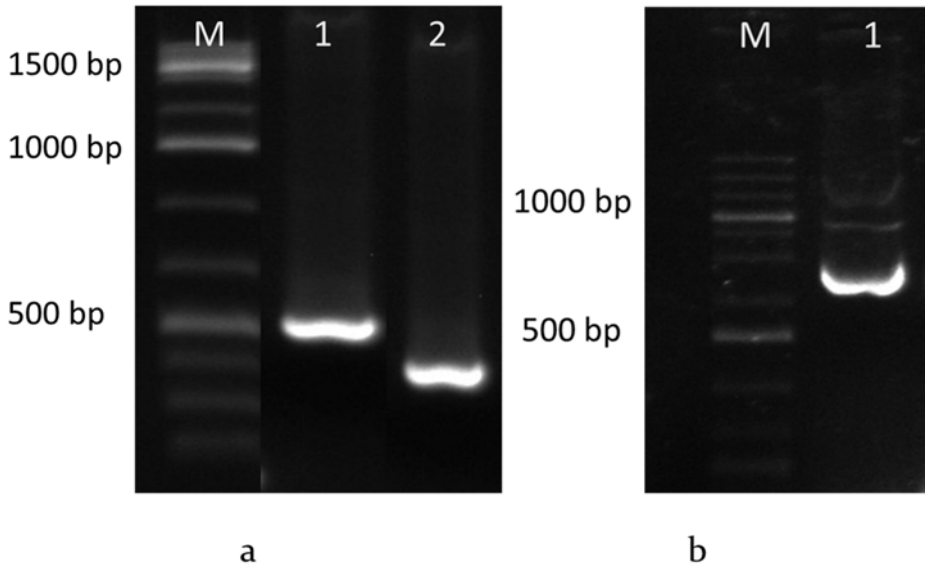

Fig. 2.5 Agarose gel electrophoretogram (a) of *Fi*-crustin2 colony PCR, Lane M: 100 bp ladder; Lane 1: amplicon (495 bp) obtained for PCR with vector specific primers and Lane 2: amplicon (354 bp) of PCR performed using gene specific primers (b) Plasmid extracted from positive clones of pGEMT-*Fi*-crustin2 vector constructs. Lane M : 1 kb marker, Lane 1: plasmid with *Fi*-crustin2 insert.

```
atgctgaagtttgtagtattatccgttgtcgccgtggctgtggtacagagtcaagaagat
 M  L  K  F  V  V  L  S  V  V  A  V  A  V  V  Q  S  Q  E  D
actcgcttcctaggtgtttctgggggtgttgctgggggtggattcgttccgggggttcca
 T  R  F  L  G  V  S  G  G  V  A  G  G  G  F  V  P  G  V  P
gggcatggcggcattgcccctggattcgaatgcaattactgcagaacgaggtatgggtac
 G  H  G  G  I  A  P  G  F  E  C  N  Y  C  R  T  R  Y  G  Y
gtatgctgcaagcccggcaggtgtccaccggttcgcgatacctgcccaggcatcaggaac
 V  C  C  K  P  G  R  C  P  P  V  R  D  T  C  P  G  I  R  N
agacccccgatctgccgtcaggacactgagtgcttcggctccgacaagtgctgctacgac
 R  P  P  I  C  R  Q  D  T  E  C  F  G  S  D  K  C  C  Y  D
acctgcttgaacgacaccgtctgcaaacccatcgtgctgggttctgagggatag
 T  C  L  N  D  T  V  C  K  P  I  V  L  G  S  E  G  -
```

Fig. 2.6 Nucleic acid and deduced amino acid sequence of *Fi*-crustin2 (GenBank ID: **KX622789)**. The turquoise coloured highlighted region is the signal peptide sequence and grey coloured region is the mature peptide region within which yellow coloured highlighted region is the putative WAP domain.

2.3.1.2 *Sequence analysis and characterization using bioinformatics tools*

Similarity searches using homology analysis tool BLAST algorithm showed that the 117 mer *Fi*-crustin2 exhibited similarity to previously described crustin isoforms by 98 % to *F. indicus* (ACT82963.1); 92 % to *P. monodon* (GQ334395.1); 84 % to *M. rosenbergii* (JQ413342.1); 71 % to *C. maenas.* The SignalP software revealed that the first 17 residues of *Fi*-crustin2 are predicted to be highly hydrophobic and encompass a signal / leader sequence with a clear cleavage site identified between residues 17 and 18 (Fig. 2.7). The ORF encoded 117 amino acid residues with a predicted molecular weight (MW) of 12.32 kDa, net charge of +2 and theoretical isoelectric point (*p*I) of 7.97. For the mature peptide region, the aforesaid parameters were found to be 10.61 kDa, +1 and 7.59 respectively, as predicted by the ProtParam software.

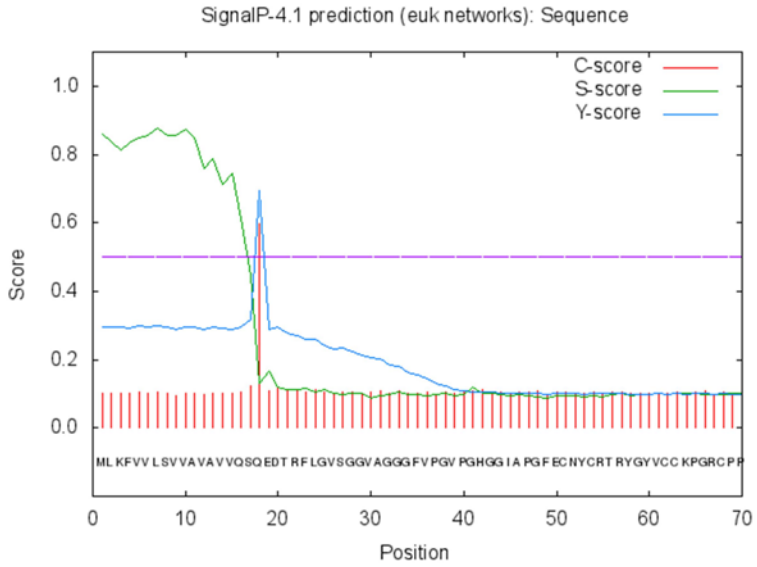

Fig. 2.7 Signal peptide analysis of *F. indicus, Fi*-crustin2 (GenBank ID: **KX622789)** as predicted by the SignalP 4.1 server.

The +1 charge of putative mature peptide region was found to be because of the contribution of 10 negatively charged amino acid residues (6 Asp + 4 Glu) and 11 positively charged residues (8 Arg + 3 Lys). The deduced amino acid sequence of *Fi*-crustin2 was found to be rich in amino acid residues glycine (14.5 %) and valine (12.8 %). The ScanProsite tool predicted a whey-acidic protein (WAP) domain in the C-terminus region of *Fi*-crustin2. At the N-terminal of the mature peptide, *Fi*-crustin2 contained a number of glycine-rich repeats between positions 25 and 49. Following the repeat region is a cysteine-rich region just like that of other crustin isoforms from *F. indicus*, *F. chinensis* and *F. japonicus*; though lack the Pro-rich domain related with those of *M. japonicus*. Whereas the C-terminal part was found to be rich in Cys-rich region (10.3 %), with 12 Cys residues engaged in the formation of disulphide bonds and forms the WAP domain. Disulfide bonds were predicted to be between Cys_{61}-$Cys_{112;}$ Cys_{68}-Cys_{98}; Cys_{75}-Cys_{102}; Cys_{85}-Cys_{97} and Cys_{91}-Cys_{108} by the ScanProsite tool.

Antimicrobial activity prediction by APD analysis of mature peptide region predicts it as a potent AMP with cationicity of +1, hydrophobic ratio of 33 % and Boman index of 1.63 kcal/mol, with an estimated half-life of 0.8 h (mammalian reticulocytes, *in vitro*), 10 min (yeast, *in vivo*) and 10 h (*E. coli*, *in vivo*). Amphipathicity of peptide was analysed by ProtScale tool and the Kyte-Doolittle plot obtained is given in Fig. 2.8.

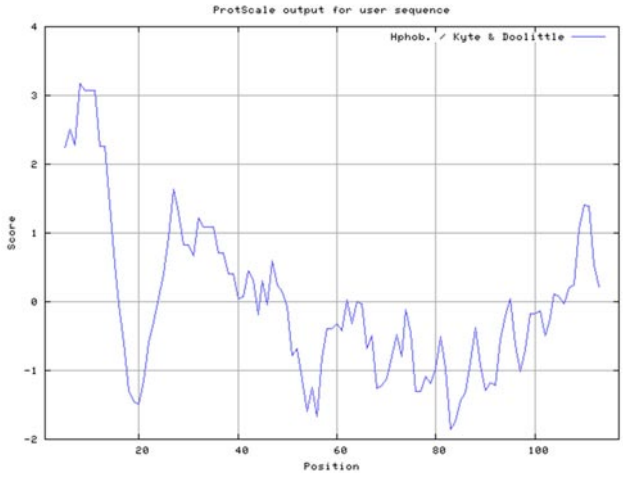

Fig. 2.8 Kyte-Doolittle plot showing hydrophobicity of *Fi*-crustin2 (GenBank ID: **KX622789).** The peaks above the score (0.0) indicate the hydrophobic nature of the predicted protein.

Secondary structure prediction using PSIPRED tool exposed the existence of one α-helix and two β-sheeted regions in *Fi*-crustin2 (Fig. 2.9).

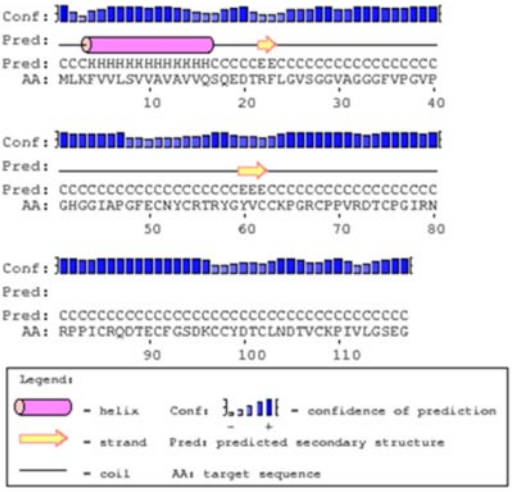

Fig. 2.9 Secondary structure of *Fi*-crustin2 (GenBank ID: **KX622789**) predicted using PSIPRED server. The α-helix region is shown in pink coloured cylinders, β-strand is shown in yellow arrows and the coil region is shown in black lines.

Spatial structure prediction was not possible since no similar sequences were found in SWISS-MODEL tool. Predicted RNA secondary structure was found to be stable with both paired and non-paired regions (Fig. 2.10).

Fig. 2.10 Predicted secondary structure of *Fi*-crustin2 (GenBank ID: **KX622789**) RNA with minimal free energy prediction.

2.3.1.3 *Sequence alignment and phylogenetic analysis*

The multiple protein sequence alignment of *Fi*-crustin2 with representatives of other crustin isoforms using ClustalW in BioEdit revealed the existence of preserved sequence features (Fig. 2.11). The phylogenetic tree topologies revealed the relationships of *Fi*-crustin2 with other invertebrate crustins and found to be assembled according to species (Fig. 2.12).

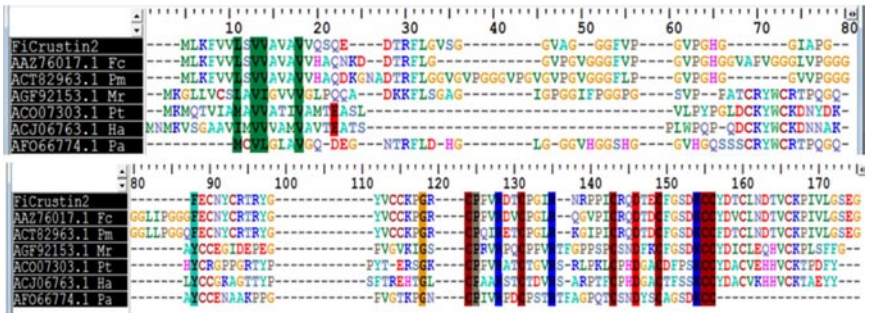

Fig. 2.11 Multiple alignment of amino acid sequence of the *Fi*-crustin2 (GenBank ID: **KX622789**) with other crustacean crustins obtained using BioEdit**),** *Fenneropenaeus chinensis* crustin (GenBank ID **AAZ76017.1**), *P. monodon* crustin (GenBank ID **ACT82963.1**), *Macrobrachium rosengergii* crustin (GenBank ID **AGF92153.1**), *Portunus trituberculatus* crustin (GenBank ID **ACO07303.1**), *Hyas araneus* crustin (GenBank ID **ACJ06763.1**) and *Panulirus argus* crustin (GenBank ID **AFO66774.1**). The conserved residues are highlighted with uniform background colours.

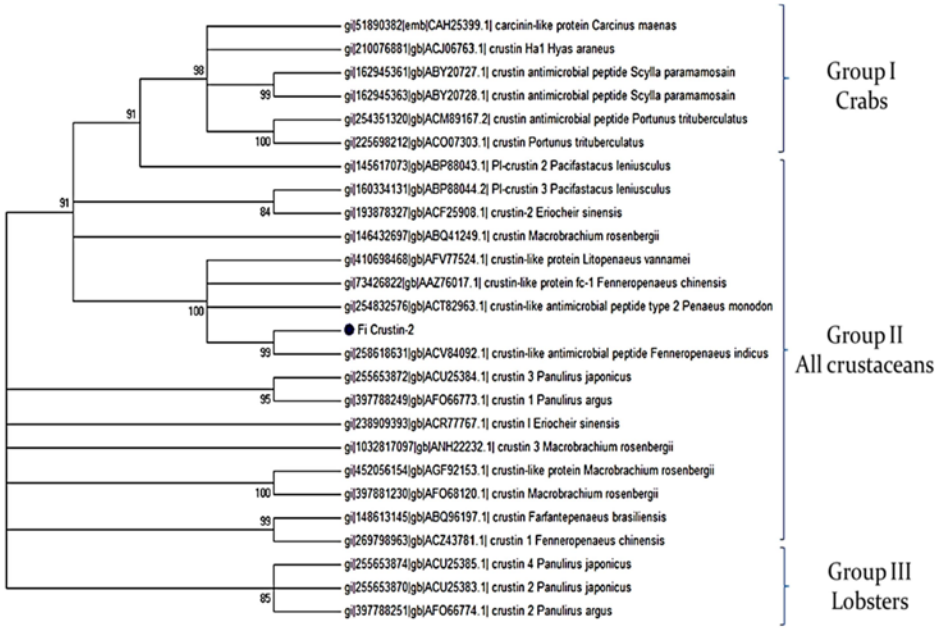

Fig. 2.12 A bootstrapped neighbor-joining tree obtained using MEGA 7 illustrating relationships between the deduced amino acid sequences of the *Fi*-crustin2 (GenBank ID: **KX622789**) with other crustins of decapod crustaceans. Values at the node indicate the percentage of times the particular node occurred in 1000 trees generated by bootstrapping the original deduced protein sequences. Branches corresponding to partitions reproduced in less than 75 % bootstrap replicates are collapsed.

2.3.2 Recombinant production and functional characterization of *Fi*-crustin2

2.3.2.1 *PCR amplification and TA cloning of the target gene with restriction sites*

Selective PCR amplification of mature peptide of *Fi*-crustin2 was achieved by primers with NcoI site in the 5' end of forward primer (pET *Fi*-crustin2 F) and HindIII site in the 3' end of reverse primer(pET *Fi*-crustin2 R) (Table 2.2). Amplicon of size 334 bp was obtained with pGEMT-*Fi*-crustin2 as template (Fig. 2.13). Purified amplicons were cloned using pGEM®-T Easy cloning vector and transformed to competent cells of the cloning host *E. coli* DH5α. Colony PCR was performed with

gene specific and vector specific primers to confirm the insertion of target gene. Amplicons of size 334 bp (comprising restriction sites) was obtained using gene specific (pET *Fi*-crustin2 F and R) and 475 bp (334 bp + 141 bp) with vector specific PCR (T7 F and SP6 R) respectively (Fig. 2.13). Recombinant clones were selected for plasmid extraction and sequencing of the plasmid was completed to check the existence of restriction site.

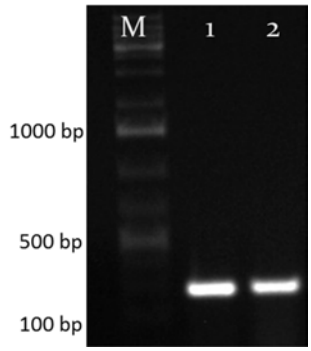

Fig. 2.13 Agarose gel electrophoretogram of the PCR amplified mature peptide region of *Fi*-crustin2 with restriction primers, Lane M: 100 bp ladder; Lane 1-2: PCR amplified product (334 bp).

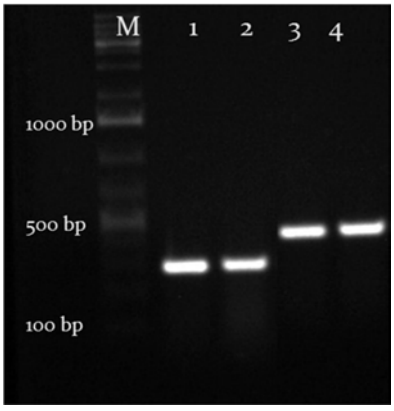

Fig. 2.14 Agarose gel electrophoretogram of *Fi*-crustin2 colony PCR, Lane M: 1 kb ladder; Lane 1-2: amplicon (334 bp) of PCR using insert specific primers; Lane 3-4: amplicon (475 bp) obtained for PCR with vector specific primers.

2.3.2.2 *Restriction enzyme digestion and cloning into pET 32a+ expression vector*

Plasmids confirmed with *Fi*-crustin2 mature peptide flanking the RE sites and the expression vector pET-32a(+) were selected for RE digestion using NcoI and HindIII. Insert release and vector digestion were confirmed by AGE and the released insert of size 334 bp (Fig. 2.15a) and the linearized vector (Fig. 2.15b) is shown. Followed by RE digestion, the insert and vector were gel eluted using GenJET™ Gel Extraction Kit (Thermo Scientific, USA).

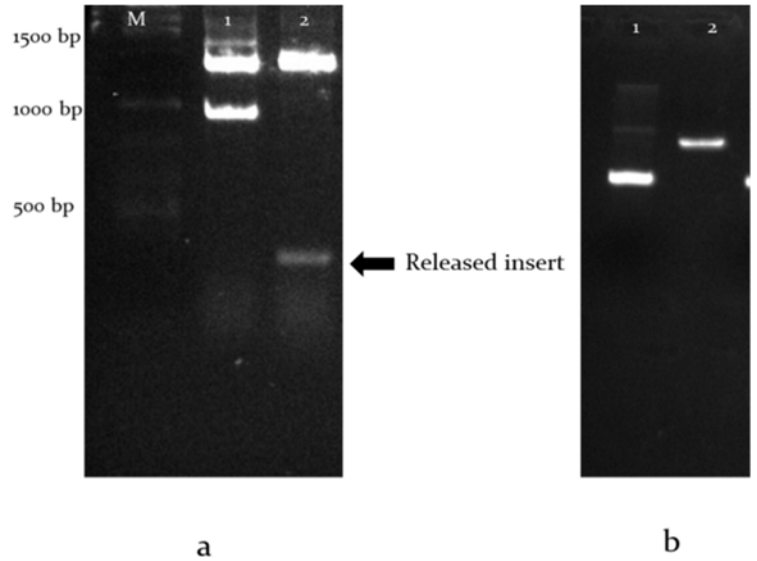

Fig. 2.15 Agarose gel electrophoretogram of the plasmids digested with NcoI and HindIII restriction enzymes **(a)** Lane M: 1kb ladder, Lane 1: Un-digested pGEMT-*Fi*-crustin2 plasmid. Lane 2: Restriction enzyme digested pGEMT-*Fi*-crustin2 with released insert **(b)** Lane 1: Un-digested pET-32(a+) vector, Lane 2: restriction enzyme digested linearized pET-32(a+) vector.

After RE digestion and gel extraction, the vector and insert were subjected to ligation and transformed to *E. coli* DH5α. Screening for the

recombinant clones were done by colony PCR and amplicons of size 1084 bp (334 bp + 750 bp) and 334 bp were obtained (Fig. 2.16) for vector specific primers (T7 F and T7 R) and gene specific primers respectively. Plasmids were extracted from positive clones and sequenced using T7 F and R primers to authorize orientation and the expression cassette without any frame shift. The recombinant vector pET-32a(+)-*Fi*-crustin2 was transformed to expression host *E. coli* Rosettagami^{TM} B (DE3) pLysS and colonies were obtained in LB agar plates with ampicillin and kanamycin.

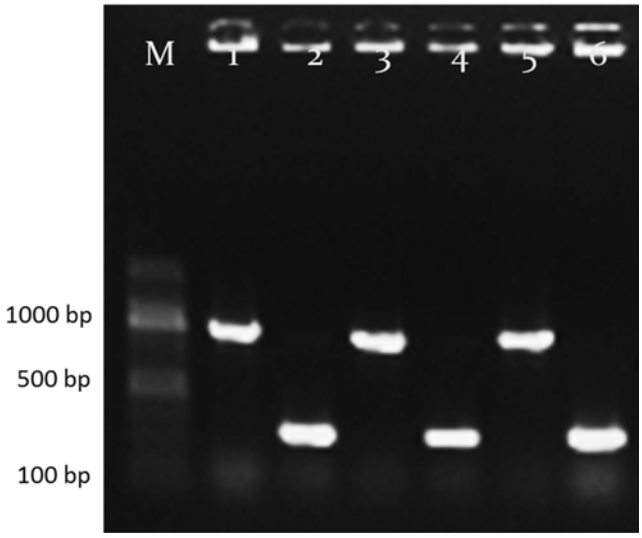

Fig. 2.16 Agarose gel electrophoretogram of *Fi*-crustin2 colony PCR, Lane M: 1 kb ladder; Lane 1, 3, and 5: amplicons (1084 bp) of PCR performed using vector specific primers; Lane 2, 4 and 6: amplicons of PCR performed using insert specific primers (334 bp).

2.3.2.3 *Recombinant expression of Fi*-crustin2 *as fusion protein*

The crustin isoform *Fi*-crustin2 from *F. indicus* was successfully produced as a fusion protein containing 6 x His tag and thioredoxin tag. Single colony of recombinant expression host with pET-32a(+)-*Fi*-crustin2

was cultured in LB broth with preferred antibiotics and kept for overnight incubation. For heterologous production of *Fi*-crustin2 and thioredoxin (Trx) with 6 × His-tag (negative control), 1 ml overnight culture was used as inoculum to 100 ml LB broth supplemented with antibiotics and incubated further at 37 °C with shaking at 250 rpm. The protein production was persuaded using the inducer, 1 mM IPTG when OD_{600nm} reached 0.8. An un-induced sample was also maintained throughout the process. After induction, cultures were incubated further up to 8 h at 37 °C with shaking at 250 rpm. In order to analyse the level of protein expression, at an interval of one hour, 2 ml of culture was collected and centrifuged; the cell pellet obtained was kept in -20 °C for SDS-PAGE analysis.

In SDS-PAGE analysis, a prominent band of recombinant *Fi*-crustin2 (r*Fi*-crustin2) at 29.81 kDa (which is the combined molecular weight of *Fi*-crustin2 (10.61 kDa) and the fusion tags (19.2 kDa) including 6XHis tag and of Trx tag) could be observed from the first hour post induction (Fig. 2.17). The expression level of r*Fi*-crustin2 was found to be higher and stable from third hour. Thus by giving the same conditions of pilot scale production, the r*Fi*-crustin2 was produced in 2 Litre of culture medium. Meanwhile, the transformants with pET-32a(+) vector was induced with 0.1 mM IPTG and a distinct 20.4 kDa expressed product representing Trx was detected after induction from 1st h itself with under the same growth conditions and thus induced cells were harvested from 2 l, LB medium at 1st h only and kept in -20°C.

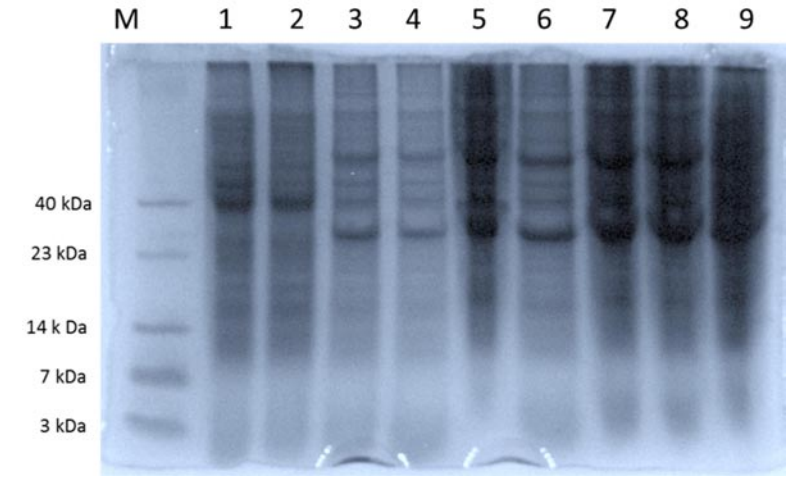

Fig. 2.17 Tricine SDS-PAGE analysis of the cells containing recombinantly expressed *F. indicus* r*Fi*-crustin2, before and after IPTG induction on a time-course basis. Lane M: Mid-range protein ladder; Lane 1: uninduced control (before IPTG induction); Lane 2-9: IPTG induced cells after 1-8 hours of induction.

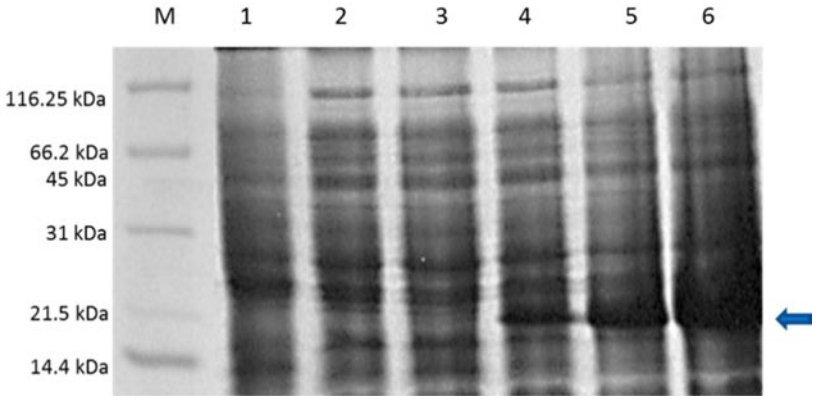

Fig. 2.18 Tricine SDS-PAGE analysis of the cells containing recombinantly expressed Thioredoxin, rTrx, before and after IPTG induction on a time-course basis. Lane M: Mid-range protein ladder; Lane 1: un-induced control (before IPTG induction); Lane 2-6: IPTG induced cells after 0-4 hours of induction.

2.3.2.4 *Purification, refolding and quantification of the recombinant protein*

The r*Fi*-crustin2 and rTrx samples were purified using Ni-NTA spin columns and the eluted fraction was evaluated by SDS-PAGE (Fig. 2.19a) and also by western blotting (Fig. 2.19b). Amicon cut off filtration unit was used for concentrating and refolding the purified r*Fi*-crustin2 from the eluted fraction. Protein concentration of r*Fi*-crustin2 and rTrx were quantified using Quant-iT^{TM} protein assay kit and the concentration was found to be 1.5 mg/ml and 1.42 mg/ml.

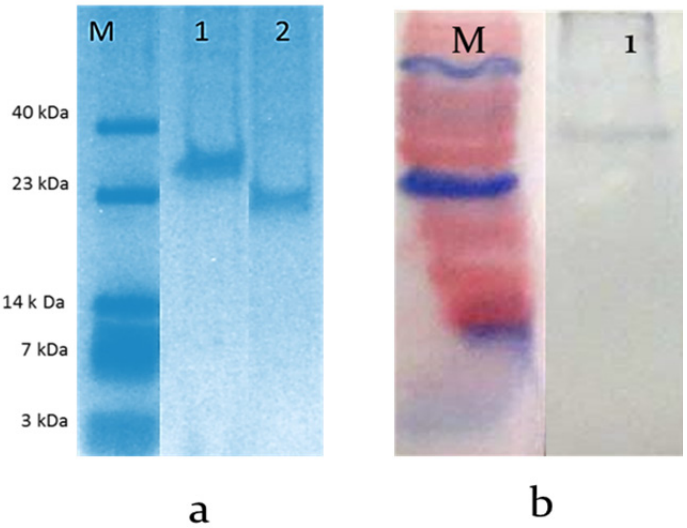

Fig. 2.19a Tricine SDS-PAGE analysis of Ni-NTA purified r*Fi*-crustin2 (29.81 kDa) Lane M: Low range weight protein marker; Lane 1: purified recombinant r*Fi*-crustin2 (29.81 kDa); Lane 2: purified recombinant Trx (20.4 kDa); **2.19b** Western blot showing the purified r*Fi*-crustin2, Lane M: Mid-range coloured marker; Lane 1: purified r*Fi*-crustin2.

2.3.2.5 *In vitro cytotoxicity and haemolytic activity*

Cytotoxicity of the peptide, r*Fi*-crustin2 and the control (rTrx) was tested ranging from 20 µM to 0.625 µM in NCI-H460 cell lines by using XTT assay. Melliitin, a positive control, was also tested from 20 µM to 0.625 µM and exhibited an IC_{50} of 16.6 µM. At higher concentration of r*Fi*-crustin2 and rTrx, the peptide exhibited only a reduction of 9 % and 4 % growth in NCI H460 cells and thus found to be non-cytotoxic to the cancer cells (Fig. 2.20).

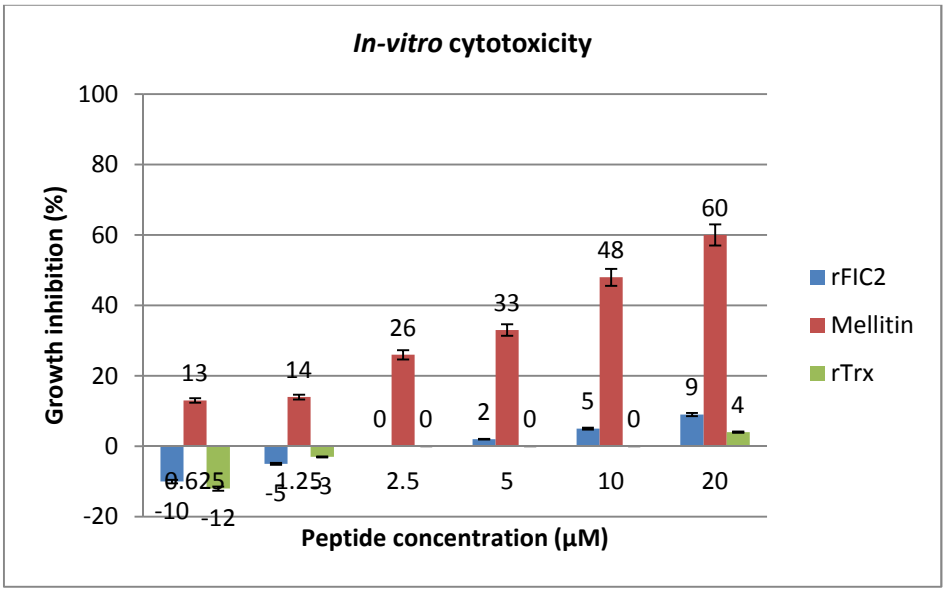

Fig. 2.20 *In vitro* cytotoxicity of the recombinant *Fi*-crustin2, r*Fi*-crustin2, rTrx and Mellitin in NCI-H460 cells at various concentrations

In order to test the cytotoxicity against normal mammalian cells, human RBCs were used to analyse the haemolytic activity of the peptide. The recombinant peptide was found to be non-haemolytic at the tested concentrations (Fig. 2.21).

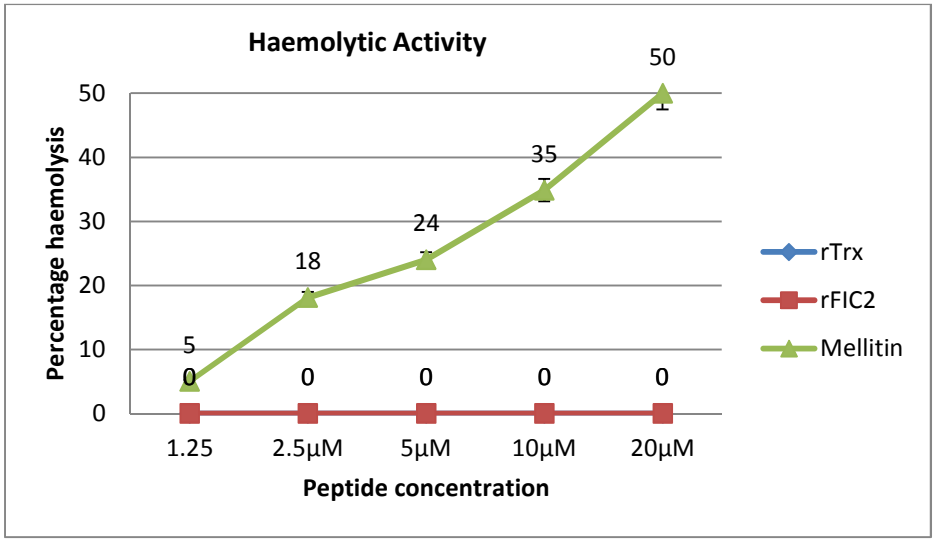

Fig. 2.21 Haemolytic activity of the recombinant *Fi*-crustin2, r*Fi*-crustin2, rTrx and control peptide Mellitin in human RBCs at various concentrations

2.3.2.6 *Antimicrobial activity*

Broth microdilution assay was performed to analyse the antimicrobial activity of recombinant *Fi*-crustin2, at a concentration ranging from 20 µM to 0.625 µM. The protein expression control, rTrx was used as the negative control in the assays. Like the untreated control, rTrx was also found to favour the bacterial growth. The test peptide r*Fi*-crustin2 demonstrated substantial antimicrobial activity against Gram-negative *E. tarda* (99 %; MIC of 5 µM and MBC of 10 µM) and *A. hydrophila* (98 %; MIC and MBC of 10 µM). Though, all the other tested pathogens were found to be sensitive to r*Fi*-crustin2, the MIC and MBC values were observed to be >20 µM.

The growth inhibition percentage of r*Fi*-crustin2 at 20 µM, were *B. cereus* - 70 %, *S. aureus* - 82 %, *V. proteolyticus* - 89 %, *V. alginolyticus* - 83 %, *V. parahaemolyticus* - 92 %, *V. vulnificus* - 75 %, *V. cholera* - 93%, *P. aeruginosa* - 91 % and *E. coli* - 86 % (Fig. 2.22).

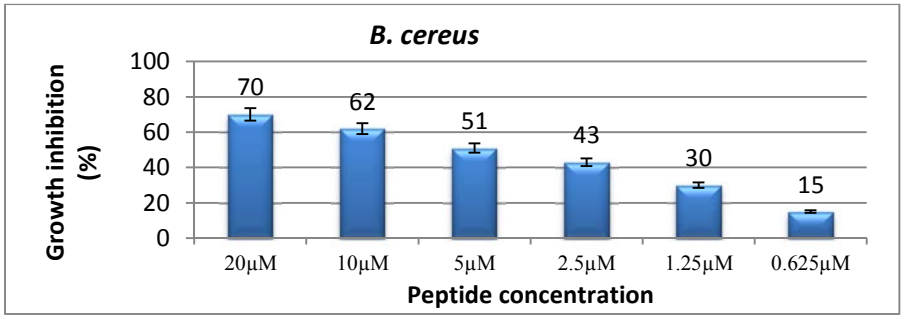
B. cereus
Growth inhibition (%)
100
80
60
40
20
0
70
62
51
43
30
15
20µM
10µM
5µM
2.5µM
1.25µM
0.625µM
Peptide concentration

(a)

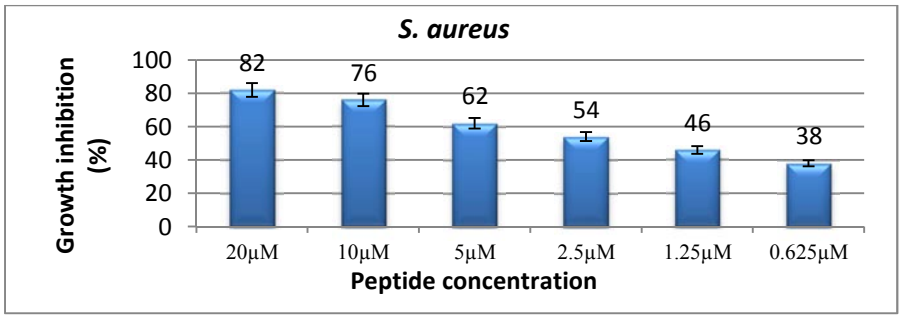
S. aureus
Growth inhibition (%)
100
80
60
40
20
0
82
76
62
54
46
38
20µM
10µM
5µM
2.5µM
1.25µM
0.625µM
Peptide concentration

(b)

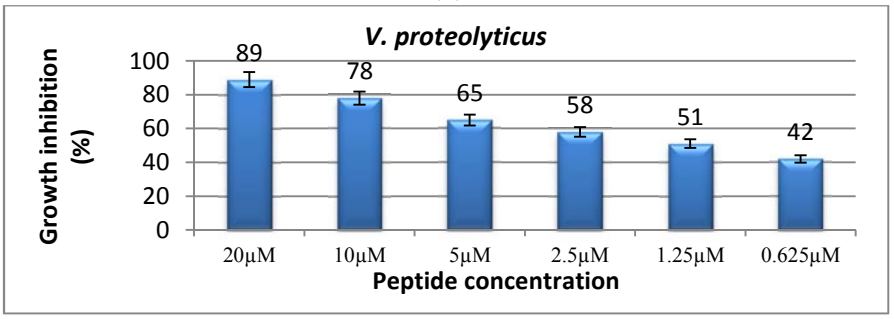
V. proteolyticus
Growth inhibition (%)
100
80
60
40
20
0
89
78
65
58
51
42
20µM
10µM
5µM
2.5µM
1.25µM
0.625µM
Peptide concentration

(c)

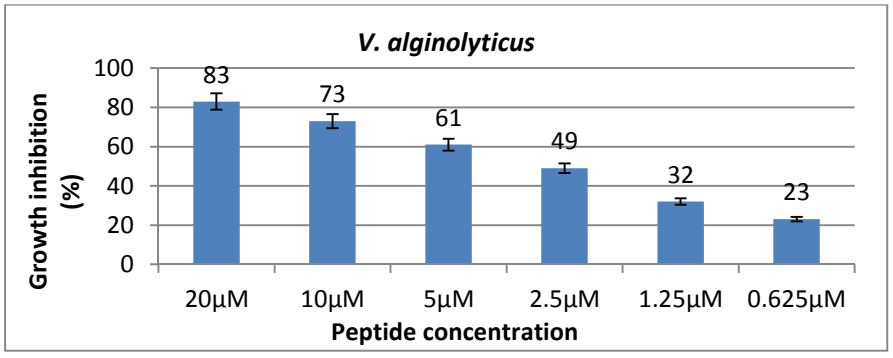
V. alginolyticus
Growth inhibition (%)
100
80
60
40
20
0
83
73
61
49
32
23
20µM
10µM
5µM
2.5µM
1.25µM
0.625µM
Peptide concentration

(d)

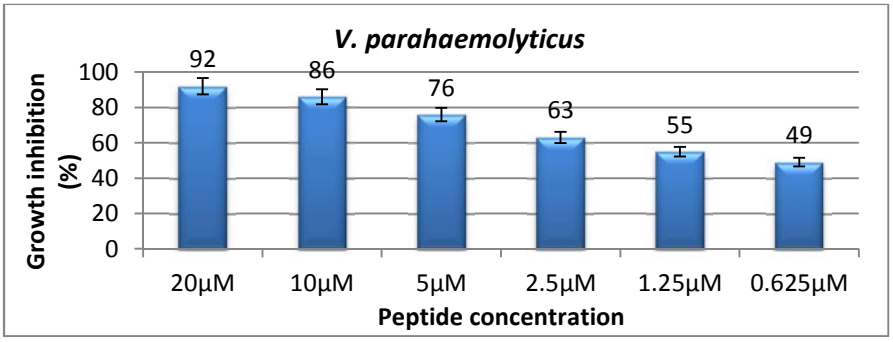
V. parahaemolyticus
Growth inhibition (%)
100
80
60
40
20
0
92
86
76
63
55
49
20µM
10µM
5µM
2.5µM
1.25µM
0.625µM
Peptide concentration

(e)

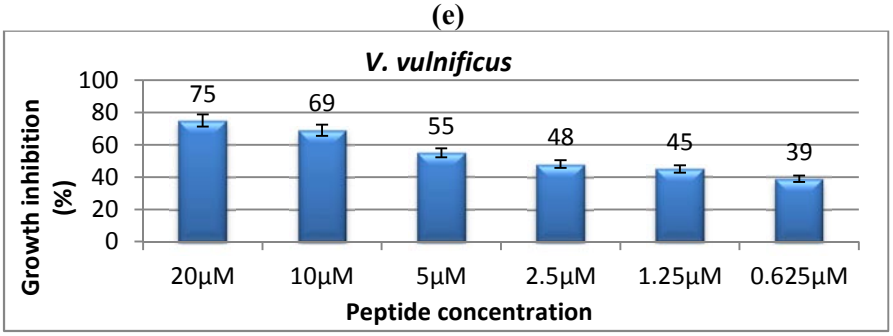
V. vulnificus
Growth inhibition (%)
100
80
60
40
20
0
75
69
55
48
45
39
20µM
10µM
5µM
2.5µM
1.25µM
0.625µM
Peptide concentration

(f)

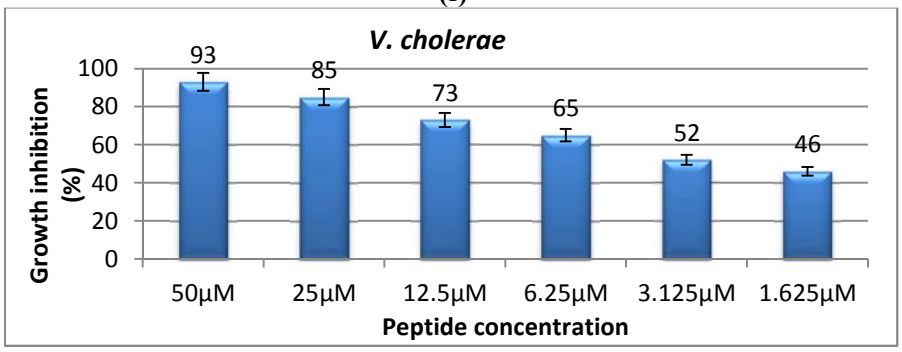
V. cholerae
Growth inhibition (%)
100
80
60
40
20
0
93
85
73
65
52
46
50µM
25µM
12.5µM
6.25µM
3.125µM
1.625µM
Peptide concentration

(g)

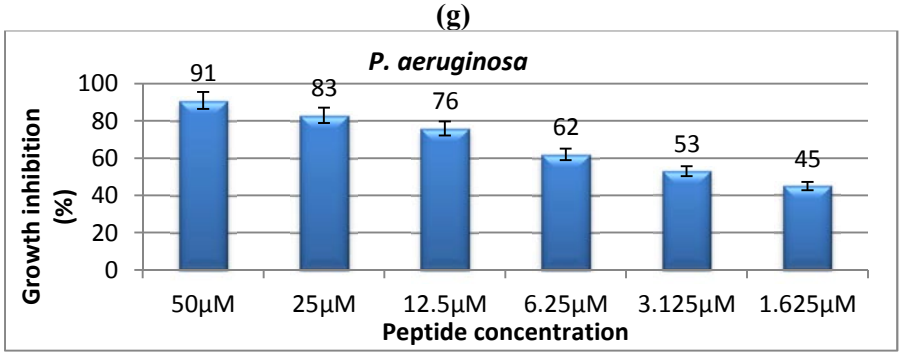
P. aeruginosa
Growth inhibition (%)
100
80
60
40
20
0
91
83
76
62
53
45
50µM
25µM
12.5µM
6.25µM
3.125µM
1.625µM
Peptide concentration

(h)

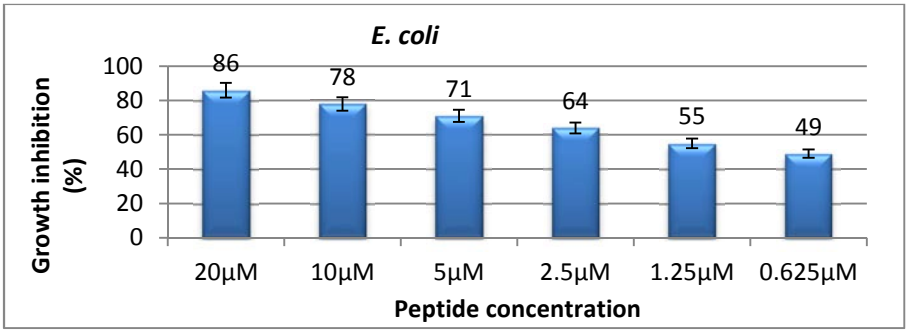

(i)

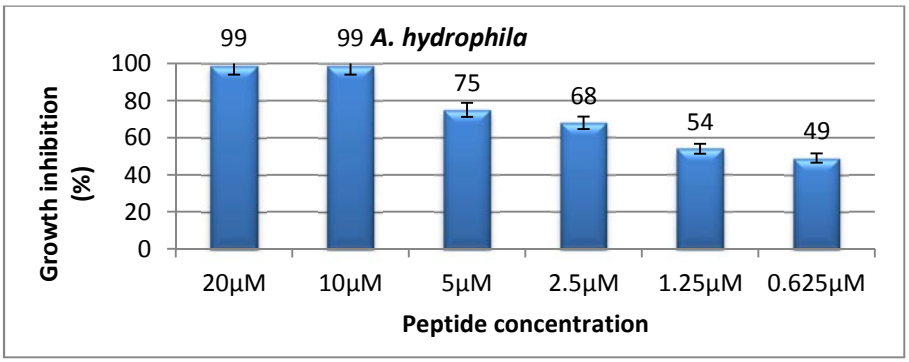

(j)

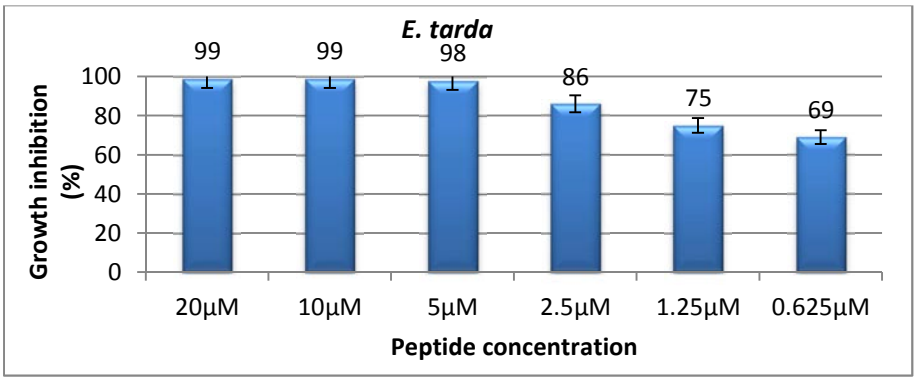

(k)

Fig. 2.22 (a-k) Antimicrobial activity of r*Fi*-crustin2 against different bacteria at various concentrations.

2.3.2.7 *PI staining*

In PI staining, majority of the peptide treated *E. tarda* appeared red (stained red since PI intercalates with the DNA of dead cells) (Fig. 2.23). This also confirms that the killing of *E. tarda* could be by membrane pore development or by perturbation.

Fig. 2.23 PI staining image of untreated control *E. tarda* and r*Fi*-crustin2 treated *E. tarda* (magnification 100 x).

2.3.2.8 SEM analysis

Scanning electron microscopy (SEM) was used to perceive the morphological changes in control and *E. tarda* cells treated with r*Fi*-crustin2. It is evident that the r*Fi*-crustin2 disrupts the membrane of *E. tarda*, with noticeable blebbing on contrary to the untreated control (Fig. 2.24).

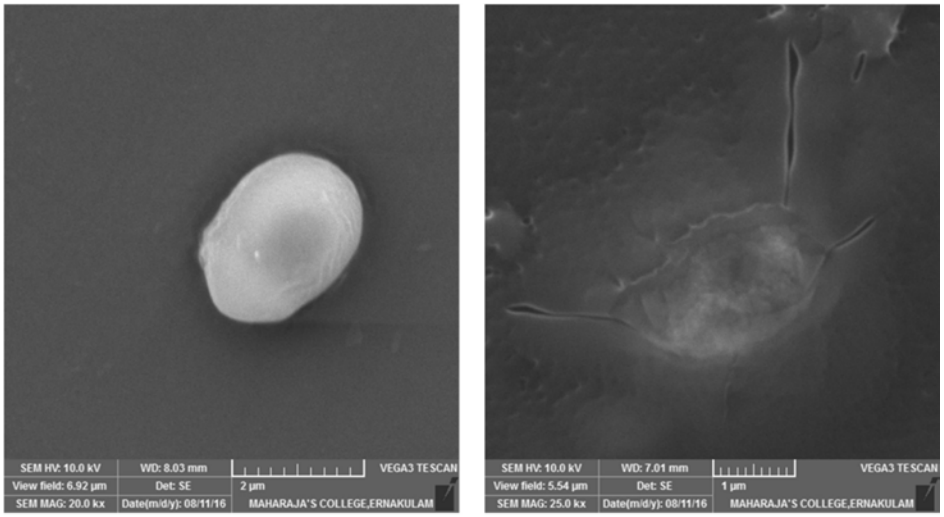

Untreated control *E. tarda* Peptide treated *E.tarda*

Fig. 2.24 SEM image of untreated control *E. tarda* and r*Fi*-crustin2 peptide treated *E. tarda.*

2.3.2.9 *DNA binding assay*

The r*Fi*-crustin2 peptide was tested for DNA binding activity using 50 ng of pUC-18 plasmid vector at a concentration of 20 µM.

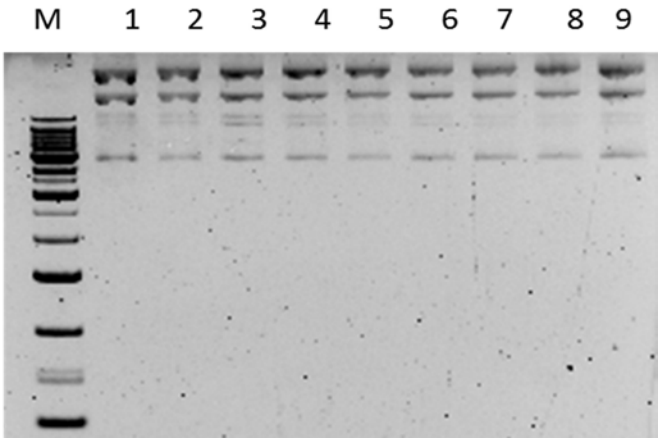

Fig. 2.25 Agarose gel electrophoretogram of DNA binding assay of r*Fi*-crustin2 using pUC-18 vector with different concentration of peptide. Lane M: 1 kb ladder, Lane 1: Control untreated plasmid, Lane 2 to 9: 20 µM to 0.1625 µM concentration of peptide with 50 ng of pUC-18.

The recombinant peptide was found to be non-DNA binding even at the highest tested concentration of 20 μM. The agarose gel electrophoretogram showing the non-retarded plasmid DNA in the treated and untreated group is evident in Fig. 2.25.

2.4 Discussion

Survival of invertebrates especially crustaceans in the microbe-laden aquatic environment mainly depend on the innate immune system to combat pathogenic infection. AMPs act at the front line to counter attack pathogenic incursion with their ability to kill or inhibit microorganisms. Along with other major crustacean AMPs including ALFs and penaeidins, the WAP domain-containing, crustin also exerts a key role in immune mechanisms. Crustins are formed and retained in haemocyte granules and released into the haemolymph by degranulation upon microbial stimulation. Crustins are found to be responsive to the pathogenic bacterial infection and exhibits antimicrobial activity against Gram-positive bacteria (Supungul et al., 2008; Imjongjirak et al., 2009; Mu et al., 2010), Gram-negative bacteria (Donpudsa et al., 2014), antiviral activity (Antony et al., 2011b; Jiang et al., 2015a) and also exhibits protease-inhibiting activity, which could be involved in interfering the nutrient attainment and bacterial pathogenicity (Jia et al., 2008). Thus crustins accentuate their significance in crustacean immunity with varied role and broad-spectrum antimicrobial activity and thus further studies are required for investigation of their biological functions. Emergence of antibiotic resistant pathogen due to the overuse of antibiotics in fish farming necessitates novel molecules to combat the

pathogens and thus (Greenlees et al., 1998) studies on the identification and characterization of potent AMPs is of great importance.

More than one type of crustin has been reported from the same organism differing from each other by just 1–4 amino acids (Bartlett et al., 2002). Present study involves the identification, cloning, molecular and biological characterization of the crustin isoform, *Fi*-crustin2, from the Indian white shrimp, *F. indicus.* This study reports the second crustin isoform from *F. indicus* with variation in signal peptide region when compared with the previously reported crustin (Antony et al., 2010). Since the previous work only dealt with the molecular and phylogenetic analysis, we performed the functional characterization using recombinant peptide.

Fi-crustin2 identified from *F. indicus* possessed an ORF with 354 bp encoding 117 amino acids with a signal peptide cleavage site between S_{17} and Q_{18}. The *Fi*-crustin2 exhibited an expected MW of 12.32 kDa, net charge of +2 and *p*I of 7.97 and, for 100 mer mature peptide above-mentioned constraints were found to be 10.61 kDa, +1 and 7.59 respectively. PROSITE analysis revealed the presence of WAP domain in the C-terminus and Gly-rich region in the N-terminus of the mature peptide region.

Structural analysis of *Fi*-crustin2 by PSI-PRED tool revealed the existence of one α-helix and two ß-sheeted regions in the WAP domain (Fig. 2.9). Cysteine residues existing in the WAP domain of the crustin were described to have functions in upholding the tertiary structure of crustins (Gross et al., 2001). According to the previous reports on crustin-

like proteins, the 4DSC domain played important roles in the biological function (Zhang et al., 2007). Structural models of the WAP domain from three types of crustins proposed that the tertiary structure of WAP domain is well maintained between decapod species (Smith et al., 2008).

According to Smith et al. (2008) crustins are classified into three; Type I crustins possessing a Cys-rich region and a WAP domain; Type II crustins with an additional Gly-rich region before a Cys-rich region and Type III crustins, the Gly-rich and Cys-rich regions are replaced by a Pro-Arg-rich region. Thus, the amino acid sequence of *Fi*-crustin2 shows that they belong to Type II. Also, the ClustalW alignment of *Fi*-crustin2 amino acid sequence with other crustin representatives exposed a conserved primary structure with a signal peptide, a glycine-rich region and 12 conserved cysteine residues containing a single WAP domain at the C-terminus (Fig. 2.11). These 12 Cys residues are believed to be significant in the establishment and preservation of tertiary structure (Relf et al., 1999). ClustalW multiple sequence alignment and the phylogenetic analysis by NJ tree of *Fi*-crustin2 with other crustin isoforms showed more similarity to Type-II crustin, especially to penaeid crustins (Fig. 2.12). Also it revealed that *Fi*-crustin2 hold the same ancestral origin and an analogous evolutionary status like other crustins, which has later diverged at diverse phases of evolution. Phylogenetic tree analysis of crustins further revealed that crustin sequences were grouped according to species.

Functional characterization of *Fi*-crustin2 was done using the recombinant peptide. The recombinant *Fi*-crustin2 (r*Fi*-crustin2) was

produced in an *E. coli* expression system. The PCR product of the *Fi*-crustin2 encoding the mature peptide was cloned into a pET-32a(+) vector (Li et al., 2012) and expressed in *E. coli* Rosettagami^{TM}B (DE3) pLysS (Donpudsa et al. 2014). After over-expression of the r*Fi*-crustin2 by adding IPTG, the bacterial cells were collected, lysed and analyzed on a 16 % SDS–PAGE. As shown in Fig. 2.17, r*Fi*-crustin2 could be successfully over-expressed as soluble protein from the first hour itself. The r*Fi*-crustin2 was purified through the Ni-NTA agarose columns and eluted protein was found as one major band on 16 % SDS–PAGE (Fig. 2.19a) and was confirmed by western blotting using Anti-His antibody (Fig. 2.19b). The r*Fi*-crustin2 was purified, concentrated and refolded, and characterized for antimicrobial, DNA binding, cytotoxic and haemolytic activity.

To study the antimicrobial activity of r*Fi*-crustin2, 11 bacterial strains including two Gram-positive strains viz. *B. cereus* and *S. aureus* and nine Gram-negative bacterial strains including *E. tarda, P. aeruginosa, A. hydrophila, E. coli, V. cholera*, *V. vulnificus, V. proteolyticus, V. alginolyticus* and *V. parahaemolyticus* were screened by broth microdilution assay from 20 µM to 0.625 µM to calculate the MIC. The bactericidal activity was confirmed by plating the peptide treated pathogens on to MH agar plates and thus MBC was calculated for each pathogen. Even though the recombinant peptide, r*Fi*-crustin2 was found to be active against both Gram-positive and Gram-negative pathogens the degree of growth inhibition was found to be varied. Among the tested pathogens r*Fi*-crustin2 exhibited an increased activity towards Gram-negative, *E. tarda* with an MIC of 5 µM and MBC of 10 µM, and

A. hydrophila with MIC and MBC of 10 μM. *E. tarda is* a fish pathogen and is of significance to aquaculture, specifically to commercial fish farms. *A. hydrophila* is also capable of affecting disease in fish and amphibians as well as in humans. Previous studies regarding crustin isoforms showed that bactericidal activity is mainly by disrupting the integrity of the bacterial cell wall (Liu et al., 2016). In addition, protease inhibition property also might contribute to the inhibition of bacterial growth. Further research is needed to reveal how r*Fi*-crustin2 retains such broad-spectrum antimicrobial activity.

As in the case of other recombinant crustins already reported, r*Fi*-crustin2 also exhibited activity against both Gram-positive and Gram-negative bacterial pathogens, but the MIC and MBC values were found to be greater than 20 μM. Further, the result indicated that the recombinant *Fi*-crustin2 exhibited antimicrobial activity as a bactericidal agent. Among the controls, the thioredoxin showed more number of surviving bacteria than the PBS control group. Similar results were observed for other crustins such as Cru*Fc* (Zhang et al., 2007), crustin-like*Pm* (Amparyup et al., 2008b), crustin*Pm*7 (Krusong et al., 2012), *Mr*Crs (Arockiaraj et al., 2013a), crustin*Pm*4-1 (Donpudsa et al., 2014), rCrustin (Banerjee et al., 2015) and *Pc*Cru (Liu et al., 2016). According to the prior reports on the crustin-like proteins, the four-disulfide core domain could play an imperative role in the biological function of r*Fi*-crustin2.

Morphological changes induced in *E. tarda* followed by r*Fi*-crustin2 treatment was analysed by SEM and observed significant blebbing of membrane (Fig. 2.24). After the outer membrane disruption, r*Fi*-crustin2

may enter bacterial cells and interact with the inner membrane. Inner membrane permeabilization can cause loss of cell content and eventually leads to the lysis of the bacterial cell. Similar kinds of changes were also observed with rcrustin*Pm*1 and rcrustinP*m*7 treated *E. coli* and *S. aureus* (Krusong et al., 2012). The recombinant peptide was found to be non-cytotoxic to NCI-H460 cancer cell lines at the tested concentrations (Fig. 2.20). Cytotoxicity of r*Fi*-crustin2 to human erythrocytes was tested from 20 µM and found to be non-haemolytic (Fig. 2.21).

In conclusion, a novel isoform of AMP, Type-II crustin from the Indian white shrimp, *F. indicus* named, *Fi*-crustin2 was cloned and characterized. The peptide *Fi*-crustin2 encodes for a 17 mer signal peptide and a 100 mer mature peptide encompassing a WAP domain. Recombinant expression was done in *E. coli* Rosettagami^{TM}B (DE3) pLysS and the purified and refolded r*Fi*-crustin2 was found to be active against both Gram-positive and Gram-negative pathogens and also found to be non-haemolytic and non-cytotoxic at the tested concentrations. Nonetheless, advance research is desired to elucidate the antimicrobial mechanism of r*Fi*-crustin2 in detail. The antimicrobial activity against environmental as well as clinical isolates displayed in this study is also remarkable and reveals the antibacterial potential of this recombinant peptide. Hence, r*Fi*-crustin2 is particularly significant as a prospective candidate in pre-clinical studies as an antimicrobial agent in aquaculture and human medicine.

Chapter 3

MOLECULAR AND FUNCTIONAL CHARACTERIZATION OF ANTI-LIPOPOLYSACCHARIDE FACTORS FROM THE CRUCIFIX CRAB, *CHARYBDIS FERIATUS*

Contents

3.1 Introduction

Crustaceans including crabs do not possess the adaptive immunity and thus mainly depend on the innate immunity including antimicrobial peptides (AMPs), prophenoloxidase (proPO)-activating system, phagocytosis, encapsulation, nodule formation etc. to protect against extraneous invasions (Söderhäll and Cerenius, 1992). Cationic AMPs act as the critical immune effectors which are keenly engaged in exclusion of pathogens and usually non-cytotoxic to the host at concentrations of killing microorganisms (Hoffmann et al., 1999). So far, many AMPs have been identified and characterized from crab species, which includes the Pro-rich peptide (6.5 kDa) (Schnapp et al., 1996) and a Cys-rich peptide carcinin, (11.5 kDa) from shore crab *Carcinus maenas* (Relf et al., 1999), callinectin (3.7 kDa) from the blue crab *Callinectes sapidus* (Khoo et al.,

1999), scygonadin from the mud crab *S. paramamosain* (Wang et al., 2007), arasin (proline-arginine-rich peptide) and hyastatin (glycine-rich multi-domain peptide) from the spider crab *Hyas araneus* (Sperstad et al., 2009a) and crustins from mud crab (Imjongjirak et al., 2009).

Anti-lipopolysaccharide factor (ALF) represents one of the evolutionarily conserved cationic AMPs distributed among horseshoe crabs and crustaceans which can bind against LPS by neutralizing lipid-A moiety of LPS (Ried et al., 1996). ALFs are single domain amphipathic peptides encompassing 114–124 amino acid residues with a 16–26 amino acid residue containing short signal peptide sequence at the N-terminal region followed by a mature peptide with conserved LPS-binding domain (Rosa et al., 2010). The first ALF was isolated from the amebocytes of the horseshoe crab *Tachypleus tridentatus* and *Limulus polyphemus* (Tanaka et al., 1982) and later numerous ALF homologs have been identified and characterized from decapod crustaceans including Penaeid shrimps (Gross et al., 2001; Supungul et al., 2004; Liu et al., 2005; de la Vega et al., 2008); non-penaeid shrimps (Lu et al., 2009); lobsters (Beale et al., 2008; Zhang et al., 2010); crabs (Imjongjirak et al., 2007; Afsal et al., 2011; Afsal et al., 2012) and cray fishes (Sun et al., 2011). Different ALF isoforms and variants are either encoded by distinct genes or formed as a consequence of alternative mRNA splicing (Tharntada et al., 2008). As per the previous studies, the structure of ALF was elucidated using NMR and found that it comprises of three α-helices packed against a four-stranded β-sheet (Hoess et al., 1993; Yang et al., 2009).

From diverse group of crustaceans various isoforms of ALFs have been identified and characterized. In penaeid shrimps, four groups of ALFs were identified based on the sequence similarity and the range of theoretical isoelectric points (*p*I). Group A consists of both anionic and cationic ALF peptides; group B consists of highly cationic ALF peptides; group C includes cationic ALF peptides and group D contains highly anionic ALF peptides (Rosa et al., 2013; Tassanakajon et al., 2014). Two isoforms of ALF from *Marsupenaeus japonicus*, MjALF-E1 and MjALF-E2 comes under a new group of shrimp ALFs, group E with cationic mature peptide and anionic LPS binding domain. While considering the gene expression of any particular ALF isoform, it is found to be tissue specific; however, sometimes ALF transcripts are found in many tissues. ALFs are mainly expressed in the hemocytes, which are the major immune tissues of crustaceans (Nagoshi et al., 2006; Liu et al., 2012a; Ponprateep et al., 2012; Arockiaraj et al., 2013b).

The LPS-binding domain is the functional unit of ALFs and is composed of conserved cluster of cationic amino acids and forms a disulfide loop between two cysteine residues (Hoess et al., 1993; Somboonwiwat et al., 2008; Yang et al., 2009). These typical structures are closely associated with the biological activities of ALFs. Functional characterization of ALFs was done by means of chemically synthesized LPS domain (Vallespi et al., 2000; Nagoshi et al., 2006; Pan et al., 2007; Ren et al., 2010; Imjongjirak et al., 2011; Arockiaraj et al., 2013b; Li et al., 2014) and by recombinant expression of mature peptides as fusion protein in prokaryotic *E. coli* system (Somboonwiwat et al., 2005; Yedery et al., 2009; Zhang et al., 2010; Sun et al., 2011; Liu et al., 2012a; Zhu et al.,

2014; Sun et al., 2015;) and eukaryotic yeast expression system (Somboonwiwat et al., 2005; Liu et al., 2012b; Yang et al., 2016a). Biological activity reported so far for ALFs include anti-bacterial activity (Pan et al., 2007; de la Vega et al., 2008; Zhang et al., 2010), anti-fungal (de la Vega et al., 2008; Yedery et al., 2009), anti-viral (Liu et al., 2006; Antony et al., 2011c; Yang et al., 2016b), immunomodulatory (Montero et al., 2003), anti-protozoan (Pan et al., 2009), antitumour and anti-inflammatory (Lin et al., 2013) activities.

For the first time, in order to characterize the properties and biological activities of the most abundant isoform of ALF found in *P. monodon*, ALFPm3 was expressed in the yeast *Pichia pastoris* by Somboonwiwat et al. in 2005. Large-scale production in fermentor provided 262 mg/l of recombinant ALFPm3 which was purified to homogeneity by single chromatography step on expanded-bed Streamline SP6XL. The rALFPm3 was further characterized in terms of N-terminal sequencing and mass spectrometry. Antimicrobial assays demonstrated that rALFPm3 has a broad spectrum of anti-fungal properties against filamentous fungi and anti-bacterial activities against both Gram-positive and Gram-negative bacteria, associated with a bactericidal effect.

Yedery and Reddy (2009) identified, characterized and cloned the gene coding for *Scylla serrata* anti-lipopolysaccharide factor (SsALF) by following a combined approach of degenerate and RACE PCR. The recombinant form of SsALF protein (rSsALF) was expressed with a His-tag, in *Escherichia coli* Rosetta B (DE3) pLacI, using the pTriEx-4 Ek/LIC vector. The purified rSsALF protein demonstrated antimicrobial

activity against both Gram-positive and Gram-negative bacteria. The recombinant protein was able to neutralize LPS-induced expression on SsALF *in vivo* as demonstrated by real-time PCR. The rSsALF was able to permeabilize artificial phospholipid membranes as demonstrated by calcein enclosed liposome model.

From *Eriocher sinensis,* Zhang et al. (2010) identified, cloned and recombinantly expressed the second ALF isoform (EsALF-2). Recombinant expression was carried out with a His-tag, in *Escherichia coli* BL21 (DE3)-pLysS, using the pET-32a(+) vector. The recombinant EsALF-2 protein (rEsALF-2) was purified by nickel affinity chromatography Mag Extractor His-TagNPK-700. The purified and refolded rEsALF-2 showed antimicrobial activity against *L. anguillarum* (75 μg/ml) and *P. pastoris* (18.75 μg/ml).

Sun et al. (2011) identified, an ALF cDNA sequence (PcALF1) from red swamp crayfish, *Procambarus clarki*. PcALF1 was heterologously expressed as inclusion bodies in *E. coli* BL21-DE3 cells using pET30a(+) and thus purified under denaturing conditions using high-affinity Ni-IDA Resin (Gen-Script). Purified and refolded recombinant protein of PcALF1 (rPcALF1) revealed multiple biological activities. *In vitro,* the antimicrobial activity assay was demonstrated as broad spectrum against Gram-positive and Gram-negative bacteria and a fungus. The rPcALF1 also exhibited a clearance activity on *Vibrio anguillarum* in a dose-dependent manner *in vivo* and it could bind microbial polysaccharides (LPS, LTA, and β-glucan) as well.

Liu et al. (2012a) reported the characterization of two isoforms of the mud crab ALF (*Scylla paramamosain*) *Sp*-ALF1 and *Sp*-ALF2 and the recombinant proteins obtained by expression in *P. pastoris*, using *Pichia* expression vector pPIC9K (r*Sp*-ALFs: designated as r*Sp*-ALF1 and r*Sp*-ALF2, respectively) and the synthetic peptide fragments (s*Sp*- ALFs: designated as s*Sp*-ALF1 and s*Sp*-ALF2, respectively) including the putative LPS binding loop were also prepared for antimicrobial test. Both r*Sp*-ALFs and s*Sp*-ALFs were highly effective against most of the Gram-positive bacteria and Gram-negative bacteria tested. In the same year, fifth isoform of ALF was identified from swimming crab *Portunus trituberculatus* (*Pt*ALF5). PtALF5 was expressed in inclusion bodies using pET-32a(+)vector in *E. coli* BL21 (DE3)-pLysS. The recombinant PtALF5 revealed antimicrobial activity only against tested Gram-negative bacteria *V. alginolyticus* (MIC value of 3.89-7.78 μM) and a lower activity against *E. tarda* (MIC value of 7.78-15.54 μM) and *P. aeruginosa* (MIC value of 15.54-31.08 μM).

Later in 2014, Zhu and co-workers identified and characterized another novel ALF homolog with 126 amino acid residues (*Sp*ALF4) from the mud crab *Scylla paramamosain*. Recombinant expression was attained by cloning to pGEX4T1 expression vector. The recombinant plasmid was transformed into competent *E. coli* Rosetta (DE3) cells for overexpression. Purified protein was used for different assays and found that r*Sp*ALF4 could inhibit the growth with an MIC ranging from 1.66 μM-12.18 μM for Gram-negative bacteria (*V. harveyi, V. anguillarum, V. alginolyticus, A. hydrophila, P. putida*), Gram-positive bacteria (*S. aureus and Bacillus megaterium*), and a yeast, *C. albicans* to varying

degrees. Bacterial binding disclosed that it could also bind to all the aforementioned microorganisms except *S. aureus*.

In 2015, Sun et al. reported fifth isoform of ALF (SpALF5) from the hemocytes of mud crab, *S. paramamosain*. Recombinant pET 32a+ with SpALF5 was transformed to *E. coli* Rosetta-gamiTM2 (DE3) pLysS competent cells. The recombinant SpALF5 protein showed varying degrees of binding activity towards bacteria and yeast. Moreover, *in vitro*, the recombinant SpALF5 revealed a strong antimicrobial activity against Gram-negative bacteria (*V. parahaemolyticus, V. alginolyticus, E. coli, A. hydrophila*) and yeast (*S. cerevisiae*), but could only inhibit the growth of some Gram-positive bacteria like *S. aureus.* Recombinant expression of modified FcALF2 gene (mFcALF2) from the Chinese shrimp *F. chinensis* was performed in yeast *P. pastoris* GS115 eukaryotic expression system (Yang et al., 2016a). The *mFcALF2* gene was synthesized with a modified LBD, compared to the FcALF2. The recombinant *mFcALF2* exhibited both antimicrobial and antiviral activity (WSSV). The peptide showed activity against *E. coli, V. alginolyticus*, *V. harveyi*, *V. parahaemolyticus*, *B. licheniformis* and *S. epidermidis*.

Thus far there are quite several studies concerning the molecular and phylogenetic characterization, gene expression analysis, structural and functional analysis of ALFs from decapod crustaceans and chelicerates. Hardly there is any report of AMPs from Crucifix crab, *Charybdis feriatus,* belonging to the family Portunidae. *C. feriatus* (Linnaeus, 1758), forms one of the important commercial crabs in markets of East Asia where it commands substantially higher premium prices than

Portunus spp., being sold for US$8 to US$15 per kg. Also it is a potential candidate species for aquaculture because of its meat quality, taste and size. The present chapter is focussed on identifying AMPs from Crucifix crab, *C. feriatus*. This chapter includes molecular cloning, bioinformatics analysis and phylogenetic study of ALFs identified from *C. feriatus* as well as its heterologous production, purification and functional characterization.

3.2 Materials and Methods

3.2.1 Experimental organism

Live and healthy adult Crucifix crab, *C. feriatus* was collected from Cochin estuary along Vypeen, Kerala, India. Samples were transported to the laboratory in live condition by providing aeration.

Fig. 3.1 Experimental organism used for the study Crucifix crab, *Charybdis feriatus*

3.2.2 Precautions for RNA preparation

Precautionary measures were taken while working with RNA as explained in section 2.2.2 of Chapter 2.

3.2.3 Haemolymph collection

Live and healthy crab, *C. feriatus* (Fig. 3.1) was washed with DEPC treated water to remove dirt and other organic matter and wiped using a tissue paper to remove excess water. Haemolymph was collected from the base of abdominal appendages of crab carefully using DEPC treated RNase-free capillary tubes rinsed using pre-cooled anticoagulant solution (RNase free 10 % sodium citrate, pH 7.0 in DEPC treated water). Haemolymph was homogenised in TRI reagent (Sigma) using RNase free micro-pestle and kept at -20˚C for total RNA isolation.

3.2.4 Total RNA isolation

Total RNA was isolated from haemocytes using TRI reagent (Sigma) following manufacturer's instructions as given in section 2.2.4 of Chapter 2. RNA pellet obtained was dissolved by adding 30 µl of RNase free water, followed by incubation at 55 °C for 5 min in a water bath for complete dissolution.

3.2.5 Quality assessment and quantification of RNA

Quality checking and quantification of total RNA obtained was done as specified in section 2.2.5 of Chapter 2.

3.2.6 Reverse transcription

Single stranded cDNA was synthesized from total RNA using specific oligo-d(T20) primers targeting the mRNA as described previously in section 2.2.6 of Chapter 2.

3.2.7 PCR amplification

PCR amplification of cDNA was done using gene-specific primers of the constitutively expressed gene beta-actin and antimicrobial peptide ALF primers (Tharantada et al., 2008). Primer sequences used for both the genes are given in the Table 3.1. Amplification of cDNA with gene specific primers were performed in a 25 µl reaction volume as explained in the section 2.2.7 of Chapter 2. The thermal profile used was 95 ˚C for 2 min followed by 35 cycles of 94 ˚C for 15 s, 57 ˚C for 30 s and 72 ˚C for 30 s and a final extension at 72 ˚C for 10 min.

3.2.8 Agarose gel electrophoresis

Amplicons were visualized and analysed using agarose gel electrophoresis as described in the section 2.2.8 of Chapter 2.

3.2.9 TA cloning of PCR products

Amplicons from PCR reaction using ALF F and R primers was chosen for TA cloning as explained in section 2.2.9 of Chapter 2.

PCR product with A-tail was cloned into pGEM®-T Easy cloning vector (Promega) and transformed to *E. coli* DH5α. Recombinant clones were confirmed by colony PCR using vector specific (T7 F & SP6 R) and gene specific primers (Table 3.1) and selected for plasmid isolation. Cloned plasmid with insert was sent for sequencing at SciGenom Labs Pvt. Ltd, Cochin, India. For details please refer section 2.2.10 of Chapter 2.

Table 3.1 List of primers used in the present chapter.

Target gene	Sequence (5'-3')	Product Size (bp)	Annealing Temp. (°C)	$MgCl_2$ Conc. (mM)
ALF	F: CAAGGGTGGGAGGCTGTGG R: TGAGCTGAGCCACTGGTTGG	300	60	1.5
β-actin	F: CTTGTGGTTGACAATGGCTCCG R: TGGTGAAGGAGTAGCCACGCTC	520	60	1.5
T7	F: TGTAATACGACTCACTATAGGG R: CTAGTTATTGCTCAGCGGTG	--	57	1.5
SP6	R: GATTTAGGTGACACTATAG	--	57	1.5

3.2.10 Sequence characterization and phylogenetic analysis

Analysis of the sequence was performed *in silico* using various softwares / programmes as described in section 2.2.11 of Chapter 2. Phylogenetic analysis was done by comparison with other ALF encoding sequences reported from crustaceans.

3.2.11 Selection of active peptide region for recombinant expression

In order to characterize the biological activities, among the two isoforms of ALFs identified from *C. feriatus,* the active mature peptide region of *Cf*-ALF1 was found to be 100% similar to recombinant *Scylla serrata* ALF (Yedery and Reddy, 2009). Thus the putative *Cf*-ALF2 which possesses only the mature peptide region and showing a high degree of variation from other crustacean ALFs was selected for recombinant expression and further functional characterization. Physico-

chemical features and phylogenetic analysis of the peptide have already been studied in the previous section (3.2.10).

3.2.12 Details of expression vector: pET-32a(+)

Specifications and features regarding the expression vector were already discussed in the section 2.2.13 of Chapter 2.

3.2.13 Primer designing for restriction cloning into expression vector

Active peptide region of *Cf*-ALF2 without signal peptide region was selectively amplified using the primers with added RE site, based on the MCS of pET-32a+ and gene sequence. Sequence and details of primer designed is given in the Table 3.2.

Table 3.2 Restriction primers designed for *Cf*-ALF2

Target gene	Sequence (5'-3')
pET *Cf*-ALF2 F	TAAGCACCATGGGCCAAGGGTGGGAGGCTGTG
pET *Cf*-ALF2 R	TAAGCAGAATTCTTATGAGCTGAGCCACTGGTTG

*** Colour definitions**

Nucleotide bases included to ensure enzyme digestion.

Nucleotide bases added to make the frame correct

Restriction enzyme site NcoI in F and EcoRI in R primer

Target gene sequence

Stop codon

3.2.14 PCR amplification of mature peptide

Mature peptide region was selectively amplified with pET-*Cf*-ALF2 F and R primers using pGEMT-*Cf*-ALF2 as template. PCR was done as explained in section 2.2.7 of Chapter 2.

3.2.15 Restriction digestion

Amplicons with restriction site and pET-32a(+) expression vector were subjected to restriction digestion using the restriction enzymes NcoI and EcoRI (FastDigest restriction enzymes, Thermo). Double digestion of insert and vector, pET-32a(+) was done in separate reactions. For performing restriction digestion, 50 µl of PCR product and pET-32a(+) plasmid were incubated with 5 µl of reaction buffer and 0.5 unit each of NcoI and EcoRI for 1 h at 37 °C followed by an inactivation at 65 °C for 20 min. Restriction digestion was confirmed by agarose gel electrophoresis.

3.2.16 Purification of restriction digested insert and expression vector by gel elution

Restriction enzyme digested insert and vector, pET-32a+ (Novagen, UK) were gel purified using GenJET™ Gel Extraction Kit (Thermo Scientific, USA) as explained in section 2.2.17 of Chapter 2.

3.2.17 Construction of recombinant expression vector pET-32a(+) and transformation into *E. coli* DH5α

Directional cloning of RE treated insert and vector was ligated using T4 DNA ligase following manufacturer's instruction. Ligation mix was prepared as given earlier in section 2.2.18 of Chapter 2 and the ligated vector was transformed to *E. coli* DH5α competent cells as discussed in section 2.2.9.3 of Chapter 2.

Positive recombinant colonies were selected on LB/ampicillin (50 µg/µl) plates to confirm the presence of vector with insert. Confirmation of clones were done by colony PCR using insert specific restriction primers (Table 3.2) and vector specific T7 F and T7 R primers

(Table 3.1) as discussed earlier in section 2.2.7 of Chapter 2. Positive clones were propagated for plasmid isolation and for that a single colony was inoculated in 10 ml LB broth supplemented with ampicillin (50 µg/ml) and incubated at 37 °C, with shaking at 250 rpm for 16 hours.

3.2.18 Plasmid extraction and sequencing

Plasmid extraction of pET-*Cf*-ALF2 was carried out from the overnight culture of recombinant clone as discussed in section 2.2.9.5 of Chapter 2. Recombinant plasmids were sequenced using vector specific primers with an ABI Prism Sequencing kit (Big-Dye Terminator Cycle) at SciGenom, Kochi, India and the sequences obtained were analyzed using GeneTool software to confirm whether the insert is in-frame with the start codon ATG of the pET-32a(+) system and to ensure the presence of stop codon TAA in insert for proper expression of fusion protein.

3.2.19 Expression host transformation

Recombinant plasmid pET-*Cf*-ALF2 was introduced to *E. coli* Rosettagami^{TM}B (DE3) pLysS strain by transformation and was confirmed by colony PCR as described in the section 2.2.20 of Chapter 2.

3.2.20 Induction and optimization of target protein expression

Confirmed recombinant colony was inoculated to 100 ml LB broth supplemented with antibiotics viz., ampicillin (50 µg /µl), kanamycin (15 µg/µl) chloramphenicol (12.5 µg/µl) and tetracycline (34 µg/ µl) and incubated at 37 °C with shaking at 250 rpm till OD_{600nm} attained 0.5–0.7. In order to induce the expression of *Cf*-ALF2 as fusion protein the inducer for transcription, IPTG was added to the medium to a final

concentration of 1 mM. Expression vector without insert, Thioredoxin was used as the negative control (See section 2.2.21 of Chapter 2).

As explained in section 2.2.21 of Chapter 2 un-induced culture was maintained and both the cultures were incubated further for 5-7 h at 37 °C with shaking at 250 rpm. At an interval of 1 h, the cell pellet was collected from 2 ml of broth cultures and stored at -20 °C for SDS-PAGE analysis.

3.2.21 Target protein detection by Sodium Dodecyl Sulphate Polyacrylamide Gel Electrophoresis (SDS- PAGE)

Production of recombinant *Cf*-ALF2 (r*Cf*-ALF2 as a fusion protein was detected using SDS-PAGE analysis as described previously in section 2.2.22 of Chapter 2.

3.2.22 Western blotting

SDS-PAGE of recombinant peptide, r*Cf*-ALF2 was done as explained in the previous section. Western blotting of r*Cf*-ALF2 was done as described previously in section 2.2.23 of Chapter 2.

3.2.23 Scale-up production of recombinant *Cf*-ALF2

Recombinant ALF, *Cf*-ALF2 production was done in Rosetta-gami™ B (DE3) pLysS cells as described in section 3.2.20. A total of 2L culture was produced in four 1L conical flasks. The culture was induced with 1mM IPTG when OD_{600nm} reached 0.8. Cells were harvested by centrifugation at 12000 x g for 2-5 min at room temperature after 4 hr incubation at 37 °C and shaking at 250 rpm. The cell pellets were stored at -20 °C for further analysis.

3.2.24 Extraction and affinity purification of recombinant *Cf*-ALF2

Recombinant *Cf*-ALF2 (r*Cf*-ALF2) was selectively purified from the crude cell proteins by using Ni-NTA spin column (Qiagen®) as described previously in the section 2.2.25 of Chapter 2.

3.2.25 *In vitro* refolding of the recombinant protein

The recombinant *Cf*-ALF2 was refolded in refolding buffer using Amicon ultra centrifugal filters with 3 kDa cut-off membranes (Millipore) as defined in the section 2.2.26 of Chapter 2.

3.2.26 Protein quantification of recombinant *Cf*-ALF2

Purified and concentrated r*Cf*-ALF2 was quantified using Quant-iT^{TM} protein assay kit using Qubit fluorometer (Invitrogen, UK) as described in section 2.2.27 of Chapter 2.

3.2.27 Haemolytic activity

Haemolytic activity of r*Cf*-ALF2 was determined using human red blood cells (hRBCs) and percentage haemolysis was calculated and plotted as explained in the section 2.2.28 of Chapter 2.

3.2.28 *In vitro* cytotoxicity assay

Toxicity of r*Cf*-ALF2 to eukaryotic cells and its effect on cellular metabolic process was tested using NCI-H460, human cancer cells. Cells were treated with desired concentration of the peptide (double dilution) and assayed for the cellular metabolism by XTT assay as described earlier in the section 2.2.29 of Chapter 2.

3.2.29 Antimicrobial activity

Screening for antimicrobial activity of r*Cf*-ALF2 was done against bacterial pathogens by microdilution assay and bactericidal activity was also confirmed. Microscopic observation of peptide treated pathogens was carried out employing epi-fluorescence microscopy (Propidium Iodide staining) and scanning electron microscopy (SEM) as described in section 2.2.30 of Chapter 2.

3.2.30 DNA binding assay

DNA binding activity of r*Cf*-ALF2 was performed as explained in the section 2.2.31 of Chapter 2.

3.3 Results

3.3.1 Molecular characterization of ALF isoforms in *C. feriatus*

In the present study, two AMPs belonging to ALF family was identified and characterized from the haemocytes of *C. feriatus*, herein after denoted to as *Cf*-ALF1 and *Cf*-ALF2.

3.3.1.1 *PCR amplification, TA cloning and sequencing of ALF isoforms*

Amplicons of 524 bp and 297 bp encoding an ORF of 123 and 98 amino acids were obtained from the haemocytes cDNA of *C. feriatus* (Fig. 3.2a and b). Amplicons were cloned into pGEM®-T Easy cloning vector and transformed into *E. coli* DH5α competent cells. Using gene specific and vector-specific primers colony PCR was performed to confirm the presence of insert within the plasmid (Fig. 3.3a and b). Plasmids with *Cf*-ALF1 and *Cf*-ALF2 were extracted from the positive recombinant clones, purity was analysed by agarose gel electrophoresis (Fig. 3.3c and d) and sequenced.

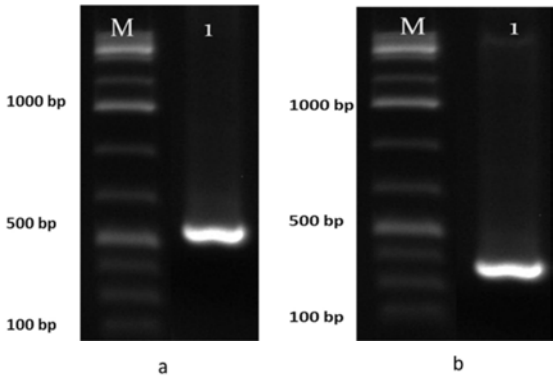

Fig. 3.2 Agarose gel electrophoretogram of PCR amplification of (a) *Cf*-ALF1, Lane M: 100 bp marker Lane 1: *Cf*-ALF1 amplicons of 524 bp (b) *Cf*-ALF2. Lane M: 100 bp marker Lane 1: *Cf*-ALF2 amplicons of 297 bp

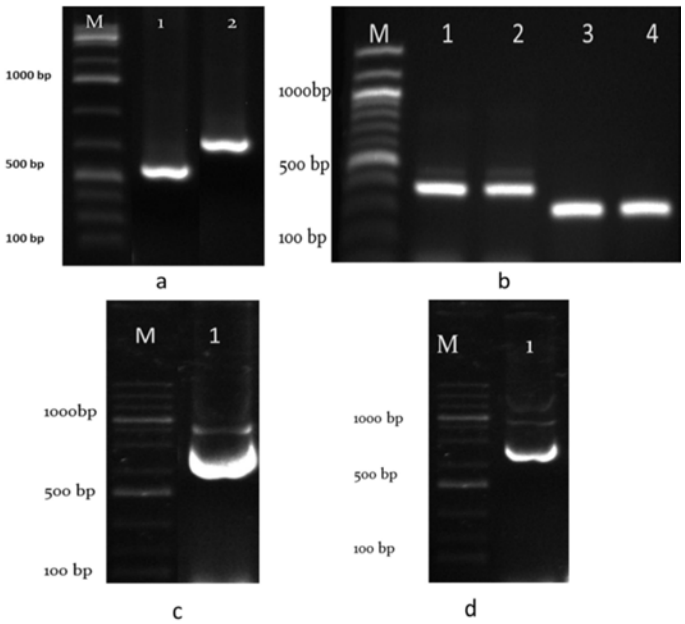

Fig. 3.3 Agarose gel electrophoretogram of (a) *Cf*-ALF1 colony PCR, Lane M: 100 bp ladder; Lane 1: 524 bp amplicon obtained for PCR with gene specific primers and Lane 2: 665 bp amplicon obtained for PCR performed using vector specific primers; (b) *Cf*-ALF2 colony PCR, Lane M: 100 bp ladder; Lane 1, 2: 438 bp amplicon obtained for PCR with vector specific primers and Lane 3, 4: 297 bp amplicon obtained for PCR performed using vector specific primers. (c) Plasmid extracted from positive clones of pGEMT-*Cf*-ALF1 vector constructs. Lane M shows 1 kb marker, Lane 1 plasmid with *Cf*-ALF1 insert; (d) Plasmid extracted from positive clones of pGEMT-*Cf*-ALF2 vector constructs. Lane M shows 1 kb ladder, Lane 1 plasmid with *Cf*-ALF2 insert.

The *Cf*-ALF1 and *Cf*-ALF2 nucleotide and deduced amino acid sequences are shown in Fig. 3.4a and b, and the sequence data has been deposited in the GenBank under the accession number of **KP688577** and **KT224347.**

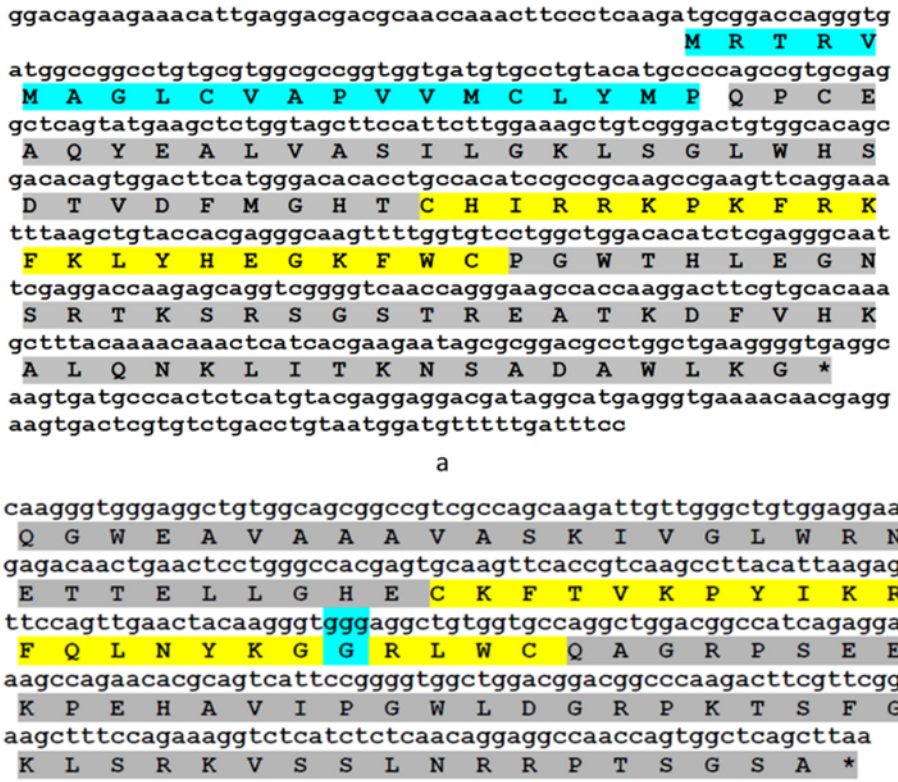

Fig. 3.4 Nucleic acid and deduced amino acid sequence of *C. feriatus* (a) *Cf*-ALF1 and (b) *Cf*-ALF2. The turquoise coloured highlighted region is the signal peptide sequence and grey coloured region is the mature peptide region within which is the putative lipopolysaccharide binding domain, the underlined sequence. Amino acid 'Gly' (G), in *Cf*-ALF2, usually absent in other ALFs is highlighted in turquoise colour.

3.3.1.2 *Sequence analysis and characterization using bioinformatics tools*

Homology search by BLASTn and BLASTp of the nucleotide sequence and deduced amino acid sequence of *Cf*-ALF1 and *Cf*-ALf2 revealed that both belong to the DUF3254 superfamily which includes the family of ALFs. BLASTn analysis of *Cf*-ALF1 nucleotide sequence showed that it exhibited 99 % similarity to an ALF isoform from *Scylla serrata* (SsALF) (GenBank ID: ACH87655.1), followed by 97 % identity to *Scylla paramamosain* ALF (GenBank ID: EF207786.1), 96 % with *Portunus pelagicus* ALF (GenBank ID: JQ899452.1), 87 % with *Portunus trituberculatus* ALF (GenBank ID: GQ165621.2) and 72 % similarity to *Eriochier sinensis* ALF (GenBank ID: HQ850572.1) respectively.

Interestingly, *Cf*-ALF2 showed more similarity to shrimp ALFs than to crab ALFs. BLASTp analysis of amino acid sequence of *Cf*-ALF2 exhibited identity of 94 % to *Fenneropenaeus indicus* ALF (GenBank ID ADK94454.1) and *Macrobrachium rosenbergii* ALF (GenBank ID AEP84102.1), 55 % to *Procambarus clarki* ALF (GenBank ID ADX60063.1), 52 % to *Homarus americanus* ALF (GenBank ID ACC94269.1), 35 % to *P. trituberculatus* ALF (GenBank ID ADU25042.1) and 37 % to *S. paramamosain* ALF (GenBank ID AEI88034.1)

SignalP analysis of 123-mer predicted the existence of 26 amino acid length signal peptide with an exceedingly hydrophobic core region and a putative cleavage site after 26^{th} amino acid (CEA_{26}-$Q_{27}Y$) which demarcates the highly cationic mature peptide of 97 amino acid residues (Fig. 3.5).

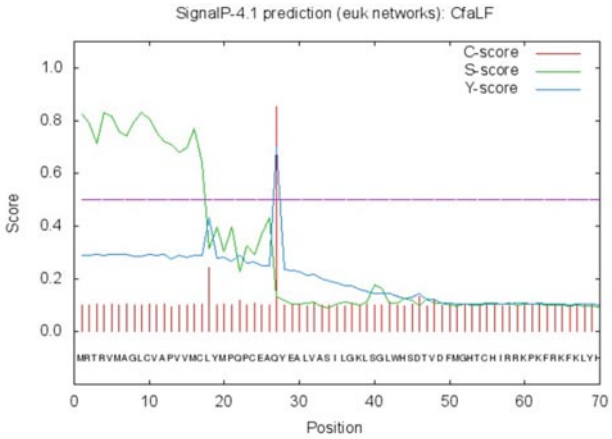

Fig. 3.5 Signal peptide analysis of *Cf*-ALF1 as predicted by the SignalP 4.1 server.

Cf-ALF1 was found to have an estimated molecular weight of 14.025 kDa, net charge of +11 and a theoretical isoelectric point (*p*I) of 9.78 and for mature peptide region the aforementioned parameters were 11.172 kDa, +10 and 10.01 respectively based on PROTPARAM tool. Cationicity of *Cf*-ALF1 mature peptide was mainly contributed by 18 positive amino acid residues (Lys (12) + Arg (6)) against 8 negative residues (Asp (4) + Glu (4)). The calculated molecular weight of the 98-mer *Cf*-ALF2 was 10.923 kDa. The putative peptide was highly cationic with a net charge of +9, total hydrophobic ratio of 34 % and an estimated isoelectric point (*p*I) of 10.09. While considering the composition of *Cf*-ALF2, the cationicity of +9 was due to the contribution of positively charged amino acids viz., K: 9, R: 8, H: 2 and negatively charged amino acids viz., E: 7 and D: 1.

The estimated half-life of mature peptide of both *Cf*-ALF1 and *Cf*-ALf2 was found to be 0.8 h (mammalian reticulocytes, *in vitro*), 10 min (yeast, *in vivo*) and 10 h (*Escherichia coli, in vivo*). Instability index is computed as 34.37 classifing the protein as stable. A

transmembrane helical region was predicted in the *Cf*-ALF1 starting from L_{43}SGLWHSDTVDFMGHT$_{59}$ and amino acid residues from G_2GWEAVAAAVASKIVGLW$_{18}$ in *Cf*-ALF2 could assist in the peptide and bacterial membrane interaction.

Secondary structure prediction using PSIPRED tool revealed the existence of 3 α helices and 4 β sheeted regions in *Cf*-ALF1 (Fig. 3.6a) and 2 α helices and 3 β sheets in *Cf*-ALF2 (Fig. 3.6b). Prediction of spatial 3D structure of *Cf*-ALF1 (Fig. 3.7a) and *Cf*-ALF2 (Fig. 3.7b) was done by homology modelling using the template, rALF-Pm3 (SMTL id: 2job.1) NMR structure, since it shared similarity of 38.61 % and 82.14 % respectively. Predicted RNA secondary structure of *Cf*-ALF1 (Fig. 3.8a) and *Cf*-ALF2 (Fig. 3.8b) with minimum free energy was found to be consisting of both double stranded and looped region.

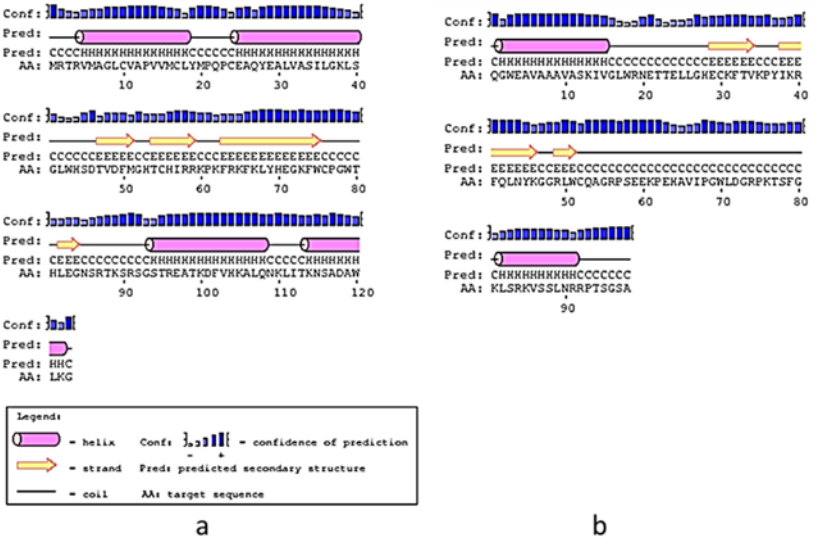

Fig. 3.6 Secondary structure of (a) *C. feriatus Cf*-ALF1 (GenBank ID: **KP688577**) and (b) *Cf*-ALF2 (GenBank ID: **KT224347**) predicted using PSIPRED server. The αhelix region is shown in pink coloured cylinders, β strand is shown in yellow arrows and the coil region is shown in black lines.

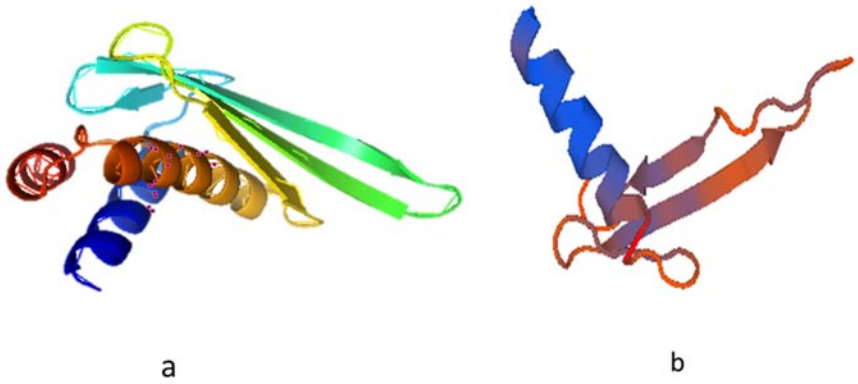

Fig. 3.7 Structural model of *C. feriatus* (a) *Cf*-ALF1 (GenBank ID: **KP688577**) and (b) *Cf*-ALF2 (GenBank ID: **KT224347**) created with the PyMol software using the pdb data generated by SWISSMODEL server.

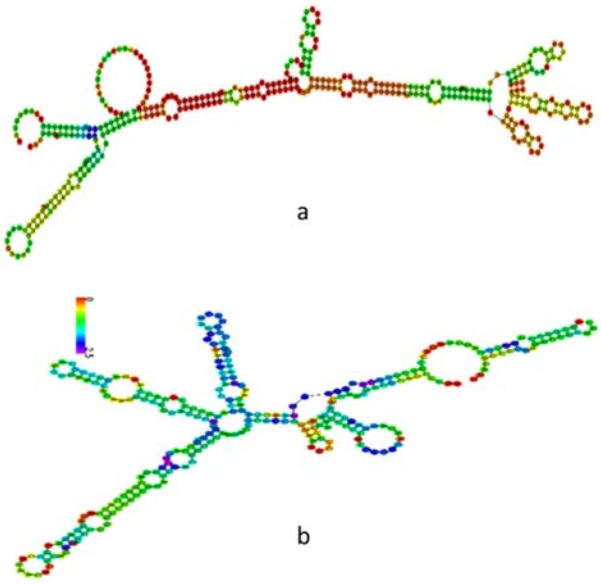

Fig. 3.8 Predicted secondary structure of *C. feriatus,* (a) *Cf*-ALF1 (GenBank ID: **KP688577**) and (b) *Cf*-ALF2 (GenBank ID: **KT224347**) RNA with minimal free energy prediction.

Antimicrobial activity of *Cf*-ALF1 predicted by APD2 revealed it as a potent AMP with a protein-binding potential (Boman index) and Wimley-White whole-residue hydrophobicity of 2.1 kcal/mol and 15.8 kcal/mol respectively. In the case of *Cf*-ALF2, the aforesaid parameters were 1.92 kcal/mol and 21.86 kcal/mol respectively. *In silico* analysis of anticipated LPS binding domain of *Cf*-ALF1 (C_{55}HIRRKPKFRKFKLYHEGKFWC_{76}) and *Cf*-ALF2 (C_{30}KFTVKPYIKRFQLNYKGGRLWC_{52}) based on amphipathicity using HeliQuest tool is shown in Fig. 3.9. Hydrophobicity analysis of mature peptide region by Kyte-Doolittle plot validated the significant presence of hydrophobic amino acids in the first 30 residues of *CF*-ALF1 (Fig. 3.10a) and in first twenty amino acid residues and 65 -70th amino acid residues of *Cf*-ALF2 (Fig. 3.10b).

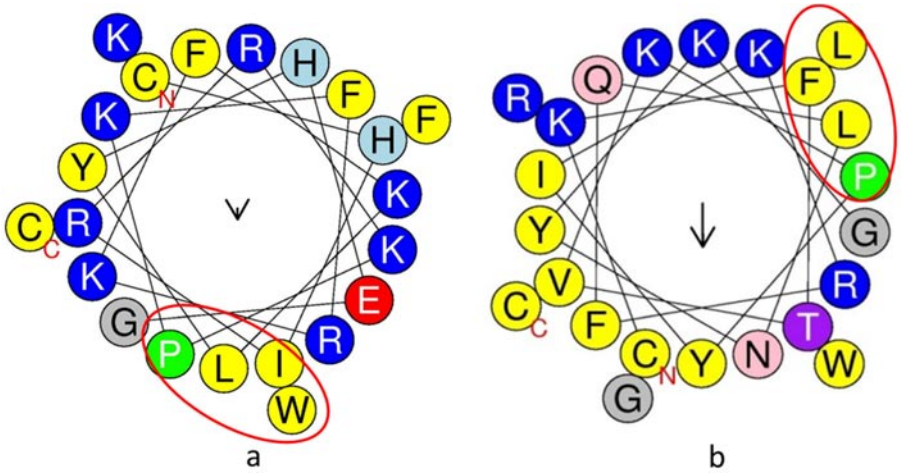

Fig. 3.9 The helical wheel diagram of (a) *C. feriatus Cf*-ALF1 (GenBank ID: **KP688577**) and (b) *Cf*-ALF2 (GenBank ID: **KT224347**). LPS domain predicted using Heliquest online tool. The structure was built to identify the amphipathicity of the LPS binding domain. The amino and carboxy terminal ends are mentioned as N and C, respectively. The expected hydrophobic face is shown in the red circle.

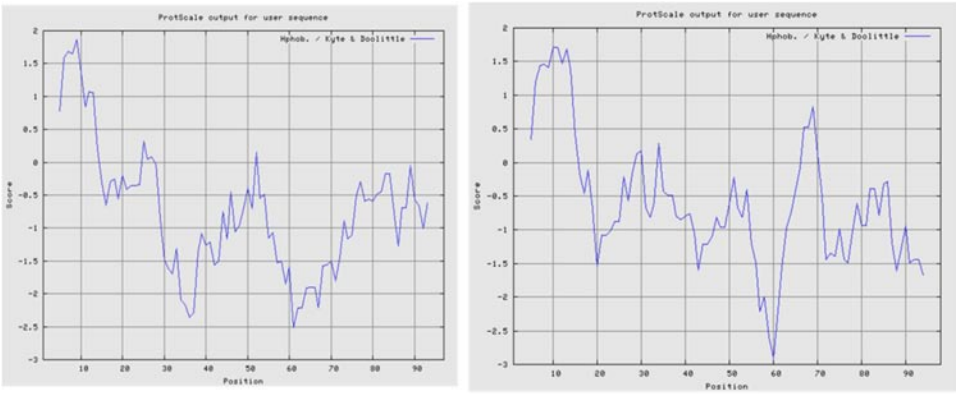

Fig. 3.10 Kyte-Doolittle plot showing hydrophobicity of mature peptide region of *C. feriatus Cf*-ALF1 (GenBank ID: **KP688577**) and (b) *Cf*-ALF2 (GenBank ID: **KT224347**). The peaks above the score (0.0) indicate the hydrophobic nature of the predicted protein.

3.3.1.3 *Sequence alignment and phylogenetic analysis*

The multiple protein sequence alignment of *Cf*-ALF1 and *Cf*-ALF2 with representatives of each crustacean ALFs using ClustalW in BioEdit revealed the existence of conserved sequence features (Fig. 3.11).

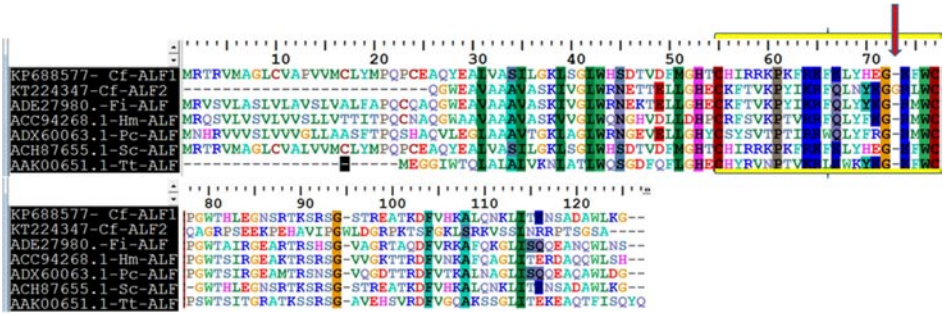

Fig. 3.11 Multiple alignment of amino acid sequence of the *C. feriatus Cf*-ALF1 (GenBank ID: **KP688577**) and (b) *Cf*-ALF2 (GenBank ID: **KT224347**) with other crustacean and limulid ALFs obtained using BioEdit.**,** *Fenneropenaeus indicus* ALF (GenBank ID **ADE27980.**1), *Homarus americanus* ALF (GenBank ID **ACC94268.1**), *Procambarus clarkii* ALF (GenBank ID **ADX60063.1**), *Scylla serrata* ALF (GenBank ID **ACH87655.1**), *Tachypleus tridentatus* (GenBank ID **AAK00651.1**).The LPS-binding domains are enclosed within the yellow square. The conserved residues are highlighted with uniform background colours.

Analysis of phylogenetic tree of *Cf*-ALF1 and *Cf*-ALF2 constructed using Neighbor-Joining method clearly showed that ALF sequences clustered according to species (Fig. 3.12).

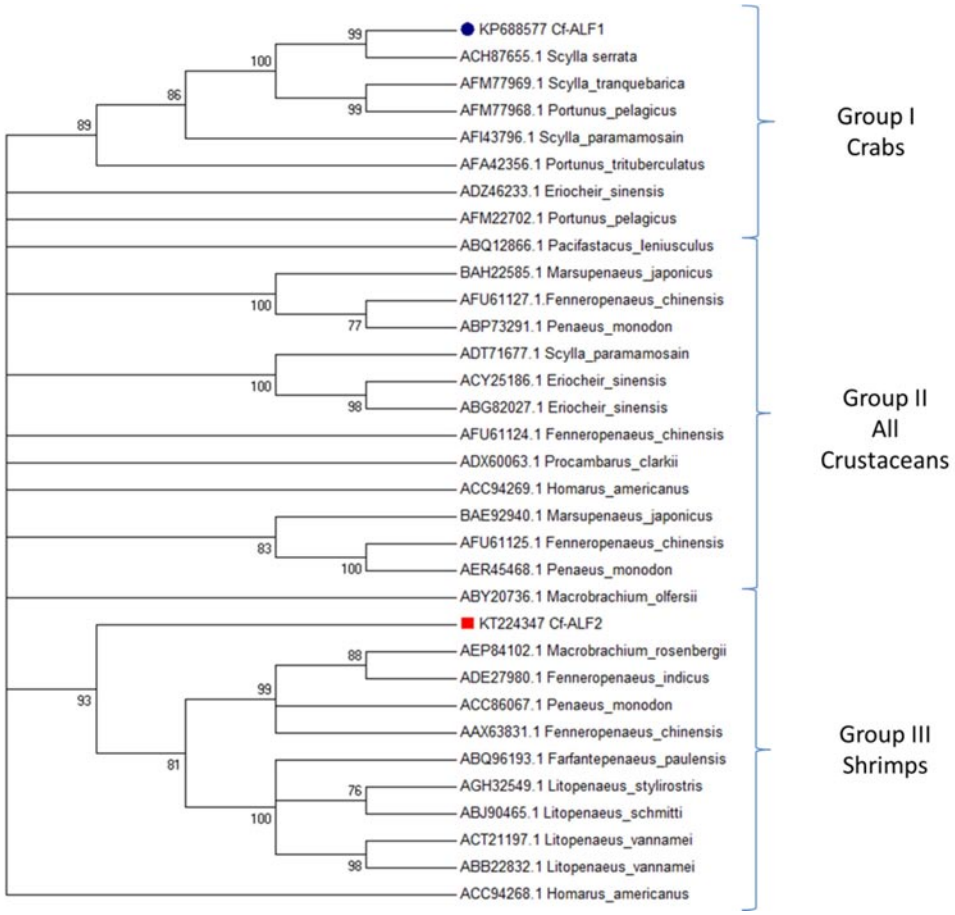

Fig. 3.12 A bootstrapped neighbor-joining tree obtained using MEGA 7 illustrating relationships between the deduced amino acid sequences of the *C. feriatus Cf*-ALF1 and *Cf*-ALF2 with other crustacean ALFs. Values at the node indicate the percentage of times the particular node occurred in 1000 trees generated by bootstrapping the original deduced protein sequences. Branches corresponding to partitions reproduced in less than 75 % bootstrap replicates are collapsed.

3.3.2 Recombinant production and functional characterization of *Cf*-ALF2

Among the two isoforms of ALFs from *C. feriatus*, the mature peptide region of *Cf*-ALF1 was found to be 100 % similar to Ss-ALF, which was already produced to recombinantly in bacterial expression system. The second isoform, *Cf*-ALF2 was predicted to be a potent AMP by *in silico* analysis and thus selected for recombinant production in bacterial system.

3.3.2.1 *PCR amplification and TA cloning of target gene with restriction sites*

A putative ALF isoform from *C. feriatus, Cf*-ALF2 was selected for cloning into expression vector. Details regarding the physicochemical parameters have been explained in the previous section (3.3.1.2).

PCR mediated amplification of active peptide was done with forward primer (pET *Cf*-ALF2 F) having NcoI site in the 5' end and reverse primer (pET *Cf*-ALF2 R) with EcoRI site in the 3' end (Table 3.2). Amplicon of size 314 bp (including restriction sites) was obtained after the PCR with pGEMT-*Cf*-ALF2 as template (Fig. 3.13). Purified PCR product was cloned using pGEM®-T Easy cloning vector and transformed to competent cells of cloning host *E. coli* DH5α. Colony PCR was performed with gene specific and vector specific primers to confirm the insertion of target gene. Amplicons of size 314 bp and 455 bp (314 bp + 141 bp) were obtained from gene specific (pET *Cf*-ALF2 F and R) and vector specific PCR (T7 F and Sp6 R) respectively (Fig. 3.14). Positive colonies were selected for plasmid isolation and sequencing of the plasmid was done to confirm the presence of restriction site.

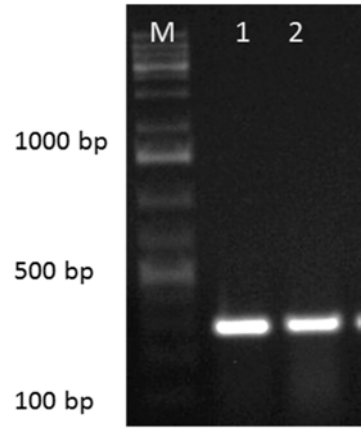

Fig. 3.13 Agarose gel electrophoretogram of the PCR amplified mature peptide region of *Cf*-ALF2 with restriction primers, Lane M: 100 bp ladder; Lane 1-2: PCR amplified product (314 bp).

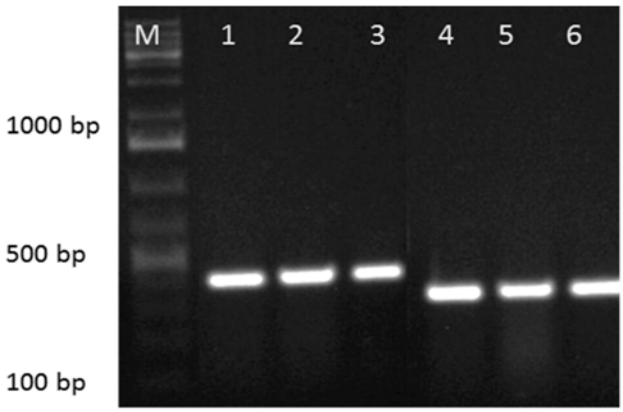

Fig. 3.14 Agarose gel electrophoretogram of *Cf*-ALF2 colony PCR, Lane M: 100 bp ladder; Lane 1-3: amplicon (455 bp) obtained for PCR with vector specific primers and Lane 3, 4 amplicon (314 bp) of PCR performed using insert specific primers

3.3.2.2 *Restriction enzyme digestion and cloning into pET-32a(+) expression vector*

Plasmids with inserts having restriction sites and in correct frame with the expression unit were selected after sequencing for RE digestion

using NcoI and EcoRI. Expression vector, pET-32a(+) was also digested with the same enzymes for restriction cloning. RE digestion was confirmed using agarose gel electrophoresis. In the case of pGEMT vector with *Cf*-ALF2, released insert of size 314 bp was observed (Fig. 3.15a). Because of pET-32a(+) vector linearization due to RE digestion, it was found as a single band unlike the control vector (uncut) in agarose gel electrophoretogram (Fig. 3.15b). Restricted insert and vector was gel purified using GenJET™ Gel Extraction Kit (Thermo Scientific, USA).

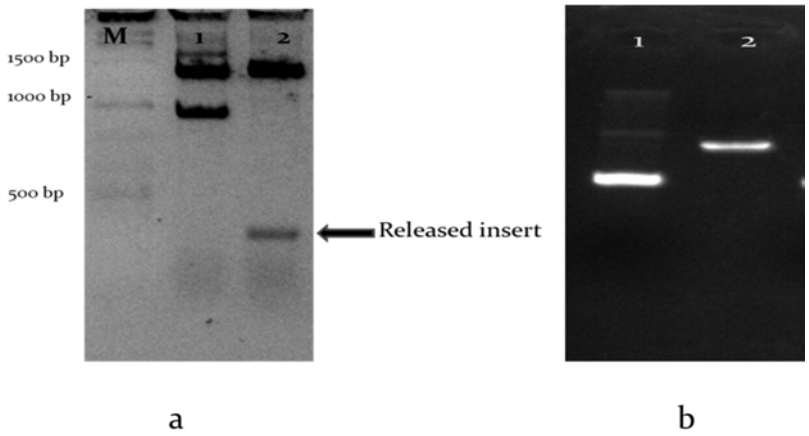

Fig. 3.15 Agarose gel electrophoretogram of the plasmids digested with NcoI and EcoRI restriction enzymes. **(a)** Lane M: 1kb ladder, Lane 1: Un-digested pGEMT-*Cf*-ALF2 plasmid. Lane 2: Restriction enzyme digested pGEMT-*Cf*-ALF2 with released insert; **(b)** Lane 1: un-digested pET-32(a+) vector, Lane 2: restriction enzyme digested linearized pET-32(a+) vector.

Purified vector and insert were ligated and transformed into the cloning host *E. coli* DH5α. Colonies obtained were screened by colony PCR using vector specific primers (T7 F and T7 R) and gene specific primers and visualized amplicons of size 1064 bp (314 bp + 750 bp) and 314 bp respectively (Fig. 3.16). Plasmids were sequenced using T7 F and

R primers in order to confirm orientation and to check any frame shift within the expression cassette. Confirmed expression vector with insert, pET-32a(+)-*Cf*-ALF2 and control vector pET-32a(+) without insert were transformed to expression host Rosettagami^{TM} B (DE3) pLysS and colonies were obtained in LB agar plates with ampicillin and kanamycin.

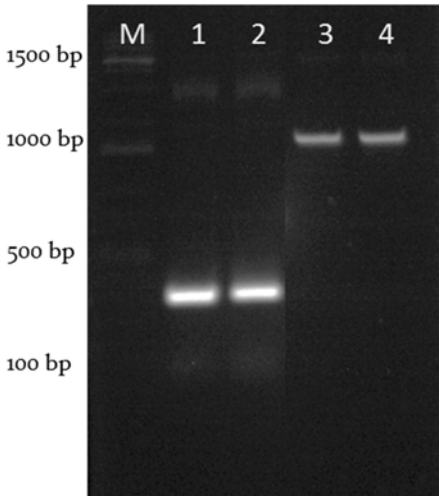

Fig. 3.16 Agarose gel electrophoretogram of (a) *Cf*-ALF2 colony PCR, Lane M: 1 kb ladder; Lane 1-2: amplicons (314 bp) using insert specific primers; Lane 3-4 amplicons (1064 bp) using vector specific primers.

3.3.2.3 *Recombinant expression of Cf-ALF2 as fusion protein*

The novel isoform of ALF, *Cf*-ALF2 from *C. feriatus* was produced by recombinant expression as a fusion protein containing 6X His tag and thioredoxin tag. Single colony of expression host with pET-32a(+)-*Cf*-ALF2 were grown in LB broth with necessary antibiotics and kept for overnight incubation. From the overnight culture, 1 ml of inoculum was added to 100 ml LB broth supplemented with antibiotics and incubated at 37 °C with shaking at 250 rpm. The expression was induced using 1mM

IPTG, when OD_{600nm} reached 0.8. An un-induced sample was also collected before induction for comparison of protein expression level. After induction, cultures were incubated further for 8 h at 37 °C with shaking at 250 rpm and from each flask 2 ml of culture were removed after every hour, centrifuged and the cell pellet was stored at -20 °C for SDS-PAGE analysis to check the expression level of recombinant *Cf*-ALF2 (r*Cf*-ALF2). SDS-PAGE analysis of the cell lysates clearly showed a band at 30.1 kDa, which is the combined molecular weight of *Cf*-ALF2 (10.923 kDa) and the fusion tags (19.2 kDa) including 6 X His tag and Trx tag (Fig. 3.17). Expression of r*Cf*-ALF2 was found to be induced from the first hour itself with a maximum from 3rd hour and found to be consistent up to 5 h. The cell pellet was collected 3 h post induction and stored in -20 °C for further analysis.

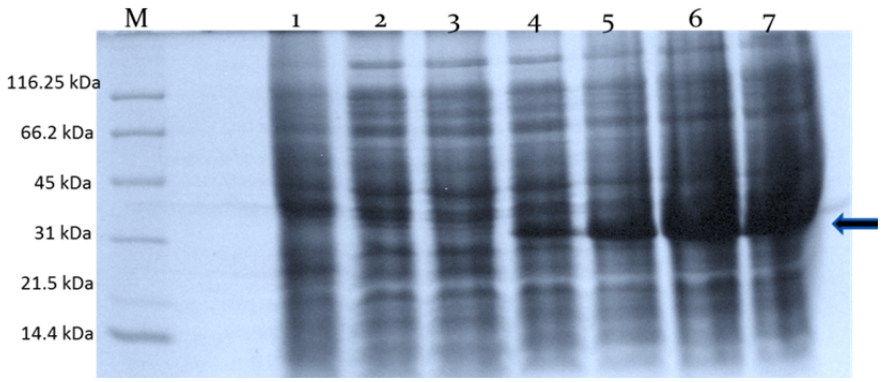

Fig. 3.17 Tricine SDS-PAGE analysis of the cells containing recombinantly expressed *C. feriatus* ALF, r*Cf*-ALF2 before and after IPTG induction on a time-course basis. Lane M: Mid-range protein ladder; Lane 1: un-induced control (before IPTG induction); Lane 2-7: IPTG induced cells after 0-5 hours of induction.

3.3.2.4 *Purification, refolding and quantification of recombinant Cf*-ALF2

Ni-NTA spin columns were used for the purification of r*Cf*-ALF2 (30.1 kDa) and eluted samples were analysed by SDS-PAGE (Fig. 3.18a) and western blotting (Fig. 3.18b). Column eluted fusion proteins with 6XHis tag were collected and stored at -20 °C to avoid the degradation of protein due to the action of bacterial proteases. Eluted fractions were concentrated using Amicon cut off filtration unit and get refolded in refolding buffer. Purified and refolded r*Cf*-ALF2 was quantified using Quant-iT^{TM} protein assay kit and the concentration was found to be 1.34 mg/ml.

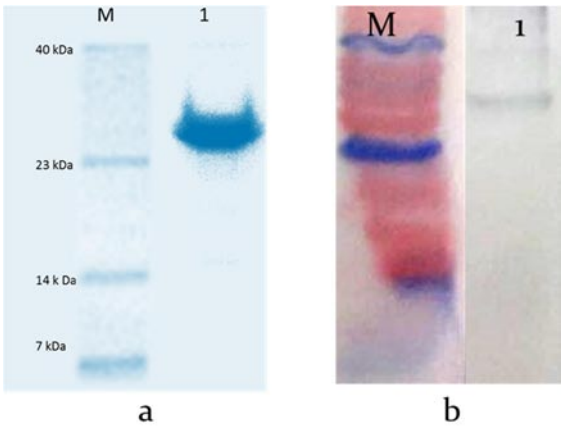

Fig. 3.18a Tricine SDS-PAGE analysis of Ni-NTA purified recombinantly expressed *C. feriatus* ALF, r*Cf*-ALF2 (30.1 kDa) Lane M: Low range weight protein marker; Lane 1: purified recombinant *Cf*-ALF2 (30.1 kDa); Lane 2: purified recombinant Trx (20.4 kDa); **3.18b** Western blot showing the purified r*Cf*-ALF2, Lane M: Mid-range coloured marker; Lane 1: purified r*Cf*-ALF2.

3.3.2.5 *In vitro cytotoxicity and haemolytic activity*

While considering the biological activity of an AMP, testing the toxicity of peptides to eukaryotic cells is of immense significance.

Cytotoxicity of the peptide, r*Cf*-ALF2was studied in NCI-H460 cell lines by employing XTT assay. Recombinant peptide, r*Cf*-ALF2 was tested for cytotoxicity from 20 µM to 0.625 µM. As explained in section 2.3.2.5 of Chapter 2, Mellitin was used as the positive control and rTrx as negative control. At 20 µM level, r*Cf*-ALF2 exhibited only a reduction of 6 % and 4 % growth respectively in NCI H460 cells and thus found to be less cytotoxic (Fig. 3.19).

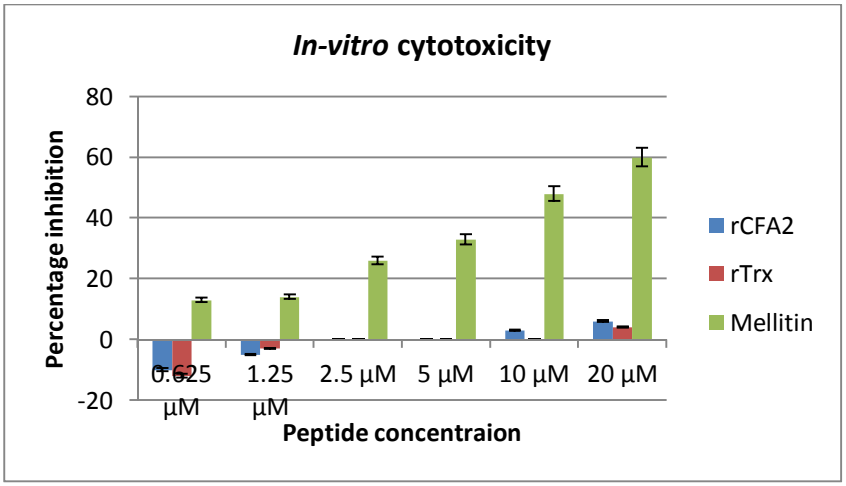

Fig. 3.19 *In vitro* cytotoxicity of the recombinant *C. feriatus* ALF, r*Cf*-ALF2, rTrx and Mellitin in NCI-H460 cells at various concentrations

Haemolytic activity of the recombinant peptides was tested using human RBCs and observed that the r*Cf*-ALF2 and rTrx showed zero percent haemolysis even at the highest concentration tested (20 µM). Whereas, the control peptide mellitin exhibited 50 % at 20 µM. Result of the haemolytic assay is showed in Fig. 3.20

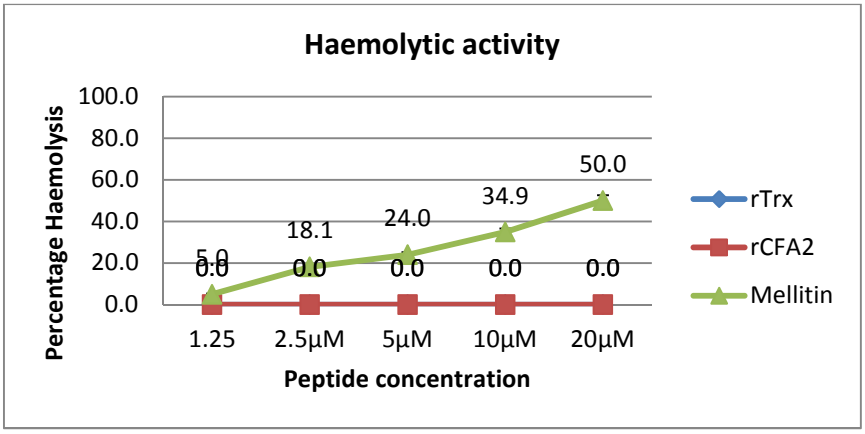

Fig. 3.20 Haemolytic activity of the recombinant *C. feriatus* ALF, r*Cf*-ALF2, rTrx and control peptide mellitin in human RBCs at various concentrations

3.3.2.6 Antimicrobial activity

Antimicrobial activity of recombinant ALF, r*Cf*-ALF2 and rTrx (negative control) was tested using broth microdilution assay from a concentration of 20 µM to 0.625 µM. Control peptide rTrx did not exhibit activity against the tested pathogens and growth was almost same as that of untreated control group. The peptide r*Cf*-ALF2 exhibited significant activity against Gram positive *S. aureus* (MIC and MBC of 5 µM) and Gram negative *E. coli* (MIC of 10 µM and MBC of 20 µM). Other tested pathogens were also found to be sensitive to r*Cf*-ALF2, but the MIC and MBC values were found to be >20 µM. At a concentration of 20 µM, the peptide was found to inhibit the growth of other pathogens viz., *E. tarda* by 78 %, *B. cereus* by 76 %, *V. proteolyticus* by 85 %, *V. parahaemolyticus* by 72 %, *V. vulnificus* by 80 %, *V. cholerae* by 74 %, *V. alginolyticus* by 89 %, *P. aeruginosa* by 65 % and *A. hydrophila* by 83 % (Fig 3.21 (a-k)).

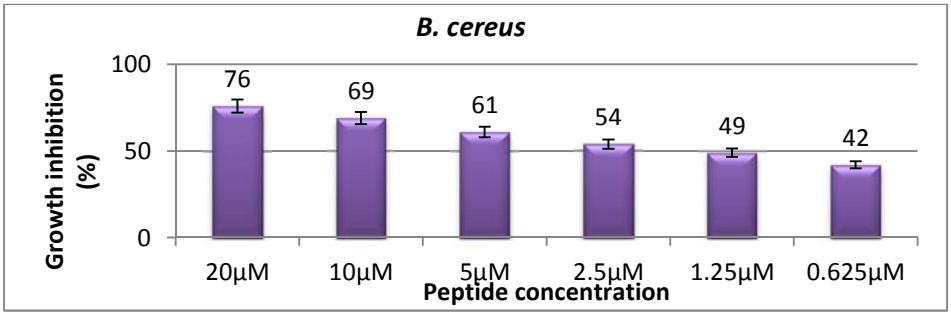
B. cereus
Growth inhibition (%)
100
50
0
76
69
61
54
49
42
20µM
10µM
5µM
2.5µM
1.25µM
0.625µM
Peptide concentration

(a)

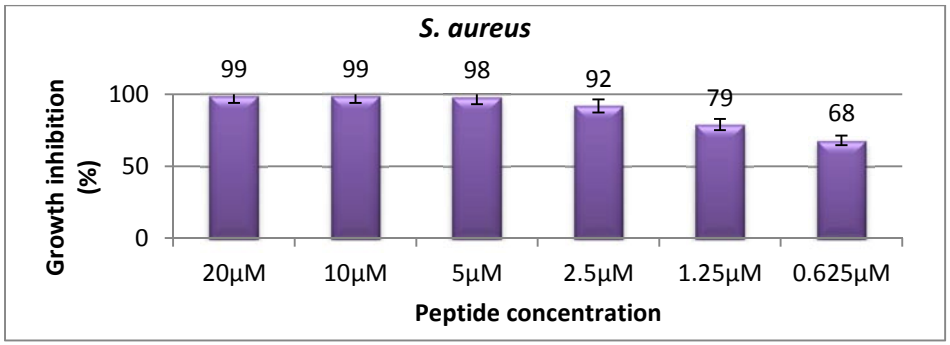
S. aureus
Growth inhibition (%)
100
50
0
99
99
98
92
79
68
20µM
10µM
5µM
2.5µM
1.25µM
0.625µM
Peptide concentration

(b)

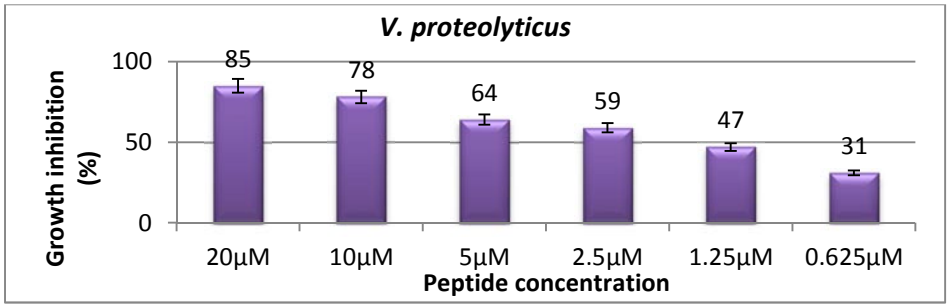
V. proteolyticus
Growth inhibition (%)
100
50
0
85
78
64
59
47
31
20µM
10µM
5µM
2.5µM
1.25µM
0.625µM
Peptide concentration

(c)

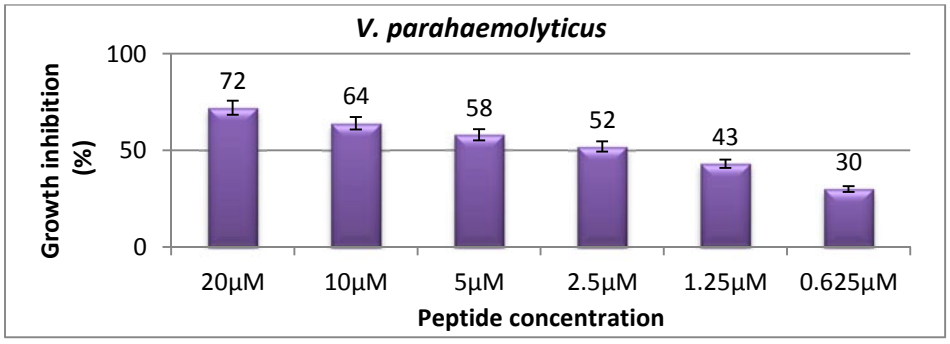
V. parahaemolyticus
Growth inhibition (%)
100
50
0
72
64
58
52
43
30
20µM
10µM
5µM
2.5µM
1.25µM
0.625µM
Peptide concentration

(d)

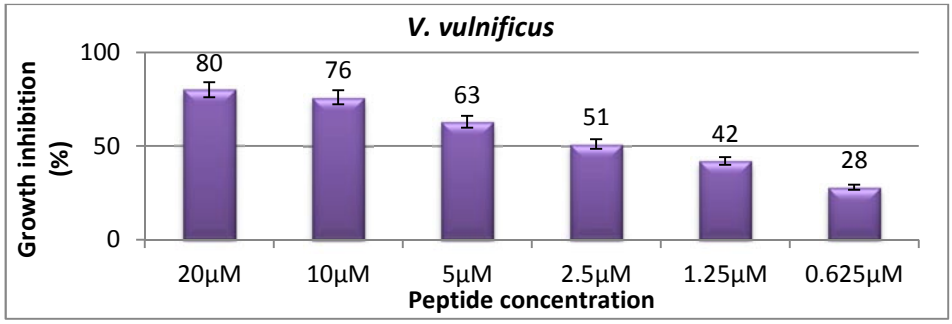
V. vulnificus
Growth inhibition (%)
100
50
0
80
76
63
51
42
28
20µM
10µM
5µM
2.5µM
1.25µM
0.625µM
Peptide concentration

(e)

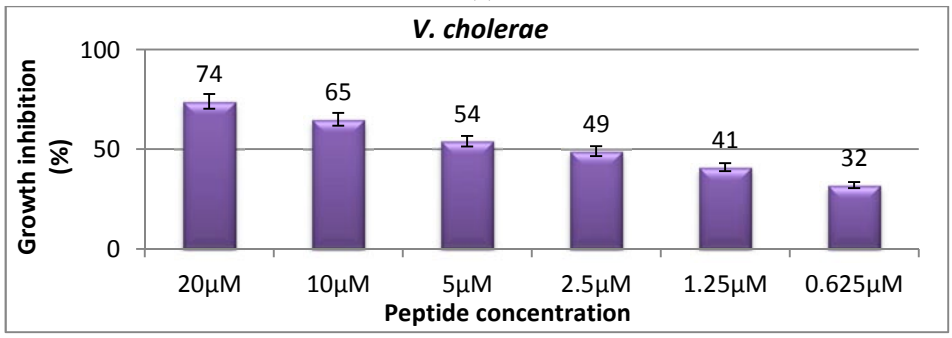
V. cholerae
Growth inhibition (%)
100
50
0
74
65
54
49
41
32
20µM
10µM
5µM
2.5µM
1.25µM
0.625µM
Peptide concentration

(f)

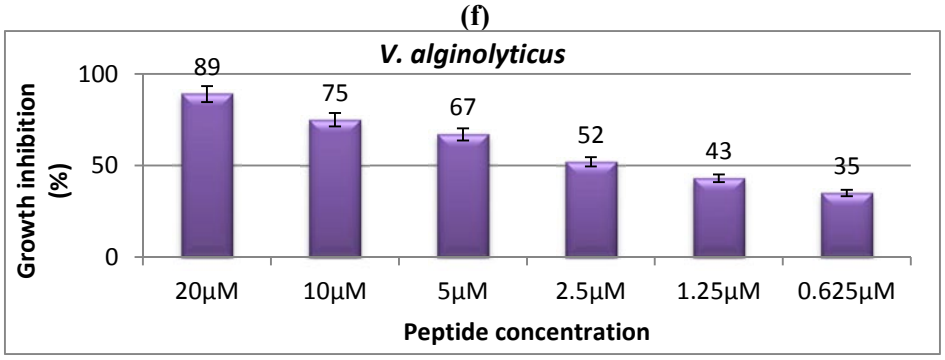
V. alginolyticus
Growth inhibition (%)
100
50
0
89
75
67
52
43
35
20µM
10µM
5µM
2.5µM
1.25µM
0.625µM
Peptide concentration

(g)

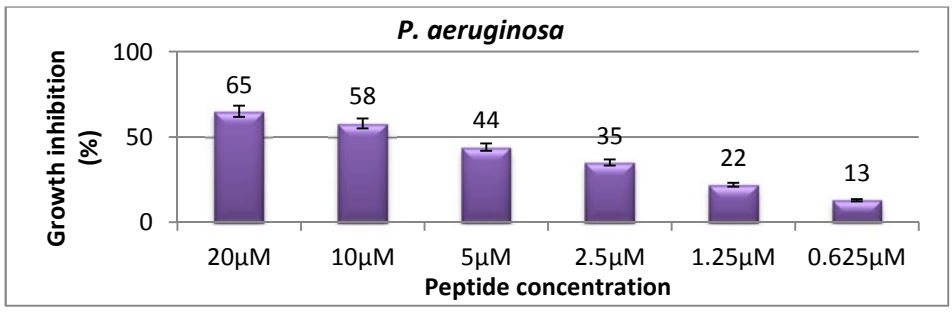
P. aeruginosa
Growth inhibition (%)
100
50
0
65
58
44
35
22
13
20µM
10µM
5µM
2.5µM
1.25µM
0.625µM
Peptide concentration

(h)

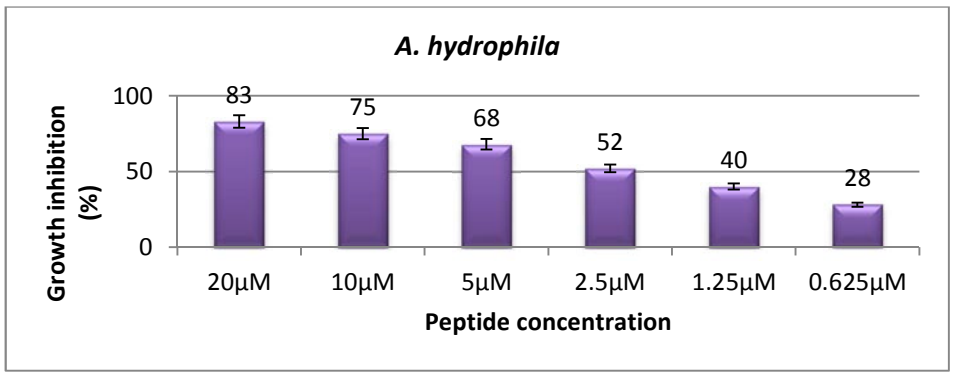

(i)

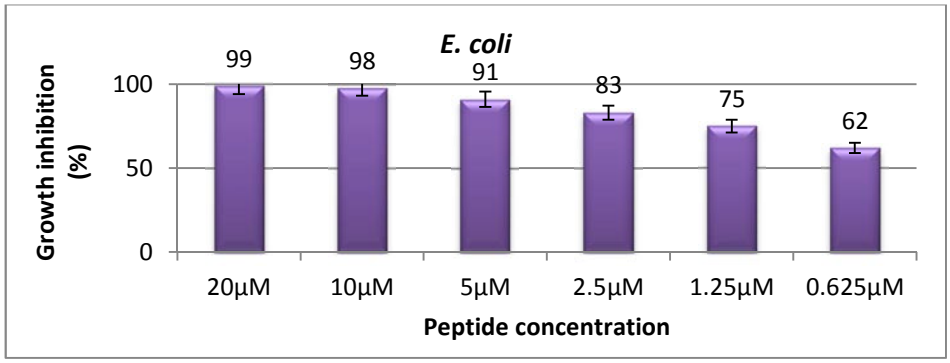

(j)

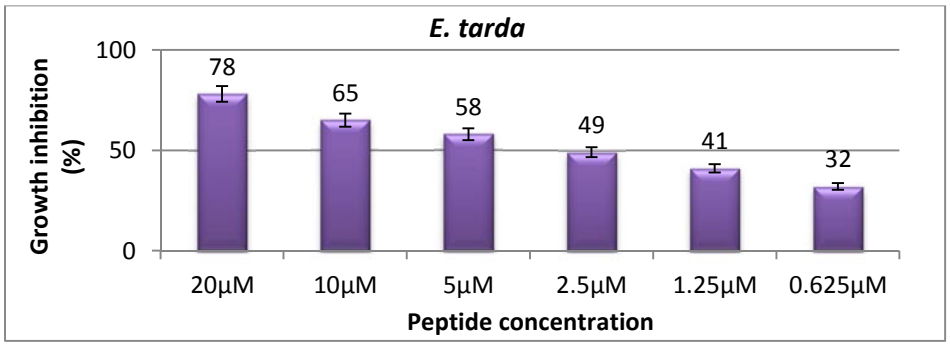

(k)

Fig. 3.21 (a-k) Antimicrobial activity of r*Cf*-ALF2 against different bacteria at various concentrations

3.3.2.7 *Propidium Iodide (PI) staining*

In PI staining of peptide treated *S. aureus* compared to the untreated control, majority of the bacteria were observed as red (dead cells stained red) (Fig. 3.22). Since propidium iodide is a DNA intercalating agent and stains DNA of dead cells. This confirms that the anti-bacterial activity of peptide is caused by membrane pore formation.

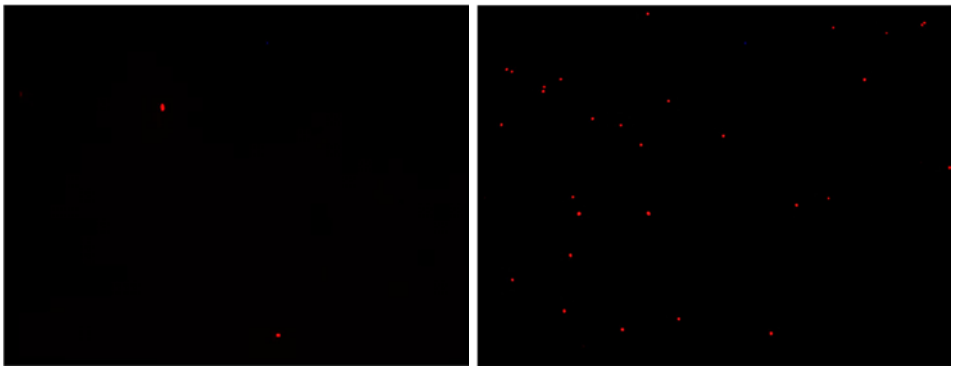

Fig. 3.22 PI staining image of untreated control *S. aureus* and r*Cf*-ALF2 treated *S. aureus* (magnification 100 x).

3.3.2.8 *SEM analysis*

Scanning electron microscopy (SEM) was used to observe the cells of Gram-positive bacteria *S. aureus* and Gram-negative bacteria *E. coli* after exposure to r*Cf*-ALF2. Compared with the control, *S. aureus* cells treated with r*Cf*-ALF2 was observed to be distorted (Fig. 3.23). Whereas in the case of *E. coli* cells incubated with r*Cf*-ALF2, compared to the untreated control, severe damage to cell membrane and the cytoplasmic content leakage could be clearly observed (Fig. 3.24).

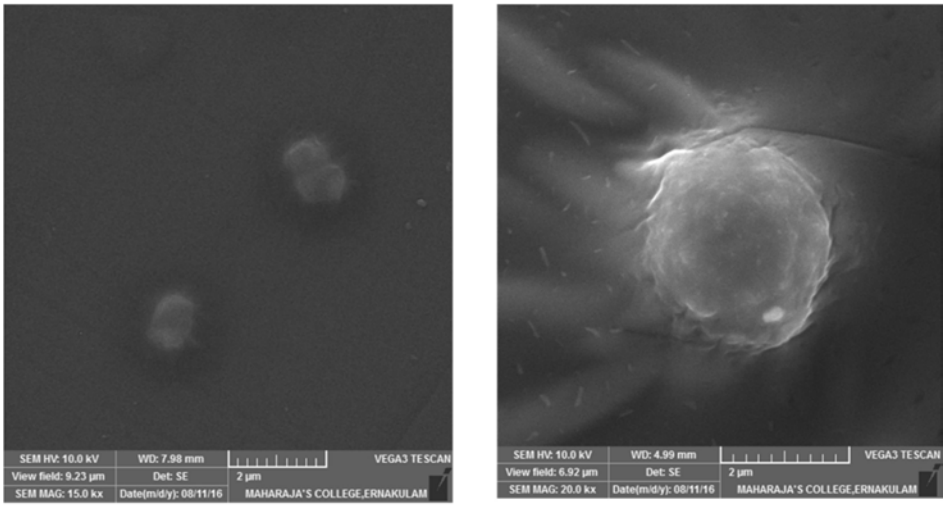

Fig. 3.23 SEM image of untreated control *S. aureus* and r*Cf*-ALF2 peptide treated *S. aureus*

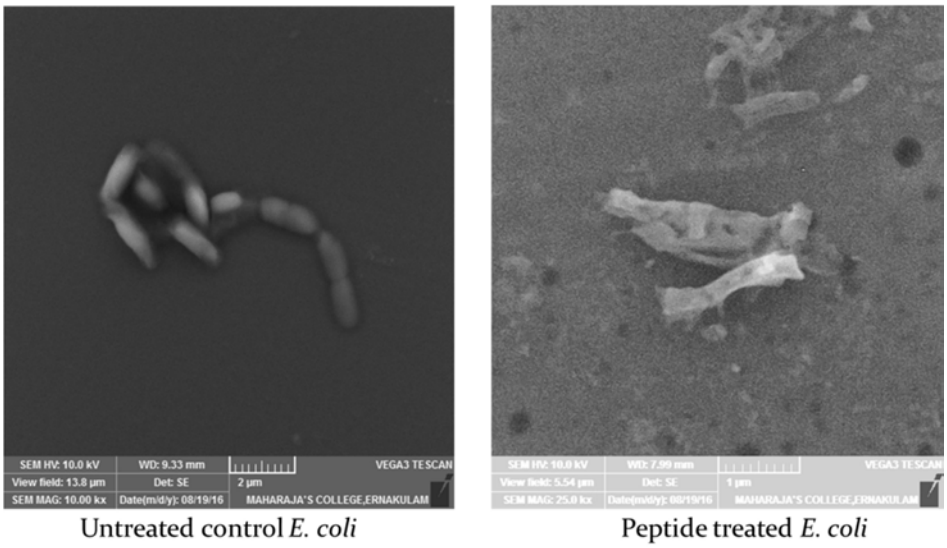

Fig. 3.24 SEM image of untreated control *E. coli* and r*Cf*-ALF2 peptide treated *E. coli*

3.3.2.9 *DNA Binding assay*

DNA binding activity of r*Cf*-ALF2 was tested using 50 ng of pUC-18 plasmid vector and even at the highest tested concentration (20 µM) the peptides did not exhibit remarkable DNA binding activity. Agarose gel image showing the non-retarded plasmid DNA in the treated and untreated group is clearly visible in Fig. 3.25.

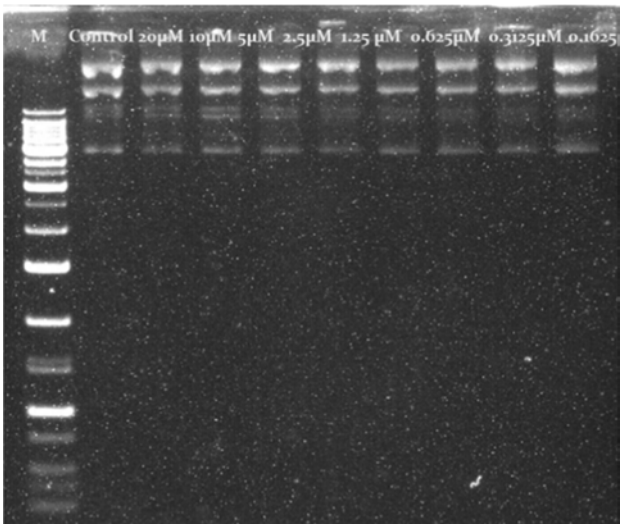

Fig. 3.25 Agarose gel electrophoretogram of DNA binding assay of r*Cf*-ALF2 using pUC-18 vector with various concentration of peptide. Lane 1: 1 kb ladder, Lane 2: Control untreated plasmid, Lane 3 to 10: 20 µM to 0.1625 µM concentration of peptide with 50 ng of pUC-18

3.4 Discussion

Anti-lipopolysaccharide factors (ALFs) in crustaceans display an imperative role in the innate immune defense mechanisms and demonstrate an extensive antimicrobial activity against different pathogenic strains of Gram-positive or Gram-negative bacteria, fungi and viruses (Liu et al.,

2005). In context of the emergence of antibiotic resistant pathogens and restrictions in antibiotic therapy in aquaculture, ALFs are becoming a promising substitutes to traditional antibiotics and as potential candidates as therapeutic agents for disease management in aquaculture (de la Vega et al., 2008; Zhang et al., 2010). The occurrence of sequence variation mainly in mature peptide of ALFs could be an important factor that leads to the functional divergence of ALF isoforms from limulids to decapod crustaceans.

Charybdis feriatus is an emerging candidate in aquaculture in order to compensate the decreasing trend in the catch from wild and to satisfy the demand in aquaculture. Also, *C. feriatus* has been scheduled as one of the appropriate species for stock enhancement and culture in the international forum on the culture of portunid crabs (Williams and Primevara, 2001). To date, there is hardly any study regarding the physiological process involved in the immune system or the host defense peptides from the portunid crab, *C. feriatus*. In the existing scenario of restriction on the usage of antibiotics and emergence of multi-drug resistant strains, the present study is of great significance; particularly in the culture system of *C. feriatus* in order to combat with pathogenic microorganisms.

In the present study, we presented the cloning, identification and phylogenetic analysis of two novel homologs of ALF from hemocytes of crucifix crab, *C. feriatus* (*Cf*-ALF1 and *Cf*-ALF2). The two isoforms exhibited a great extent of sequence variation in nucleotide and amino acid to each other and with other reported ALF isoforms. At the same

time they share similarity in the conserved characteristic motifs with other crustacean ALFs. Apparently both isoforms *Cf*-ALF1 and *Cf*-ALF2 belonged to the member of ALF family with conserved features, comprising the LPS-binding domain with a conserved cysteine residue at both ends of the domain (Somboonwiwat et al., 2008; Yang et al., 2009). Several homologs of ALFs usually co-occur in single species with miscellaneous functions and dissimilar expression level in different organs. For example, six isoforms from *P. monodon* (ALFPm1-6) (Supungul et al., 2004; Ponprateep et al., 2012], seven isoforms from *P. trituberculatus* (PtALF1-7) (Liu et al., 2011; 2012b; 2013) and seven isoforms from *F. chinensis* (ALFFc, FcALF1-6) (Liu et al., 2005; Li et al., 2013) respectively were identified.

The *Cf*-ALF1 isoform possessed an ORF of 123 amino acids with a 26 amino acid length signal peptide followed by a 97 mer mature peptide. Whereas for *Cf*-ALF2, we were able to identify only the cDNA of 297 bp encoding 98 mer mature peptide region. Considering the active peptide region, both isoforms exhibited two conserved cysteine residues forming a disulfide loop, within which the cationic amino acid residues were mainly clustered. While considering the physico-chemical parameters of the active peptide region, *Cf*-ALF1 possess a molecular weight of 11.172 kDa with a net charge of +10 and a theoretical isoelectric point (*p*I) of 10.01; Whereas *Cf*-ALF2 is a 10.923 kDa cationic peptide with a net charge of +9 and p*I* of 10.09. Hydrophobicity analysis of both peptides showed that *Cf*-ALF1 and *Cf*-ALF2 possess a total hydrophobic ratio of 34 %. Distribution of hydrophobic residues of *Cf*-ALF1 and *Cf*-ALF2 was identified using Kyte-Doolitle plot (Fig. 3.10). Detailed analysis of

Cf-ALF1 and *Cf*-ALF2, LPS binding domain revealed the hydrophobic face responsible for interaction with LPS, LTA and other bacterial polysaccharides for antimicrobial activity (Sun et al., 2012).

Amino acid sequence alignment of *Cf*-ALF1 with other crustacean and limulid ALFs (Fig. 3.11) revealed the existence of conserved residues and two cysteines flanking LPS- binding domain i.e., Cys residues (C_{55} – C_{76}) establishing a disulfide bridge with a highly conserved sequence embracing 7 positively charged amino acid residue cluster within the disulfide loop forming the functional LPS domain of ALF, which is mandatory for LPS binding and neutralization (Hoess et al., 1993). Sequence alignment also revealed that the amino acid sequence of signal peptide is not conserved among different groups, but that of mature peptide region showed a conserved pattern of amino acid motif K_{71}GR/KM/FWCPGW_{79} straddling across the LPS domain that interact with microbial polysaccharides. Compared to *Scylla serrata* SsALF, *Cf*-ALF1 differs only in a single amino acid residue in the signal peptide and the mature peptide region was found to be highly conserved.

The *Cf*-ALF2 amino acid sequence multiple alignment with other reported ALFs revealed the existence of conserved region including the LPS binding domain flanked by Cys residues (C_{24} – C_{47}) and connected by a disulfide bond (Fig. 3.20). LPS binding domain is composed of 6 positively charged amino acid residues (Lys- 4 Nos; Arg- 2 Nos) and compared to other crustacean ALFs, *Cf*-ALF2 possess an extra amino acid within the region; 23 amino acids instead of 22 amino acids. Sequence alignment also revealed that the *Cf*-ALF2 peptide exhibited

increased variation in amino acid sequences in contrary to other ALFs, by maintaining the conserved regions and motifs responsible for biological activity. The ALFs were verified to bind to the anionic microbial membrane constituents including the lipid A site of the LPS from Gram-negative bacteria, the lipo-teichoic acid (LTA) from Gram-positive bacteria (Somboonwiwat et al., 2008; Yang et al., 2009) and β glucan of fungus (Sun et al., 2011). In the case of anionic ALFs the absence of a positively charged amino acid cluster in the anionic LPS binding domain causes the deficient LPS binding ability leading to the lack of antimicrobial activity of the ALF (Rosa et al., 2013).

Molecular evolutionary pattern of two novel ALF isoforms from *C. feriatus*, *Cf*-ALF1 and *Cf*-ALF2 were analysed by employing phylogenetic tree with other reported ALF amino acid sequences using NJ method. Phylogenetic tree of *Cf*-ALF1and *Cf*-ALF2 could be divided into three groups, group I consist of crab ALFs, group II comprise of all crustacean ALFs and group III including both penaeid and non-penaeid shrimp ALFs. *Cf*-ALF1 grouped along with SsALF and other portunid crab ALFs in group I. Interestingly *Cf*-ALF2 grouped along with the shrimp ALFs (group III); similarity of *Cf*-ALF2 with other shrimp ALFs is of great significance, while considering the evolution of AMPs, especially ALF in crustaceans. The results of phylogenetic tree suggest that compared to *Cf*-ALF2, *Cf*-ALF1 is evolutionarily conserved with crab ALFs than other family members from crustacean groups. Phylogenetic tree revealed that ALFs including *Cf*-ALF1 and *Cf*-ALF2 shared a common ancestral origin and could be subsequently diverged in the course of evolution.

The HeliQuest analysis of *Cf*-ALF1 (Fig. 3.9a) unveiled that it is composed of 22 amino acids of which 45.45 % is contributed by polar residues and the rest by non-polar residues establishing a hydrophobic face with 'IWLP' residues and thus having a hydrophobicity of 0.342 H with a +7 net charge and *p*I of 10.31 this could assist in the binding of LPS domain with the highly negative charged lipid A moiety of LPS confirming the antimicrobial activity. The Kyte-Doolitle plot (Fig. 3.10a) shows that the hydrophobic residues falls in the first 30 residues which could be the part of α-helix and thus involved in the microbial membrane interaction. Overall *Cf*-ALF1 demonstrated the presence of amphipathic regions, a characteristic feature of well-studied AMPs including ALFs (Yedery and Reddy, 2009). Likewise, *Cf*-ALF2 LPS binding domain analysis revealed that the 23 amino acids containing domain has got 47.83 % amphipathicity with a hydrophobic face formed by 'FLLP'. The cationic LPS binding domain with cationicity of +6, *p*I of 10.04 possess a hydrophobicity of 0.497; all the features could aid, *Cf*-ALF2 in the interaction with negatively charged microbial membrane (Fig. 3.9b). Both the peptides *Cf*-ALF1 and *Cf*-ALF2 exhibited a highly basic *p*I due to the presence of cationic amino acids (arginine and lysine) in LPS-binding domain and this could account for the different antimicrobial activities of ALFs (Brogden, 2005).

Structural analysis of *Cf*-ALF1 demonstrates that this newly identified crab ALF contains three α-helices packed against four β-sheet strands (fig. 3.7a) analogous to the 3D structures of LALF and ALFPm3 (Hoess et al., 1993 and Yang et al., 2009). Since we were only able to identify the mature peptide region of *Cf*-ALF2, the predicted spatial

structure by homology modelling includes two α-helices and three β-sheets (fig. 3.7b). The predicted LPS-binding site is present in *Cf*-ALF1 at β2 and β3 and for *Cf*-ALF2 at β1 and β2. Usually the number of α-helices in ALF varies from species to species, but the number of β-sheets were found to be constant i.e., 4 β-sheets (Somboonwiwat et al., 2008). The structural differences along with other features such as net charge, hydrophobicity and *p*I also contribute to the biological activity of peptide (Arockiaraj et al., 2013b).

Elucidation of bioactivity potential of ALF was mainly done using synthetic and recombinant production of the LPS binding domain or the active peptide region. Biological activity of recombinant ALFs characterized so far, includes bactericidal activity against both Gram positive and Gram negative bacterial pathogens (Imjongjirak et al., 2007; Somboonwiwat et al., 2008; Zhang et al., 2010; Liu et al., 2012b; Zhu et al., 2014, Sun et al., 2015; Jiang et al., 2015b; Yang et al., 2015), antifungal activity (Zhang et al., 2010; Ren et al., 2012) and antiviral activity (Liu et al., 2012b; Sun et al., 2015; Yang et al., 2015). Since the mature peptide region of *Cf*-ALF1 showed 100 % similarity to Ss-ALF from *Scylla serrata*, which was recombinantly produced and characterized by Yedery and Reddy, 2009, *Cf*-ALF2 was selected for heterologous production and functional characterization.

Recombinant protein production by prokaryotic expression system was considered as the most effective large scale method to achieve functional protein (Hannig and Makrides, 1998). We decided to select the *E. coli* expression host Rosettagami^{TM}B (DE3) pLysS along with the

pET-32a(+) expression vector system for recombinant production of *Cf*-ALF2, since it has been used earlier to successfully produce several recombinant ALFs (Zhu et al., 2014; Sun et al., 2015). Main challenges faced while producing AMPs in *E. coli* systems include toxicity of peptide to host and proteolytic degradation by host proteases (Li, 2011). The features of pET-32a(+) vector including the solubility increasing fusion tag Thioredoxin (Trx) and the protease deficient host *E. coli* Rosettagami^{TM}B (DE3) pLysS (lon protease and ompT outer membrane protease deficient) could help to overcome the complications of recombinant production of *Cf*-ALF2.

Recombinant protein *Cf*-ALF2 was successfully produced. Protein production was found to be more after 3 h when induced with 1mM IPTG at OD_{600nm} of 0.8 (Fig. 3.17). This expression system assisted the production of *Cf*-ALF2 protein with an N-terminal 6 X His tag to aid the purification using Ni-NTA column and a Trx tag to increase the solubility and folding of peptide. Thioredoxin (Trx) with 6 X His-tag was also expressed using parent vector pET-32a(+) in *E. coli* Rosettagami^{TM}B (DE3) pLysS and purified. The rTrx was used as the negative control in the functional assays as done previously in the case of other recombinant ALFs viz., Es-ALF2 (Zhang et al., 2010); Pt-ALF5 (Liu et al., 2012b); Sp-ALF5 (Sun et al., 2015) and Mj-ALFE2 (Jiang et al., 2015b).

The purified r*Cf*-ALF2 peptide exhibited inhibition to both Gram-positive and Gram-negative bacteria, but the specific antibacterial activities to different bacteria were dissimilar. The recombinant peptide exhibited noticeable activity against *S. aureus* and *E. coli* with an MIC of 5 μM and

10 µM. *Staphylococcus aureus* is the most dangerous of all common staphylococcal bacteria causing infections ranging from minor skin lesions to life threatening diseases such as pneumonia, meningitis, osteomyelitis, endocarditis, toxic shock syndrome, bacteraemia, and sepsis. They are also involved in food spoilage. Likewise *E. coli* is also pathogenic bacteria which mainly cause urinary tract infections and diarrhoea. The r*Cf*-ALF2 exhibited a lower MIC (5 µM) against *S. aureus* when compared with other recombinant ALFs including rSsALF with an MIC of 100-200 µg/ml (Yedery and Reddy, 2009); rPcALF1 with 20 µg (Sun et al., 2011); rSpALF4 with 5.66 -7.76 µM (Zhu et al., 2014). Compared to other recombinant ALFs produced in *E. coli* system such as Pt-ALF4 (Liu et al., 2012b) and Fc-ALF5 (Yang et al., 2015), r*Cf*-ALf2 exhibited significant inhibition against *E. coli.*

Effect of peptide treatment on the bacterial morphology was analysed by SEM. Morphological changes including membrane damage, bleb formation, pore formation and cytoplasmic content leakage was evidently detected in the SEM images of *S. aureus* and *E. coli* treated with r*Cf*-ALF2 (Fig. 3.23 and Fig. 3.24). Similar morphological changes in SEM analysis was also reported previously by Jaree et al. (2012) in rALF-Pm3 treated *V. harveyii* and by Yang et al. (2016) in mFcALF2 peptide treated *E. coli, S. epidermidis* and *V. alginolyticus*. Absence of cytotoxicity in NCI-H460 cell lines and haemolytic activity against hRBCs has been observed with r*Cf*-ALF2 at the tested concentrations. This is in agreement with the previous works showing that T-ALF from *T. tridentatus* (Ohashi et al., 1984) was able to lyse only RBCs sensitised with Gram-negative bacterial LPS but not untreated RBCs and, rALFPm3

was also found to be non-haemolytic even at 100 µM (Somboonwiwat et al., 2005).

In conclusion, two novel ALF isoforms, *Cf*-ALF1 and *Cf*-ALF2 were identified and characterized by *in silico* analysis. The recombinant *Cf*-ALF2 exhibited strong bactericidal activity against tested Gram-negative bacteria and Gram-positive bacteria. In the existing scenario of emergence of drug resistance by bacteria, antimicrobial activity against aquatic and human pathogens and, lack of toxicity towards hRBCs suggests that r*Cf*-ALF2 could find application as a potential therapeutic agent in aquaculture and medicine.

Chapter 4

MOLECULAR CHARACTERIZATION OF AN ALF ISOFORM FROM THE MANTIS SHRIMP, *MIYAKEA NEPA* AND FUNCTIONAL ANALYSIS OF THE SYNTHETIC PEPTIDE

Contents

4.1 Introduction

Crustaceans are widespread and comprise diverse invertebrate groups with a highly efficient innate immune system. They are persistently exposed to the microbial challenges in the marine environment and therefore would be a potent source of antimicrobial compounds. Anti-lipopolysaccharide factor (ALF) is a cationic AMP which constitutes one of the key effector molecules in the innate immune system of crustaceans and is capable of binding and neutralizing lipopolysaccharides (LPS). Also ALF represents the humoral defense system and exhibits a diverse spectrum of activity against microbial pathogens, including Gram-negative and Gram-positive bacteria, fungi, parasites and viruses. The first ALF was identified from the amoebocytes of the horseshoe crab, *Limulus polyphemus* (Tanaka et al., 1982) and later numerous ALFs were identified and characterized from decapod crustaceans including

Penaeid shrimps (Gross et al., 2001; Supungul et al. 2004; Liu et al., 2005; de la Vega et al., 2009), non-penaeid shrimps (Lu et al., 2009), lobsters (Beale et al., 2008), crabs (Imjongjirak et al., 2007; Zhang et al., 2010; Afsal et al., 2011; Afsal et al., 2012) and cray fishes (Sun et al., 2011). Structure of ALF was elucidated using NMR and found that it consists of three α-helices packed against a four-stranded β-sheet (Hoess et al., 1993; Yang et al., 2009). Genomic organization analysis of most of the ALFs showed that it consists of three exons and two introns and the LPS-binding domain is included in the second exon. In case of *Pt*-ALF (from *Portunus trituberculatus*), there is only one intron in between two exons and in ALFPm3 (*P. monodon*), there are four exons and two introns (Beale et al., 2008; Li et al., 2008b; Tharntada et al., 2008; Imjongjirak et al., 2011).

ALF possess the ability to bind with microbial polysaccharides including LPS, lipoteichoic acid (LTA) and β-glucan, an evidence for its antimicrobial activity (Sun et al., 2011). *In vivo* and *in vitro* activity of synthetic LPS domain and recombinant ALFs were tested against different pathogens (Liu et al., 2006; de la Vega et al., 2008; Pan et al., 2009; Zhang et al., 2010). In addition to anti-microbial activity, ALFs also exhibit anti-fungal (de la Vega et al., 2008), anti-viral (Lin et al. 2010; Antony et al., 2011b), immunomodulatory (Montero et al. 2003; Ren et al. 2010), antitumour (Lin et al., 2013) anti-inflammatory (Montero et al. 2003) and anti-protozoan activity (Pan et al., 2009). ALF is a constitutively expressed AMP in haemocytes and found up-regulated followed by viral and bacterial challenge (Nagoshi et al., 2006). The transcription elements in the promoter of ALF gene was also studied which will be

useful to know about the gene regulation mechanism involved in its expression (Tang et al., 2014).

In order to unveil the potential of an AMP, it should be either produced by chemical synthesis or recombinant production. Chemical synthesis of peptides can be used for applications demanding peptides labelled with fluorescent tags, incorporation of unnatural amino acids and production of peptides that are toxic to biological expression systems. Nowadays chemical synthesis is getting cheaper and thus can rely for synthesis of short peptides with minor modifications. Functional characterization of ALFs was also done by chemical synthesis of functional domain, LPS binding domain.

Pioneer works regarding the functional study of ALF from crustaceans using synthetic LPS binding domains was started by Alpert et al. (1992). His work was mainly about the *in vivo* neutralization effect of synthetic limulus LALF ($LALF_{31–52}$: CHYRIKPTFRRLKWKYKGKFWC). Later Vallespi et al. in 2000 characterized the anti-inflammatory property of synthetic LALF. In 2002, Hirakura et al. studied about the specific interactions of the synthetic cyclic β-sheeted AMP tachyplesin I from *Tachypleus tridentatus* with lipopolysaccharides. They found that recognition site for interaction by cyclic peptide was the lipid A moiety and also exposed that the cyclic structure is required for outer membrane permeabilization. Vallespi and co-workers in 2003 observed the effects of the $LALF_{31–52}$ peptide (CHYRIKPTFRRLKWKYKGKFWC) in an experimental model of *P. aeruginosa* peritoneal sepsis and evaluated the cytokine gene expression in the spleen and liver of peptide-treated mice. They found that peptide exhibits immunomodulatory activity by reducing the TNF-α level and

upregulating the IL-2, IL-12 and IL-13, level and finally endorsing a significant increase in mice survival.

Later in 2007, Imura et al. performed a comparative study on the mechanism of action of synthetic tachyplesin and PEGylated peptide. They found that both peptides induced a toroidal pore in lipid bilayer and found no difference in biological activity compared to parent peptide. Also found that PEGylation reduces the cytotoxicity of peptides. Imjongjirak et al. 2007, for the first time studied about crab ALFs functional aspect using the synthetic ALFSp peptide containing putative LPS binding domain (TCHIRRRPKFRKFKLYHEGKFWCP) and revealed that the peptide exhibited a strong antimicrobial activity against Gram-positive bacteria, *Micrococcus luteus* and Gram-negative bacteria, *Vibrio harveyi.* LPS binding domain of a shrimp ALF, was synthesized for the first time by Pan et al. (2007). Synthetic linear and cyclic peptide forms of *P. monodon, S*ALF$_{55\text{-}76}$ (ECKFTVKPYLKRFQVYYKGRMWCP) were tested against clinical bacterial isolates and found them as potent peptides that can be applied as a prophylactic tool as well as a therapeutant for bacterial infectious diseases, as well as for septic shock.

In 2008, Ren et al. investigated synthetic peptides based on Limulus ALF (LALF), named CLP-19 (CRKPTFRRLKWKIKFKFKC) and alternative peptide equivalent to an essential part of the LPS-binding domain in the LALF, LALF$_{31–52}$. Both peptides were found to be non-cytotoxic, inhibited the cytokines, and provided a survival benefit to the mice. Later in 2010, Pan and co-workers investigated the activity of synthetic peptides derived from epinecidin-1 and SALF against *Propionibacterium*

acnes, *Candida albicans*, and *Trichomonas vaginalis* and found that both linear and cyclic forms exhibited activity against the tested pathogens with an MIC between 6-25 μM.

In 2010, Pan and coworkers studied the antibacterial activity of SALF against *Riemerella anatipestifer*, a Gram-negative bacterium which infect ducks. The minimum inhibitory concentrations (MICs) of SALF cyclic peptide ranged between 12.5–25 μg/ml and those of $SALF_{55-76}$ linear peptide ranged between 6.25– 25 μg /ml. Later in 2011, Imjongjirak and co-workers studied about antimicrobial activity of the synthetic LPS-binding domain (VCNYRVMPRFKDWELYFRGDVWCP) of ALFSp2 from crab *Scylla paramamosain* and exposed antimicrobial activity against Gram-positive (*A. viridans* and *M. luteus*) and Gram-negative (*V. harveyi* and *V. anguillarum*) bacteria. Arockiaraj et al. (2013b) reported the antimicrobial activity of the LPS binding domain of an ALF isoform (MrALF: TCQYSVNPKIKRFELYFKGRMWCP) from the freshwater prawn, *Macrobrachium rosenbergii*. The synthetic peptide showed antimicrobial activity against both Gram-negative and Gram-positive bacteria recognizing the LPS of bacterial cell wall and binding on its domain and thereby efficiently distinguishing the pathogens.

Also in the present decade, the number of people suffering from cancer-related diseases is increasing each day and conventional cancer therapies, especially chemotherapy impose lot of problems. Novel therapeutics is of great demand for the suppression of cancer cells. In this circumstance, AMPs exhibiting anticancer activity (anticancer peptides, ACPs) have been demonstrated to be a potential approach in

directed cancer drug discovery and development process (Gaspar et al., 2013). The anticancer property of the synthetic SALF cyclic peptide (Ac-ECKFTVKPYLKRFQVYYKGRMWCP-NH2) was tested in HeLa cell lines by Lin et al. (2010). Peptide induced apoptosis of HeLa cell lines via activation of caspases-6, -7, and -9, and down-regulation of Bcl-2 and nuclear factor (NF)-KB was reported in this study. *In vivo* analysis also exposed that the SALF revealed tumor suppressing activity in mice with tumor xenografts.

In 2014, Li et al. characterized one isoform of ALF from the Chinese shrimp, *Fenneropenaeus chinensis* (FcALF2). A peptide corresponding to the LPS-binding domain of FcALF2 (FcALF2-LBD: CSFNVTPKFKRWQLYFRGRMWC) and the modified LBD peptides (FcALF2-LBDb, FcALF2-LBDv) were also synthesized by solid phase peptide synthesis (SPPS) to analyze its antimicrobial activities. Data demonstrated that FcALF2-LBD possessed strong antibacterial activity against Gram-positive bacteria *M. luteus* and *M. lysodeikticus* and white spot syndrome virus (WSSV). In the same year, Guo et al. (2014) studied the antimicrobial activity of the synthetic FcALF LPS binding domain with modifications such as flanking amino acid residue in both N and C terminal end and a disulfide bond between two cysteine residues (FcALF-LBDc).

They also studied about linear peptide with same amino acid sequence (FcALF- LBDl), peptide containing Lys/Arg replaced with neutral amino acids (FcALF-LBDk and FcALF-LBDr) and peptide with neutral amino acids replaced with other neutral amino acids (FcALF-LBDn). The cyclic form exhibited improved antimicrobial activities

against Gram-negative bacteria such as *E. coli* and *V. anguillarum* and also Gram-positive bacteria such as *M. luteus* and *M. lysodeikticus* with an MIC ranging from 32–64, 2–4, 1–2, and 32–64 μM, respectively. Wang et al. (2015) studied about the antimicrobial activity of synthetic LPS binding domain of *Macrobrachium nipponense* ALF, MnALF2, and the cyclic peptide exhibited broad-spectrum antibacterial activity against Gram-positive and Gram-negative bacteria with a weak haemolytic activity.

Recently Yang et al. (2016) studied about the bioactivity of a modified peptide based on the LPS binding domain of FcALF2. The synthetic peptide was named as LBDv (Ac-YCKFKVKPKFKRWKLKFKGRMWCP-NH2). The parent peptide was LBD-2(Ac-TTGKLPVPWPTLVTTFSYGVQCFS-NH2), and in the synthetic form (LBDv), the basic amino acids number was increased by replacing six residues (S, N, T, Q, Y and R) with lysine (K). The peptide, LBDv showed higher antimicrobial and bactericidal activities compared with LBD-2. LBD-v also exhibited *in vivo* antimicrobial activity to *V. harveyi.* While comparing the bioactivity of two peptides, it was found that the net positive charge and amphipathicity were speculated as two important properties for their antimicrobial activity.

Even though there are quite a lot studies regarding the molecular characterization, structural and functional analysis of ALFs from decapod crustaceans and chelicerates (Tanaka et al., 1982; Alpert et al., 1992; Gross et al., 2001; Supungul et al., 2002; Liu et al., 2006; Imjongjirak et al., 2007; Li et al., 2008b; Beale et al., 2008; Rosa et al., 2008; Yedery and Reddy, 2009a; Tassanakajon et al., 2010;), hardly there is any report on AMPs from stomatopod crustaceans. Combined with their wide

occurrence in crustaceans and their reported diverse biological activity, this specifies the prospective prominence of the ALF group of peptides in the innate immune system. Molecular analysis of immune effectors from animals lacking economic importance is less understood. Stomatopods are predatory crustaceans distributed in tropical or subtropical regions, with few species in cool temperate regions and found to be highest in the Indo-West Pacific region (Ahyong, 2001). The present chapter mainly focuses on molecular characterization and phylogenetic analysis of ALF from a stomatopod crustacean, Mantis shrimp, *Miyakea nepa* and its functional characterization using the synthetic peptide corresponding to the LPS binding domain of the putative peptide. Present study is of great significance, since it will serve as a connecting link in the evaluation of sequence divergence, mode of evolution of innate immune effectors and its functional role from chelicerates to decapod crustaceans.

4.2 Materials and Methods

4.2.1 Experimental organism

Live and healthy adult Mantis shrimp, *Miyakea nepa* was collected from Cochin estuary along Vallarpadam, Kerala, India. Samples were transported to the laboratory in live condition by providing aeration.

Fig. 4.1 Experimental organism used for the study Mantis shrimp, *Miyakea nepa.*

4.2.2 Molecular identification by DNA Barcoding

Identification of the experimental organism by examining only the morphological characters was difficult; thus identity was confirmed with the aid of DNA barcoding. An approximate of 650 base pair (bp) fragment of the cytochrome c oxidase subunit 1 (CO1) was selected as DNA barcode which represents a very successful mtDNA-based approach for the identification. In order to perform DNA barcoding, the genomic DNA was isolated from the gills of squilla, *M. nepa* using TRI reagent (Sigma) according to manufacturer's instruction with minor modifications.

Concisely, about 100 mg of tissue was homogenized in 0.3 ml of TRI reagent in a DNase free 1.5 ml MCT using sterile micro pestle and finally 0.7 ml of TRI reagent was added and mixed well by vortexing. The homogenate was transferred to 1.5 ml MCTs. Followed by homogenization, the homogenate was centrifuged at 12000 × g for 10 min at 2–8 °C to remove the insoluble material (extracellular membranes and polysaccharides). The supernatant was then transferred to fresh MCT for phase separation using 0.2 ml chloroform. After vigorous shaking for 15 sec, the samples were allowed to stand at room temperature for 15 min. Homogenate was then centrifuged at 12000 x g for 15 min at 4 ˚C so as to separate the mixture into three phases: a red organic phase (containing protein), an interphase (containing DNA) and a colourless upper aqueous phase (containing RNA).

The aqueous phase containing RNA overlaying the interphase was carefully removed and DNA was precipitated from the interphase and organic phase by adding 0.3 ml of 100 % ethanol per 1 ml of TRI reagent

used in sample preparation. Gently mixed by inversion to avoid DNA shearing and allowed to stand for 5 min at room temperature. Precipitated DNA pellets were collected by centrifugation at 2000 × g for 5 min. DNA pellet was then washed twice in 1 ml of 0.1 M Tri-sodium citrate in 10 % ethanol solution. During each washing step, the DNA pellet was allowed to stand for at least 30 min with occasional mixing to remove phenol completely from DNA. Subsequently centrifuged at 2000 × g for 5 min at 4° C and DNA pellet was re-suspended in 75 % ethanol (1 ml), allowed to stand for 10–20 min at room temperature followed by centrifugation at 2000 × g for 5 min at 4° C. The DNA pellet was air dried for about 30 min at room temperature and dissolved in DNase free water with repeated slow pipetting to avoid shearing of DNA and stored at -20 °C for further use. The quality of the DNA was analysed by agarose gel electrophoresis using 0.8 % gel. Quantity and purity of DNA was determined using a UV Spectrophotometer (U-2900, Hitachi) by measuring the optical density (OD) at 260 and 280 nm. Only the DNA preparations having an absorbance ratio (A260: A280) ≥1.8 were used for molecular barcoding.

1 OD at 260 nm is equivalent to about 50 µg/ml of DNA

∴ DNA concentration (µg/ml) = OD at 260 nm x Dilution factor x 50

Amplification of the cytochrome oxidase-I (CO1) gene was performed in a 25 µl reaction mix using 1 µl of genomic DNA as template with a concentration of 50 ng / µl. The sequence details of primers used for the amplification of CO1 gene is given in Table 4.1. (Folmer et al., 1994). The thermal regime consisted of an initial denaturation at 95 ˚C for 5 min followed by 35 cycles of 95 ˚C for 45 sec, 50 ˚C for 45 sec, and

72 ˚C for 45 sec and a final extension at 72 ˚C for 10 min. Amplicons obtained were purified and sequenced using ABI Prism Sequencing kit (BigDye Terminator Cycle) at SciGenom, India.

Table 4.1 Primer sequence and details of COI primer used.

Target gene	Sequence (5'-3')	Product Size (bp)	Annealing Temp. (°C)	$MgCl_2$ Conc. (mM)
COI	F: GGTCAACAAATCATAAAGATATTGG R: TAAACTTCAGGGTGACCAAAAAATCA	650	50	1.5

4.2.3 Precautions for RNA preparation

Haemolymph and tissue collection for total RNA isolation and the sample processing were done with necessary cautionary measures. Basic precautions taken during and before RNA isolation have been explained in section 2.2.2 of Chapter 2.

4.2.4 Haemolymph collection

Haemolymph was extracted from the ventral sinus using DEPC treated capillary tubes (RNase-free) rinsed using pre-cooled anticoagulant solution (RNase free 10 % sodium citrate, pH 7.0). Haemolymph was homogenised in TRI reagent (Sigma) and kept at -20 ˚C for total RNA isolation.

4.2.5 Total RNA isolation

As per manufacturer's instructions with slight modification, total RNA was isolated from *M. nepa* haemocytes using TRI reagent (Sigma) as explained in section 2.2.4 of Chapter 2. RNA pellet obtained was dissolved by adding 30 µl of DEPC treated RNase free water and for

complete dissolution of RNA pellet was incubated further at 55 °C for 5 min.

4.2.6 Quality assessment and quantification of RNA

Quality of total RNA was analysed by agarose gel electrophoresis and quantified by using UV-Vis spectroscopy as described in section 2.2.5 of Chapter 2.

4.2.7 Reverse transcription

Single stranded cDNA was synthesised using specific oligo-d(T20) primers targeting the poly-A tail of mRNA from total RNA as explained previously in section 2.2.6 of Chapter 2.

4.2.8 PCR amplification

In order to confirm the reverse transcription reaction, PCR with primers for house-keeping gene, beta-actin was performed using cDNA as the template. Followed by confirmation, cDNA was used for PCR amplification using the primers, ALF-F and ALF-R (Table 4.2) (Tharntada et al. 2008). The thermal profile used was 95 ˚C for 2 min followed by 35 cycles of 94 ˚C for 15 s, 57 ˚C for 30 s and 72 ˚C for 30 s and a final extension at 72 ˚C for 10 min.

Table 4.2 Primer sequence and details of ALF primer used.

Target gene	Sequence (5'-3')	Product Size (bp)	Annealing Temp. (°C)	$MgCl_2$ Conc. (mM)
ALF	F: CAAGGGTGGGAGGCTGTGG R: TGAGCTGAGCCACTGGTTGG	350	57	1.5
β-actin	F:CTTGTGGTTGACAATGGCTCCG R: TGGTGAAGGAGTAGCCACGCTC	520	60	1.5

4.2.9 Agarose gel electrophoresis

PCR product was analysed by AGE as explained in the section 2.2.8 of Chapter 2.

4.2.10 TA cloning of amplicons and sequencing

PCR product obtained from the amplification with ALF-F and ALF-R primers were cloned into pGEM®-T Easy cloning vector as described in section 2.2.9 of Chapter 2. Recombinant plasmid was isolated and sequenced as described in detail in the section 2.2.9.5 and 2.2.10 of Chapter 2.

4.2.11 Sequence characterization and phylogenetic analysis

Various biological computational tools were used for the molecular characterization including physicochemical properties and *in silico* analysis of antimicrobial activity as described in section 2.2.11 of Chapter 2. Phylogenetic analysis of nucleotide and deduced amino acid sequences were done by multiple sequence alignment and phylogenetic tree analysis by comparison with other ALF isoforms from crustaceans.

4.2.12 Peptide synthesis and characterization

In order to study the biological activity of the peptide, the functional domain of the peptide i.e. the putative LPS binding domain was selected for peptide synthesis. Physicochemical characteristics of the synthetic peptide were also studied using different bioinformatics tools as explained in the section 2.2.11.

The peptide was synthesized at M/s Zhejiang Ontores Biotechnologies Co., Ltd China by Solid phase procedure of Fmoc chemistry with >95 % final purity.

4.2.13 Mass spectrometry analysis of the synthetic peptide

Mass spectrometry was performed at Zhejiang Ontores Biotechnologies Co., Ltd, China to verify the molecular mass and quality of peptide. The spectra analysis was performed with a Thermo Finnigan LCQ Duo mass spectrometer with an electrospray source and Xcaliber software. Synthetic peptide was reconstituted in 50 % (v/v) acetonitrile and 50 % 0.1 % trifluoracetic acid (v/v) and analyzed using Electrospray Ionization (ESI) probe with a probe bias of -3.5kv and the nebulizer gas flow was maintained at 1.5 L/min. The spectra were obtained by scanning from 400 to 2000 m/z at a scan time of 5 s.

4.2.14 Purity determination of synthetic peptide using HPLC

The homogeneity of the synthetic peptide was determined using HPLC (at Zhejiang Ontores Biotechnologies Co., Ltd, China). Synthetic peptide was dissolved in 50 µl of 0.1 % trifluoroacetic acid (TFA) and 10 µl of the sample was injected to the Inertsil ODS-SP column of dimensions 4.6 mm x 250 mm. Solvent system comprised of Solvent A (0.1 % TFA in 100 % acetonitrile) and Solvent B (0.1 % TFA in 100 % H_2O). Purification was performed with a step gradient system. During purification, a solvent gradient of 23 % Solvent A and 77 % solvent B was maintained for 0.01 min in the beginning, followed by a gradient of 48 % solvent A and 52 % solvent B for 25 min. Finally a flow of 100 % solvent A was maintained for 25 min. Flow rate was adjusted and maintained at 1 ml/min throughout the purification and eluent was monitored at 220 nm.

4.2.15 Haemolytic activity

Synthetic peptide was tested for its haemolytic activity using hRBCs. Haemolytic activity of the peptide was tested for eight different concentrations, ranging from 400 µM to 3.125 µM and the activity was represented as percentage haemolysis, calculated as described in the section 2.2.28 of Chapter 2.

4.2.16 Antimicrobial activity

Antimicrobial activity of the synthetic peptide (cyclic) was performed against bacterial pathogens by broth microdilution assay. Bactericidal activity confirmed by plating the pathogens treated with peptide after 12 h incubation. Along with that microscopic observation of pathogens sensitive to the peptide were accomplished using epi-fluorescence microscopy and SEM. The experimental procedure of all the above mentioned tests are same as explained in the section 2.2.30 of Chapter 2.

4.2.17 DNA binding assay

DNA binding activity of the synthetic peptide was tested as described in section 2.2.31 of Chapter 2.

4.2.18 Anticancer activity

4.2.18.1 *In vitro cytotoxicity assay*

Cell lines for toxicity studies, human non-small cell lung carcinoma cell lines NCI-H460 and human laryngeal carcinoma derived human epithelial type 2 cell lines, HEp-2 were purchased from NCCS, Pune. The cells were sustained in DMEM/F-12 augmented with 10 % fetal bovine

serum (FBS), penicillin and streptomycin at 37 °C in a humidified atmosphere containing 5 % CO_2.

Cell viability was determined using XTT assay in NCI-H460 and HEp2 cell lines. Cells were treated with eight different concentrations of synthetic peptide (double dilution ranging from 200 µM to 0.78 µM) and assayed for the cellular metabolism by XTT assay as described earlier in the section 2.2.28 of Chapter 2. Experiments were done in triplicate. Results are expressed as a percentage inhibition rate of viable cells. Synthetic Mellitin with FITC label was used as the positive control. IC_{50} values for each cell line were evaluated, representing the concentration at which cell viability were determined for each assay. IC_{50} value was calculated by probit analysis using SPSS 21.0 for Windows.

4.2.18.2 *Gene expression analysis using real-time reverse-transcription polymerase chain reaction (RT-PCR)*

To evaluate the anticancer activity of the synthetic peptide, the NCI-H460 cell lines and HEp2 cell lines were incubated in DMEM supplemented with 10 % FBS and antibiotic mixture containing 1% penicillin-streptomycin and co-treated with 25 µM and 50 µM of the peptide for 24 h. Cells incubated without peptide was treated as the control. After incubation cells were suspended in TRI reagent (Sigma) for RNA isolation as explained in section 2.2.4 of Chapter 2.

Single stranded cDNA was synthesised from total RNA as described in the section 2.2.4 and 2.2.6 of Chapter 2. Confirmation of cDNA conversion was done by PCR amplification with primers for house-keeping gene, GAPDH (Table 4.1). A real-time RT-PCR analysis was used to understand

the effect of peptide on the cell function by analysing the gene expression pattern of twenty three different genes viz., Bcl-2, Bax, Caspase-3, Caspase-9, Cathepsin-G, Calpain-5, Rb1, p-53, Akt1, MAPK-1, JNK, IL-1β, IL-2, IL-6, IL-10, IL-12, IFN-β, IFN-γ, TNF-α, viperin, MX1, ISG15 and IFITM3 (Table 4.2) by NCI-H460 and HEp2 cell lines following the treatment with and without peptide.

The SYBR® Green PCR Master Mix (ABI, USA) and specific primer pairs were used for selected genes, and the primer pair for GAPDH was used as the reference gene. Quantitative real time PCR (qRT-PCR) was performed in StepOnePlus real-time PCR system (Applied Biosystems) according to the following conditions: 2 min at 50 °C, 10 min at 95 °C, and 40 cycles of 15 s at 95 °C and 1 min at 60 °C using 0.5 µg of cDNA, 2X SYBR Green PCR Master Mix, and 500 nM of the forward and reverse primers. The threshold cycle number (C_T) was calculated with ABI software. Relative transcript quantities were calculated using the $\Delta\Delta C_T$ method (Livak and Schmittgen, 2001) with GAPDH as the reference gene amplified from the same samples. The results were expressed as the ratio of reference gene to target gene by using the following formula: $\Delta C_T = C_T$ (Target genes) - C_T (GAPDH). To determine the relative expression levels, the following formula was used: $\Delta\Delta C_T = \Delta C_T$ (Treated) - ΔC_T (Control). The qPCR was performed in triplicate for each experimental group. Normalized fold difference in gene expression is presented graphically to compare the level of transcription.

Table 4.3 List of primers of the various genes used for real time qPCR analysis

Sl. No.	Primer Name	Sequence (5'-3')
1	GAPDH – F	CGGAGTCAACGGATTTGGTC
	GAPDH – R	AGCCTTCTCCATGGTCGTGA
2	Bcl2 – F	ACCTGCACACCTGGATCCA
	Bcl2 – R	AGAGACAGCCAGGAGAAATCAAA
3	Bax – F	AAGCTGAGCGAGTGTCTCCGGCG
	Bax – R	CAGATGCCGGTTCAGGTACTCAGTC
4	Caspase 3 – F	ATACCAGTGGAGGCCGACTTC
	Caspase 3 – R	CAAAGCGACTGGATGAACCA
5	Caspase 9 – F	TGTCCTACTCTACTTTCCCAGGTTTT
	Caspase 9 – R	GTGAGCCCACTGCTCAAAGAT
6	Cathepsin G – F	TCAAGTTTCCTGCCCTGGAT
	Cathepsin G – R	CCTGTGTCCCCGAGAAGAAG
7	Calpain 5 – F	CAGGTCCTCTCAGAGGCAGATAC
	Calpain 5 – R	ACCTCTCCAGGGACCTTAACG
8	Rb1 – F	GAACATCGAATCATGGAATCCCT
	Rb1 – R	AGAGGACAAGCAGATTCAAGGTGAT
9	p-53 – F	GGGTTAGTTTACAATCAGCCACATT
	p-53 – R	GGGCCTTGAAGTTAGAGAAAATTCA
10	Akt 1 – F	GCACAAACGAGGGGAGTACAT
	Akt 1 – R	CCTCACGTTGGTCCACATC
11	MAPK – F	CAATGGCGGTGTGGTGTTC
	MAPK – R	AGCTCCCTTATGATCTGGTTCC
12	JNK – F	TGGACTTGGAGGAGAGAACCA
	JNK – R	CGACGATGATGATGGATGCT
13	IL-1β – F	GCAGCCATGGCAGAAGTACCTGA
	IL-1β – R	CCAGAGGGCAGAGGTCCAGGTC
14	IL-2 – F	CTGCTGGATTTACAGATGATTTGA
	IL-2 – R	TGGCCTTCTTGGGCATGT
15	IL-6 – F	CCTGACCCAACCACAAATGC
	IL-6 – R	CCTTAAAGCTGCGCAGAATGA
16	IL-10 – F	CTGGGTTGCCAAGCCTTGT
	IL-10 – R	AGTTCACATGCGCCTTGATG
17	IL-12 – F	CCTGGACCACCTCAGTTTGG
	IL-12 – R	ACGGCCCTCAGCAGGTT
18	IFN-β – F	CTCCTGTTGTGCTTCTCCACT
	IFN-β – R	GGCAGTATTCAAGCCTCCCA
19	IFN-γ – F	CTTTAAAGATGACCAGAGCATCCA
	IFN-γ – R	ATCTCGTTTCTTTTTGTTGCTATTGA
20	TNF-α – F	CCCAGGGACCTCTCTCTAATC
	TNF-α – R	ATGGCTACAGGCTTGTCACT
21	Viperin – F	CGTGAGCATCGTGAGCAATG
	Viperin – R	GCTGTCACAGGAGATAGCGA
22	Mx1 – F	CCAGCTGCTGCATCCCACCC
	Mx1 – R	AGGGGCGCACCTTCTCCTCA
23	ISG15 – F	TGGCGGGCAACGAATT
	ISG15 – R	GGGTGATCTGCGCCTTCA
24	IFITM3 – F	TCCCACGTACTCCAACTTCCA
	IFITM3 – R	AGCACCAGAAACACGTGCACT

4.3 Results

In the present study, a novel isoform of ALF was identified and characterized from the haemocytes of *M. nepa*, herein after denoted as *Mn*-ALF

4.3.1 PCR amplification, TA cloning and sequencing of *Mn*-ALF

Taxonomic identification based on amplification of a region of the mitochondrial gene, cytochrome oxidase subunit-I (GenBank ID: **KM034808**) and homology analysis by BLASTn confirmed it as *Miyakea nepa*, with 99 % similarity to *Miyakea nepa* (GenBank ID: **J229778**).

The RT-PCR of cDNA from the haemocytes of the Mantis shrimp, *M. nepa* using the ALF specific primers yielded a 372 bp amplicon (Fig. 4.2). Amplicons obtained were cloned into pGEM®-T Easy cloning vector and further transformed into *E. coli* DH5α competent cells. Insert presence was ensured by colony PCR using gene specific and vector specific primers. Approximately 513 bp (372 bp+141bp) length amplicon was obtained with vector specific primers and 372 bp with gene specific primers (Fig. 4.3a). The pGEMT-*Mn*-ALF plasmids were isolated from positive clones and confirmed by agarose gel electrophoresis (Fig. 4.3b).

The nucleotide and deduced amino acid sequences obtained by translation tool of ExPASY (Fig. 4.4) were deposited in GenBank database (GenBank ID: **KJ995817**). BLAST analysis of the 372 bp of cDNA sequence and its deduced amino acid sequence revealed that it belongs to the DUF3254 superfamily which includes the family of ALFs.

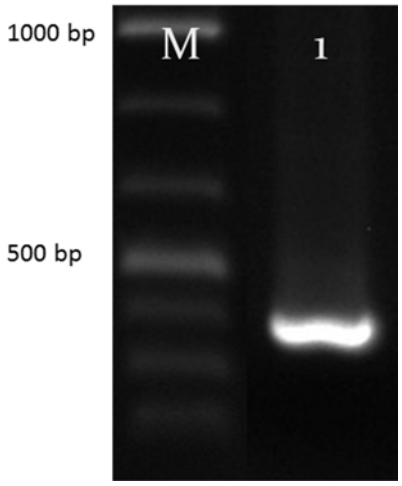

Fig. 4.2 Agarose gel electrophoretogram of PCR amplification of *Mn*-ALF primers. Lane M: 100 bp marker, Lane 1*Mn*-ALF amplicons of 372 bp

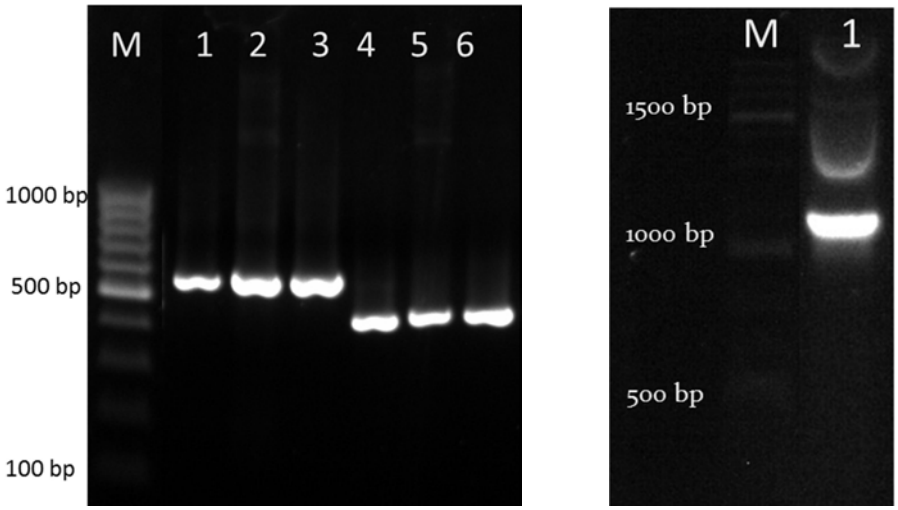

a b

Fig. 4.3 Agarose gel electrophoretogram (a) of *Mn*-ALF colony PCR, Lane M: 100 bp ladder; Lane 1-3: amplicon (513 bp) obtained for PCR with vector specific primers and Lane 4-6: amplicon (372 bp) of PCR performed using gene specific primers. (b) Plasmid extracted from positive clones of pGEMT-*Mn*-ALF vector constructs. Lane M: 1 kb marker, Lane 1: PGEM®-T Easy plasmids with Mn-ALF insert.

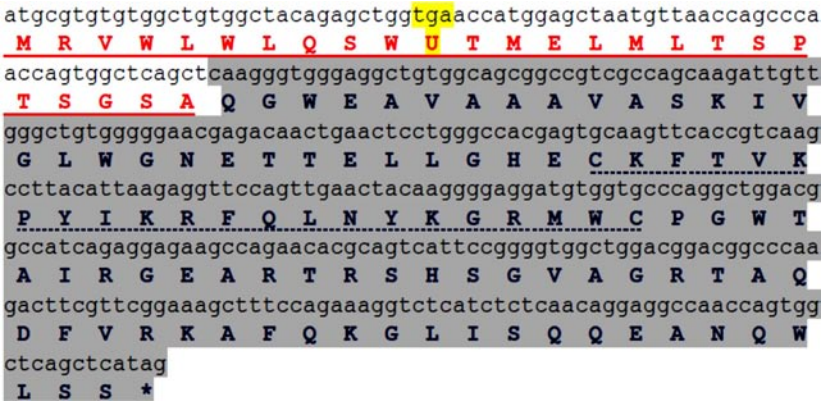

Fig. 4.4 Nucleotide and deduced amino acid sequence of the ALF isoform from the haemocyte mRNA transcripts of *M. nepa* – *Mn*-ALF (GenBank ID: **KJ995817**). Red underlined portion specifies the 25 amino acid signal peptide within which, SeC encoding TGA and its amino acid single letter code 'U' is highlighted in yellow. The bioactive mature peptide is highlighted in grey, and dashed underlined region within the mature peptide is the LPS binding domain.

4.3.2 Sequence analysis and characterization using bioinformatics tools

Evaluation of amino acid sequence homology to different crustacean ALFs and limulid ALFs showed that *Mn*-ALF possess 80 % identity to *M. rosenbergii* ALF (GenBank ID **AEP84102.1**) and *F. indicus* ALF (GenBank ID **ADE27980.1**) followed by 69 %, 62 %, 45 %, 40 % and 36 % identity to *Homarus americanus* ALF (GenBank ID **ACC94268.1**), *Procambarus clarkii* ALF (GenBank ID **ADX60063.1**), *Portunus trituberculatus* ALF (GenBank ID **ADU25083.1**), *Tachypleus tridentatus* (GenBank ID **AAK00651.1**)and *Limulus polyphemus* (GenBank ID **1307201A**) respectively.

SignalP analysis of 123-mer predicted the existence of 25 amino acid length SP with a highly hydrophobic core region and a putative

cleavage site after 25th amino acid (SA_{25}-$Q_{26}G$) which delineates the highly cationic mature peptide of 98 amino acid residues (Fig. 4.5).

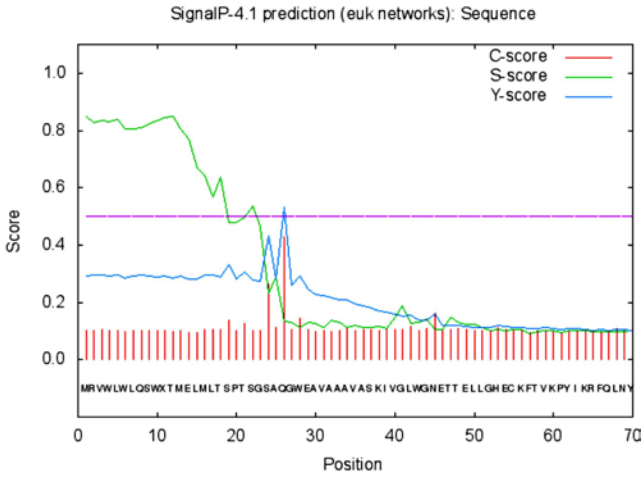

Fig.4.5 Signal peptide analysis of *Mn*-ALF as predicted by the SignalP 4.1 server.

The *Mn*-ALF was found to have a predicted molecular weight of 13.942 kDa, net charge of +7 and a theoretical isoelectric point (*p*I) of 9.93. For mature peptide region, the aforesaid parameters were 10.998 kDa, +7 and 9.93 respectively (PROTPARAM tool). Cationicity of the mature peptide was mainly contributed by 14 positive amino acid residues (Lys + Arg) against 7 negative residues (Asp + Glu). Antimicrobial activity prediction using APD envisages this peptide as a potent AMP with a protein-binding potential (Boman index) and Wimley-White whole-residue hydrophobicity as 1.69 kcal/mol and 15.56 kcal/mol respectively. The estimated half-life of *Mn*-ALF was anticipated to be 30 h (mammalian reticulocytes, *in vitro*), >20 h (yeast, *in vivo*) and >10 h (*E. coli, in vivo*).

Simultaneously the instability index (II) of *Mn*-ALF was computed to be 38.45 which categorize the protein as stable. Analysis of proposed LPS

binding domain of *Mn*-ALF (C_{55}KFTVKPYIKRFQLNYKGRMWC_{76}) based on amphipathicity using HeliQuest tool disclosed that it is composed of 22 amino acids of which 45.45 % is contributed by polar residues and the rest by non-polar residues establishing a hydrophobic face with 'FVYI' residues and thus having a hydrophobicity of 0.498 H with a +6 net charge confirming the antimicrobial activity (Fig. 4.6).

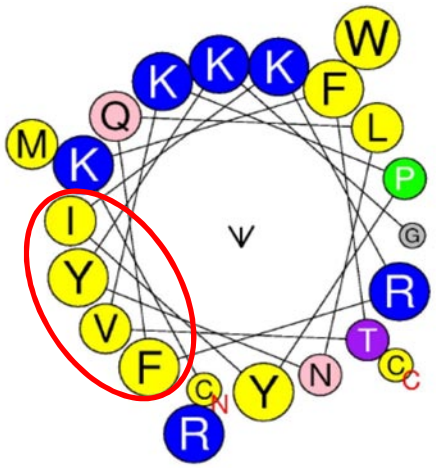

Fig. 4.6 The helical wheel diagram of *M. nepa* – *Mn*-ALF (GenBank ID: **KJ995817**) LPS domain predicted using Heliquest online tool. The structure was built to identify the amphipathicity of the LPS binding domain. The Amino and Carboxy terminal ends are mentioned as N and C, respectively. The expected hydrophobic face FVYI is shown in the red circle.

Secondary structure prediction of mature peptide of *Mn*-ALF using PSIPRED tool found that it consists of one α-helix in the hydrophobic N-terminal region and the other two α-helices towards C-terminus (Fig. 4.7). Spatial structure of *Mn*-ALF was constructed based on homology modelling using NMR structure of *P. monodon* rALF-Pm3 as template since it shared 89.9 % similarity with *Mn*-ALF (Fig. 4.8). Peptide

structure predicted in PyMOL using the pdb file (SMTL id: 2job.1) as template consisted of three α-helices packed against four strands of β-sheets.

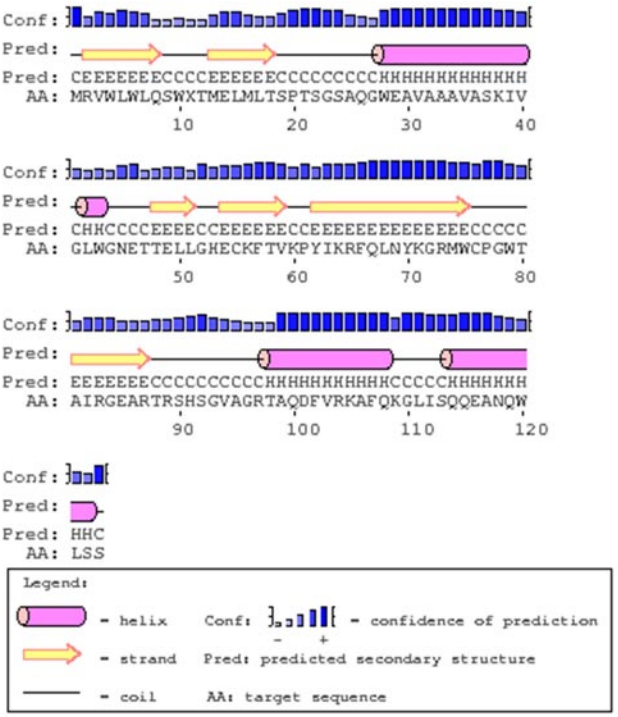

Fig 4.7 Secondary structure of *M. nepa, Mn*-ALF (GenBank ID: **KJ995817)** predicted using PSIPRED server. The α-helix region is shown in pink coloured cylinders, β-strand is shown in yellow arrows and the coil region is shown in black lines.

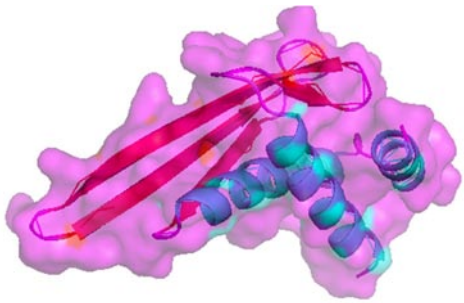

Fig.4.8 Spatial structure of *M. nepa, Mn*-ALF (GenBank ID: **KJ995817)** created with the PyMol software using the pdb data generated by SWISSMODEL server.

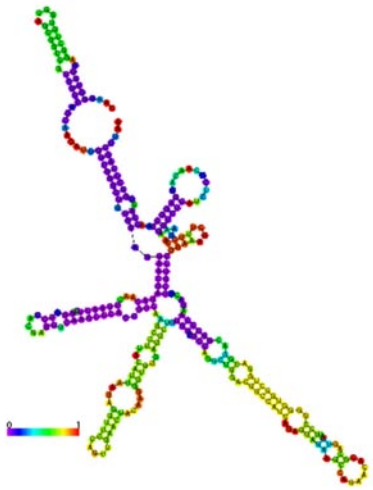

Fig. 4.9 Predicted secondary structure of *M. nepa, Mn*-ALF (GenBank ID: **KJ995817)** RNA with minimal free energy prediction.

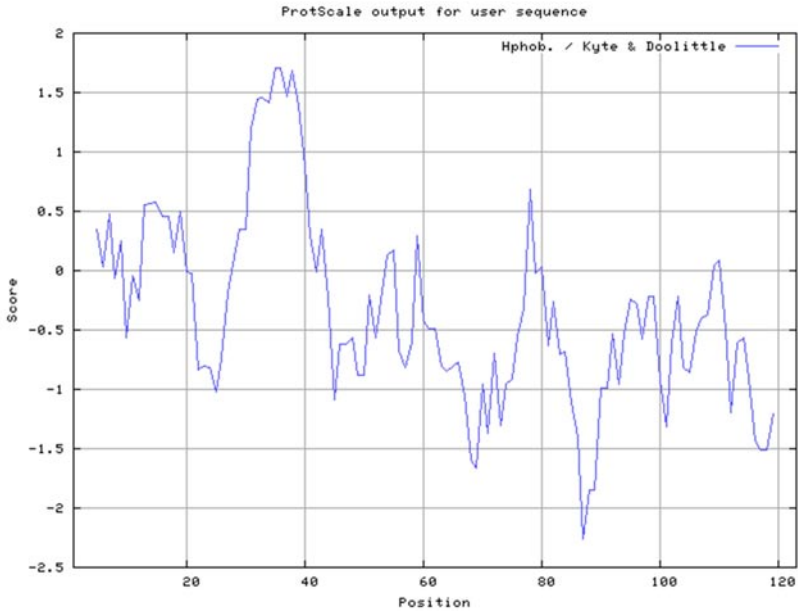

Fig. 4.10 Kyte-Doolittle plot showing hydrophobicity of *M. nepa, Mn*-ALF (GenBank ID: **KJ995817)**. The peaks above the score (0.0) indicate the hydrophobic nature of the predicted protein.

4.3.3 Phylogenetic analysis of *Mn*-ALF

Multiple alignment performed for *Mn*-ALF with representatives of ALF from limulids and decapod crustaceans revealed the existence of conserved regions within the sequence (Fig. 4.11). Detailed analysis of aligned sequences displayed that the amino acid sequences in SP region are not conserved when compared to that of mature peptide.

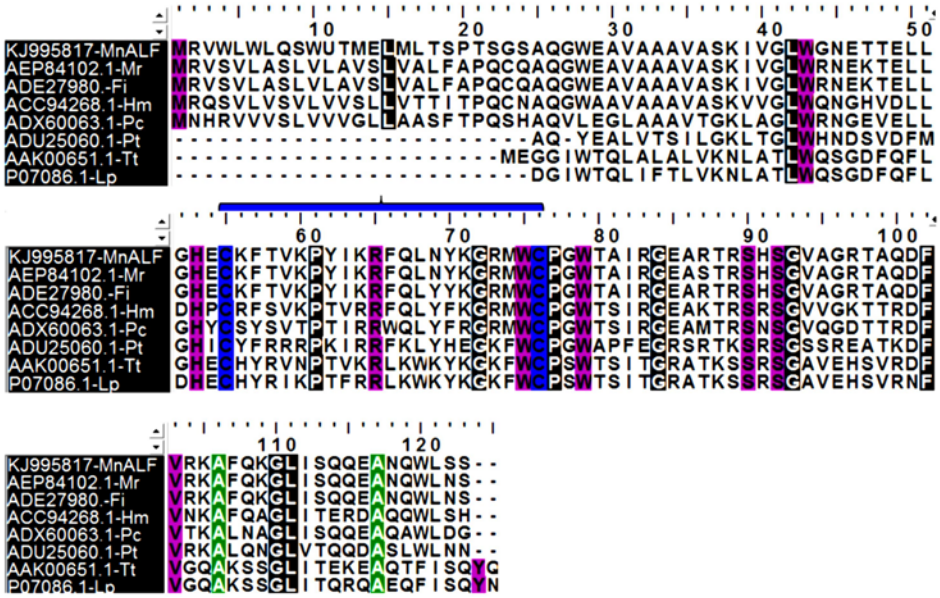

Fig. 4.11 Multiple alignment of amino acid sequence of the *M. nepa, Mn*-ALF (**KJ995817**) with other crustacean and limulid ALFs obtained using BioEdit. *Macrobrachium rosenbergii* ALF (GenBank ID **AEP84102.1),** *Fenneropenaeus indicus* ALF (GenBank ID **ADE27980**), *Homarus americanus* ALF (GenBank ID **ACC94268.1**), *Procambarus clarkii* ALF (GenBank ID **ADX60063.1**), *Portunus trituberculatus* ALF (GenBank ID **ADU25060.1**), *Tachypleus tridentatus* (GenBank ID **AAK00651.1**) and *Limulus polyphemus* (GenBank ID **P07086.1**) The LPS-binding domains are enclosed within a blue bracket. The conserved residues are highlighted with background colours.

Evolutionary history of *Mn*-ALF with other 38 ALF amino acid sequences of decapod crustaceans were inferred by constructing phylogenetic tree using NJ-method (Fig. 4.12).

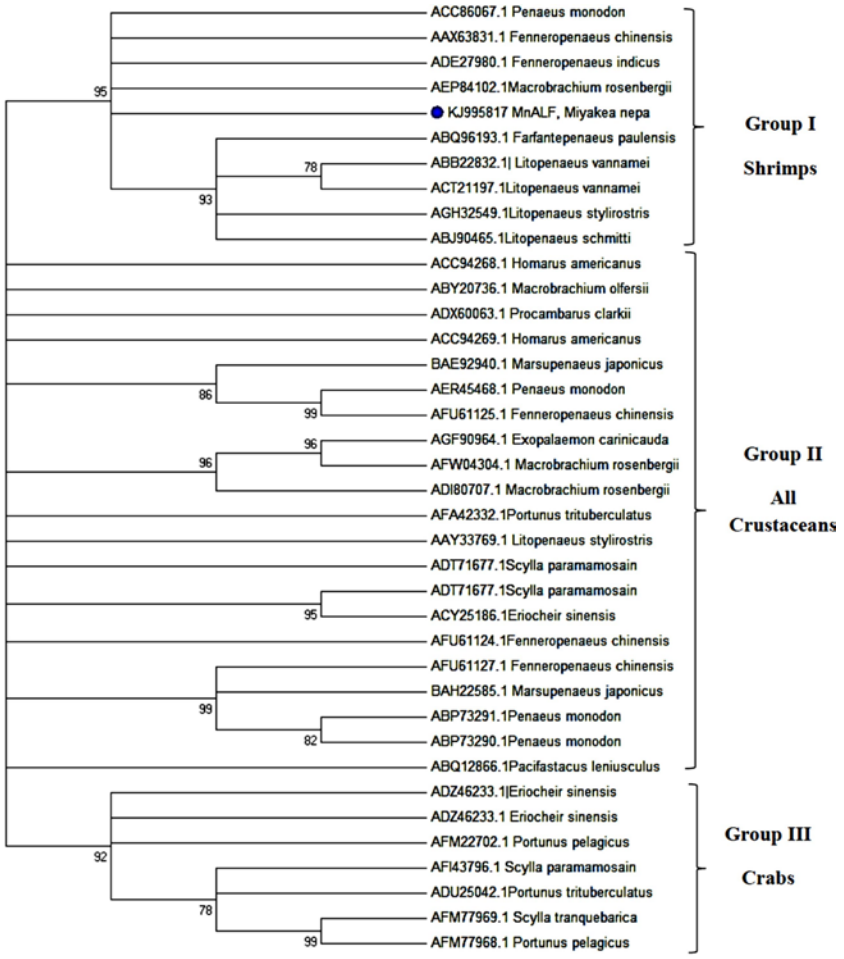

Fig. 4.12 A bootstrapped neighbor-joining tree obtained using MEGA 6 illustrating relationships between the deduced amino acid sequences of the *Mn*-ALF (**KJ9958170**) with other ALFs of decapod crustaceans. Values at the node indicate the percentage of times the particular node occurred in 1000 trees generated by bootstrapping the original deduced protein sequences. Branches corresponding to partitions reproduced in less than 75 % bootstrap replicates are collapsed.

4.3.4 Peptide synthesis and molecular characterization

The putative LPS binding domain of *Mn*-ALF with extra amino acid residue (ECKFTVKPYIKRFQLNYKGRMWCP), was identified by multiple sequence alignment with other crustacean ALFs (Fig. 4.11) and selected for chemical synthesis. The peptide was synthesized from C-terminus to N-terminus of the peptide sequence with a Fluorescein isothiocynate (FITC) labeling. The N-terminal residue of peptide was blocked by acetylation, and the C-terminal residue was amidated to increase the peptide stability. Also a disulfide bond was incorporated between the cysteine residues of peptide for cyclization. The synthetic peptide was supplied at >95 % purity in lyophilized form and was dissolved in sterile water to minimize the LPS contamination (Somboonwiwat et al., 2005) and stored at -20 °C. Herein after the synthetic peptide will be mentioned as MNA-LBD

The synthetic MNA-LBD is a cationic peptide with a net charge of +5 and consists of 24 amino acids with a theoretical mass and *p*I of 3.036 kDa and 9.79, respectively. Cationicity was contributed by six positively charged residues (Arg + Lys) and one negatively charged residue (Asp + Glu). *In silico* analysis of antimicrobial activity using the APD3 reveals that MNA-LBD is a potent AMP with a hydrophobic ratio of 37 %; boman index of 1.91 kcal/mol and the Wimley-White whole-residue hydrophobicity of 2.15 kcal/mol. The helical property prediction and amphipathicity analysis was done using Heliquest tool (Fig. 4.13) and the synthetic MNA-LBD was found to be alpha helical peptide with a hydrophobicity of 0.460, and the FVPYI region of the helix forming the hydrophobic face involved in the microbial membrane interaction.

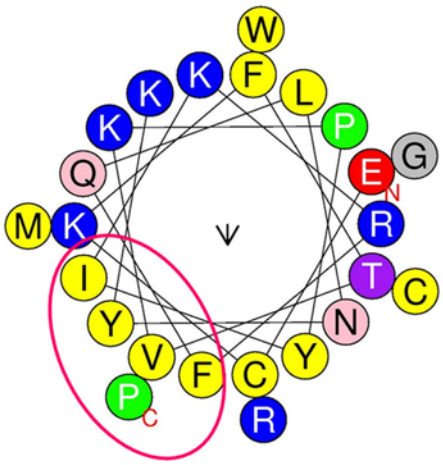

Fig. 4.13 The helical wheel diagram of synthetic peptide MNA-LBD predicted using Heliquest online tool. The structure was built to identify the amphipathicity of the LPS binding domain. The amino and carboxy terminal ends are mentioned as N and C respectively. The expected hydrophobic face FVPYI is shown in the red circle.

4.3.5 Determination of molecular mass and purity of synthetic MNA-LBD

The molecular weight of the synthetic peptide MNA-LBD (3592.31 Da) was confirmed by ESI mass spectroscopy. The ESI mass spectrum of MNA-LBD is shown in Fig. 4.14. The mass spectrum depicts the mass to charge ratio (m/z) from 400 to 1800 of all the ionized molecules present in the sample. The most abundant ion in the spectrum is seen at a mass to charge ratio of 898.98. This m/z matches the MNA-LBD ionized to +4 (rounded off MW = 3592.31 Da + 4H+ = 3596.31). The mass to charge ratio is thus 3596.31/4 = 899.07. The other comparatively abundant ion recognised to MNA-LBD was m/z of 1198.13 ionized to +3 (round off MW = 3592.31 Da + 3H+ = 3595.31) and thus the m/z is 2450/5 = 1198.43.

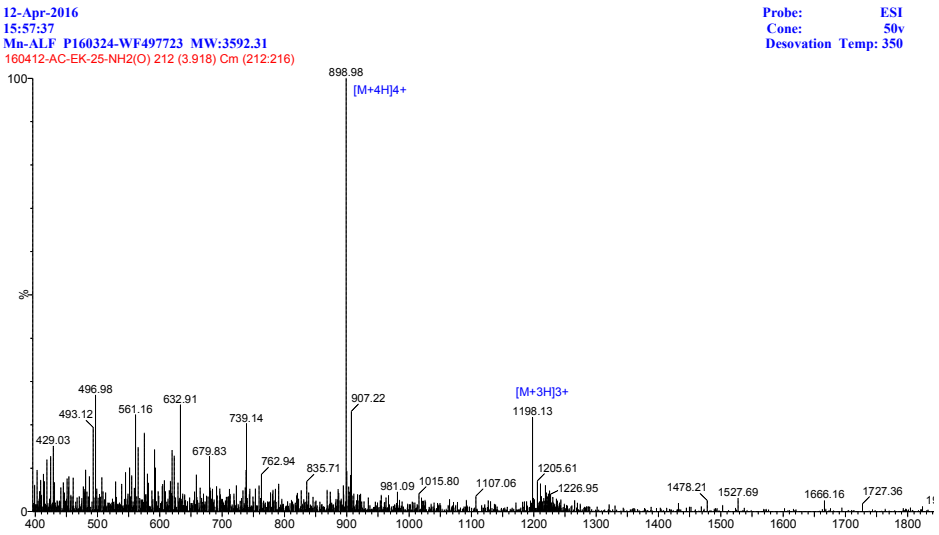

Fig. 4.14 ESI Mass Spectrum of Synthetic MNA-LBD, Most abundant ion in the spectrum is seen at m/z of 898.98 [M+4H]4+ followed by 1198.13 [M+3H]3+.

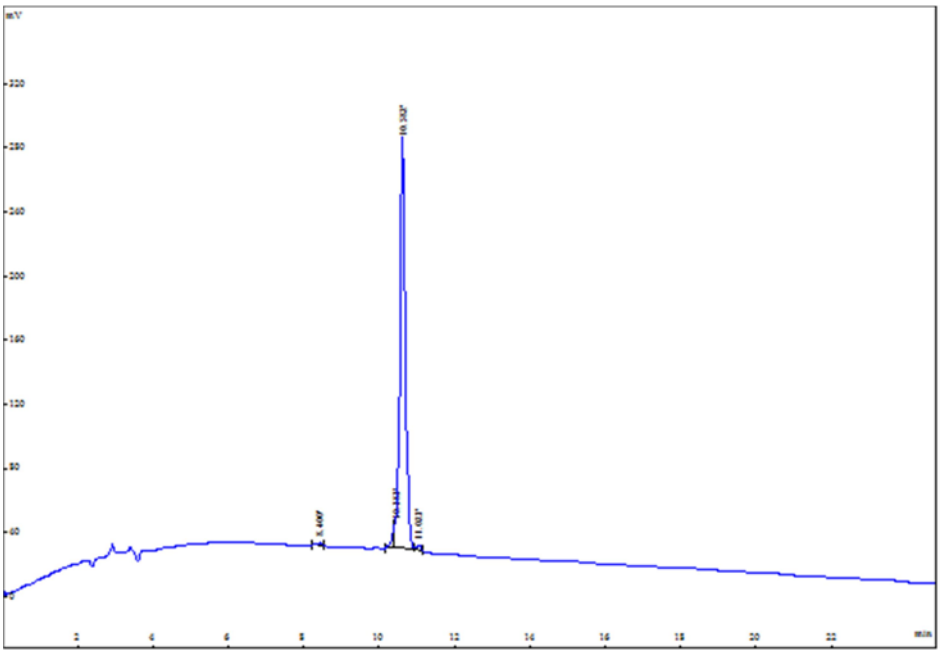

Fig. 4.15 HPLC chromatogram of synthetic MNA-LBD showing a major peak at retention time of 10.582 min.

Since the synthetic peptide had the correct molecular mass, the peptide was checked for purity by HPLC. The HPLC chromatogram obtained for synthetic MNA-LBD is shown in Fig. 4.14. The peptide was found to be >95 % pure by the percent area of the main peak at retention time 10.582 min as seen in Fig. 4.15.

4.3.6 Haemolytic activity

Synthetic MNA-LBD peptide at different concentrations (400 µM to 3.125 µM) was tested for haemolytic activity towards human RBCs. After incubation for 1 h, weak haemolysis (around 9 % to 15 %) was observed from a concentration of 200 µM – 400 µM peptide. The reference peptide Mellitin, exhibited about 71 % and 85 % haemolytic activity at 200 µM and 400 µM. Thus the peptide showed only weak haemolysis in hRBCs even at a higher concentration (Fig. 4.16).

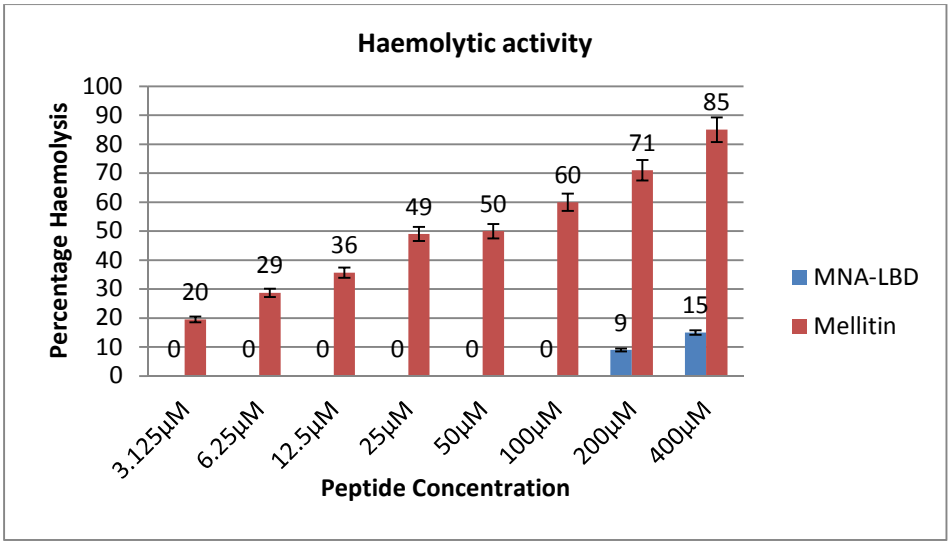

Fig. 4.16 Haemolytic activity of the synthetic MNA-LBD and Mellitin in human RBCs at various concentrations.

4.3.7 Antimicrobial activity

Antimicrobial activity of the synthetic peptide, MNA-LBD was tested against two Gram-positive and nine Gram-negative bacteria by broth microdilution assay from a concentration of 50 µM to 1.562 µM. The antibacterial activity of synthetic MNA-LBD against the tested bacteria is shown in Fig. 4.17 (a-k). Synthetic peptide, MNA-LBD exhibited antibacterial activity against all tested pathogens. The peptide displayed significant activity against Gram-negative *E. coli* (MIC and MBC of 25µM). In case of *B. cereus, P. aeruginosa, E. tarda, V. parahaemolyticus* and *V. alginolyticus,* the MIC value was found to be 50 µM, but the MBC value was found to be greater than the highest concentration tested. Other pathogens were also found to be sensitive to MNA-LBD, but the MIC and MBC values were found to be >50 µM.

Inhibition level of other pathogens were 75 % for *S. aureus,* 55 % for *A. hydrophila,* 78 % for *V. cholera,* 85% for *V. fluvialis* and 82 % for *V. vulnificus* respectively (Fig. 4.17 (a-k)). Bactericidal activity of *E. coli, B. cereus, P. aeruginosa, E. tarda, V. parahaemolyticus* and *V. alginolyticus* was assessed by plating cultures and counting the CFUs after 24 h incubation. The result showed that the peptide exhibited bactericidal activity against *E. coli* at 25 µM (MBC) and for others it was found to be greater than 50 µM. These results proposed that the growth inhibitory properties of the peptide are due to bactericidal activity.

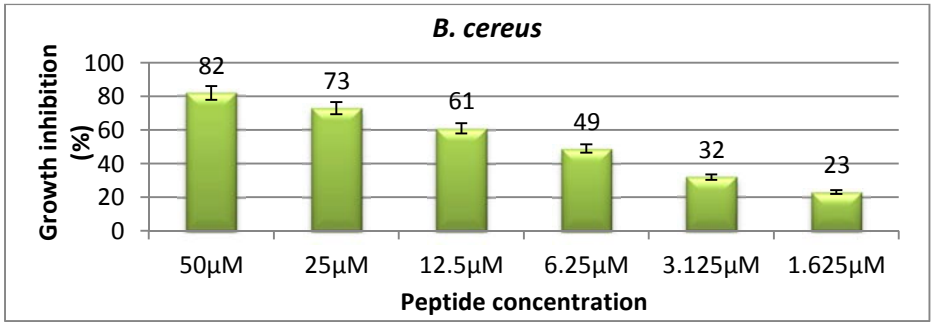
B. cereus
Growth inhibition (%)
100
80
60
40
20
0
82
73
61
49
32
23
50µM
25µM
12.5µM
6.25µM
3.125µM
1.625µM
Peptide concentration

(a)

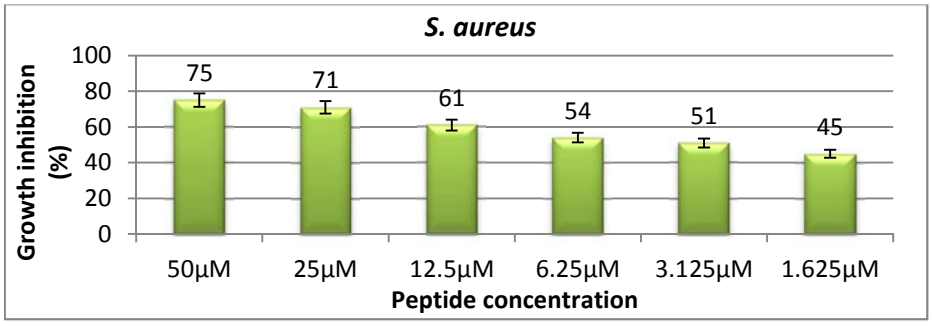
S. aureus
Growth inhibition (%)
100
80
60
40
20
0
75
71
61
54
51
45
50µM
25µM
12.5µM
6.25µM
3.125µM
1.625µM
Peptide concentration

(b)

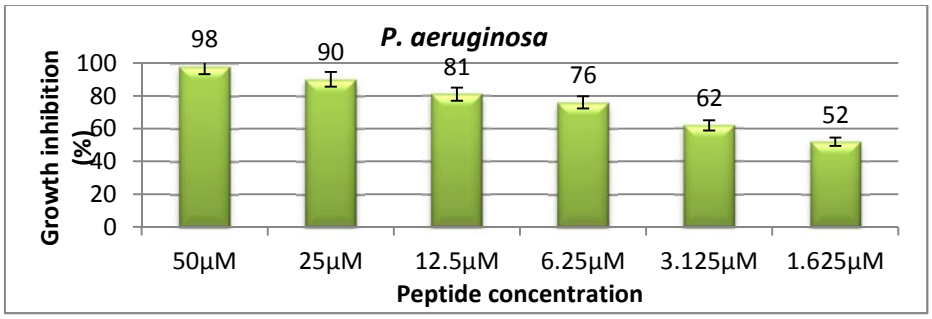
P. aeruginosa
Growth inhibition (%)
100
80
60
40
20
0
98
90
81
76
62
52
50µM
25µM
12.5µM
6.25µM
3.125µM
1.625µM
Peptide concentration

(c)

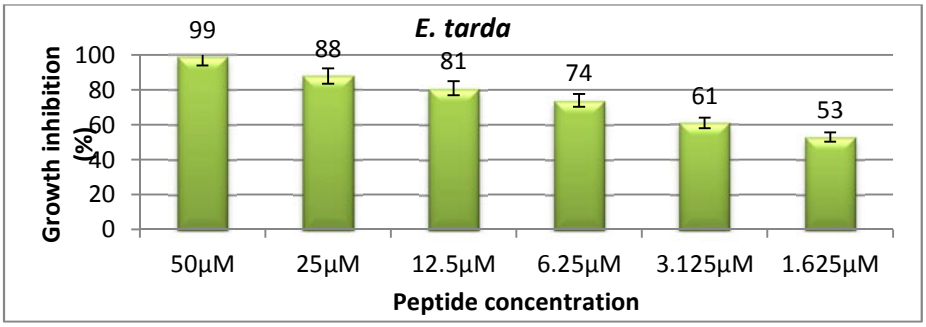
E. tarda
Growth inhibition (%)
100
80
60
40
20
0
99
88
81
74
61
53
50µM
25µM
12.5µM
6.25µM
3.125µM
1.625µM
Peptide concentration

(d)

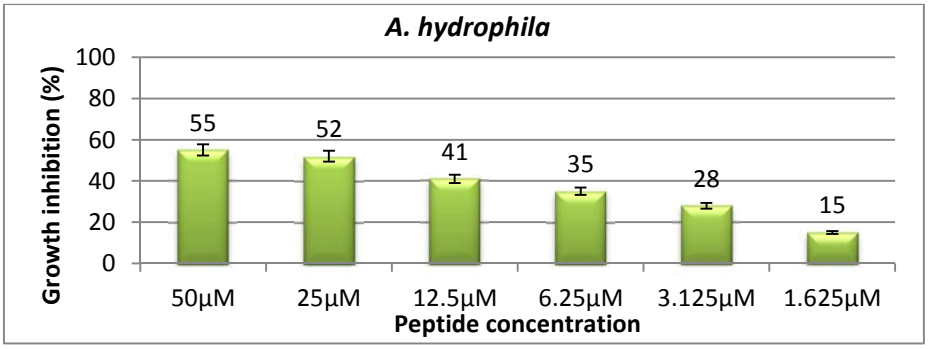
A. hydrophila
Growth inhibition (%)
100
80
60
40
20
0
55
52
41
35
28
15
50µM
25µM
12.5µM
6.25µM
3.125µM
1.625µM
Peptide concentration

(e)

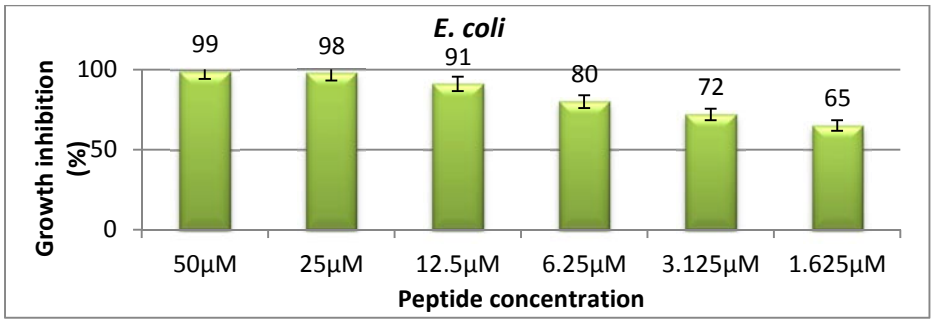
E. coli
Growth inhibition (%)
100
50
0
99
98
91
80
72
65
50µM
25µM
12.5µM
6.25µM
3.125µM
1.625µM
Peptide concentration

(f)

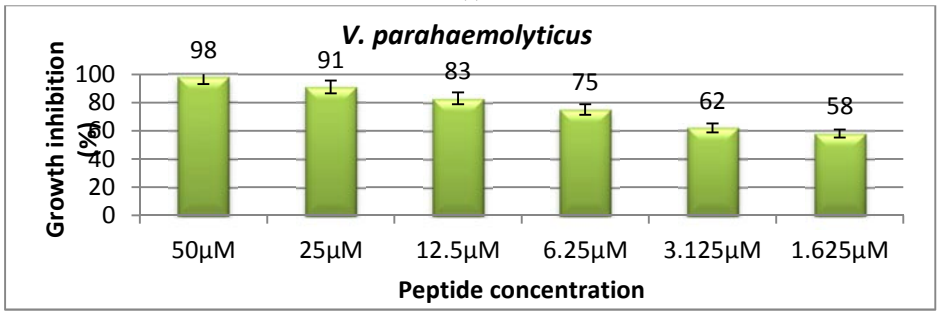
V. parahaemolyticus
Growth inhibition (%)
100
80
60
40
20
0
98
91
83
75
62
58
50µM
25µM
12.5µM
6.25µM
3.125µM
1.625µM
Peptide concentration

(g)

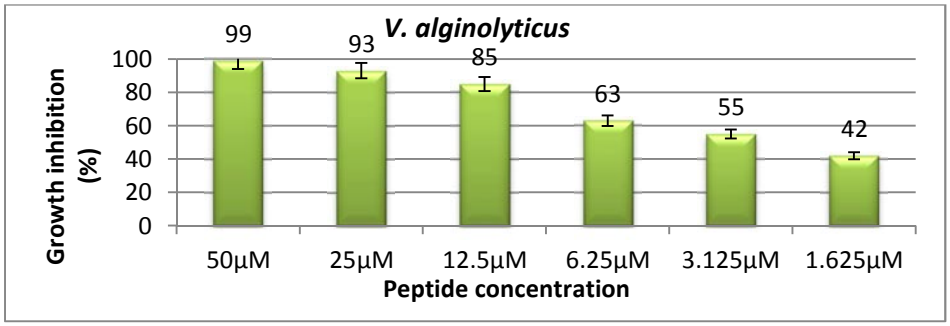
V. alginolyticus
Growth inhibition (%)
100
80
60
40
20
0
99
93
85
63
55
42
50µM
25µM
12.5µM
6.25µM
3.125µM
1.625µM
Peptide concentration

(h)

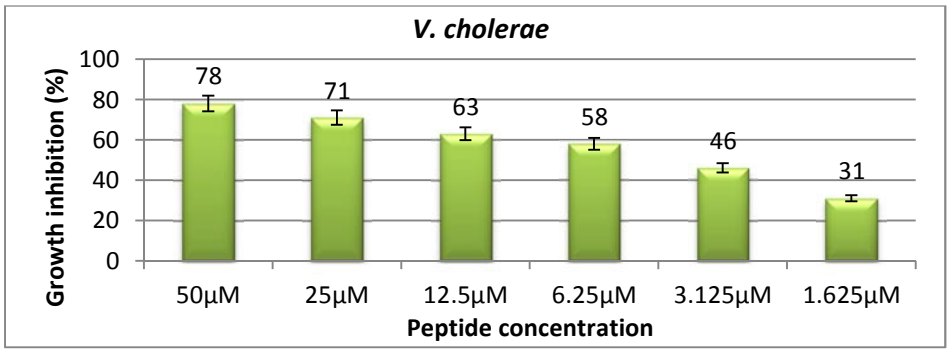

(i)

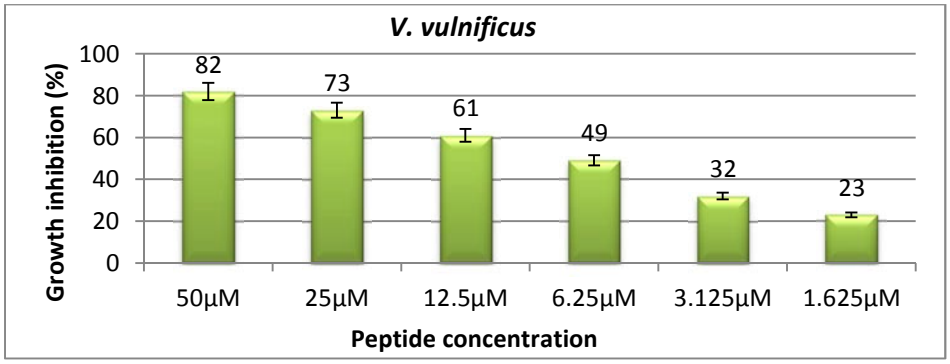

(j)

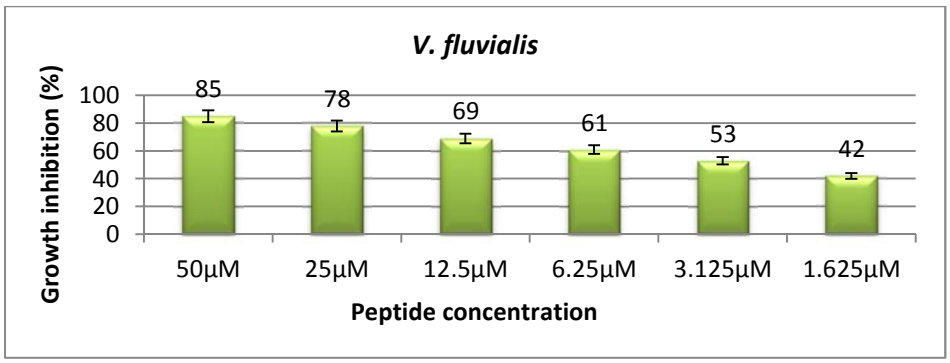

(k)

Fig. 4.17 (a-k) Antibacterial activity of synthetic MNA-LBD against the bacterial pathogens at various concentrations

4.3.8 PI staining

The PI stained image of MNA-LBD peptide treated *E. coli* were detected as red cells due to the intercaltion of PI with bacterial DNA in dead cells (Fig. 4.18). Since the peptide is labelled with FITC tag, the presence of peptide in the cells could be observed as green. Pictures were taken at two different filters for PI and FITC on the same field. Most of the cells in green also appeared red, which confirms that the bacterial death is due to peptide interaction. Thus the mode of action could be mainly due to membrane pore formation.

Untreated control

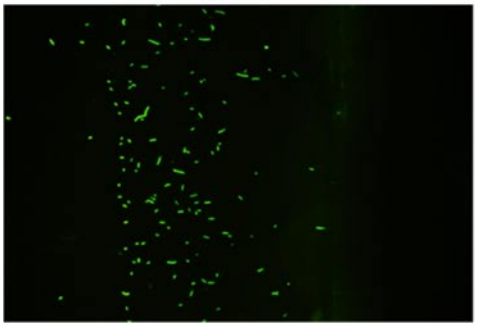

MNA-LBD treated *E.coli* under FITC filer

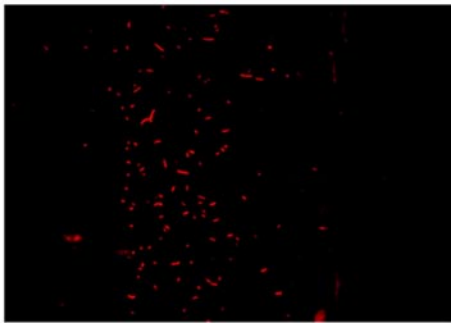

MNA-LBD treated *E.coli* under PI filer

Fig. 4.18 PI stained untreated control *E. coli* and synthetic MNA-LBD treated *E. coli* under FITC filter and PI filter (magnification 100 x).

4.3.9 SEM analysis

Morphological changes in MNA-LBD treated *E. coli* was analysed by scanning electron microscopy (SEM). On contrary to untreated control, *E. coli* cells treated with MNA-LBD was noticed with blebbing of membrane and also there was marked extensive damage to bacterial membrane with cytoplasmic content loss (Fig. 4.18).

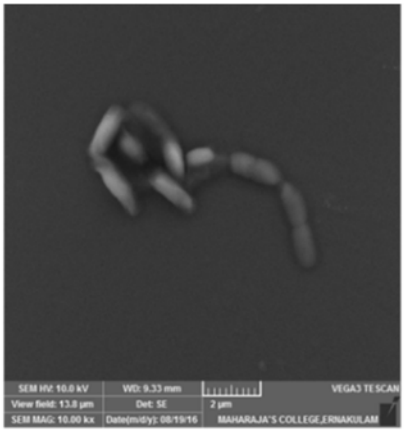

Untreated control

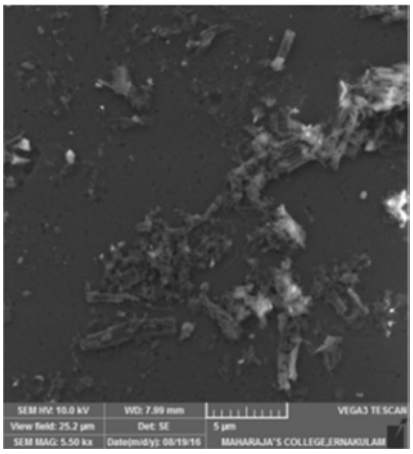

MNA-LBD treated *E.coli*

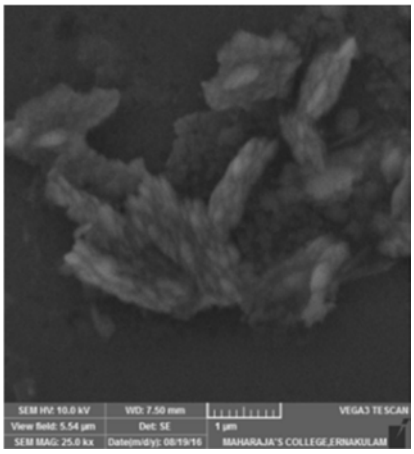

MNA-LBD treated *E.coli*

Fig. 4.19 SEM image of untreated control *E. coli* and synthetic peptide, MNA-LBD peptide treated *E. coli* showing the leakage of cytoplasmic content and blebbing.

4.3.10 DNA Binding assay

In addition to the membrane disruptive mode of bacterial killing, the MNA-LBD peptide was tested for its DNA binding activity. DNA binding activity of synthetic MNA-LBD was tested with 50 ng of pUC-18 plasmid vector from a concentration of 200 µM – 3.125 µM. Peptide exhibited remarkable DNA binding from a concentration of 200 µM to 25 µM and the retarded plasmid DNA could be clearly seen when compared to the untreated plasmid control. The agarose gel electrophoretogram showing the retarded plasmid DNA in the peptide treated and non-retarded plasmid DNA in untreated group is evident in Fig. 4.20.

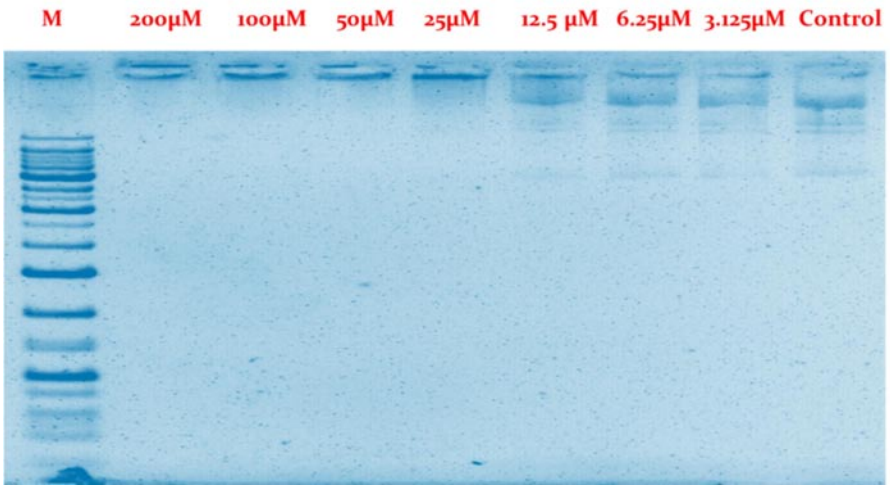

Fig. 4.20 Agarose gel electrophoretogram of DNA binding assay of synthetic MNA-LBD using pUC-18 vector with various concentration of peptide. Lane M: 1 kb ladder, Lane 1-7: 200 µM to 3.125 µM concentration of peptide with 50 ng of pUC-18, Lane 8: Control untreated plasmid.

4.3.11 *In vitro* cytotoxicity assay

Cell viability of MNA-LBD treated HEp-2 and NCI-H460 cell lines were tested from 200 µM to 1.625 µM by employing XTT assay. The *in vitro* cytotoxic activity displayed by MNA-LBD peptide against HEp2 and NCI-H460 cell lines is represented in Fig. 4.21. The peptide was found to be cytotoxic to both cell lines at the highest concentration tested. A growth inhibition of 92 % was observed for NCI-H460 and 86 % for HEp-2 cell lines at 200 µM. The IC_{50} of synthetic peptide against HEp2 cells was estimated to be 34.317±43.901 µM and for NCI-H460, 28.018±21.725 µM.

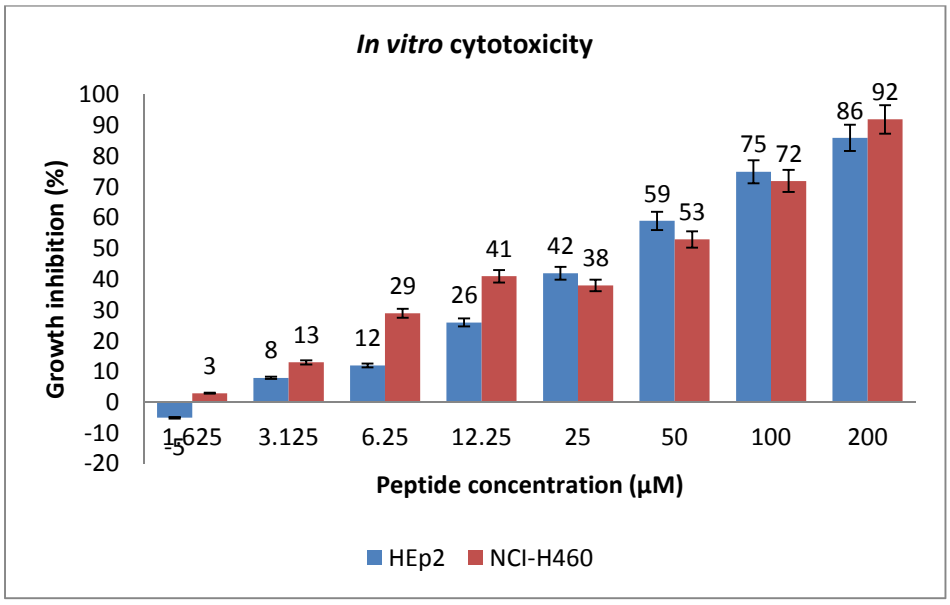

Fig. 4.21 *In vitro* cytotoxicity of MNA-LBD in HEp2 and NCI-H460 cells at various tested concentrations

4.3.12 Anticancer activity

4.3.12.1 *Relative gene expression analysis of cancer related genes in MNA-LBD treated NCI-H460 lung cancer cells*

In vitro anticancer activity of synthetic peptide MNA-LBD was tested against NCI-H460 non-small cell lung cancer cell lines. Activity was analysed by treating the cell lines with two concentrations of the peptide viz., 25 µM and 50 µM. Relative gene expression of peptide treated NCI-H460 cell lines was studied using quantitative real-time PCR (RT-PCR or qPCR) and found to be expressed differentially at the tested concentrations with respect to the untreated control (Fig. 4.22 a-e). Significant up-regulation of Caspase-3, Caspase-9, IK-BA and Rb-1 could be observed. Noticeable up-regulation of Bax gene expression and downregulation of Bcl2 was also detected. Compared to the control group, an increased gene expression was noticed for non-caspase protease, Calpain-5 and cell cycle associated genes viz., JNK, Akt 1 and MAPK-1. The immune genes (IFN-c, IL-1b, IL-2, IL-6, IL-10, Il-12) and IFN induced genes (ISIG, IFIT-M3) also showed marked up-regulation., Down-regulation of Cathepsin-G, Mx1, Viperin, IFN-b and TNF-α were noteworthy in NCI-H460 cells on peptide treatment. Thus the peptide, MNA-LBD could exhibit anticancer activity in NCI-H460 cells.

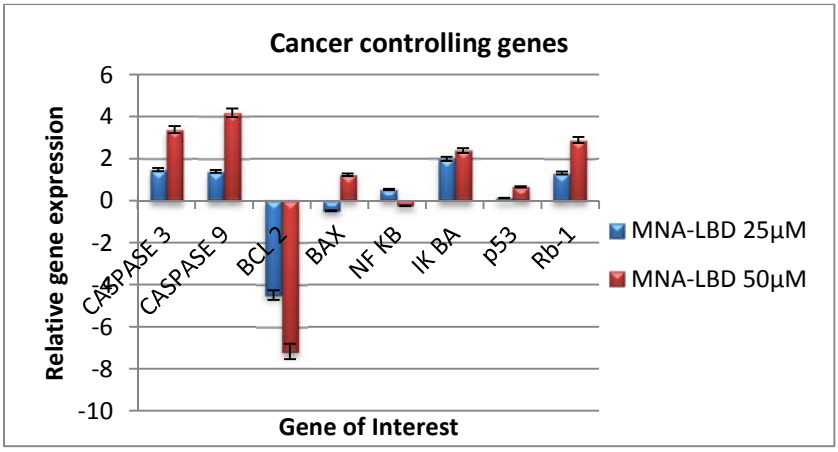
Cancer controlling genes
Relative gene expression
6
4
2
0
-2
-4
-6
-8
-10
CASPASE 3
CASPASE 9
BCL 2
BAX
NF KB
IK BA
p53
Rb-1
Gene of Interest
MNA-LBD 25µM
MNA-LBD 50µM

(a)

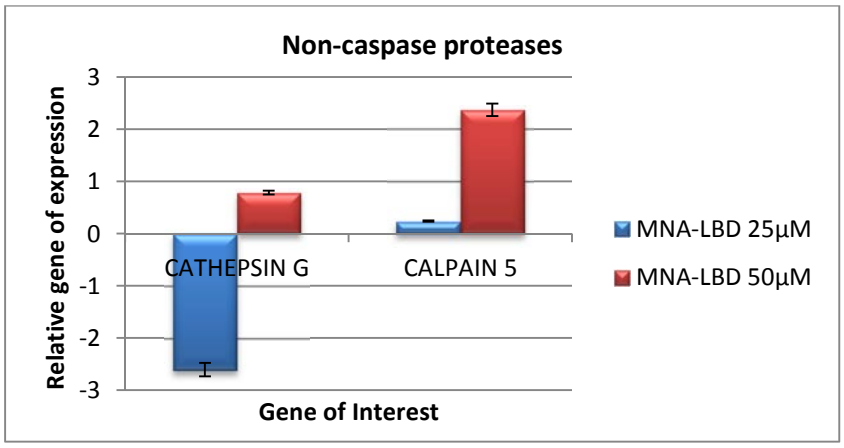
Non-caspase proteases
Relative gene of expression
3
2
1
0
-1
-2
-3
CATHEPSIN G
CALPAIN 5
Gene of Interest
MNA-LBD 25µM
MNA-LBD 50µM

(b)

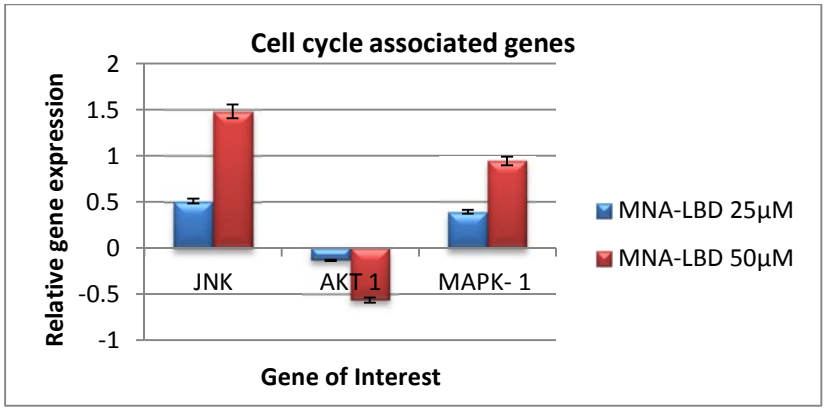
Cell cycle associated genes
Relative gene expression
2
1.5
1
0.5
0
-0.5
-1
JNK
AKT 1
MAPK- 1
Gene of Interest
MNA-LBD 25µM
MNA-LBD 50µM

(c)

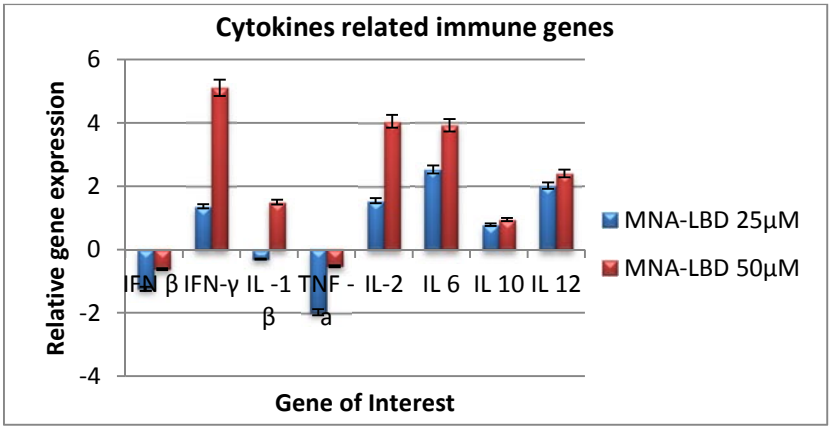

(d)

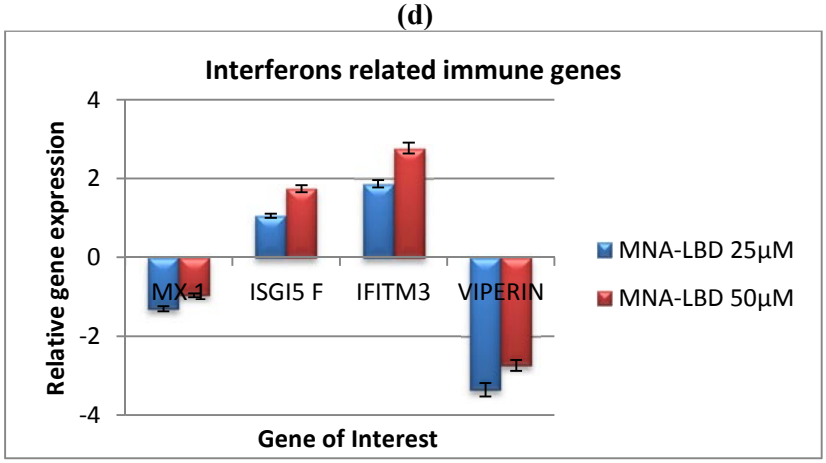

(e)

Fig. 4.22 (a-e) Relative gene expression profile of different cancer related genes using real time PCR and the $\Delta\Delta C_T$ method in MNA-LBD peptide treated in NCI-H460 cell lines.

4.3.12.2 *Relative gene expression of cancer related genes in MNA-LBD treated HEp-2 pharyngeal cancer cells*

The synthetic peptide, MNA-LBD was screened for its *in vitro* anticancer activity in HEp-2 cell lines using 25 µM and 100 µM of peptide. Relative expression of different genes controlling and regulating cancer was analysed by qPCR. Peptide treatment in HEp-2 cells were found to be involved in the up-regulation of cancer controlling genes viz.,

Bax, Caspase-3, Caspase-9, p53, Ik-BA and Rb1. The gene expression level of Cathepsin-G, Calpain-5 and the non-caspase proteases were found to be higher. Enhanced expression of cell cycle associated genes (JNK, Akt-1, ISG15), immune gens (IFN-c, IFn-b, TNF-α) and interleukins (IL-2, IL-6, IL- 10, IL-12) were also detected. Down-regulation of cancer controlling Bcl2 and interleukin IL-1b were observed when compared to untreated control (Fig. 4.23).

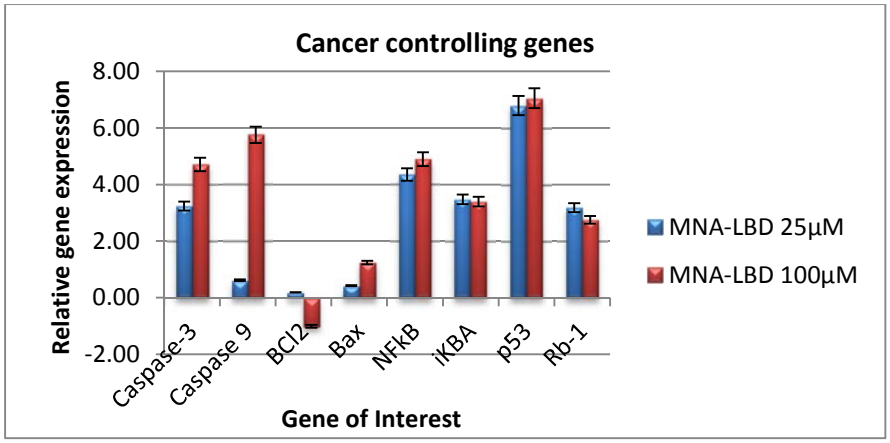

(a)

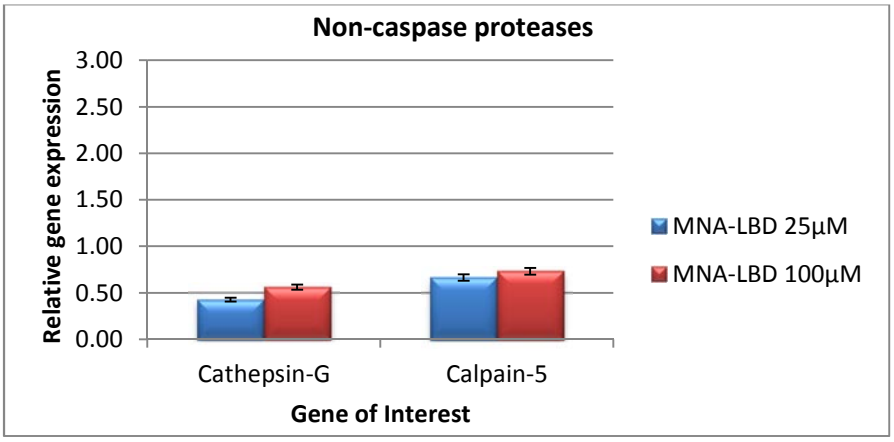

(b)

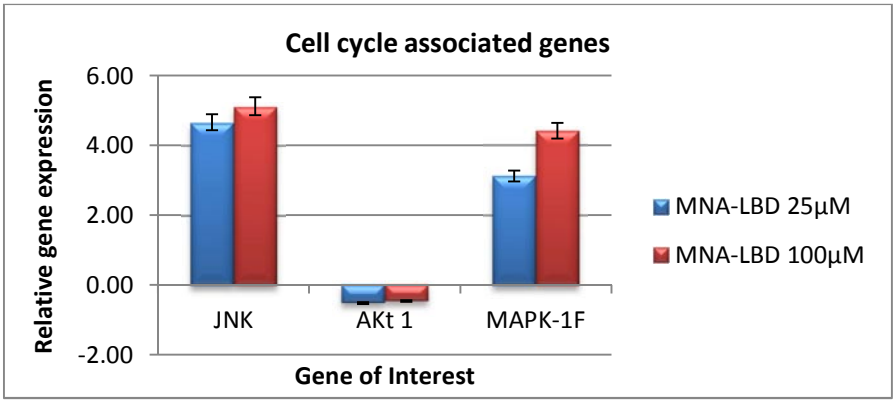

(c)

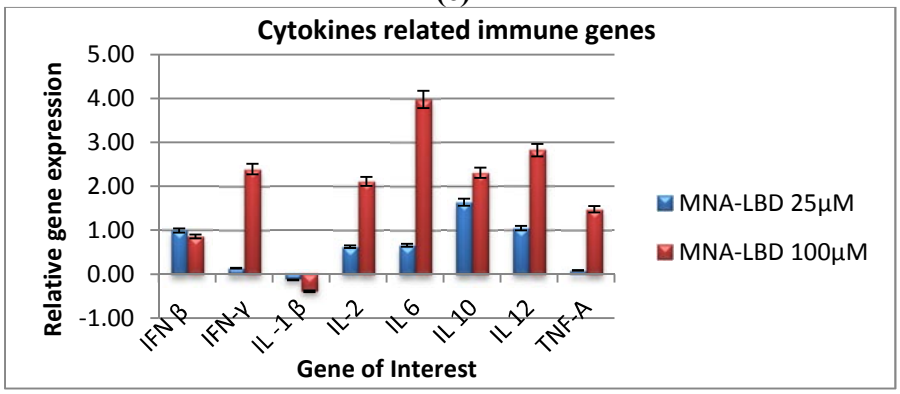

(d)

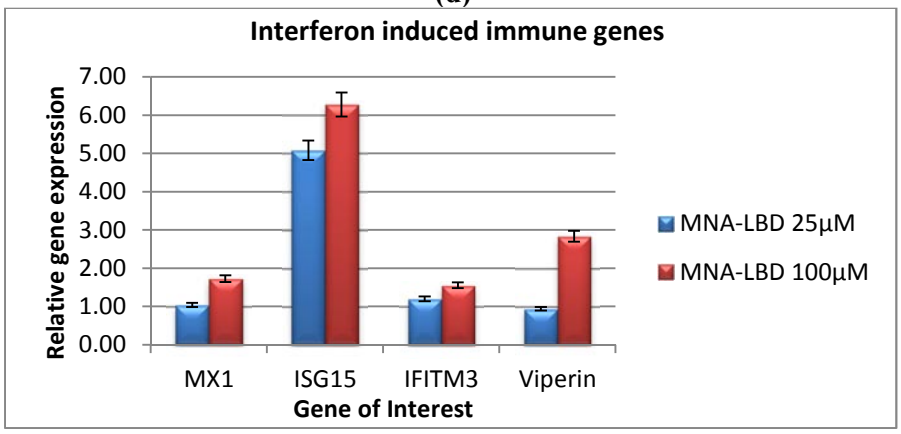

(e)

Fig. 4.23 (a-e) Relative gene expression profile of different cancer related genes using real time PCR and the $\Delta\Delta C_T$ method in MNA-LBD peptide treated in HEp-2 cell lines.

4.4 Discussion

Indiscriminate use of antibiotics has resulted in the emergence of multi-drug resistant pathogens. Thus, understanding the significance of biological and biomedical application of antimicrobial peptides (AMPs) might be promising with respect to resistance-free therapies for contagious diseases. AMPs are small amphipathic molecules, comprehending cationic and hydrophobic amino acids in higher proportion and thus through non-specific interactions with the membrane lipids, the AMPs are capable of interaction with microbial membranes (Brandenburg et al., 2012; Seo et al., 2012). The rapid microbial death by membrane interaction decreases the possibility of resistance development against AMPs (Fernebro, 2011).

Anti-lipopolysaccharide factors (ALFs) are class of AMPs which possess broad spectrum antimicrobial, anticancer, anti-inflammatory, immunomodulatory and endotoxin binding activity. ALFs are amphipathic peptides that comprise of a LPS-binding domain (LPS-BD) within a conserved disulfide bridge. According to Brandenburg et al. (2016), three approaches seem to be promising for the advance of AMPs as remedy against bacteria and their toxins: (i) amino acid sequence variations of the endogenous AMPs to diminish their inherent toxicity, but sustaining antibacterial action, (ii) analysis of LPS-binding domains from natural defense proteins and consequent synthesis of these protein-derived polypeptides, and (iii) expansion of polypeptides which are not antibacterial but modulate the immune system. Thus ALFs are promising candidates for therapy against drug resistant pathogens, sepsis induced shock and cancer.

The present study introduces for the first time molecular characterization and phylogenetic analysis of an isoform of ALF (*Mn*-ALF) from a stomatopod crustacean, haemocyte mRNA of mantis shrimp, *M. nepa.* Predicted SP cleavage between A_{25}-Q_{26} yields a 98-mer mature peptide with a net charge of +7, hydrophobicity of 39% and amphipathic LPS binding domain (LPS-BD) which together with the structural features confirmed MnALF as an isoform of ALF with potent antimicrobial activity. The amphipathic loop structure of LPS-BD is supposed to bind a single fatty acid with the phospho-glucosamine portion of lipid A (Nagoshi et al., 2006). The secondary structure prediction using PSIPRED tool and PyMOL revealed that the *Mn*-ALF possesses three α-helices and four strands of β-sheets (Fig. 4.8). Between α-helical regions are segments of β-strands and random coil which includes the amphipathic LPS binding domain. Two of the β-sheets were linked by a disulphide bond forming the amphipathic, highly cationic LPS binding domain with net charge +7 and *p*I of 10.01. Three dimensional structure of *Mn*-ALF consists of patches of hydrophobic and charged residues that permit the peptides to interact strongly with membranes.

The multiple protein sequence alignment of *Mn*-ALF with other crustacean ALFs using ClustalW in BioEdit (Fig. 4.11) revealed the existence of conserved structural features i.e. Cys residues (C_{55}–C_{76}) forming a disulfide bridge with a highly conserved sequence comprising six positively charged amino acid residue cluster within the disulfide loop forming the functional LPS binding domain of ALF, which is obligatory for LPS binding and neutralization (Yang et al., 2009). Detailed analysis of the alignment revealed that mature peptide region Cys residues at 55

and 76 are responsible for disulphide bond in the LPS binding domain were found to be highly conserved. In addition to this, residues including L_{42}, W_{43}, H_{53}, P_{61}, R_{65}, G_{72}, W_{75}, P_{77}, W_{79}, G_{84}, S_{90}, S_{92}, G_{93}, F_{102}, V_{103}, A_{106}, G_{110}, L_{111} and A_{117} were also found to be conserved within the homologous groups. While the sequence homology of *Mn*-ALF with limulid and decapod ALFs showed the existence of a conserved amino acid motif K_{71}-G-R/K-M/F-W-C-P-G-W_{79} spanning across the LPS binding domain that interact with microbial polysaccharides.

The molecular bootstrapped phylogenetic tree revealing the relationship between *M. nepa, Mn*-ALF and previously reported ALF amino acid sequences from other crustaceans and limulids was constructed (Fig. 4.12). The NJ tree validates that the members of the ALF family are resultant from a common ancestor by a succession of evolutionary fluctuations. In the phylogenetic tree, the ALF sequences clustered with respect to species. The tree could be broadly categorized into three. *Mn*-ALF was found to be included in Group I, which includes ALF sequences from only shrimps. Group II comprised of the ALF sequences from different groups of crustaceans (lobsters, crayfish, crabs and shrimps) whereas Group III comprised of ALF sequences from only crabs.

In fact we have tried to produce the peptide *Mn*-ALF recombinantly, by cloning into pET-32a(+). Successful transformation of *Mn*-ALF to *E. coli* Rosetta-gamiTM B (DE3) pLysS could be achieved; while induction of protein expression using IPTG, the host *E. coli* cells were observed to be lysed. This may be due to the increased toxicity of the peptide to bacterial host. Interestingly, it was reported that there were no differences in

antimicrobial activities between recombinant and synthetic variants of mud crab ALF (*Scylla paramamosain*), *Sp*-ALFs; both showed remarkable bactericidal activity against Gram-positive and Gram-negative bacteria (Liu et al., 2012a). Hence, we synthesized the peptide (LPS binding domain of *Mn*-ALF) to test the the biological activity. According to Guo et al. (2014) the incorporation of modifications such as disulfide bond between cysteine residues of LPS binding domain, N-terminal acetylation, C-terminal Amidation and modification of amino acid sequence in LBD has demonstrated crucial roles in its biological activities. Similarly, Pan et al. (2007) and Guo et al. (2014) found that synthetic linear LBD of *Pm*ALF and *Fc*ALF showed a reduced antibacterial potential compared to the cyclic peptide. Thus in the present study the synthetic cyclic peptide MNA-LBD corresponding to the LPS binding domain of *Mn*-ALF was synthesized with disulfide bond, end modifications (N-terminal acetylation and the C-terminal amidation) and disulfide bond between the Cys residues at M/s Zhejiang Ontores Biotechnologies Co., Ltd China with >95 % purity. The synthetic MNA-LBD possessed the sequence 'ECKFTVKPYIKRFQLNYKGRMWCP' with a net charge of +5, rich in amino acids; 16 % each of Lys, Arg; 8 % of Phe, Cys, Pro, Tyr and 4 % of Ile, Val, Leu, Met, Trp, Gly, Thr, Gln, Asn and Glu..

The synthetic cyclic peptide, MNA-LBD was further characterized for its biological activity including antimicrobial activity, DNA binding, cytotoxicity against cancer cells, gene expression analysis of the peptide treated cancer cell lines and haemolytic activity against human RBCs. First of all antimicrobial activity of cyclic peptide, MNA-LBD was performed against eleven selected bacterial pathogens (2 Gram-positive

and 9 Gram-negative) by broth microdilution assay and the bactericidal activity was confirmed by plating the peptide treated bacteria on MH agar plates. We observed that the synthetic peptide MNA-LBD revealed antimicrobial activity similar to the earlier reports (Arockiaraj et al., (2013b); Wang et al. (2015) and Yang et al. (2016). Peptide was found to be active against both Gram-positive and Gram-negative bacteria at the highest tested concentration (50 μM), but the highest activity was shown against Gram-negative *E. coli* followed by *P. aeruginosa, E. tarda, V. parahaemolyticus, V. alginolyticus* and Gram-positive *B. cereus*. The MIC and MBC values obtained for MNA-LBD was compared to be low with respect to other reported synthetic LBD peptide. The modified LBD, LBD2 of FcALF exhibited MIC and MBC >64 μM against *E. coli*; 32 μM-64 μM for *V. parahaemolyticus* (Yang et al., 2016a).

The microbicidal activity against *E. coli* was further confirmed by epifluorescence microscopy of FITC labelled MNA-LBD treatment followed by staining with permeability indicator stain, PI. Thus the peptide treated cells were seen as green because of the FITC tag and the dead cells were observed as red due to the interaction of PI with the DNA of dead cells, indicating the altered/permeabilized bacterial membrane (Fig. 4.17). Morphological discrepancies because of bactericidal activity in MNA-LBD treated *E. coli* was detected through observation of the morphology of bacteria by SEM. Bacteria with blebbing, pores and cytoplasmic content lost was clearly observed in comparison to the untreated control (Fig. 4.18). Similar kind of surface changes were observed in scanning electron micrograph of modified LBD of FcALF2, LBDv treated *E. coli* with 64 μM of peptide (Yang et al., 2016a). Peptide

was also tested for its DNA binding activity using pUC-18 plasmid and found a significant retardation of plasmid DNA from peptide concentration of 12.5 μM to 200 μM. Thus at a higher concentration, the peptide could inhibit the bacterial growth by DNA binding mechanism also. Till now there is no studies regarding the DNA interacting property of ALF, but Tachyplesin I a cyclic β-sheet AMP from horseshoe crab, *Tachypleus tridentatus* exhibited DNA binding activity in gel retardation assay (Yonezawa et al., 1992).

Currently, a variety of mechanisms have been putforth for antimicrobial activity of AMPs, including the membrane interactive carpet, barrel-stave pore, toroidal pore, and aggregate models (Matsuzaki et al., 1998; Wu et al., 1999; Shai, 2002). After translocation into the cytoplasm, AMPs could bind to cellular polyanions including DNA and RNA, inhibition of enzymatic activity such as protein synthesis or chaperone assisted protein folding (Brandenburg et al., 2012). Also it could be attributed that, as in the case of other cationic non-amphipathic AMPs, the net positive charge is essential for electrostatic interaction between peptide residues with anionic phospholipids resulting in membrane binding and disruption of the membraneand subsequent death of the microbes (Lamaziere et al., 2007). Also the basic amino acids along with the LPS-binding domain have been found critical for the antibacterial activities of ALFs (Guo et al., 2014). Development of an appropriate model for MNA-LBD needs further research.

Among the AMPs identified so far from bacteria to humans, a few have anticancer activity (Lin et al., 2010). The electrostatic interactions

between cationic anticancer peptides (ACPs) and anionic cell membrane components of malignant cells are supposed to be a key factor in the selective killing of cancer cells by ACPs (Hoskin et al., 2008). Also alpha helical AMP, BMAP-28 and beta sheeted AMP tachyplesin favourably disrupt mitochondrial membranes and evoke the classic complement pathway to kill tumour cells (Risso et al., 2002; Chen et al., 2005).

AMPs due to their amphipathic and cationic nature aids to disrupt negatively charged membranes via electrostatic interactions. Compared to normal mammalian cell membranes with neutral zwitterionic phospholipids and sterols, the cancer cells carry a net negative charge because of elevated expressions of phosphatidylserine, O-glycosylated mucins, sialilated gangliosides and heparin sulfates in plasma membrane and thus AMPs have a higher selectivity towards malignant cells. Besides, the anticancer properties of AMPs may include the selective lysis of cancer cell membranes, permeation and engorgement of mitochondria, resulting in the release of cytochrome c and induction of apoptosis (Chang et al., 2011).

Regarding the ALF or ALF derived peptides there are only very few studies about anticancer/antitumour activity. This includes the antitumour activity of synthetic peptide shrimp ALF (SALF, Ac-ECKFTVKPYLKRFQVYYKGRMWCP-NH_2) using HeLa cells as the study model. The SEM and transmission electron microscopy (TEM) analysis showed that the SALF altered the cancer cell membrane structure similar to a lytic peptide. The qRT-PCR analysis revealed that the peptide SALF induced apoptosis through the death receptor/NF-KB signalling pathway (Lin et al., 2010).

The qRT-PCR analysis of both cell lines after peptide treatment showed almost similar trend of gene regulation. In both cell lines, the treatment of cyclic peptide MNA-LBD leads to the marked up-regulation of mRNA of pro-apoptotic protein Bax and down-regulation of anti-apoptotic, Bcl2 (Dewson and Kluc, 2010). The ratio of Bax: Bcl-2 protein was found to increase during apoptosis (Leung and Wang, 1999). While considering the level of Caspases, the initiator caspase, caspase-9 and effector caspase, caspase-3 were found to be up-regulated in both cells as a result of peptide treatment and these are believed to be responsible in the cleavage of cellular components during apoptosis (Fink and Cookson, 2005). Increased level of caspases also indicates the activation of apoptosis by intrinsic apoptotic pathway which involves the release of cytochrome-c from mitochondria. While considering the mRNA level of tumour suppressor genes (p53 and Rb1), the gene expression level was found to be up-regulated in both cells after MNA-LBD treatment. Non-caspase proteases, Cathepsin-G and Calpain-5 were also up-regulated in both cell lines and thus could be involved in the breakdown of cellular components leading to apoptosis. Droga-Mazovec et al. (2008) proposed that the Cathepsin-G is involved in the activation of Bcl-2 family pro-apoptotic gene Bid, and thus induce the mitochondrial pathway of apoptosis.

The c-Jun N-terminal protein kinase (JNK) is a subfamily of the mitogen activated protein kinase (MAPK) superfamily which in the absence of NF-κB activation, contributes to TNF-α induced apoptosis (Liu and Lin, 2005). TNF-α is an activator of extrinsic pathway of apoptosis (Wang et al., 2009). In HEp2 cells after peptide treatment an up-regulation of JNK and TNF-α could be observed and thus the peptide

could initiate a dual mode of apoptosis induction; one by intrinsic pathway and the other by extrinsic pathway.

AKT1 is a crucial intermediate of the AKT kinase signalling pathway and exerts an anti-apoptotic activity by preventing the release of cytochrome c from the mitochondria and by phosphorylating and inactivating the pro-apoptotic factors BAD and procaspase-9 (Whang et al., 2004). The mitogen-activated protein kinase 1 (MAPK-1), also known as extracellular signal-regulated kinases (ERKs), act as a combination point for multiple biochemical signals, and are engaged in a wide variety of cellular processes such as proliferation, differentiation, transcription regulation and development. In both cell lines, followed by peptide treatment, the expression of MAPK-1 is improved and Akt-1 is down regulated enhancing the anticancer activity of the peptide.

Cytokines are considered as the chemical communicators of different parts of the immune system and comprise of interleukins, interferons and growth factors (Razavi and Allen. 2014). In the present study on gene expression, the interleukins (IL-1β, IL-2, IL-6, IL-10 and IL-12) and interferons (β and γ) were found to be up-regulated in both cell lines, except IL-1β in HEp-2 and IFN- β in NCI-H460 cell lines. As a result of enhanced interferon expression, the IFN-inducible proteins, such as GTPase Mx1 (myxovirus resistance 1), ISG15 (IFN-stimulated protein of 15 kDa), Viperin (virus inhibitory protein, endoplasmic reticulum-associated, interferon-inducible) and IFIT (IFN-induced proteins with tetratricopeptide repeat) were found to be differentially expressed in both cell lines. All the four genes were observed to be up-regulated in HEp-2

cell lines, whereas Mx1 and Viperin found to be down-regulated in NCI-H460. Thus the present observation of anticancer potential screening of MNA-LBD in NCI-H460 and HEp-2 cells revealed that the peptide exhibited an immunomodulatory activity in addition to anticancer activity by regulating the gene expression of cytokines and other immune genes. Also the cytotoxicity exerted by peptide in the tested cancer cell lines could be mainly due to the modulation and induction of apoptosis rather than necrotic cell death.

In summary, we have successfully cloned and characterized a novel isoform of ALF, *Mn*-ALF from mantis shrimp, *Miyakea nepa*. The synthetic cyclic peptide MNA-LBD corresponding to the LPS binding domain of *Mn*-ALF was used for functional characterization. The synthetic MNA-LBD exhibited marked activity against both Gram positive *B. cereus* and Gram negative pathogens including *P. aeruginosa, E. tarda, V. parahaemolyticus, V. alginolyticus* which are important pathogens of concern in aquaculture and medicine. Broad spectrum antimicrobial activity, anticancer potential and low toxicity to human erythrocytes exhibited by synthetic MNA-LBD endorse it as a potential therapeutic agent for application in aquaculture and medicine. Present study is only a preliminary one with respect to the biological activity of MNA-LBD peptide. Further preclinical assays pertaining to the mode of antibacterial activity and anticancer mechanism need to be performed.

Chapter 5

MOLECULAR CHARACTERIZATION OF A HISTONE H2A DERIVED AMP FROM THE INDIAN WHITE SHRIMP, *FENNEROPENAEUS INDICUS* AND FUNCTIONAL ANALYSIS OF THE SYNTHETIC PEPTIDE

Contents

5.1 Introduction

In the current scenario of emergence of multidrug resistant pathogens and cancer cells, antimicrobial peptide (AMP) would be a potential alternative to conventional antibiotics and cancer therapeutics (Hancock and Patrzykat, 2002; Nguyen et al., 2011; Conlon, 2015). AMPs are produced in active form after proteolytic cleavage of a precursor proteins/ peptides which are pre-arranged by the host genome and ribosomally synthesized. These are short peptides (10–100 amino acids) and with a net positive charge (in general, +2 to +9) and a considerable proportion (>30 %) of hydrophobic residues (Boman, 1995; Hancock and Sahl, 2006). Most of the peptides either fold into an amphipathic α-helix and/or β- sheet structures upon contact with anionic microbial membranes.

Histones are the integral protein part of chromatin which is involved in various biological activities (Parseghian and Luhrs, 2006). Histone proteins are primarily engaged in the packing of genomic DNA, fundamentally aiding the folding of extensive DNA strands to a coin like manner and transcription regulation (Wyrick and Parra, 2009). Eukaryotic nuclei is mainly comprised of histone proteins and this includes the nucleosome with core histones encompassing H2A, H2B, H3 and H4 and the linker histones containing H1 and H5 proteins. Histone proteins are also highly alkaline peptides rich in Lys/Arg residues, which make them potent antimicrobial agents against negatively-charged cell membranes. Among which, histone H1, H2A, and H2B are rich in Lys residues whereas H3 and H4 are rich in Arg residues (Tagai et al., 2011).

For the first time Kim and co-workers identified and characterized a 39 amino acid residue histone derived antimicrobial peptide (HDAP) named, buforin I from the stomach tissue of Asian toad, *Bufo gargarizans* (Kim et al., 1996). Later in the same year Park et al. (1996) identified a 21 amino acid peptide named buforin II, exhibiting broad spectrum antimicrobial activity with no haemolytic activity. They also revealed the structure of peptide by NMR and found that it is composed of amphipathic helix. Using synthetic buforin II peptide labelled with FITC, the mechanism of antimicrobial activity was revealed and found to be non-membrane lytic mode of killing via interaction with nucleic acid (Park et al., 1998a). In the same year antimicrobial activity of a H2A derived peptide, parasin-I (2 kDa) from the epithelial mucous layer of *Parasilurus asotus* was studied in response to epidermal injury (Park et al., 1998b). Parasin-I also exhibited 8 fold increases in antimicrobial activity than buforin-I with an MIC in the

range of 1-4 μg/ml without any haemolytic activity. Mechanism of parasin-I production from *Parasilurus asotus* histone H2A was studied by Cho et al. (2002) and established that enzyme cathepsin D cleaves between Ser_{19}-Arg_{20} of histone H2A from N-terminus to yield parasin-I. In 2003, Birkemo et al. performed the identification, purification and characterization of a 51-residue containing HDAP from H2A of Atlantic halibut, (*Hippoglossus hippoglossus L.*) and named as hipposin. Both synthetic and natural hipposin exhibited remarkable antimicrobial activity against Gram-positive and Gram-negative bacteria and the activity could be detected down to concentrations of 0.3 μM.

Report of HDAPs from invertebrates includes the identification of histone H2A fragments with antimicrobial activity by employing biochemical approach from shrimps, *Litopenaeus vannamei* (Patat et al., 2004). And in the same year from coelomocyte extract of the starfish, *Asterias rubens* a peptide of approximately 2 kDa showing similarity to H2A with antimicrobial activity was identified (Maltseva et al., 2004). Li et al. (2007) reported H2A derived AMP from the scallop, *Chlamys farreri* and also produced recombinant peptide in *Pichia pastoris* GS115, and the antibacterial activity of the recombinant peptide against Gram-positive bacteria was found to be 2.5 times more than that against Gram-negative bacteria.

'Abhisin,' derived from H2A histone was identified and characterized by De Zoysa et al. (2009) from disk abalone, *H. discus.* In order to characterize the antimicrobial activity and anticancer activity, the 40 amino acid length peptide was synthesized and found that the peptide inhibited the growth of

Gram-positive *Listeria monocytogenes*, Gram-negative *Vibrio ichthyoenteri*, and fungi *Pityrosporum ovale* at 250 μg/ml. The peptide exhibited growth inhibition of THP-1 leukemia cancer cells by 25 %, but there was no cytotoxicity to the normal vero cells.

In 2012, Sathyan and co-workers identified and characterized a putative 68 amino acid HDAP Himanturin from H2A N-terminus of Whip Ray, *Himantura pastinacoides* (Sathyan et al., 2012a). Later, in the same year HDAP sequences derived from histone-H2A of back water oyster, *Crassostrea madrasensis*; rock oyster, *Saccostrea cucullata*; grey clam, *Meretrix casta*; fig shell, *Ficus gracilis* and ribbon bullia, *Bullia vittata* were identified and characterized *in silico*. The 75 bp fragment encoding 25 amino acid residues was named as molluskin (Sathyan et al., 2012b).

Molecular characterization and evolutionary divergence of a 52 amino acid residue designated as Harriottin-1, a 40 mer Harriottin-2, and a 21 mer Harriottin-3 were identified from N-terminus histone H2A of sickle fin chimaera, *Neoharriotta pinnata* (Sathyan et al., 2013). Chaithanya et al. (2013) reported a 52 mer HDAP of H2A from two teleost fishes, *Tachysurus jella* and *Cynoglossus semifasciatus*, and designated as teleostin. From the mud crab *S. paramamosain,* Chen et al. (2015) identified a histone H2A derived peptide and designated it as Sphistin. The synthetic peptide Sphistin exhibited high antimicrobial activity against Gram-positive and Gram-negative bacteria and yeast, especially *A. hydrophila, P. fluorescens* and *P. stutzeri*.

In addition to AMPs derived from H2A, there are reports of antimicrobial activity of other histone proteins against bacteria, fungi,

viruses and protozoa (Chen et al., 2015). In case of H2B, antimicrobial activity was first reported from murine macrophage H2B (Hiemstra et al. 1993). Later, Robinette and co-workers reported the same from skin secretions of *Ictalurus punctatus.* The secretion was found to inhibit the growth of fish pathogens *A. hydrophilia* and *Saprolegnia* sp. (Robinette et al., 1998). Antimicrobial activity were also reported from the shrimp, *Litopenaeus vannamei* (Patat et al., 2004); skin mucus of Atlantic cod, *Gadus morhua* (Bergsson et al., 2005) and H2B derived AMP cv-H2B-1 (Seo et al., 2010) and cv-H2B-2, -3 & -4 (Seo et al., 2011) from the mollusc, *Crassostrea virginica.* H3 core histone HDAPs were reported from the haemocytes of *L. vannamei* (Patat et al., 2004) and skin mucus of the hagfish *Myxine glutinous* (Subramanian et al., 2007).

In terms of antimicrobial activity the role of histone H4 is under explored. Kai-Larsen et al. (2007) purified a HDAP from H4 of human meconium. Likewise, Lee et al. (2009) isolated HDAP from H4 of human sebocyte secretions and exposed its antimicrobial property against *S. aureus* and *Propionibacterium acnes*. Antimicrobial activity of recombinant H4 peptide from *Xenopus laevis* was observed by Dorrington et al. (2011). Chaurasia et al. (2015) performed the molecular characterization, gene expression analysis, and antimicrobial activity of synthetic N and C terminal peptides from the core histone 4 (H4) of freshwater giant prawn *M. rosenbergii.* Linker histone H1 derived AMPs were also identified and characterized from humans (Kashima, 1991); Salmon, *Salmo salar* (Richards et al., 2001); Rainbow trout, *Onchorynchus mykiss* (Fernandes et al., 2002); shrimp, *L. vannamei* (Patat et al., 2004) and Olive flounder, *Paralichthys olivaceous* (Nam et al., 2012).

The histone proteins also function as endotoxin-neutralizing proteins (Kim et al., 2002), leucocyte stimulatory factor (Pedersen et al., 2003) homeostatic thymus hormone (Reichhart et al., 1985) as well as apoptotic signal transmitting factor (Konishi et al., 2003) and activation of haemolymph to generate the pro-inflammatory cytokine (Chen et al., 2015).

Histone-derived antimicrobial peptides (HDAPs) exhibiting antimicrobial properties were identified from various vertebrates, such as mammals (Rose et al., 1998, Howell et al., 2003, Jacobsen et al., 2005), chicken (Silphaduang et al., 2006), frog (Park et al., 1996) and fish (Park et al., 1998b, Robinette et al., 1998, Richards et al., 2001, Fernandes et al., 2002, Birkemo et al., 2003, Fernandes et al., 2004, Bergsson et al., 2005). In the meantime a few studies regarding antimicrobial activity of HDAPs have been reported from invertebrates, including histone H2A fragments in scallop (*Chlamys farreri*) (Li et al., 2007), abalone (*Haliotis discus discus*) (De Zoysa et al., 2009), Pacific white shrimp (*L. vannamei*) (Patat, et al., 2004), freshwater prawn (*M. rosenbergii*) (Arockiaraj et al., 2013, Chaurasia et al., 2015) and mud crab *S. paramamosain* (Chen et al. 2015).

In addition to antimicrobial activity, the HDAPs also exhibited potent anticancer activity (Cho et al. 2009). Among the HDAPs, buforin IIb, the synthetic analogue of buforin II was found to aim cancer cells selectively by interacting with the cell-surface gangliosides and was found to be able to pass through cancer cell membranes without damaging it effecting mitochondria-dependent apoptosis (Lee et al., 2008). Another reported HDAP from disk abalone (*H. discus discus*), abhisin, a potential

AMP derived from histone H2A, also showed antimicrobial and anticancer activity similar to that of buforin IIb (De Zoysa et al., 2009).

To date only few H2A-derived AMPs are reported from shrimp species and so far no HDAPs were characterized from *F. indicus*. In the present study, based on the obtained nucleotide sequence of histone H2A of Indian white shrimp, *F. indicus,* a 28 mer N-terminal peptide was recognised and named as *Fi*-Histin. To unveil the biological activity of *Fi*-Histin, a synthetic peptide having sequence homology to buforin-II was custom synthesized as a linear peptide. Antimicrobial activity of the synthetic peptide was tested against selected Gram-positive and Gram-negative bacteria. Mechanism behind the antimicrobial activity was studied using epi-fluorescence microscopy, SEM and DNA binding assay. Anticancer potential of the peptide was screened in NCI-H460 and HEp-2 cell lines. Finally, toxicity was tested by haemolytic assay using human RBCs. From the study, the antimicrobial and anticancer activity of the new HDAP from *F. indicus* will be assessed and thus would add more information about the innate immune system of crustaceans.

5.2 Materials and methods

5.2.1 Experimental organism

Live and healthy shrimp, *Fenneropenaeus indicus* was collected and maintained as described in section 2.2.1 of Chapter 3.

5.2.2 Precautions for RNA preparation

Basic cautionary measures were followed before and during RNA isolation as explained in section 2.2.2 of Chapter 2.

5.2.3 Haemolymph collection

Haemolymph was collected from the rostral sinus of live *F. indicus* and stored in TRI reagent (Sigma) for total RNA isolation as defined in section 2.2.3 of Chapter 2.

5.2.4 Total RNA isolation

As per manufacturer's instructions, total RNA was isolated from *F. indicus* haemocytes using TRI reagent (Sigma) as explained in section 2.2.4 of Chapter 2. RNA pellet was dissolved by adding 25 µl of DEPC treated RNase free water and incubated at 55 °C for 5 min in a water bath for complete dissolution.

5.2.5 Quality assessment and quantification of RNA

Total RNA was quantified and analysed for purity and quality as explained in section 2.2.5 of Chapter 2.

5.2.6 Reverse transcription

First strand of cDNA was synthesized using specific oligo-d(T20) primers targeting the mRNA from total RNA as explained previously in section 2.2.6 of Chapter 2.

5.2.7 PCR amplification

Amplification of the house-keeping gene, beta-actin was done using single stranded cDNA as the template for ensuring the reverse transcription. After confirmation, the cDNA was used as the template for amplification using HDAP, Hipposin primers (Birkemo et al., 2003) in a 25 µl reaction volume as explained in the section 2.2.7 of Chapter 2. Sequences of primers are given in Table 5.1.

Table 5.1 List of primers used in the present chapter.

Target gene	Sequence (5'-3')	Product Size (bp)	Annealing Temp. (°C)	$MgCl_2$ Conc. (mM)
Hipposin	F: ATGTCCGGRMGMGGSAARAC R: GGGATGATGCGMGTCTTCTTGTT	354	55	1.5
β-actin	F:CTTGTGGTTGACAATGGCTCCG R: TGGTGAAGGAGTAGCCACGCTC	520	60	1.5

5.2.8 Agarose gel electrophoresis

PCR product was visualized and examined using agarose gel electrophoresis as explained in the section 2.2.8 of Chapter 2.

5.2.9 TA cloning of amplicons and sequencing

Amplicons obtained using Histin primers were cloned into pGEM®-T Easy cloning vector (Promega) and transformed to *E. coli* DH5α. Detailed methodology has already been explained in section 2.2.9 of Chapter 2. Plasmid with insert was selected for sequencing as described in section 2.2.10 of Chapter 2.

5.2.10 Sequence characterization and phylogenetic analysis

In silico analysis of the sequences were performed using various bioinformatics tools as mentioned in section 2.2.11 of Chapter 2. Phylogenetic analysis of nucleotide and deduced amino acid sequences were compared with other histone derived AMPs from different phylum.

5.2.11 Peptide synthesis and characterization

Chemical synthesis of peptide with FITC labelling was carried out at M/s Zhejiang Ontores Biotechnologies Co., Ltd China by Solid phase procedure of Fmoc chemistry with >95 % final purity. As explained in the previous chapter in section 4.2.12, synthesis was performed from N to C terminus with end modifications. Linear synthetic peptide supplied as lyophilized powder was solubilized in sterile water and stored at -20 °C for further use.

5.2.12 Mass spectrometry analysis of synthetic peptide

Mass spectra analysis was performed with a Thermo Finnigan LCQ Duo mass spectrometer as explained in section 4.2.13 of Chapter 4.

5.2.13 Purity determination of synthetic peptide using HPLC

The purity of synthetic peptide was determined using HPLC as described in section 4.2.14 of Chapter 4. A step gradient system of solvents were used for purification; beginning with a solvent gradient of 27 % Solvent A (0.1 % TFA in 100 % acetonitrile) and 73 % solvent B (0.1 % TFA in 100 % H_2O) for 0.01 min, followed by a gradient of 52 % solvent A and 48 % solvent B for 25 min and finally a flow of 100 % solvent A for 25 min.

5.2.14 Haemolytic activity

Haemolytic activity of the synthetic peptide is an inevitable part before going to other functional studies including antimicrobial and anticancer activity. Thus haemolytic assay was performed with using

hRBCs from concentration of 400 µM to 3.125 µM (by double dilution) as described in section 2.2.28 of Chapter 2.

5.2.15 Antimicrobial activity

In order to determine the MIC, six dilutions (50 µM to 3.125 µM concentrations) of the synthetic peptide were tested for antimicrobial activity against eleven bacterial strains (Refer section 2.2.30 of Chapter 2). Broth microdilution assay and bactericidal assay were performed to detect the antimicrobial activity of synthetic peptide against bacterial pathogens. To confirm the interaction of the peptide with pathogens, microscopic observation of peptide treated pathogens were done using PI staining for epi-fluorescence microscopy and by SEM as described in section 2.2.30.4 and 2.2.30.5 of Chapter 2.

5.2.16 DNA binding assay

DNA binding activity of the synthetic peptide was performed as explained in the section 2.2.31 of Chapter 2.

5.2.17 Anticancer activity

5.2.17.1 *In vitro cytotoxicity assay*

Cytotoxicity was determined using XTT assay in NCI-H460, and HEp2 cell lines. Cells were treated with desired concentration of peptide (double dilution) and assayed for the cellular metabolism by XTT assay as described earlier in section 2.2.29 of Chapter 2. Experiments were done in triplicate. The results are expressed as a percentage inhibition of viable cells. Synthetic mellitin with FITC label was used as the positive control. The IC_{50} values were calculated as explained in section 4.2.18.1 of Chapter 4.

5.2.17.2 *Real-time reverse-transcription polymerase chain reaction (RT-PCR)*

In order to study the anticancer activity of synthetic *Fi*-Histin, the NCI H460 lung cancer cell lines and HEp2 cells were incubated in DMEM supplemented with 10 % FBS with synthetic peptide for 24 h. Cells incubated without peptide was treated as the control. After incubation, cells were suspended in TRI reagent (Sigma) for RNA isolation as explained in section 2.2.4 of Chapter 2. Gene expression analysis of cancer controlling genes, immune genes and oncogenes were analysed by qRT-PCR as explained in section 4.2.18.2 of Chapter 4. Relative transcript levels were calculated using the $\Delta\Delta C_T$ method.

5.3 Results

In the current study, a novel histone H2A derived AMP was identified and characterized from the haemocytes of *F. indicus,* herein after designated as *Fi*-Histin.

5.3.1 PCR amplification, TA cloning and sequencing of *Fi*-Histin

An 81 bp amplicon encoding 27 amino acids was acquired by RT-PCR of cDNA using histone H2A specific primer (Fig. 5.1). The PCR products were cloned into pGEM®-T Easy cloning vector and transformed into *E. coli* DH5α competent cells. Presence of insert within the vector was confirmed by colony PCR with gene specific and vector specific primers, approximately 81 bp with gene specific primers (Fig. 5.2a) and 222 bp (81bp+141bp) long amplicon (Fig 5.2b) with vector specific primers. Positive colonies were inoculated and harvested for pGEMT-*Fi*-Histin plasmids and analysed by agarose gel electrophoresis (Fig. 5.2b).

BLAST analysis of the nucleotide and deduced translated amino acid sequences of *Fi*-Histin in pGEM®-T Easy vector revealed that the peptide belonged to histone H2A family (Fig. 5.3).

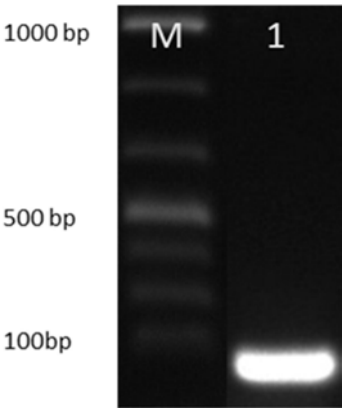

Fig. 5.1 Agarose gel electrophoretogram of PCR amplification of *Fi*-Histin using Histone H2A specific primers. Lane M: 100 bp marker, Lane 1: *Fi*-Histin amplicons of 81 bp.

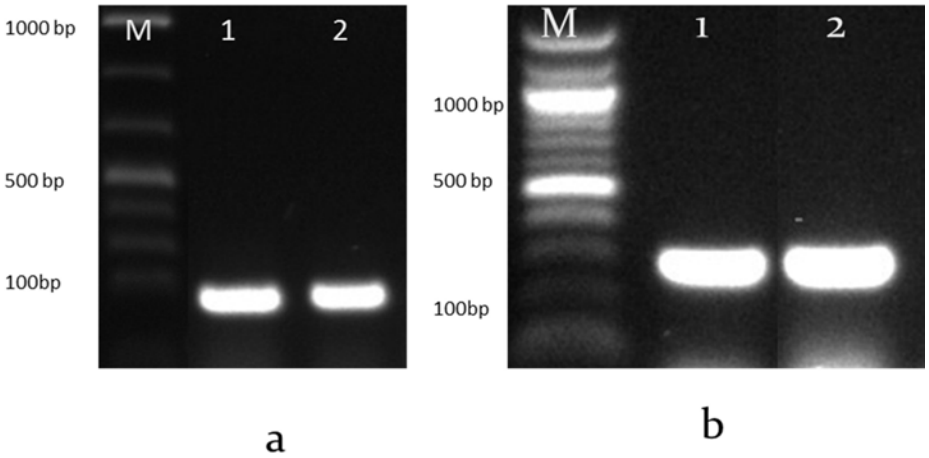

Fig. 5.2 Agarose gel electrophoretogram of *Fi*-Histin colony PCR (a) Lane M: 100 bp ladder; Lane 1-2: amplicon (81 bp) obtained for PCR with gene specific primers and (b) M: 100 bp ladder; Lane 1-2: amplicons (222 bp) of PCR performed using vector specific primers.

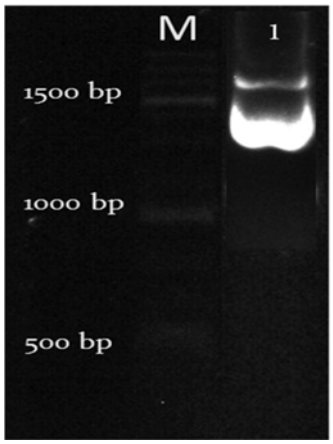

Fig. 5.3 Plasmid extracted from positive clones of pGEMT-*Fi*-Histin. Lane M shows 1 kb marker, Lane 1 pGEM®-T Easy plasmid with *Fi*-Histin insert

The nucleotide and deduced amino acid sequences of *Fi*-Histin (Fig 5.4) were deposited in NCBI GenBank database (GenBank ID: **KY126319**).

```
tcccgctcttctcgcgctggacttcagttccccgtgggtcgtatccaccgtctgctccgt
  S   R   S   S   R   A   G   L   Q   F   P   V   G   R   I   H   R   L   L   R
aagggaaactatgcggccgcc
  K   G   N   Y   A   A   A
```

Fig. 5.4 Nucleotide and deduced amino acid sequence of the HDAP from the haemocyte mRNA transcripts of *F. indicus* – *Fi*-Histin (GenBank ID: **KY126319**).

5.3.2 Sequence analysis and characterization using bioinformatics tools.

Homology analysis of *Fi*-Histin acquired nucleotide sequence and deduced amino acid sequence by BLASTn and BLASTp showed that it belongs to the histone H2A sequence of invertebrates. BLASTn analysis of *Fi*-Histin nucleotide sequence disclosed that it showed 100 % identity to *F. indicus* (GenBank ID: HM243619.1) and *Ficus gracilis* histone H2A (GenBank ID: HQ720146.1), followed by 99 % to *P. monodon* (GenBank

ID: HM243620.1) and 94 % to *S. scripta* histone H2A (GenBank ID: HQ720149.2).

Sequence analysis of *Fi*-Histin was done using ProtParam tool and APD3 and found to have a predicted molecular weight of 2.983 kDa, net charge of +6 and a theoretical isoelectric point (*p*I) of 12.18 respectively. Cationicity of the 27 mer, *Fi*-Histin was primarily due to six positive amino acid residues (Lys (1 No) + Arg (5 Nos)). The estimated half-life of the peptide was found to be 1.9 h (mammalian reticulocytes, *in vitro*), >20 h (yeast, *in vivo*) and >10 h (*Escherichia coli, in vivo*). Predicted instability index was computed to be 81.89 categorizing the peptide as unstable. *Fi*-Histin was found to be rich in Ala (A) 14.8 %, Arg (R) 18.5 %, 11.1 % each of Leu (L), Gly (G) and Ser (S) as in the case of other histone derived AMPs followed by 3.7 % each of Asn (N), Gln (Q), His (H), Ile (I), Lys (K), Phe (F), Pro (P), Tyr (Y) and Val (V). Of the total weight of *Fi*-Histin, 55.56 % was contributed by polar residues + GLY and 44.44 % by nonpolar residues.

Prediction of antimicrobial activity of *Fi*-Histin by APD3 discovered it as an effective AMP with a protein-binding potential (boman index) and wimley-white whole-residue hydrophobicity of 2.85 kcal/mol and 6.37 kcal/mol respectively. *In silico* analysis based on amphipathicity using HeliQuest tool revealed a hydrophobicity (H) of 0.221 and hydrophobic moment (μH) of 0.269. The helical wheel obtained depicting the distribution of amino acids based on amphipathicity is presented in Fig. 5.5. Hydrophobicity analysis of *Fi*-Histin by Kyte-Doolittle plot (Fig. 5.6) confirmed the substantial occurrence of hydrophobic amino acids located in the first 15 residues.

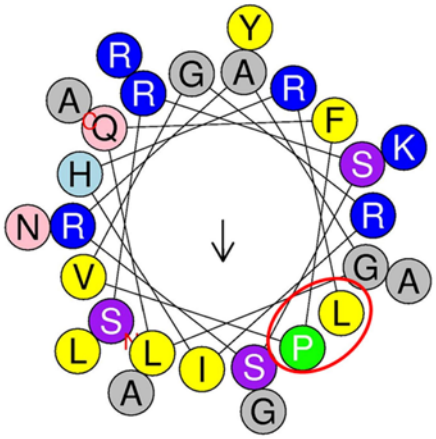

Fig. 5.5 The helical wheel diagram of *F. indicus, Fi*-Histin (GenBank ID: **KY126319**) predicted using Heliquest online tool. The structure was built to identify the amphipathicity of the peptide. The amino and carboxy terminal ends are mentioned as N and C, respectively. The expected hydrophobic face LP is shown in the red circle.

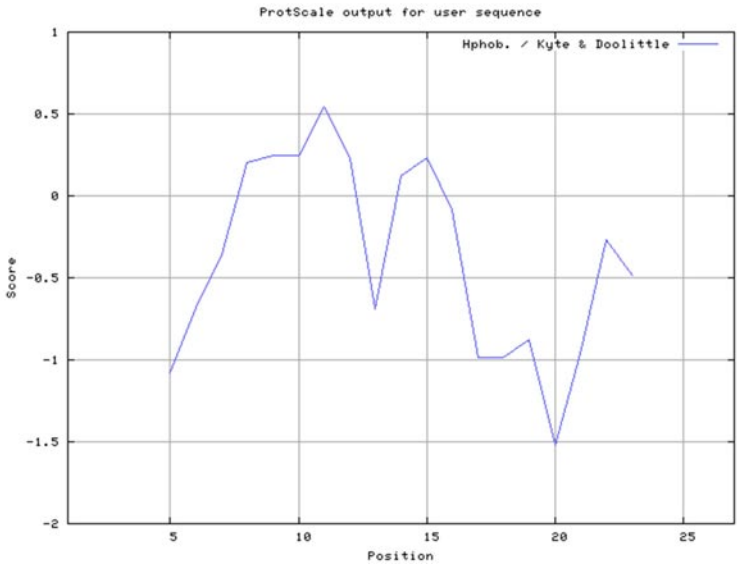

Fig. 5.6 Kyte-Doolittle plot showing hydrophobicity of *F. indicus, Fi*-Histin (GenBank ID: **KY126319**). The peaks above the score (0.0) indicate the hydrophobic nature of the predicted protein.

Secondary structure prediction using PSIPRED tool revealed the presence of one α-helix in *Fi*-Histin (Fig. 5.7). Prediction of spatial 3D structure of *Fi*-Histin by homology modelling using the SWISSMODEL sever is given in Fig. 5.8 and validated the occurrence of one extended α-helix at the N-terminus. Expected RNA sequence and model secondary structure of *Fi*-Histin with minimum free energy was found to be comprised of paired double stranded and unpaired looped region (Fig. 5.9).

Fig. 5.7 Secondary structure of *F. indicus*, *Fi*-Histin (GenBank ID: **KY126319**) predicted using PSIPRED server. The α-helix region is shown in pink coloured cylinders and the coiled region is shown in black lines.

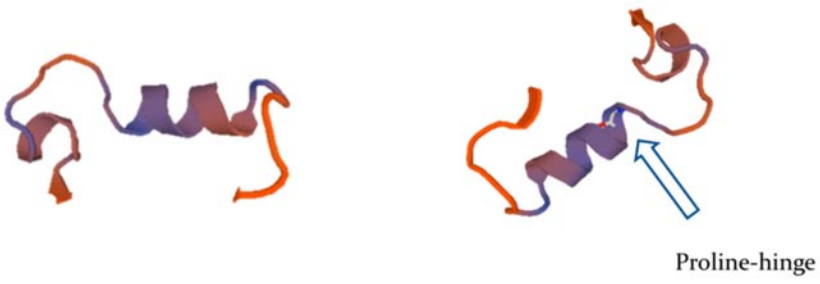

Fig. 5.8 Structural model of *F. indicus*, *Fi*-Histin (GenBank ID: **KY126319**) created with the PyMol software using the pdb data generated by SWISSMODEL server.

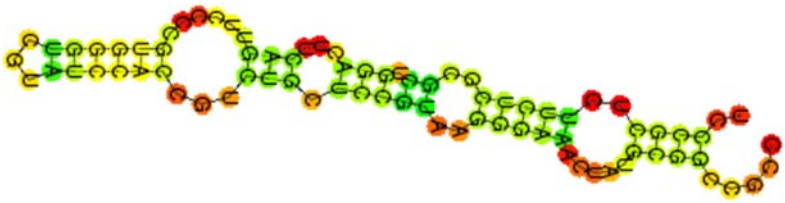

Fig. 5.9 Predicted secondary structure of *F. indicus*, *Fi*-Histin (GenBank ID: **KY126319**) RNA with minimal free energy prediction.

5.3.3 Sequence alignment and phylogenetic analysis of *Fi*-Histin

The ClustalW multiple protein sequence alignment of *Fi*-Histin with representatives of histone H2A derived AMPs in BioEdit revealed the existence of conserved sequence features (Fig. 5.10).

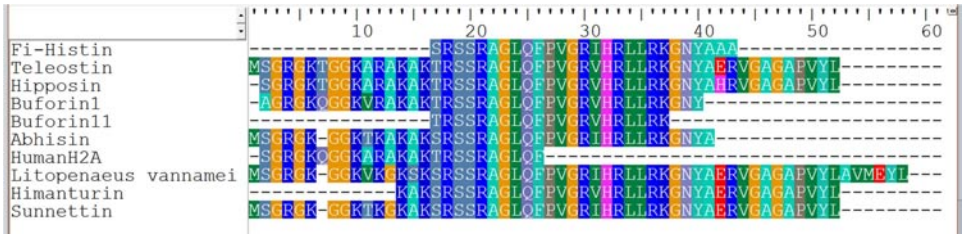

Fig. 5.10 Multiple alignment of amino acid sequence of the *F. indicus*, *Fi*-Histin (GenBank ID: **KY126319**) with other vertebrate and invertebrate H2A sequences obtained using BioEdit. Teleostin (*Tachysurus jella* and *Cynoglossus semifasciatus*), hipposin (*Hippoglossus hippoglossus*), buforin I and II (*Bufo bufo gargarizans*), abhisin (*Haliotis discus*), human H2A, *Litopenaeus vannamei* H2A, *himanturin* (*Himantura pastinacoides*) and *s*unettin (*Sunetta scripta*).

Bootstrap distance phylogenetic tree constructed using Neighbor-Joining method confirmed the similarity of *Fi*-Histin to the previously reported histone-H2A nucleotide sequences.

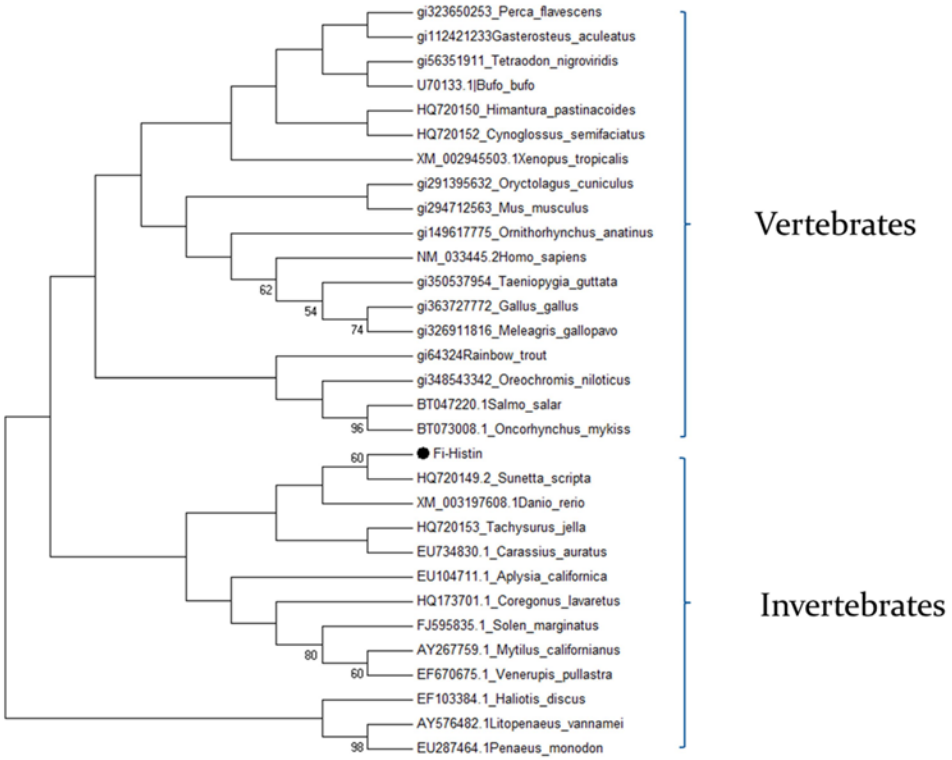

Fig. 5.11 A bootstrapped neighbor-joining tree obtained using MEGA 7 illustrating relationships between the deduced amino acid sequences of the *F. indicus*, *Fi*-Histin (GenBank ID: **KY126319**) with other histone H2A sequences from vertebrates and invertebrates. Values at the node indicate the percentage of times the particular node occurred in 1000 trees generated by bootstrapping the original deduced protein sequences. Branches corresponding to partitions reproduced in less than 75 % bootstrap replicates are collapsed.

5.3.4 Peptide synthesis and molecular characterization.

This study represents the first report of a histone, H2A derived AMP from *F. indicus*. In order to characterize the bioactivity, a 21 amino acid length region of the peptide (SRSSRAGLQFPVGRIHRLLRK) sharing similarity to buforin (histone derived AMP) identified by multiple sequence alignment was selected for solid phase peptide synthesis. The synthetic

peptide, *Fi*-His$_{1\text{-}21}$ is a cationic peptide with a net charge of +6 with a predicted mass and *p*I of 2.428 kDa and 12 respectively. Herein after, the synthetic peptide will be mentioned as *Fi*-His$_{1\text{-}21}$.

Synthetic peptide predicted to be an effective AMP with total hydrophobicity of 33 %, boman index of 3.34 kcal/mol and wimley-white whole residue hydrophobicity of 3.77 kcal/mol. Peptide cationicity was mainly subsidised by six positively charged residues (Arg (5 Nos)+ Lys (1 No)). The helical peptide analysis by Heliquest tool revealed that the hydrophobic and hydrophilic amino acids are clustered on opposite side and aid in the membrane penetration of peptide with a hydrophobic face of LP (Fig. 5.12).

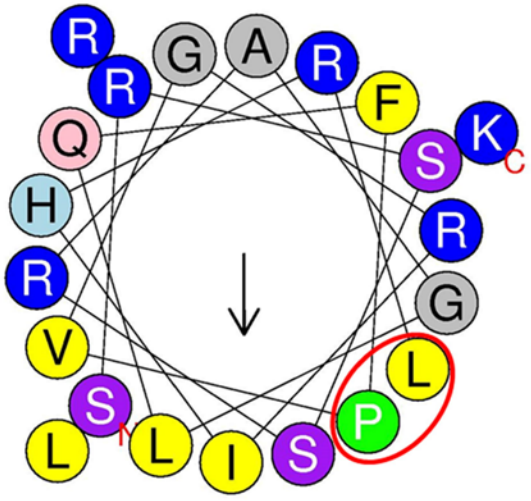

Fig. 5.12 The helical wheel diagram of synthetic *Fi*-His$_{1\text{-}21}$ predicted using Heliquest online tool. The structure was built to identify the amphipathicity of the peptide. The amino and carboxy terminal ends are mentioned as N and C, respectively. The expected hydrophobic face LP is shown in the red circle.

5.3.5 Determination of molecular mass and purity of synthetic *Fi*-His$_{1-21}$

ESI mass spectroscopy was employed to confirm the molecular weight of synthetic peptide *Fi*-His$_{1-21}$ (2865.28 Da). The ESI mass spectrum of peptide is shown in Fig. 5.13. The mass spectrum illustrates the mass to charge ratio (m/z) from 400 to 1800 of all the ionized molecules existing in the sample. The most abundant ion in the spectrum is seen at a mass to charge ratio of 955.95. This m/z matches to *Fi*-His$_{1-21}$ ionized to +3 (rounded off MW = 2867.85 Da + 3H+ = 2870.85). The mass to charge ratio is thus 2870.85/3 = 956.95. The other relatively abundant ion was m/z of 717.30 ionized to +4 (round off MW = 2869.2 Da + 4H+ = 2873.2) and thus the m/z is 2873.2/4 = 718.3.

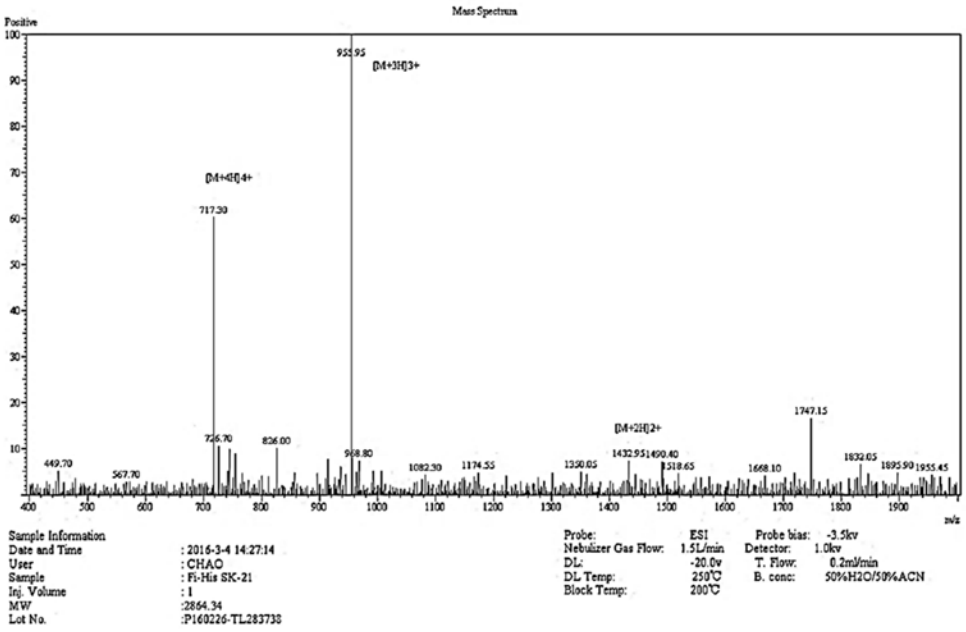

Fig. 5.13 ESI mass spectrum of synthetic *Fi*-His$_{1-21}$, Most abundant ion in spectrum is seen at m/z of 955.95 [M+3H]3+ followed by 717.30 [M+4H]4+.

The peptide was tested for its purity by HPLC and from the chromatogram, it was found to be 95 % pure by the percent area of the main peak at retention time 9.183 min as seen in Fig. 5.14.

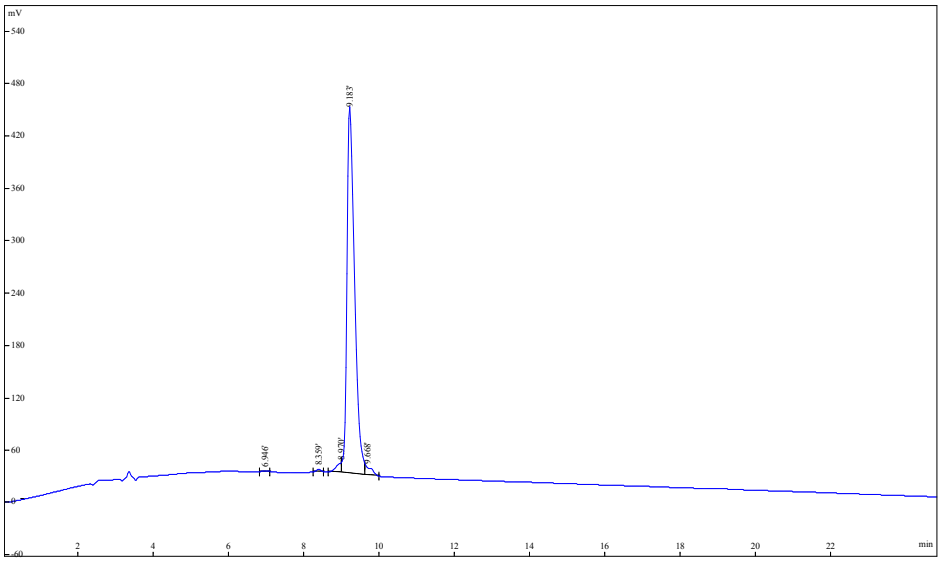

Fig. 5.14 HPLC chromatogram of synthetic peptide *Fi*-His$_{1\text{-}21}$ showing a major peak at retention time of 9.183 min.

5.3.6 Haemolytic activity

Haemolytic activity of synthetic *Fi*-His$_{1\text{-}21}$ peptide was tested against human RBCs at different concentrations. As shown in Fig. 5.15 only about 18 % of RBCs were lysed even after the treatment with 400 µM of peptide. Also the peptide was found to be non-haemolytic at the lower concentrations from 100 µM to 3.125 µM compared to mellitin.

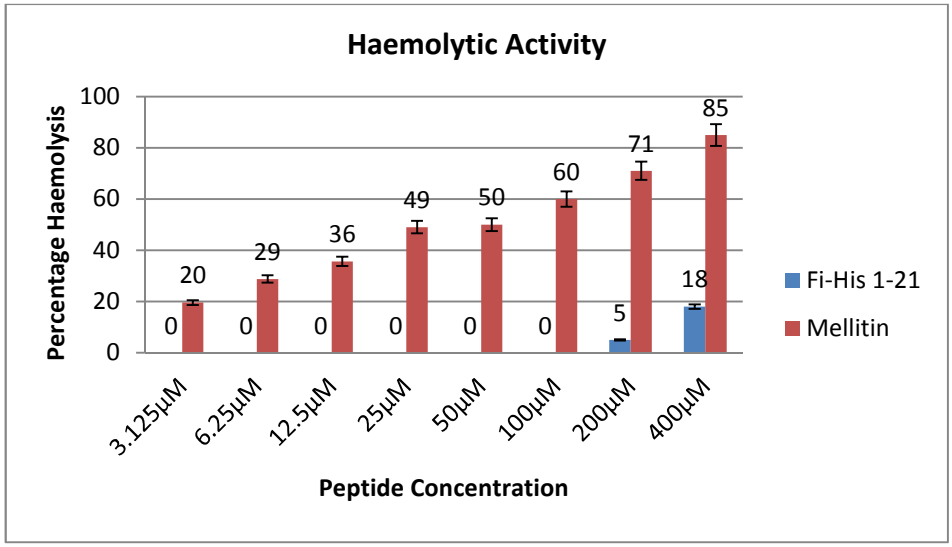

Fig. 5.15 Haemolytic activity of the synthetic *Fi*-His$_{1-21}$ and Mellitin in human RBCs at various concentrations.

5.3.7 Antimicrobial activity

To determine the antimicrobial activity of *Fi*-His$_{1-21,}$ the peptide was verified for the capability to inhibit proliferation of microorganisms using MIC and MBC method. The antibacterial activity of synthetic *Fi*-His$_{1-21}$ against the tested bacteria is shown in Fig. 5.16 (a-k). The result showed that the peptide was highly active in inhibiting the growth of Gram- negative bacteria *V. vulnificus* with an MIC and MBC of 25 µM each. Against *P. aeruginosa* and *V. parahaemolyticus* the MIC was found to be 25 µM; for *S. aureus* and *V. cholera* 50 µM was observed to be the MIC value and the MBC value was found to be greater than the highest tested concentration. Bacterial pathogens *E. coli, B. cereus, A. hydrophila, E. tarda* and *V. alginolyticus* were found to be sensitive to *Fi*-His$_{1-21}$, but the MIC and MBC values were found to be >50 µM. At the highest tested concentration (50 µM), *Fi*-His$_{1-21}$ inhibited the proliferation of *E. coli* by

79 %, *B. cereus* by 78 %, *A. hydrophila* by 68 %, *E. tarda* by 82 %, *V. fluvialis* by 85 % and *V. alginolyticus* by 89 %.

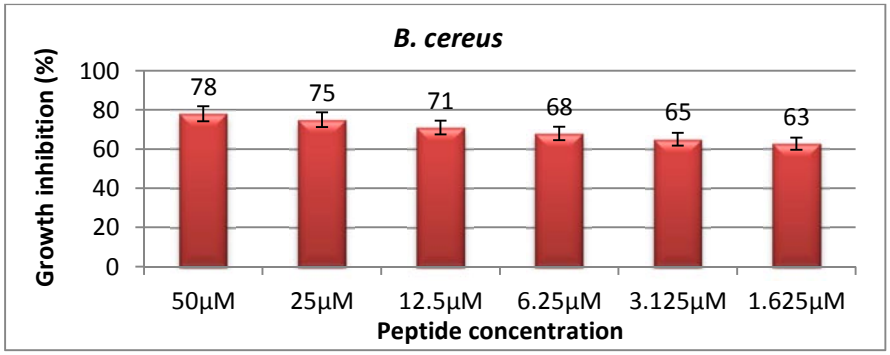

(a)

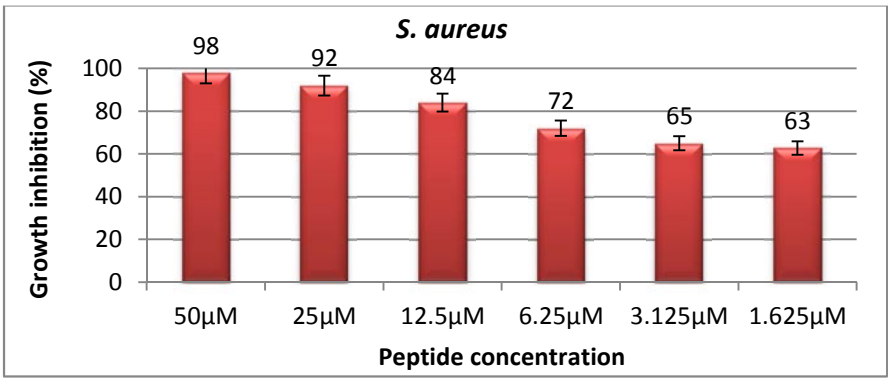

(b)

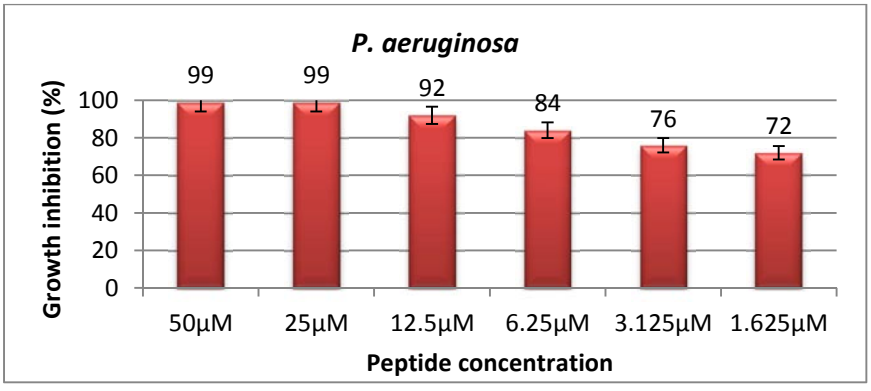

(c)

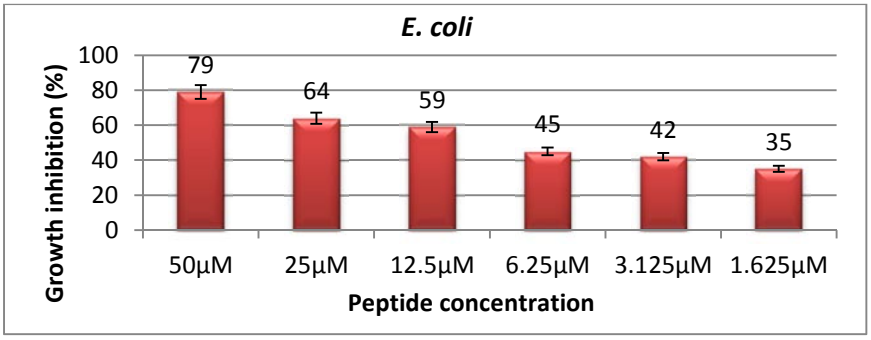
E. coli
Growth inhibition (%)
100
80
60
40
20
0
79
64
59
45
42
35
50µM
25µM
12.5µM
6.25µM
3.125µM
1.625µM
Peptide concentration

(d)

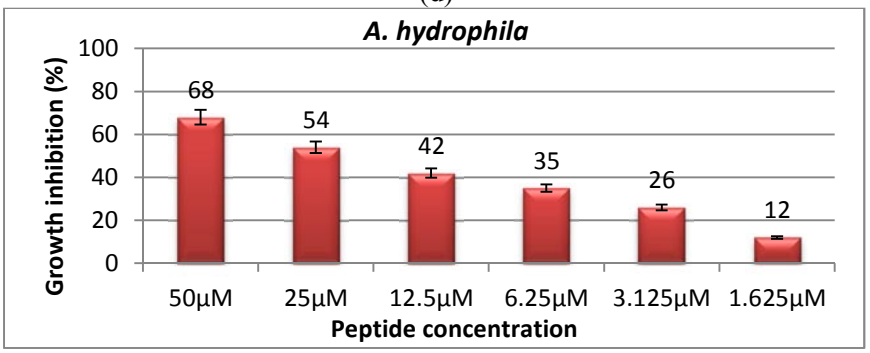
A. hydrophila
Growth inhibition (%)
100
80
60
40
20
0
68
54
42
35
26
12
50µM
25µM
12.5µM
6.25µM
3.125µM
1.625µM
Peptide concentration

(e)

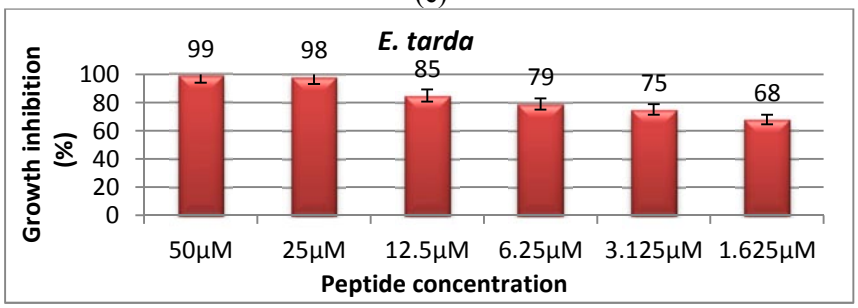
E. tarda
Growth inhibition (%)
100
80
60
40
20
0
99
98
85
79
75
68
50µM
25µM
12.5µM
6.25µM
3.125µM
1.625µM
Peptide concentration

(f)

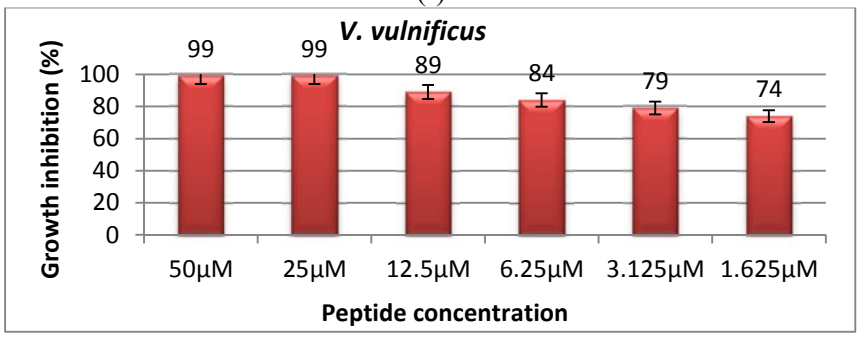
V. vulnificus
Growth inhibition (%)
100
80
60
40
20
0
99
99
89
84
79
74
50µM
25µM
12.5µM
6.25µM
3.125µM
1.625µM
Peptide concentration

(g)

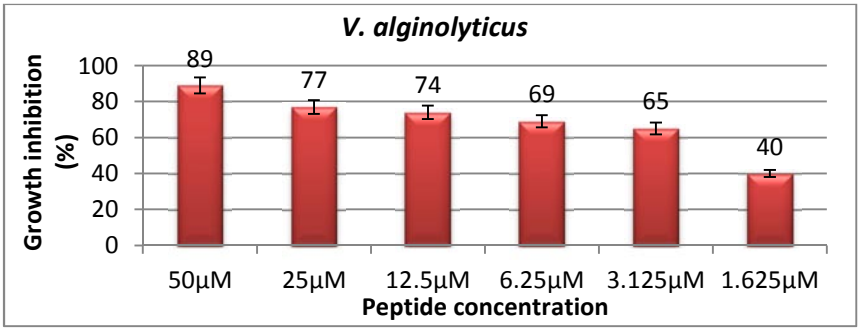

(h)

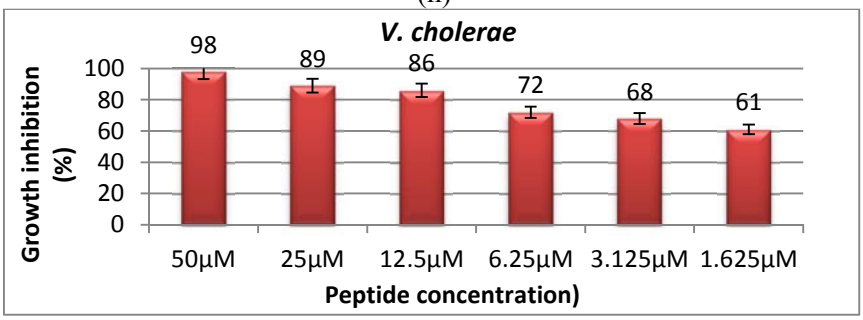

(i)

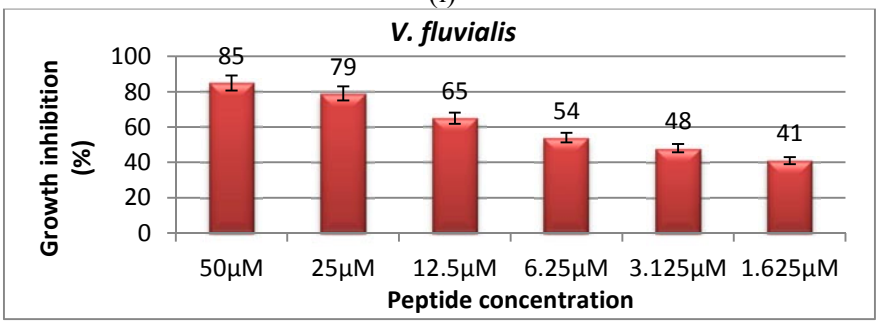

(j)

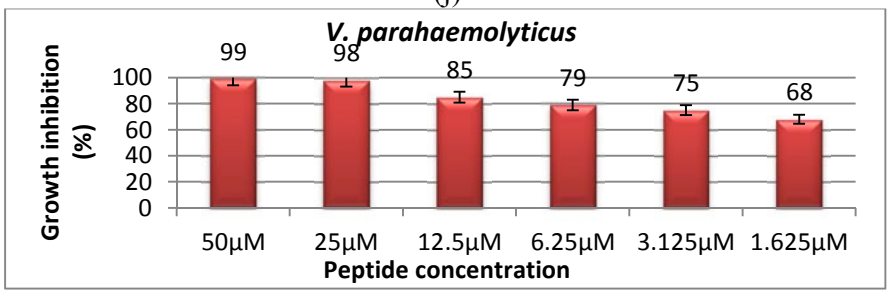

(k)

Fig. 5.16 (a-k) Antimicrobial activity of synthetic *Fi*-His$_{1-21}$ against different bacteria at various concentrations.

5.3.8 PI staining

Dead bacterial cells were observed as red in the PI stained image of *Fi*-His_{1-21} peptide treated *V. vulnificus* (Fig. 5.17). At the same time, peptide penetrated cells were detected as green because of the presence of FITC tag in the peptide. Thus the images were captured under PI and FITC filter on the same field. Green fluorescencence was observed in bacteria in high numbers showing the internalization of the flourescent peptide into the bacterial cytoplasm.

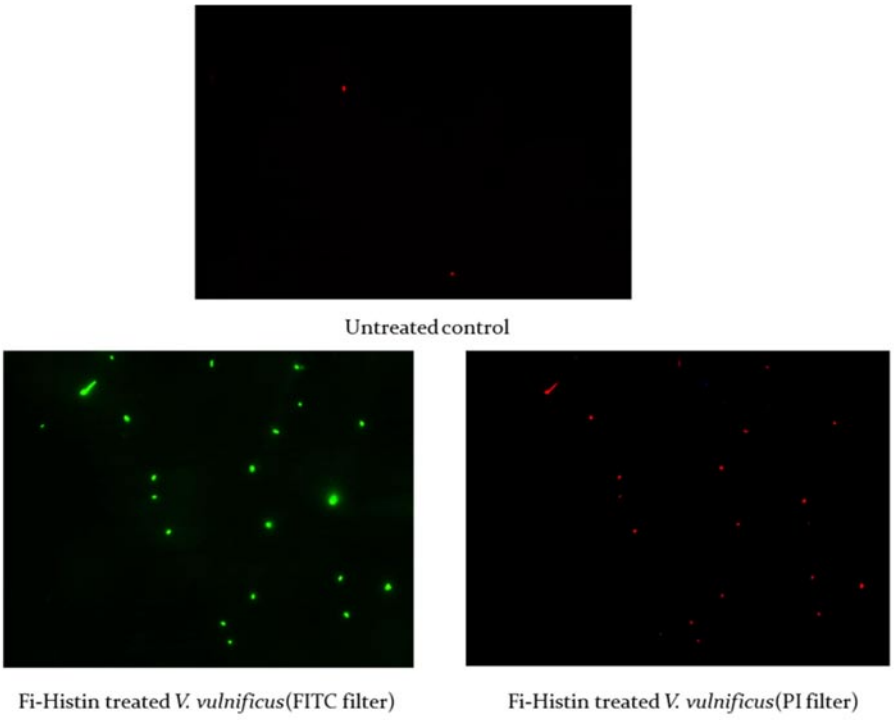

Fig. 5.17 PI stained image of untreated control *V. vulnificus* and synthetic *Fi*-His_{1-21} treated *V. vulnificus* under FITC filter and PI filter (magnification 100 x).

5.3.9 SEM analysis

Morphological alterations of *Fi*-His_{1-21} treated *V. vulnificus* were visualized by scanning electron microscopy (SEM) (Fig. 5.18). On contrary to smooth surfaced untreated control, *V. vulnificus* cells treated with *Fi*-His_{1-21} was noticed with uneven surface, altered membrane and loss of cytoplasmic content.

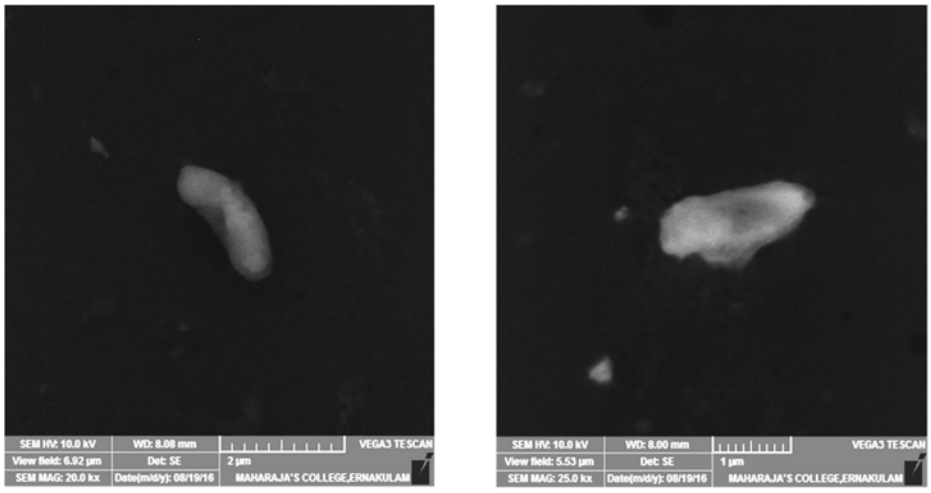

Untreated control of *V. vulnificus* Fi-His_{1-21} treated *V. vulnificus*

Fig. 5.18 SEM image of untreated control *V. vulnificus* and synthetic peptide, *Fi*-His_{1-21} treated *V. vulnificus* showing the disrupted membrane.

5.3.10 DNA Binding assay

To explore the intracellular targeting mechanisms, the DNA binding affinity of *Fi*-His_{1-21} was tested by gel retardation assay. Retardation assay of synthetic *Fi*-His_{1-21} was examined by analyzing the electrophoretic moblity of 50 ng of pUC-18 plasmid vector treated with different concentrations of peptide (200 µM – 3.125 µM). Peptide

exhibited notable retardation by DNA binding from a concentration of 200 µM to 12.5 µM. (Fig. 5.19)

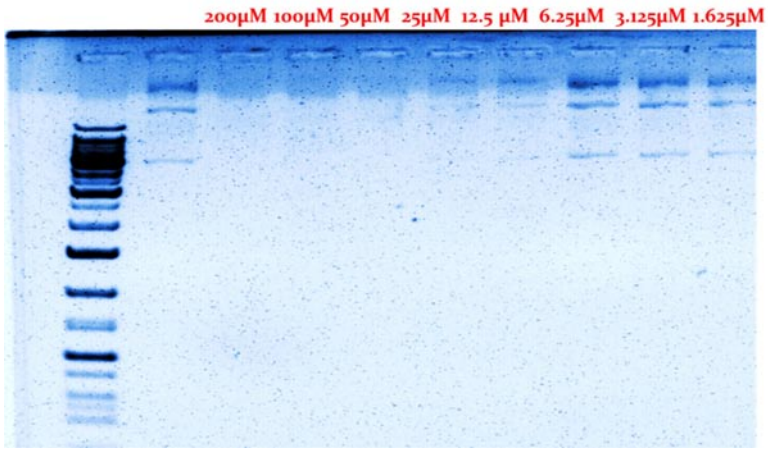

Fig. 5.19 Agarose gel electrophoretogram of DNA binding assay of synthetic *Fi*-His_{1-21} using pUC-18 vector with various concentrations of peptide. Lane M: 1 kb ladder, Lane 1: Control plasmid, Lane 2-8: 200 µM to 3.125 µM concentration of peptide with 50 ng of pUC-18.

5.3.11 *In vitro* cytotoxicity assay

Cytotoxicity of *Fi*-His_{1-21} was tested from 200 µM to 1.625 µM in HEp-2 and NCI-H460 cell lines by XTT assay and the result is represented in Fig. 5.20. At the highest tested concentration (200 µM), growth inhibition of 94 % was exhibited in NCI-H460 and 89 % in HEp-2 cell lines. The IC_{50} of *Fi*-His_{1-21} against HEp2 cells was estimated to be 31.274±24.531 µM and 22.670±13.939 µM for NCI-H460. *Fi*-His_{1-21} displayed potent cytotoxic activity against HEp2 and NCI-H460 cell lines and was found to be concentration dependent.

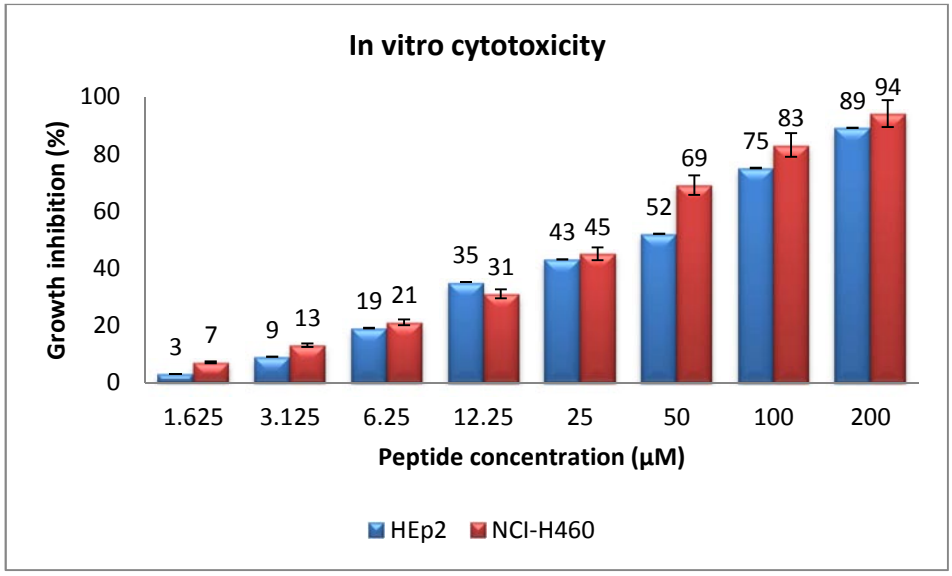

Fig. 5.20 *In vitro* cytotxicity of *Fi*-His_{1-21} against HEp2 and NCI-H460 cells at various tested concentrations

5.3.12 Anticancer activity

5.3.12.1 *Relative gene expression analysis of cancer related genes in Fi-His_{1-21} treated NCI-H460 lung cancer cells*

The *in vitro* gene expression level of cancer related genes in 25 µM and 100 µM of linear peptide, *Fi*-His_{1-21} treated NCI-H460 was analyzed by qRT-PCR. Quantitative RT-PCR analysis showed that the relative gene expression of most of the genes was differentially expressed in response to *Fi*-His_{1-21} treatment. Most of the genes were noticed to be up-regulated including the cancer controlling genes (Bax, Caspase 3, Caspase 9 and Rb1) and cytokine related immune genes (IFN-b, IFN-c, ISG 15, IFITM3, IL-1β and IL-6).

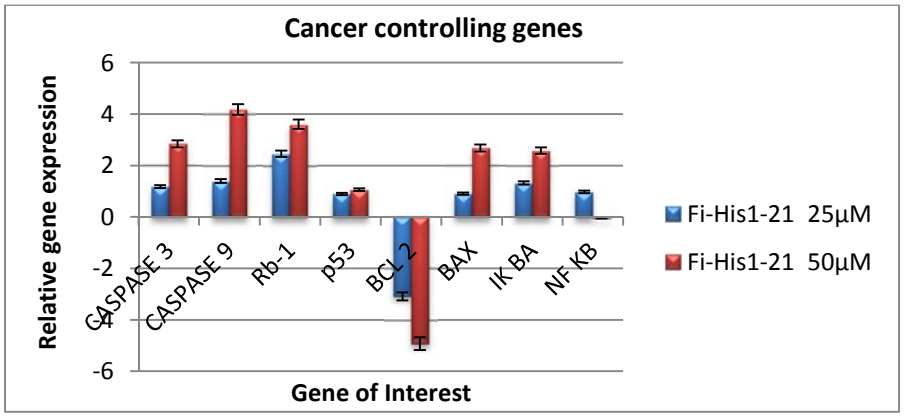
Cancer controlling genes
Relative gene expression
6
4
2
0
-2
-4
-6
CASPASE 3
CASPASE 9
Rb-1
p53
BCL 2
BAX
IK BA
NF KB
Gene of Interest
Fi-His1-21 25µM
Fi-His1-21 50µM

(a)

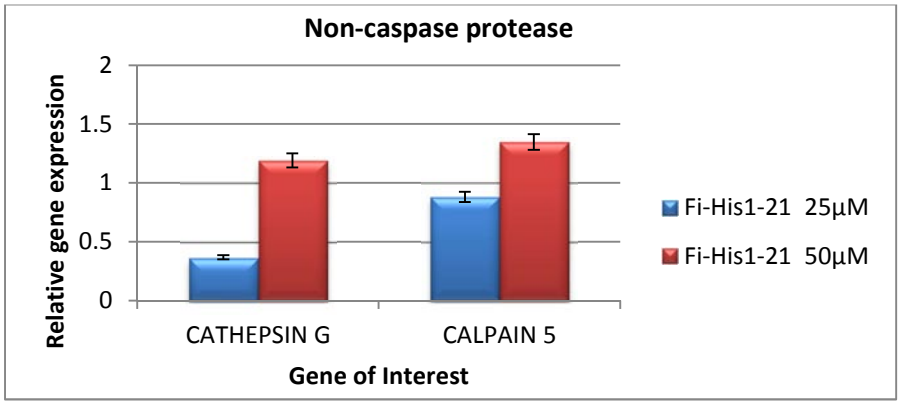
Non-caspase protease
Relative gene expression
2
1.5
1
0.5
0
CATHEPSIN G
CALPAIN 5
Gene of Interest
Fi-His1-21 25µM
Fi-His1-21 50µM

(b)

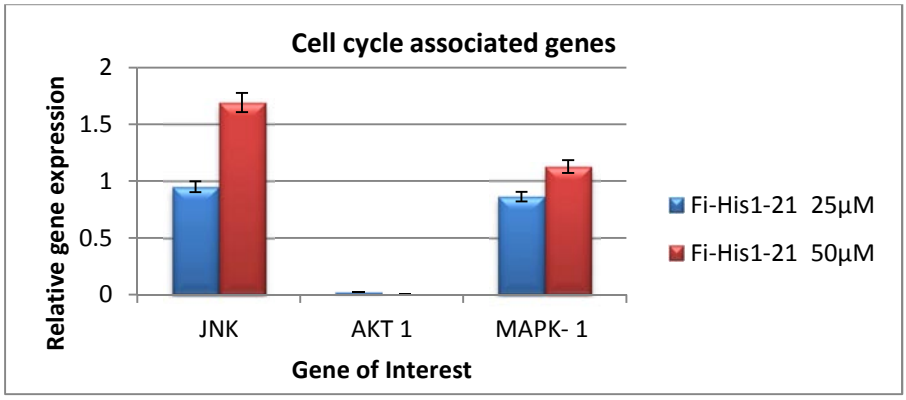
Cell cycle associated genes
Relative gene expression
2
1.5
1
0.5
0
JNK
AKT 1
MAPK- 1
Gene of Interest
Fi-His1-21 25µM
Fi-His1-21 50µM

(c)

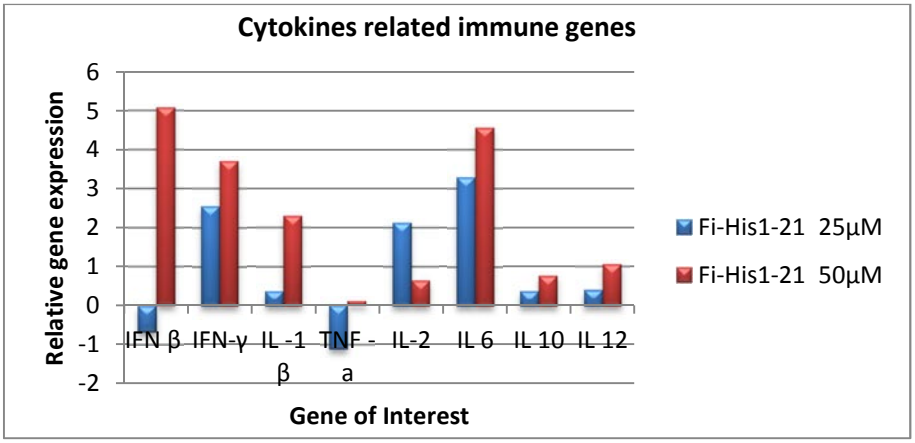

(d)

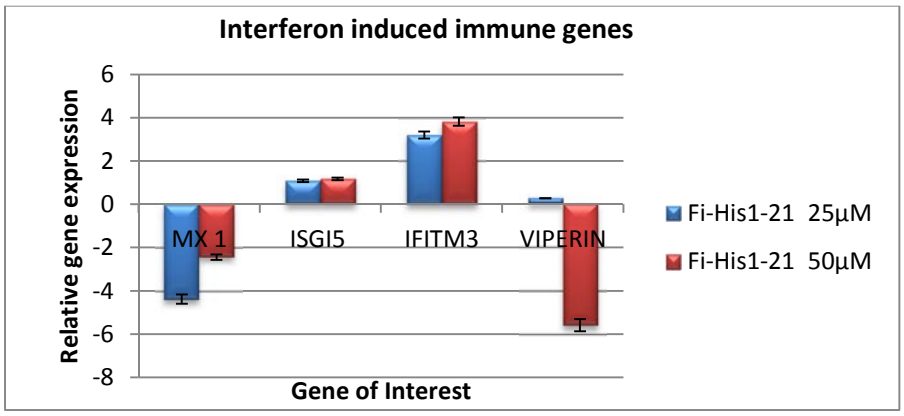

(e)

Fig. 5.21 (a-e) Relative gene expression profile of different cancer related genes using real time PCR and the $\Delta\Delta C_T$ method in *Fi*-His_{1-21} peptide treated in NCI-H460 cell lines.

5.3.12.2 *Relative gene expression analysis of cancer related genes in Fi-His_{1-21} treated HEp-2 pharyngeal cancer cells*

To examine the mode of action underlying the cytotoxic activity of *Fi*-His_{1-21} against HEp2 cell lines, 25 µM and 50 µM of peptide was treated with the cells. The gene expression of cancer controlling and immune related genes in HEp2 cell lines were analysed after peptide treatment by

qRT-PCR (Fig. 5.22 (a-e)). *Fi*-His$_{1-21}$ treatment in HEp-2 cell lines led to the noticeable up-regulation of Bax, TNF-α, Caspase-3, Caspase-9, JNK, Mx-1, IFN-c , ISG15, IFITM3, IL-6, IL-10 and IL-12 and marked down regulation of Bcl2 gene and IL-1β.

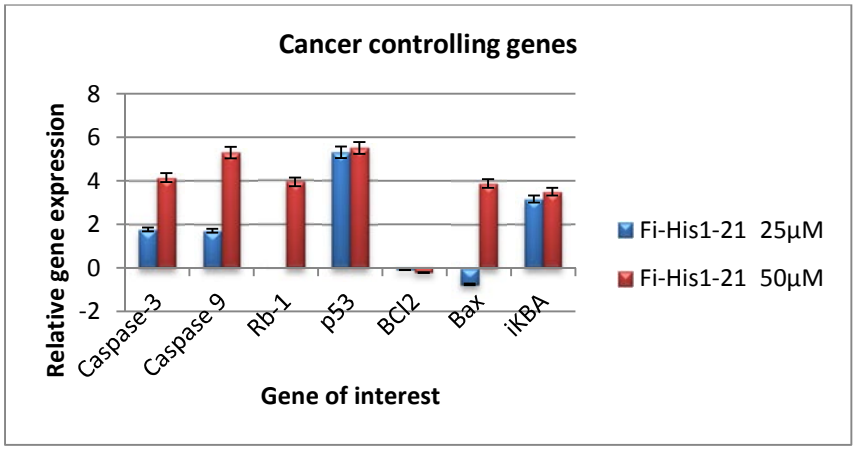

(a)

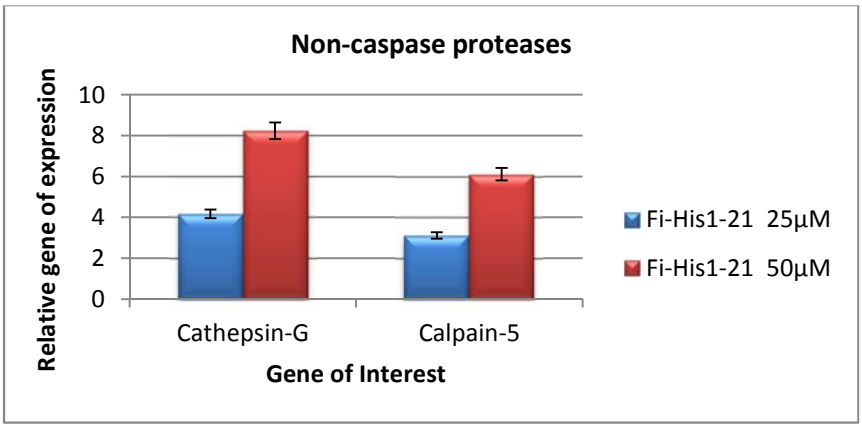

(b)

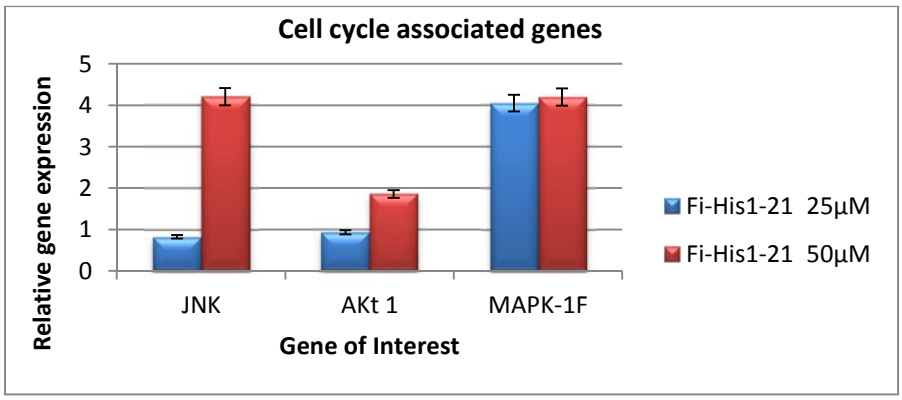

(c)

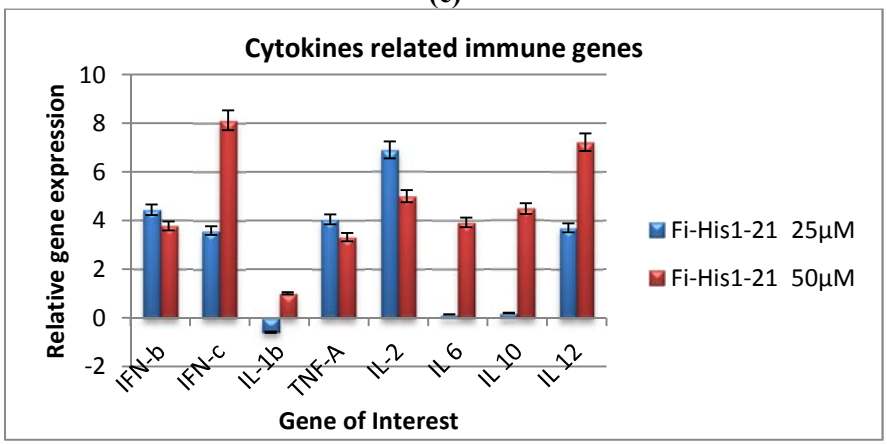

(d)

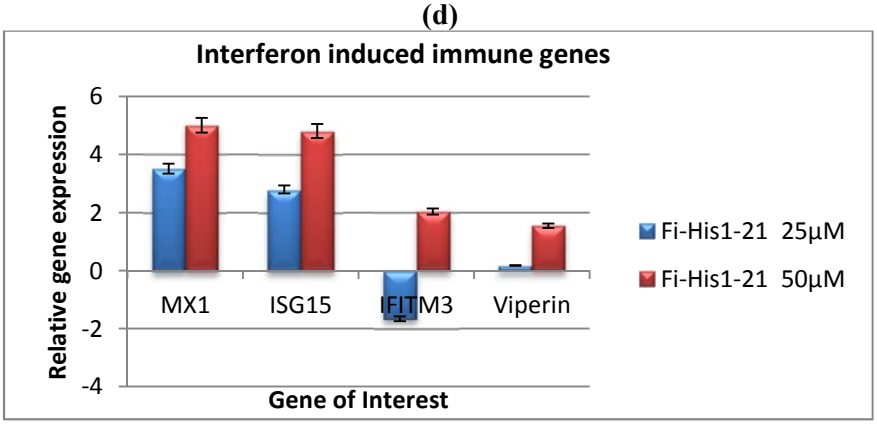

(e)

Fig. 5.22 (a-e) Relative gene expression profile of different cancer related genes using real time PCR and the $\Delta\Delta C_T$ method in *Fi*-His_{1-21} peptide treated in HEp-2 cell lines.

5.4 Discussion

Antimicrobial peptides (AMPs) are multi-functional peptides and form the integral component of the innate immune system which is mainly involved in rapid and non-specific exclusion of pathogenic microorganisms (Diamond et al., 2009). Histone H2A is identified to contribute in the host immune defense processes through producing AMPs mainly by proteolytic cleavage and thus it has been an exciting research application to explore and portray HDAPs in vertebrates and invertebrates. In eukaryotes, histone proteins play an important role in chromatin packaging in nucleus and can also turn as antimicrobials by involving in the host defense processes against pathogen infection (Patrzykat et al., 2001). The present study has reported a histone derived AMP, *Fi*-Histin from the haemocytes of *F. indicus*. The nucleotide sequence of *Fi*-Histin was characterized using biological and bioinformatics tools. The antimicrobial and anticancer activity was demonstrated using synthesizing peptide.

Homology search using BLASTn and BLASTp revealed the similarity of *Fi*-Histin to the Histone–H2A family of invertebrates. *Fi*-Histin is a 27 amino acid cationic peptide having a net positive charge of +6, molecular weight of 2.983 kDa, *p*I of 12.18 and hydrophobicity of 0.221. Secondary structure prediction using PSIPRED (Fig. 5.7) and SWISSMODEL tool (Fig. 5.8) revealed that *Fi*-Histin is an α-helical peptide. The amphipathic nature coupled with net positive charge and α-helical structure gives a strong indication of the antimicrobial nature of *Fi*-Histin.

ClustalW multiple sequence alignment of *Fi*-Histin with other reported HDAPs revealed the existence of conserved residues (Fig. 5.10). While considering the differences, *Fi*-Histin showed a hydrophilic amino acid 'Ser' residue at N-terminus region when compared to other HDAPs from vertebrates where, hydrophilic 'Thr' is present in that place. Also in *Fi*-Histin at 15th amino acid from N-term is a hydrophobic amino acid 'Ile', which is same for all other invertebrate HDAPs; but replaced by hydrophobic 'Val' in all other vertebrate HDAPs. Phylogenetic tree of *Fi*-Histin constructed based on amino acid sequences of previously reported histone H2A derived AMPs validates that the HDAPs are derived from a common ancestor by sequences of evolutionary modifications (Fig. 5.11). The invertebrate HDAPs and vertebrate HDAPs formed a separate group. Compared to other AMPs, HDAP genes evolve very slowly and thus evolutionary studies are of immense importance (Thatcher and Gorovsky, 1994).

Sequence and structural analysis, revealed *Fi*-Histin as an amphipathic and alpha helical cationic AMP with similarity to other known histone H2A derived AMPs (Park et al., 1998; Sathyan et al., 2012). Antimicrobial action of α-helical cationic peptides has been anticipated to arise through three general mechanisms: binding to the cell surface, microbial membrane permeabilization and secondary effects including DNA/protein binding, membrane compositional rearrangements, interference with essential cellular machinery, etc. (Dathe and Wieprecht, 1999; Giangaspero et al., 2001). In addition to membrane disruption antimicrobial mechanism of HDAPs also include interactions with nucleic acids (Koo et al., 2008; Bustillo et al., 2014).

Based on the multiple sequence alignment data (Fig. 5.10), from *Fi*-Histin, a 21 amino acid region was selected based on the similarity to buforin II and named as *Fi*-His_{1-21}. Peptide was synthesized as linear peptide with end modifications and an FITC-tag. Previous study of anticancer activity of buforin II with FITC labelling showed that FITC-labeling had no adverse effects on the cytotoxicity of the peptides when compared to peptide without labelling (Lee et al., 2008).

Fi-His_{1-21} has a net charge of +6 with molecular weight of 2.428 kDa, hydrophobicity of 33 %, and *p*I of 12, making it highly positively charged in physiological media. Artur et al. (2003) and Chen et al. (2007) reported that increased hydrophobicity of the peptide to a certain extent increases the antimicrobial activity. Malmsten et al. (2007), Svensson et al. (2010) and Pasupuleti et al. (2012) found that the net charge above a threshold maximum may not increase the antimicrobial activity since the robust interactions with phospholipid head groups, prevents structuring and further translocation of the peptide. Similar to the buforin II, *Fi*-His_{1-21} is also a cationic α-helical peptide. Main difference in amino acid sequence to buforin II is two amino acids, 'Ser' in first position is replaced by 'Thr' and 'Ile' at 15^{th} place by 'Val' in buforin-II. Yi et al. (1996) elucidated the structure of buforin II using NMR spectroscopy and found that it adopts a helix-hinge-helix; with an N-terminal extended α-helix from Arg_5 to Phe_{10}, and the C-terminal α-helix encompassing residues from Val_{12} to Lys_{21}. *Fi*-Histin also exhibits the same structural features including the 'Pro_{11}' hinge between the two helices (Fig. 5.8). Kobayashi et al. (2000) investigated about the role of Pro in interaction with membrane system and found that Pro_{11} distorts the helical structure of

buforin II and forms a hinge like structure, conferring the unique cell penetrating property. Later in 2004, Kobayashi et al., found that translocation of peptide, buforin II was by toroidal pore formation. Microbicidal activity and the anticancer activity of buforin II has been reported by various scientists due to the intracellular nucleic acid binding especially with DNA and RNA (Park et al., 1998a; Uyterhoeven et al., 2008; Cho et al., 2009).

Antimicrobial activity of histone H2A derived AMPs against both Gram-positive and Gram-negative bacteria especially drug resistant pathogens and fungi was described by several scientists (Park et al., 1996; Park et al., 2000; Giacometti et al., 2000; Giacometti et al., 2001; Richards et al., 2001; Birkemo et al., 2003; Fernandes et al., 2004; Patat et al., 2004; Li et al., 2007; Koo et al., 2008; Sook et al., 2008; De Zoysa et al., 2009). The antimicrobial activity showed by synthetic *Fi*-His_{1-21} was in agreement with the previously reported HDAPs such as hipposin, parasin I, buforin I and buforin II. Like other HDAPs, *Fi*-His_{1-21} also exhibited broad spectrum antibacterial activity against Gram-positive and Gram-negative bacteria which includes both aquatic and human pathogens. Activity of *Fi*-His_{1-21} was observed to be dose dependent and antimicrobial activity was detected down to a concentration of 1.625 μM. At the lowest tested concentration (1.625 μM), the peptide was found to inhibit the growth of Gram-positive bacteria *S. aureus* by 59 % and that of *B. cereus* by 62 %.

Most of the tested pathogens were found to be sensitive against *Fi*-$His_{1-21.}$ Microbicidal activity of the peptide was confirmed by plating the peptide treated bacteria in the LB agar plates and the MBC was found

to be 25 μM for *V. vulnificus*. The bactericidal activity was further analysed by epifluorescence microscopy after staining using permeability marker, PI and the dead cells were observed as red indicating that the bacterial membrane is permeabilized (Fig. 5.17). Morphological variations in peptide treated *V. vulnificus* were observed through SEM in order to better understand the mode of microbicidal activity and membrane perturbed bacteria without any blebbing or pores compared to untreated control clearly observed in the SEM image (Fig. 5.18).

Like other reported HDAPs *Fi*-His_{1-21} the cationic nature could assist in the antimicrobial action via electrostatic interaction with microbial membranes. Chen et al. (2015) observed the LPS and LTA binding activity of H2A N-terminus derived AMP, Sphistin from *S. paramamosain* and speculated that the electrostatic attraction to negatively charged microbial surfaces is involved in the initial stage of antimicrobial mechanism. The α-helical nature of *Fi*-His_{1-21} could attach to the microbial membrane with partitioning of hydrophilic and hydrophobic amino acids followed by interaction with the phospholipid bilayer of microbe. Epifluorescence microscopy image of *V. vulnificus* treated with peptide appeared fluorescent (green) through FITC filter which ensures the entry of peptide. SEM investigation revealed the cell membrane rupture and cell content leakage inferring that the killing could be via initial binding followed by permeabilization and cell damage.

DNA binding activity of buforin-II and buforin-III variants was studied and found that antimicrobial activity is correlated with DNA binding affinity of the peptide (Uyterhoeven et al., 2008; Jang et al.,

2012). Synthetic *Fi*-His_{1-21} exhibited a distinguishable DNA binding activity even at 12.5 μM, which is a lower concentration than the MIC. Thus along with the α-helical content, cationicity and hydrophobicity the DNA binding activity of synthetic *Fi*-His_{1-21} augments the antimicrobial activity. Previous studies revealed that the synthetic and purified N-terminal region of histone H2A derived AMPs exhibited antimicrobial and anticancer activity (Park et al., 1998a; Birkemo et al., 2003; Patat et al., 2004; Bergsson et al., 2005; De Zoysa et al., 2009; Chen et al., 2015).

In the development of novel antimicrobials as drug, the main hurdle is the cytotoxicity against host cells. Majority of the HDAPs are found to be non-cytotoxic to normal eukaryotic cells including Buforin IIb (Lee et al., 2008) and Sphistin (Chen et al., 2015). *Fi*-His_{1-21} was also found to be non-cytotoxic against mammalian erythrocytes through a haemolytic assay. Synthetic HDAP, abhisin exhibited cytotoxicity against leukemia cancer (THP-1) cells but not for normal fibroblast vero cells (De Zoysa et al., 2009), likewise *Fi*-His_{1-21} also displayed anticancer activity against cancer cell lines including lung cancer (NCI-H460) cells and pharyngeal cancer (HEp-2) cells without cytotoxicity against human RBCs in haemolytic assays.

Recently, anticancer peptides (ACPs) gained consideration as a substitute to chemotherapeutic drugs. ACPs have benefits over currently used anticancer therapeutics, by virtue of its potential in discriminating normal and cancer cells and ability to circumvent the multidrug-resistance mechanism (Papo and Shai, 2005). HDAPs including buforin IIb were found to be non-cytotoxic to normal cells (Jang et al., 2011). Anticancer

activity of HDAP, buforin IIb was studied by Lee et al. (2008) and found that the cytotoxic activity against cancer cells were mainly by directing cancer cells through interaction with cell surface gangliosides, phosphatidylserine (PS) and heparin sulfate (HS). Without damaging the cell membrane, the peptide induced apoptosis via intrinsic pathway mediated through induction of caspase-3 and caspase-9.

Anticancer mechanism by *Fi*-His1-21 in NCI-H460 and HEp-2 cell lines was observed by gene expression analysis using qRT-PCR. Our results propose that *Fi*-His_{1-21} up-regulates apoptosis related to caspase-3 and caspase-9 activation in both the tested cell lines. Apparently, this could be resulted from the release of cytochrome c from mitochondria which in turn get activated downstream caspase-9 and caspases-3. The linear peptide *Fi*-His_{1-21} induced the activation of caspase-9 and which could initiates mitochondrion-dependent apoptosis. In both the cell lines, the up-regulation of analysed caspases were found to be concentration dependent (Kaufmann and Earnshaw, 2000). Mitochondria dependent mode of apoptosis induction is involved in the anticancer activity of most of the AMPs. The AMPs such as RGD-tachyplesin, buforin IIb, and DP1 were also observed to persuade apoptosis in tumour cells via mitochondrion-dependent pathway (Lin et al., 2010).

The up-regulation of mRNA of pro-apoptotic protein Bax and further down-regulation of anti-apoptotic protein Bcl2 was observed in both cell lines, and the ratio of Bax : Bcl-2 proteins is believed to get augmented upon apoptosis induction (Leung and Wang, 1999). The tumour suppressor genes p53 and Rb1 which aid in the regulation of cell

growth and cell division were also found to be up-regulated followed by peptide treatment in both cell lines. Similar kind of up-regulation of p53 mRNA was noticed in epinecidin-1 treated U-937 leukaemia cell lines (Chen et al., 2009). Expression level of non-caspase proteases, Cathepsin-G and Calpain-5 were also high in both cell lines. Both the proteases expressed significantly more in NCI-H460 cells compared to HEp-2 upon peptide treatment. Thus along with other caspases, these non-caspase proteases could also assist in the apoptosis.

The pattern of gene expression level of MAPKs, MAPK1 and JNK were found to be up-regulated after peptide treatment in both cell lines. Thus the induction could lead to the phosphorylation of substrates involved in different signalling pathways for apoptosis induction, augmenting the anticancer activity of *Fi*-His_{1-21} peptide. While analysing the relative mRNA level of cytokine genes in both cell lines after *Fi*-His_{1-21} treatment, induction of all tested interleukins, TNF-α and that of interferons, IFN-α and IFN-γ have been detected. Similar kind of induction of cytokines was observed after administration of pardaxin peptide in HeLa cell lines (Hsu et al., 2011). Up-regulated gene expression of pro-inflammatory cytokines, such as TNF-α and IL-6 proposed a possible increase in phagocytosis as in the case of peptide, TH 1-5 treated HT1080 cell lines (Chang et al., 2011). Interestingly, the peptide exhibited ant-cancer activity along with immunomodulatory activity in both tested cell lines identical to other ACPs such as buforin-II, epinecidin-1, S-ALF, pardaxin and Tilapia hepcidins (TH1-5) (Chen et al., 2009; Lin et al., 2010; Hsu et al., 2011; Chang et al., 2011).

Anticancer activity of *Fi*-His_{1-21} was in par with the previous reports on cytotoxic activity of HDAPs. Further studies are needed to scrutinize the exact mode of anticancer activity exhibited by synthetic *Fi*-His_{1-21} peptide. In conclusion a putative HDAP, *Fi*-Histin was identified and cloned from haemocytes of Indian white shrimp, *F. indicus*. The synthetic peptide, *Fi*-His_{1-21} exhibited broad spectrum antimicrobial activity and remarkable anticancer activity along with low toxicity towards human erythrocytes. Thus the peptide *Fi*-His_{1-21} is a prospective contender for preclinical studies for its application as a therapeutic drug against bacterial infections and in cancer therapy.

Chapter 6

SUMMARY AND CONCLUSION

With the advent of antibiotic-resistant bacteria and the insufficiency of new classes of expedient antibiotics, there is an instantaneous prerequisite for effective substitute therapeutants. Oceans are rich with biodiversity and remain a valuable resource of bioactive molecules unexplored. Of these, the marine invertebrates are prime candidates of bioactive metabolites with potential activity which could lead to the development of new pharmaceutical products. Marine cationic antimicrobial peptides symbolize a largely untapped resource that can trail the molecular route from the oceans to the lab. AMPs display several activities that make them promising candidates as therapeutic agents. AMPs display broad-spectrum antibacterial activity or selective activity against Gram-negative or Gram-positive bacteria, or antifungal, antiviral, anti-parasitic and anticancer activity. Also AMPs exhibit, rapid killing of microbes (99.9% within 20 min), in synergy with antibiotics, and are active against both antibiotic-susceptible and antibiotic-resistant strains, and reduce sepsis shock by endotoxin neutralization.

Crustaceans lack a specific adaptive immune response to thrive in an environment comprising one million bacteria per mL and present a

robust non-specific innate immune system that controls pathogenic invasion. AMPs are short peptides that form part of the innate immune response and act by compromising microbial membranes. The present study was intended for bioprospecting of novel AMPs from marine crustaceans using genomics approach. Bioinformatics tools were employed for the molecular and phylogenetic analysis of AMPs identified in this study. Functional characterization was performed using recombinant and synthetic peptides and screened for antimicrobial, anticancer, DNA binding, haemolytic and cytotoxic activity.

Salient findings

- In the present study, marine crustaceans were screened for novel AMP genes using gene based approach. Overall five AMPs, belonging to the families of ALF, crustin and histone H2A derived peptides could be identified and characterized.
- Two novel Anti-lipopolysaccharide factor (ALF) isoforms were identified from haemocytes of Crucifix crab, *C. feriatus*, and named as *Cf*-ALF1 (GenBank ID: **KP688577**) and *Cf*-ALF2 (GenBank ID: **KT224347**). Molecular and phylogenetic characterization of ALF isoforms was done *in-silico*.
- From Indian white shrimp, *Fenneropenaeus indicus* an isoform of crustin, *Fi*-crustin2 (GenBank ID: **KX622789**) and a histone H2A derived AMP, *Fi*-Histin (GenBank ID: **KY126319**) were identified using gene based approach
- A novel isoform of ALF was also identified from stomatopod, *Miyakea nepa* and termed as *Mn*-ALF (GenBank ID: **KJ995817**).

- The AMPs, *Cf*-ALF2 and *Fi*-crustin2 were produced for functional characterization by recombinant expression using pET-32a(+) vector in expression host *E. coli* Rosetta-gami^{TM} B (DE3) pLysS.
- Two AMPs, *Mn*-ALF and *Fi*-Histin were synthesized with FITC labelling and end modifications (with >95% final purity) at M/s Zhejiang Ontores Biotechnologies Co., Ltd China by Solid phase technology (Fmoc chemistry). .
- The recombinant (2 Nos) and synthetic peptides (2 Nos) were characterized for antibacterial, anticancer, DNA binding, haemolytic and cytotoxic activity.
- Recombinant anti-lipopolysaccharide factor, *Cf*-ALF2 exhibited broad spectrum antimicrobial activity with significant activity against *S. aureus* (MIC – 5 μM) and *E. coli* (MIC – 10 μM). Membrane damages including blebbing due to the action of peptides was very clear in the Scanning Electron Micrograph (SEM) analysis.
- The r*Cf*-ALF2 was found to be non-DNA binding, non-cytotoxic and non-haemolytic at the tested concentrations (20 μM – 1.25 μM).
- Recombinant peptide, *Fi*-crustin2 exhibited broad spectrum activity against Gram positive and Gram negative bacteria with remarkable activity against *E. tarda* (MIC 5 μM) and *A. hydrophila* (MIC 10 μM) mainly by bacterial membrane disruption, revealed by SEM analysis.

- The peptide, r*Fi*-crustin2 was non-DNA binding, non-haemolytic and non-cytotoxic at the tested concentrations (20 μM – 1.25 μM).
- In order to characterize *Mn*-ALF, the putative LPS binding domain of Mn-ALF (MNA-LBD), (Sequence: ECKFTVKPY IKRFQLNYKGRMWCP), was synthesized as cyclic peptide with di-sulphide bond between Cys residues.
- Synthetic MNA-LBD revealed that it is a potential AMP with antimicrobial activity against *E. coli* (MIC and MBC of 25 μM) and *B. cereus, P. aeruginosa, E. tarda, V. parahaemolyticus* and *V. alginolyticus* (MIC of 50 μM). SEM analysis of peptide treated *E. coli* confirmed the membrane leakage of bacteria after treatment with peptide.
- Synthetic MNA-LBD was found to be DNA binding (from 12.5 μM to 200 μM) and non-haemolytic against hRBCs.
- A 21 amino acid length region of Histone derived antimicrobial peptide from *Fenneropenaeus indicus*, *Fi*-Histin (SRSSRAGL QFPVGRIHRLLRK) sharing similarity to buforin (histone derived AMP) was synthesized as linear peptide and named as *Fi*-His_{1-21}.
- Synthetic Fi-Histin exhibited antimicrobial activity against *V. vulnificus*, (MIC and MBC of 25 μM), *P. aeruginosa* and *V. parahaemolyticus* (MIC - 25 μM, MBC - > 50 μM), *S. aureus* and *V. cholera* (MIC - 50 μM, MBC - >50 μM). It was also found to exhibit DNA binding activity and displayed

membrane destabilization in SEM analysis of peptide treated *V. vulnificus* with lower toxicity towards hRBCs.

- Anticancer activity of synthetic peptides MNA-LBD and *Fi*-His_{1-21} were evaluated through *in vitro* gene expression analysis using qRT-PCR on NCI-H460 and HEp-2 cancer cell lines.
- Gene expression studies revealed that cancer related and immune related genes were differentially expressed in response to MNA-LBD and *Fi*-His_{1-21}.
- Genes related to apoptosis and tumor suppression was upregulated followed by peptide treatment in both cell lines.
- MNA-LBD and *Fi*-His_{1-21} exhibited immunomodulatory and anticancer activity in NCI-H460 and HEp2 cell lines mainly via regulation of cytokine related and intrinsic apoptotic pathway genes.

Crustaceans represent one of the most abundant animals inhabiting both aquatic and terrestrial habitats. By virtue of their diversity and abundance they have earned consideration as a potential source of bioactive compounds. Crustacean AMPs could be considered as potential therapeutants to fight against antibiotic resistance which is considered as a grave threat to public health across India and the globe. The present study generated new information regarding the innate immune system of crustacean by identifying and characterizing five novel AMPs. All the peptides demonstrated significant anti-bacterial activity against the tested aquatic and clinical pathogens and could be considered for further pre-clinical assays. Synthetic peptides projected in this study were found to

inhibit the growth of cancer cell lines including NCI-H460 and HEp-2 via apoptosis induction and immunomodulation. While considering the application of AMPs in medicine and/or aquaculture, main hurdles to overcome include degradation caused by proteases, high production cost, mode of delivery and stability *in vivo*. Incorporation of unusual amino acids or peptido-mimetics to evade proteolytic degradation and design of short peptides with antimicrobial activities in order to decrease the production cost are some of the solutions. A comprehensive analysis of the mechanism of action of antibacterial and anticancer activity of peptides mentioned in this study will aid in yielding effective therapeutics in medicine and/or aquaculture.

References

[1] Afsal, V. V, Antony, S. P., Sathyan, N., & Philip, R. (2011). Molecular characterization and phylogenetic analysis of two antimicrobial peptides: Anti-lipopolysaccharide factor and crustin from the brown mud crab, *Scylla serrata. Results in Immunology*, *1*(1), 6–10. doi:10.1016/j.rinim.2011.06.001

[2] Afsal, V. V., Antony, S. P., Philip, R., & Bright Singh, I. S. (2016). Molecular Characterization of a Newly Identified Subfamily Member of Penaeidin from two Penaeid Shrimps, *Fenneropenaeus indicus* and *Metapenaeus monoceros*. *Probiotics and Antimicrobial Proteins*, *8*(1), 46–52. doi:10.1007/s12602-015-9203-9

[3] Afsal, V. V., Antony, S. P., Sanjeevan, V. N., Anil Kumar, P. R., Singh, I. S. B., & Philip, R. (2012). A new isoform of anti-lipopolysaccharide factor identified from the blue swimmer crab, *Portunus pelagicus*: Molecular characteristics and phylogeny. *Aquaculture*, *356-357*, 119–122. doi:10.1016/j.aquaculture.2012.05.028

[4] Ahyong, S.T. (2001). Revision of the Australian Stomatopod Crustacea. *Records of the Australian Museum, Supplement* 26, 1-326.

[5] Ajesh, K. and Sreejith, K. (2009). Peptide antibiotics: an alternative and effective antimicrobial strategy to circumvent fungal infections. *Peptides*, *30,* 999–1006.

[6] Alpert, G., Baldwin, G. & Thompson, C. (1922). Limulus antilipopolysaccharide factor protects rabbits from meningococcal endotoxin shock. *Critical Care Medicine,22*, 494–500.

[7] Amparyup, P., Donpudsa, S., Tassanakajon, A. (2008a). Shrimp single WAP domain (SWD)-containing protein exhibits proteinase inhibitory and antimicrobial activities. *Developmental and Comparative Immunology*, *32*, 1497-1509.

[8] Amparyup, P., Kondo, H., Hirono, I., Aoki, T., & Tassanakajon, A. (2008b). Molecular cloning, genomic organization and recombinant expression of a crustin-like antimicrobial peptide from black tiger shrimp Penaeus monodon. *Molecular Immunology*, *45*(4), 1085–93. doi:10.1016/j.molimm.2007.07.031

[9] Andrä, J., Howe, J., Garidel, P., Rössle, M., Richter, W., Leiva-León, J. & Brandenburg, K. (2007). Mechanism of interaction of optimized Limulus-derived cyclic peptides with endotoxins: thermodynamic, biophysical and microbiological analysis. *The Biochemical Journal*, *406*(2), 297–307. doi:10.1042/BJ20070279

[10] Andra, J., Lamata, M., de Martinez Tejada, G., Bartels, R., Koch, M.H., Brandenburg, K. (2004). Cyclic antimicrobial peptides based on Limulus anti-lipopolysaccharide factor for neutralization of lipopolysaccharide. *Biochemical Pharmacology*, 68, 1297–1307.

[11] Antony, S. P., Bright Singh, I. S., & Philip, R. (2010). Molecular characterization of a crustin-like, putative antimicrobial peptide, Fi-crustin, from the Indian white shrimp, *Fenneropenaeus indicus*. *Fish & Shellfish Immunology*, *28*(1), 216–20. http://doi.org/10.1016/j.fsi.2009.10.013

[12] Antony, S. P., Singh, I. S. B., & Philip, R. (2011a). Molecular characterization and phylogenetic analysis of a penaeidin-like antimicrobial peptide, Fi-penaeidin from *Fenneropenaeus indicus*. *Aquaculture*, *319*(1-2), 298–301. doi:10.1016/j.aquaculture.2011.06.011

[13] Antony, S. P., Singh, I. S. B., Sudheer, N. S., Vrinda, S., Priyaja, P., & Philip, R. (2011b). Molecular characterization of a crustin-like antimicrobial peptide in the giant tiger shrimp, Penaeus monodon, and its expression profile in response to various immunostimulants and challenge with WSSV. *Immunobiology*, *216*(1-2), 184–94. doi:10.1016/j.imbio.2010.05.030

[14] Antony, S. P., Philip, R., Joseph, V., & Singh, I. S. B. (2011c). Anti-lipopolysaccharide factor and crustin-III, the anti-white spot virus peptides in *Penaeus monodon*: Control of viral infection by up-regulation. *Aquaculture*, *319*(1-2), 11–17. doi:10.1016/j.aquaculture.2011.06.022

[15] Arayamethakorn, S., Krusong, K., & Tassanakajon, A. (2013). Cloning , Expression and Characterization of Recombinant Crustin Pm 7 from Black Tiger Shrimp *Penaeus monodon*. In *Proceedings: International Graduate Research Conference 2013* (pp. 231–235).

[16] Arnold, K., Bordoli, L., Kopp, J., Schwede, T. 2006. The SWISS-MODEL Workspace: A web-based environment for protein structure homology modeling. *Bioinformatics*. 22, 195-201.

[17] Arockiaraj, J., Gnanam, A. J., Muthukrishnan, D., Gudimella, R., Milton, J., Singh, A., Bhassu, S. (2013a). Crustin, a WAP domain containing antimicrobial peptide from freshwater prawn *Macrobrachium rosenbergii*: immune characterization. *Fish & Shellfish Immunology*, *34*(1), 109–18. doi:10.1016/j.fsi.2012.10.009

[18] Arockiaraj, J., Kumaresan, V., Bhatt, P., Palanisamy, R., Gnanam, A. J., Pasupuleti, M., Chaurasia, M. K. (2013b). A novel single-domain peptide, anti-LPS factor from prawn: Synthesis of peptide, antimicrobial properties and complete molecular characterization. *Peptides*. doi:10.1016/j.peptides. 2013.11.008

[19] Arockiaraj, J., Gnanam, A. J., Kumaresan, V., Palanisamy, R., Bhatt, P., Kuppusamy, M., & Roy, A. (2013c). Fish & Shell fi sh Immunology An unconventional antimicrobial protein histone from freshwater prawn *Macrobrachium rosenbergii* : Analysis of immune properties. *Fish and Shellfish Immunology*, *35*(5), 1511–1522. doi:10.1016/ j.fsi.2013.08.018

[20] Arrighi, R.B.G., Nakamura, C., Miyake, J., Hurd, H., Burgess, J.G. (2002). Design and activity of antimicrobial peptides against sporogonic-stage parasites causing murine malarias. *Antimicrobial Agents and Chemotherapy, 46,* 2104-2110.

[21] Artur S., Mukesh P., Matthias M., Mina D., Jan A., Anna C. (2003). Hipposin, a histone- derived antimicrobial peptide in Atlantic halibut (*Hippoglossus hippoglossus L.*). *Biochimica et Biophysica Acta*, *1646,* 207-15

[22] Bachère, E., Mialhe, E. and Rodriguez, J. (1995) Identification of defence effectors in the haemolymph of Crustaceans with particular reference to the shrimp *Penaeus japonicus* (Bate): prospects and applications. *Fish & Shellfish Immunology, 5,* 597–612.

[23] Baker, M.A., Maloy, W.L., Zasloff, M., Jacob, L.S. (1993). Anticancer efficacy of magainin 2 and analogue peptides. *Cancer Research, 53,* 3052-3057

[24] Banerjee, D., Maiti, B., Girisha, S. K., Venugopal, M. N., & Karunasagar, I. (2015). A crustin isoform from black tiger shrimp, *Penaeus monodon* exhibits broad spectrum anti-bacterial activity. *Aquaculture Reports*, *2*, 106–111. doi:10.1016/j.aqrep.2015.08.009

[25] Bartlett, T. C., Cuthbertson, B. J., Shepard, E. F., Chapman, R. W., Gross, P. S., & Warr, G. W. (2002). Crustins, Homologues of an 11. 5-kDa Antibacterial Peptide, from Two Species of Penaeid Shrimp , *Litopenaeus vannamei* and *Litopenaeus setiferus*. *Marine Biotechnology*, 278–293. doi:10.1007/s10126-002-0020-2

[26] Battison, A. L., Summerfield, R., & Patrzykat, A. (2008). Isolation and characterisation of two antimicrobial peptides from haemocytes of the American lobster *Homarus americanus*. *Fish & Shellfish Immunology*, *25*(1-2), 181–7. doi:10.1016/j.fsi.2008.04.005

[27] Beale, K. M., Towle, D. W., Jayasundara, N., Smith, C. M., Shields, J. D., Small, H. J., & Greenwood, S. J. (2008). Anti-lipopolysaccharide factors in the American lobster *Homarus americanus*: molecular characterization and transcriptional response to Vibrio fluvialis challenge. *Comparative Biochemistry and Physiology. Part D, Genomics & Proteomics*, *3*(4), 263–9. doi:10.1016/j.cbd.2008.07.001

[28] Bechinger, B. & Salnikov, E. S. (2012) The membrane interactions of antimicrobial peptides revealed by solid-state NMR spectroscopy. *Chemistry and Physics of Lipids, 165,* 282–301.

[29] Bergsson, G., Agerberth, B., Jörnvell, H. & Gudmundsson, G. H. (2005). Isolation and identification of antimicrobial components from epidermal mucus of Atlantic cod, *Gadus morhua*. *FEBS Journal, 272,* 4960–4969.

[30] Birkemo, G. A., Lüders, T., Andersen, O., Nes, I. F., & Nissen-Meyer, J. (2003). Hipposin, a histone-derived antimicrobial peptide in Atlantic halibut (*Hippoglossus hippoglossus* L.). *Biochimica et Biophysica Acta (BBA) - Proteins and Proteomics*, *1646*(1-2), 207–215. doi:10.1016/S1570-9639(03)00018-9

[31] Boman, H. G. (2003). Antibacterial peptides: basic facts and emerging concepts. *Journal of Internal Medicine* 254, 197-215.

[32] Boman, H.G. (1995). Peptide antibiotics and their role in innate immunity, *Annual Review of Immunology, 13,* 61–92.

[33] Brandenburg, K., Heinbockel, L., Correa, W., & Lohner, K. (2016). Peptides with dual mode of action: Killing bacteria and preventing endotoxin-induced sepsis. *Biochimica et Biophysica Acta - Biomembranes*, *1858*(5), 971–979. doi:10.1016/j.bbamem.2016.01.011

[34] Brandenburg, L. O., Merres, J., Albrecht, L. J., Varoga, D., and Pufe, T. (2012). Antimicrobial peptides: multifunctional drugs for different applications. *Polymers, 4,* 539–560. doi: 10.3390/polym4010539

[35] Brockton, V., Hammond, J. a, & Smith, V. J. (2007). Gene characterisation, isoforms and recombinant expression of carcinin, an antibacterial protein from the shore crab, Carcinus maenas. *Molecular Immunology*, *44*(5), 943–9. doi:10.1016/j.molimm.2006.03.017

[36] Brogden, K.A. (2005). Antimicrobial peptides: Pore formers or metabolic inhibitors in bacteria? *Nature Reviews Microbiology* 3, 238-250.

[37] Bustillo, M. E., Fischer, A. L., LaBouyer, M. A., Klaips, J. A., Webb, A. C. & Elmore, D. E. (2014). Modular analysis of hipposin, a histone-derived antimicrobial peptide consisting of membrane translocating and membrane permeabilizing fragments. *Biochimica et Biophysica Acta (BBA) – Biomembranes*, *1838(9*), 2228–2233.

[38] Cézard, C., Silva-pires, V., Mullié, C. & Sonnet, P. (2011). Antibacterial Peptides : A Review. *Science against microbial pathogens: communicating current research and technological advances*, A. Méndez-Vilas (Ed.) 926–937.

[39] Chaithanya, E. R., Philip, R., Sathyan, N., & Kumar, P. R. A. (2013). Molecular Characterization and Phylogenetic Analysis of a Histone-Derived Antimicrobial Peptide Teleostin from the Marine Teleost Fishes, Tachysurus jella and Cynoglossus semifasciatus. *ISRN Molecular Biology*, *2013*, 1–8.

[40] Chang, W. T., Pan, C. Y., Rajanbabu, V., Cheng, C. W., & Chen, J. Y. (2011). Tilapia (Oreochromis mossambicus) antimicrobial peptide, hepcidin 1-5, shows antitumor activity in cancer cells. *Peptides*, *32*(2), 342–52. doi:10.1016/j.peptides.2010.11.003

[41] Chaurasia, M. K., Palanisamy, R., Bhatt, P., Kumaresan, V., Gnanam, A. J., Pasupuleti, M. & Arockiaraj, J. (2015). A prawn core histone 4: Derivation of N- and C-terminal peptides and their antimicrobial properties, molecular characterization and mRNA transcription. *Microbiological Research*, *170*, 78–86. doi:10.1016/j.micres.2014.08.011

[42] Chen, J., Xu, X. M., Underhill, C. B., Yang, S., Wang, L. & Chen, Y. (2005). Tachyplesin activates the classic complement pathway to kill tumor cells. *Cancer Research,* 65, 4614–22.

[43] Chen Y., Guarnieri M.T., Vasil A.I., Vasil M.L., Mant C.T., Hodges R.S. (2007). Role of peptide hydrophobicity in the mechanism of action of α-helical antimicrobial peptides. *Antimicrobial Agents and Chemotherapy, 51(4),* 1398–406.

[44] Chen, B., Fan, D. Q., Zhu, K. X., Shan, Z. G., Chen, F. Y., Hou, L. & Wang, K. J. (2015). Mechanism study on a new antimicrobial peptide Sphistin derived from the N-terminus of crab histone H2A identified in haemolymphs of *Scylla paramamosain*. *Fish and Shellfish Immunology*, *47*(2), 833–846. doi:10.1016/j.fsi.2015.10.010

[45] Chen, J. Y., Lin, W. J., Wu, J. L., Her, G. M., & Hui, C. F. (2009). Epinecidin-1 peptide induces apoptosis which enhances antitumor effects in human leukemia U937 cells. *Peptides*, *30*(12), 2365–73. doi:10.1016/j.peptides.2009.08.019

[46] Chi, C. -F., Hu, F. -Y., Wang, B., Li, T. & Ding, G. F. (2015) Antioxidant and anticancer peptides from the protein hydrolysate of blood clam (*Tegillarca granosa*) muscle. *Journal of Functional Foods*, 15, 301–313

[47] Cho, J. H., Sung, B. H., & Kim, S. C. (2009). Buforins: histone H2A-derived antimicrobial peptides from toad stomach. *Biochimica et Biophysica Acta*, *1788*(8), 1564–9. doi:10.1016/j.bbamem.2008.10.025

[48] Cho, J. U. H., Park, I. N. Y., Kim, H. S., Lee, W. T., Kim, M. S. and Kim, S. C. (2002). Cathepsin D produces antimicrobial peptide parasin I from histone H2A in the skin mucosa of fish. The FASEB Journal 16, 429–431.

[49] Conlon, J. M. (2015). Host-defense peptides of the skin with therapeutic potential: From hagfish to human. *Peptides*, *67*, 29–38. doi:10.1016/j.peptides.2015.03.005

[50] Cruciani, R. A., Barker, J. L., Zasloff, M., Chen, H. C. and Colamonici, O. (1991) Antibiotic magainins exert cytolytic activity against transformed cell lines through channel formation. *Proceedings of the National Academy of Sciences of the U S A,* 88, 3792-3796.

[51] Cui, Z., Song, C., Liu, Y., Wang, S., Li, Q., & Li, X. (2012). Crustins from eyestalk cDNA library of swimming crab *Portunus trituberculatus:* molecular characterization, genomic organization and expression analysis. *Fish & Shellfish Immunology*, *33*(4), 937–45. doi:10.1016/j.fsi.2012.08.002

[52] da Costa, J. P., Carvalhais, V., Amado, F., Silva, A., Nogueira-Ferreira, R., Ferreira, R., Helguero, L. and Vitorino, R. (2015) Anti-tumoral activity of human salivary peptides. *Peptides, 71,* 170–178.

[53] Daher, K. A., Selsted, M. E. and Lehrer, R. I. (1986). Direct inactivation of viruses by human granulocyte defensins. *Journal of Virology, 60,* 1068–1074.

[54] Dathe, M., T. Wieprecht, 1999. Structural features of helical antimicrobial peptides: their potential to modulate activity on model membranes and biological cells, *Biochimica et Biophysica Acta, 1462,* 71-87.

[55] de la Vega, E., O'Leary, N. a, Shockey, J. E., Robalino, J., Payne, C., Browdy, C. L., Gross, P. S. (2008). Anti-lipopolysaccharide factor in *Litopenaeus vannamei* (LvALF): a broad spectrum antimicrobial peptide essential for shrimp immunity against bacterial and fungal infection. *Molecular Immunology*, *45*(7), 1916–25. doi:10.1016/j.molimm.2007.10.039

[56] De Lucca, A. J., Bland, J. M., Jacks, T. J., Grimm, C., Cleveland, T. E. and Walsh, T. J. (1997) Fungicidal activity of cecropin A. *Antimicrobial Agents and Chemotherapy, 41,* 481–483.

[57] De Zoysa, M., Nikapitiya, C., Whang, I., Lee, J., & Lee, J. (2009). Abhisin : A potential antimicrobial peptide derived from histone H2A of disk abalone (*Haliotis discus discus*). *Fish and Shellfish Immunology*, *27*(5), 639–646. doi:10.1016/j.fsi.2009.08.007

[58] Desai, P. N., Shrivastava, N., & Padh, H. (2010). Production of heterologous proteins in plants : Strategies for optimal expression. *Biotechnology Advances*, *28*(4), 427–435. doi:10.1016/j.biotechadv.2010.01.005

[59] Destoumieux, D., Bulet, P., Loew, D., Dorsselaer, A. Van, Rodriguez, J., & Bache, E. (1997). Penaeidins, a New Family of Antimicrobial Peptides Isolated from the Shrimp *Penaeus vannamei* (Decapoda), *The Journal of Biological Chemistry, 272*(45), 28398–28406.

[60] Destoumieux-Garzon, D., Saulnier, D., Garnier, J., Jouffrey, C., Bulet, P., Bachère, E. (2001). Crustacean immunity. Antifungal peptides are generated from the C terminus of shrimp hemocyanin in response to microbial challenge. *The Journal of Biological Chemistry, 276,* 47070-47077.

[61] Dewson, G. & Kluc, R.M. (2010). Bcl-2 family-regulated apoptosis in health and disease. *Cell Health and Cytoskeleton*, *2,* 9-22.

[62] Diamond, G., Beckloff, N., Weinberg, A., & Kisich, K. O. (2009). The Roles of Antimicrobial Peptides in Innate Host Defense. *Current Pharmaceutical Design*, *15*(21), 2377–2392.

[63] Donpudsa, S., Rimphanitchayakit, V., Tassanakajon, A., Söderhäll, I., & Söderhäll, K. (2010). Characterization of two crustin antimicrobial peptides from the freshwater crayfish *Pacifastacus leniusculus*. *Journal of Invertebrate Pathology*, *104*(3), 234–8. doi:10.1016/j.jip.2010.04.001

[64] Donpudsa, S., Visetnan, S., Supungul, P., & Tang, S. (2014). Type I and type II crustins from *Penaeus monodon,* genetic variation and antimicrobial activity of the most abundant crustin Pm 4. *Developmental and Comparative Immunology, 47*(1), 95–103. doi:10.1016/j.dci.2014.06.015

[65] Dorrington T., Villamil L. & Gomez-Chiarri M. (2011). Upregulation in response to infection and antibacterial activity of oyster histone H4. *Fish & Shellfish Immunology*, *30,* 94–101.

[66] Droga-Mazovec, G., Bojic, L., Petelin, A., Ivanova, S., Romih, R., Repnik, U., Salvesen, G.S., Stoka, V., Turk, V., Turk, B. 2008. Cysteine cathepsins trigger caspase-dependent cell death through cleavage of Bid and antiapoptotic Bcl-2 homologues. *The Journal of Biological Chemistry*, *283,* 19140-19150.

[67] Ehrenstein, G. & Lecar, H. (1977). Electrically gated ionic channels in lipid bilayers. *Quarterly Reviews of Biophysics, 10(1),* 1-34.

[68] Falla, T. J., Karunaratne, D. N. & Hancock, R. E. (1996). Mode of action of the antimicrobial peptide indolicidin. *The Journal of Biological Chemistry, 271*, 19298-19303.

[69] Fehlbaum, P., Bulet, P., Chernysh, S., Briand, J.P., Roussel, J.P., Leitellier, L., Hetru, C., Hoffmann, J.A. (1996). Structure-activity analysis of thanatin, a 21-residue inducible insect defense peptide with sequence homology to frog skin antimicrobial peptides. *Proceedings of national academy of sciences.* USA*, 93,* 1221-1225.

[70] Fernandes, J. M. O., Gerard, M., Graham, Kemp, D. and Smith, V. J. (2004) Isolation and characterisation of oncorhyncin II , a histone H1-derived antimicrobial peptide from skin secretions of rainbow trout, *Oncorhynchus mykiss*. *Developmental and Comparative Immunology, 28,* 127–138.

[71] Fernandes, J. M. O., Kemp, G. D., Molle, M. G. & Smith, V. J. (2002). Anti-microbial properties of histone H2A from skin secretions of rainbow trout, *Oncorhynchus mykiss*. *Biochemical Journal, 368,* 611–620.

[72] Fernebro, J. (2011). Fighting bacterial infections-future treatment options. *Drug Resistance Updates, 14,* 125–139. doi: 10.1016/j.drup. 2011.02.001

[73] Fink, S.L. & Cookson, B.T. 2005. Apoptosis, pyroptosis, and necrosis: mechanistic description of dead and dying eukaryotic cells. *Infection and Immunity, 73,* 1907-1916.

[74] Folmer, O., Black, M., Hoeh, W., Lutz, R. & Vrijenhoek, R. (1994). DNA primers for amplification of mitochondrial cytochrome c oxidase subunit I from diverse metazoan invertebrates. *Molecular Marine Biology and Biotechnology, 3(5),* 294–9. Retrieved from http://www.ncbi.nlm.nih.gov/ pubmed/7881515.

[75] García, J. R. C., Jaumann, F., Schulz, S., Krause, A., Rodríguez-Jiménez, J., Forssmann, U., Bals, R. (2001). Identification of a novel, multifunctional -defensin (human -defensin 3) with specific antimicrobial activity: Its interaction with plasma membranes of *Xenopus* oocytes and the induction of macrophage chemoattraction. *Cell and Tissue Research*, *306*(2), 257–264. doi:10.1007/s004410100433

[76] Gaspar, D., Veiga, A. S., & Castanho, M. A. R. B. (2013). From antimicrobial to anticancer peptides. A review. *Frontiers in Microbiology*, *4*(October), 1–16. doi:10.3389/fmicb.2013.00294

[77] Giacometti, A., Cirioni, O., Del Prete, M.S., Barchiesi, F., Fineo, A., Scalise, G. (2001). Activity of buforin II alone and in combination with azithromycin and minocycline against *Cryptosporidium parvum* in cell culture, *Journal of Antimicrobial Chemotherapy, 47,* 97–99.

[78] Giacometti, A., Cirioni, O., Del Prete, M.S., Paggi, A.M., D'Errico, M.M., Scalise, G. (2000). Combination studies between polycationic peptides and clinically used antibiotics against Gram-positive and Gram-negative bacteria, *Peptides.* 21, 1155–1160.

[79] Giangaspero, A., Sandri, L. & Tossi, A. (2001). Amphipathic alpha helical antimicrobial peptides. *European Journal of Biochemistry,* 268, 5589-5600.

[80] Greenlees K. J., Machado J., Bell T., Sundlof S. F. (1998). Food borne microbial pathogens of cultured aquatic species. *Veterinary Clinics of North America: Food Animal Practice, 14*(1), 101-12.

[81] Gross, P.S., Bartlett, T.C., Browdy, C.L., Chapman, R.W., Warr, G.W. (2001). Immune gene discovery by expressed sequence tag analysis of hemocytes and hepato- pancreas in the Pacific white shrimp, *Litopenaeus vannamei,* and the Atlantic white shrimp, *L. setiferus*. *Developmental & Comparative Immunology*, *25,* 565-577.

[82] Guex, N. & Peitsch, M.C. (1997). SWISS-MODEL and the Swiss-PdbViewer: An environment for comparative protein modelling. *Electrophoresis, 18*, 2714-2723.

[83] Guo, S., Li, S., Li, F., Zhang, X., & Xiang, J. (2014). Modification of a synthetic LPS-binding domain of anti-lipopolysaccharide factor from shrimp reveals strong structure-activity relationship in their antimicrobial characteristics. *Developmental and Comparative Immunology*, *45*(2), 227–32. doi:10.1016/j.dci.2014.03.003

[84] Hagiwara, K., Kikuchi, T., Endo, Y., Huqun, U.K., Takahashi, M., Shibata, N. (2003). Mouse SWAM1 and SWAM2 are antibacterial proteins composed of a single whey acidic protein motif. *The Journal of Immunology*, *170*, 1973–1979.

[85] Haines, L. R., Thomas, J. M., Jackson, A. M., Eyford, B. A., Razavi, M., Watson, C. N., Gowen, B., Hancock, R.E., Pearson, T.W. (2009). Killing of trypanosomatid parasites by a modified bovine host defense peptide, bmap-18. *PLOS Neglected Tropical Diseases*, *3*, doi:10.1371/journal.pntd.0000373.g007.

[86] Hancock, R. E. & Chapple, D. S. (1999). Peptide antibiotics. *Antimicrobial Agents and Chemotherapy* 43(6), 1317-1323.

[87] Hancock, R. E. & Diamond, G. (2000). The role of cationic antimicrobial peptides in innate host defences. *Trends in Microbiology* 8, 402–410.

[88] Hancock, R. E. & Lehrer, R. (1998). Cationic peptides: a new source of antibiotics. *Trends in Biotechnology* 16(2), 82-88.

[89] Hancock, R. E. and Sahl, H. G. (2006). Antimicrobial and host-defense peptides as new anti-infective therapeutic strategies. *Nature Biotechnology,* 24, 1551–1557.

[90] Hancock, R.E., Patrzykat, A. (2002). Clinical development of cationic antimicrobial peptides: from natural to novel antibiotics, *Infectious Disorders Drug Targets*, *2*, 79–83

[91] Hancock, R.E.W. (2001). Cationic peptides: effectors in innate immunity and novel antimicrobials. *The Lancet Infectious Diseases, 1,* 156-164.

[92] Hannig, G. &Makrides, S.C., (1998). Strategies for optimizing heterologous protein expression in Escherichia coli. *Trends in Biotechnology,* 16, 54e60

[93] Hauton, C., Brockton, V., & Smith, V. J. (2006). Cloning of a crustin-like, single whey-acidic-domain, antibacterial peptide from the haemocytes of the European lobster, *Homarus gammarus*, and its response to infection with bacteria. *Molecular Immunology* (Vol. 43). doi:10.1016/j.molimm.2005.07.029

[94] Herbinière, J., Braquart-Varnier, C., Grève, P., Strub, J. M., Frère, J., Van Dorsselaer, A., & Martin, G. (2005). Armadillidin: a novel glycine-rich antibacterial peptide directed against gram-positive bacteria in the woodlouse Armadillidium vulgare (Terrestrial Isopod, Crustacean). *Developmental and Comparative Immunology*, *29(6),* 489–99. doi:10.1016/j.dci.2004.11.001

[95] Hiemstra, P. S., Eisenhauer, P. B., Harwig, S. S., van den Barselaar, M. T., van Furth, R. & Lehrer, R. I. (1993). Antimicrobial proteins of murine macrophages. *Infection and Immunity, 61,* 3038–3046.

[96] Hirakura, Y., Kobayashi, S., & Matsuzaki, K. (2002). Specific interactions of the antimicrobial peptide cyclic beta-sheet tachyplesin I with lipopolysaccharides. *Biochimica et Biophysica Acta*, *1562*(1-2), 32–6. Retrieved from http://www.ncbi.nlm.nih.gov/pubmed/11988219

[97] Hoess, A., Watson, S., Siber, G. R. & Liddington, R. (1993). Crystal structure of an endotoxin-neutralizing protein from the horseshoe crab Limulus anti-LPS factor, at 1.5 A resolution. *The EMBO Journal, 12,* 3351–3356. 29.

[98] Hoffmann, J.A., Kafatos, F.C., Janeway, C.A., Ezekowitz, R.A. (1999). Phylogenetic per- spectives in innate immunity. *Science,* 284, 1313–1318

[99] Hoskin, D. W., & Ramamoorthy, A. (2008). Studies on anticancer activities of antimicrobial peptides. *Biochimica et Biophysica Acta*, *1778*(2), 357–75. doi:10.1016/j.bbamem.2007.11.008.

[100] Howell S.J., D. Wilk, S.P. Yadav, C.L. Bevins. (2003). Antimicrobial polypeptides of the human colonic epithelium, *Peptides*, *24,* 1763-1770.

[101] Hsieh, J. C., Pan, C. Y. and Chen, J. Y. (2010). Tilapia hepcidin (TH) 2-3 as a transgene in transgenic fish enhances resistance to *Vibrio vulnificus* infection and causes variations in immune-related genes after infection by different bacterial species. *Fish and Shellfish Immunology, 29,* 430–439.

[102] Hsu, J.C., Lin, L.C., Tzen, J. T. C., & Chen, J.Y. (2011). Pardaxin-induced apoptosis enhances antitumor activity in HeLa cells. *Peptides*. 32(6), 1110–6. doi:10.1016/j.peptides.2011.04.024

[103] Huang, W.S., Wang, K.J., Yang, M., Cai, J.J., Li, S.J., Wang, G.Z. (2006). Purification and part characterization of a novel antibacterial protein Scygonadin, isolated from the seminal plasma of mud crab, *Scylla serrata* (Forskal, 1775). *Journal of Experimental Marine Biology and Ecology, 339,* 37-42.

[104] Imjongjirak, C., Amparyup, P., & Tassanakajon, A. (2011). Molecular cloning, genomic organization and antibacterial activity of a second isoform of antilipopolysaccharide factor (ALF) from the mud crab, *Scylla paramamosain. Fish & Shellfish Immunology*, *30*(1), 58–66. doi:10.1016/ j.fsi.2010.09.011

[105] Imjongjirak, C., Amparyup, P., Tassanakajon, A., & Sittipraneed, S. (2007). Antilipopolysaccharide factor (ALF) of mud crab *Scylla paramamosain*: molecular cloning, genomic organization and the antimicrobial activity of its synthetic LPS binding domain. *Molecular Immunology*, *44*(12), 3195–203. doi:10.1016/j.molimm.2007.01.028

[106] Imjongjirak, C., Amparyup, P., Tassanakajon, A., Sittipraneed, S. (2009). Molecular cloning and characterization of crustin from mud crab *Scylla paramamosain. Molecular Biology Reports, 36,* 841–850

[107] Imura, Y., Nishida, M., Ogawa, Y., Takakura, Y., & Matsuzaki, K. (2007). Action mechanism of tachyplesin I and effects of PEGylation. *Biochimica et Biophysica Acta*, *1768*(5), 1160–9. doi:10.1016/j.bbamem.2007.01.005

[108] Ishitsuka, Y., Pham, D. S., Waring, A. J., Lehrer, R. I., & Lee, K. Y. C. (2006). Insertion selectivity of antimicrobial peptide protegrin-1 into lipid monolayers: effect of head group electrostatics and tail group packing. *Biochimica et Biophysica Acta*, *1758*(9), 1450–60. doi:10.1016/j.bbamem. 2006.08.001

[109] Jacobsen, F., Baraniskin, A., Mertens, J., Mittler, D., Mohammadi-Tabrisi, A., Schubert, S. (2005). Activity of histone H1.2 in infected burn wounds, *Journal of Antimicrobial Chemotherapy, 55,* 735-741.

[110] Jang, J. H., Kim, M. Y., Lee, J.-W., Kim, S. C., & Cho, J. H. (2011). Enhancement of the cancer targeting specificity of buforin IIb by fusion with an anionic peptide via a matrix metalloproteinases-cleavable linker. *Peptides*, *32*(5), 895–9. doi:10.1016/j.peptides.2011.02.010

[111] Jang, S. A., Kim, H., Lee, J. Y., Shin, J. R., Kim, D. J., Cho, J. H., & Kim, S. C. (2012). Mechanism of action and specificity of antimicrobial peptides designed based on buforin IIb. *Peptides*, *34*(2), 283–9. doi:10.1016/j.peptides.2012.01.015

[112] Jaree, P., Tassanakajon, A., & Somboonwiwat, K. (2012). Effect of the anti-lipopolysaccharide factor isoform 3 (ALFPm3) from Penaeus monodon on Vibrio harveyi cells. *Developmental and Comparative Immunology*, *38*(4), 554–60. doi:10.1016/j.dci.2012.09.001

[113] Jia, Y. P., Sun, Y. D., Wang, Z. H., Wang, Q., Wang, X. W., Zhao, X. F., & Wang, J. X. (2008). A single whey acidic protein domain (SWD)-containing peptide from fleshy prawn with antimicrobial and proteinase inhibitory activities. *Aquaculture*, *284*(1-4), 246–259. doi:10.1016/j.aquaculture. 2008.07.046

[114] Jiang, H. S., Jia, W. M., Zhao, X. F., & Wang, J. X. (2015a). Four crustins involved in antibacterial responses in *Marsupenaeus japonicus*. *Fish and Shellfish Immunology*, *43*(2), 387–395. doi:10.1016/j.fsi.2015.01.001

[115] Jiang, H. S., Zhang, Q., Zhao, Y. R., Jia, W. M., Zhao, X. F., & Wang, J. X. (2015b). A new group of anti-lipopolysaccharide factors from *Marsupenaeus japonicus* functions in antibacterial response. *Developmental and Comparative Immunology*, *48*(1), 33–42. doi:10.1016/ j.dci.2014.09.001

[116] Jiravanichpaisal, P., Young, S., Kim, Y., Andren, T., & Soderhall, I. (2007a). Antibacterial peptides in hemocytes and hematopoietic tissue from freshwater crayfish *Pacifastacus leniusculus*: Characterization and expression pattern. *Developmental & Comparative Immunology*, *31*(31), 441–455. doi:10.1016/j.dci.2006.08.002

[117] Jiravanichpaisal, P., Puanglarp, N., Petkon, S., Donnuea, S., Söderhäll, I., & Söderhäll, K. (2007b). Expression of immune-related genes in larval stages of the giant tiger shrimp, Penaeus monodon. *Fish & Shellfish Immunology*, *23*(4), 815–24. doi:10.1016/j.fsi.2007.03.003

[118] John, H., Maronde, E., Forssmann, W. G., Meyer, M. and Adermann, K. (2008). N-terminal acetylation protects glucagon-like peptide GLP-1-(7–34)-amide from DPP-IV-mediated degradation retaining cAMP- and insulin-releasing capacity. *European Journal of Medical Research*, *13,* 73–78.

[119] Kai-Larsen Y., Bergsson G., Gudmundsson G.H., Printz G., Jornvall H., Marchini, G. (2007). Antimicrobial components of the neonatal gut affected upon colonization. *Pediatric Research,* 61, 530–6.

[120] Kashima, M. (1991). H1 histones contribute to candidacidal activities of human epidermal extract. *Journal of Dermatology* 18, 695–706.

[121] Kaufmann S.H., Earnshaw W.C. 2000. Induction of apoptosis by cancer chemotherapy. *Experimental Cell Research,* 256, 42–9.

[122] Khoo, L., Robinette, D.W., Noga, E.J., (1999). Callinectin, an antibacterial peptide from blue crab, *Callinectes sapidus,* hemocytes. *Marine Biotechnology*, 1, 44–51.

[123] Kieffer, A.E., Goumon, Y., Ruh, O., Chasserot-Golaz, S., Nullans, G., Gasnier, C., Aunis, D., Metz-Boutigue, M.H. (2003). The N- and C-terminal fragments of ubiquitin are important for the antimicrobial activities. *FASEB Journal* 17, 776-778.

[124] Kim, H.S., J.H. Cho, H.W. Park, H. Yoon, M.S. Kim, S.C. Kim, (2002). Endotoxin- neutralizing antimicrobial proteins of the human placenta, *The Journal of Immunology,* 168 2356-2364.

[125] Kim, H.S., Park, C.B., Kim, M.S., Kim, S.C. (1996). cDNA cloning and characterization of buforin I, an antimicrobial peptide: a cleavage product of histone H2A, Biochemical *and Biophysical Research Communications*, 229, 381–387.

[126] Kobayashi S., A. Chikushi, S. Tougu, Y. Imura, M. Nishida, Y. Yano, K. Matsuzaki, (2004). Membrane translocation mechanism of the antimicrobial peptide buforin 2, *Biochemistry, 43,* 15610–15616.

[127] Kobayashi, S., Takeshima, K., Park, C. B., Kim, S. C. & Matsuzaki, K. (2000). Interactions of the novel antimicrobial peptide buforin 2 with lipid bilayers: proline as a translocation promoting factor. *Biochemistry, 39*, 8648–8654.

[128] Konishi, A., Shimizu, S., Hirota, J., Takao, T., Fan, Y., Matsuoka, Y. (2003). Involvement of histone H1.2 in apoptosis induced by DNA double-strand breaks, *Cell, 114,* 673-688.

[129] Koo, Y. S., Kim, J. M., Park, I. Y., Yu, B. J., Jang, S. A., Kim, K. S. & Park, C. B. (2008). Structure-activity relations of parasin I, a histone H2A-derived antimicrobial peptide. *Peptides, 29(7),* 1102-1108.

[130] Kragol, G., Lovas, S., Varadi G., Condie B. A., Hoffmann, R. and Otvos Jr. L., (2001). The antibacterial peptide pyrrhocoricin inhibits the ATPase actions of DnaK and prevents chaperone-assisted protein folding. *Biochemistry, 40,* 3016–3026.

[131] Krusong, K., Poolpipat, P., Supungul, P., & Tassanakajon, A. (2012). A comparative study of antimicrobial properties of crustinPm1 and crustinPm7 from the black tiger shrimp Penaeus monodon. *Developmental and Comparative Immunology*, *36*(1), 208–15. doi:10.1016/j.dci.2011.08.002

[132] Kushibiki, T., Kamiya, M., Aizawa, T., Kumaki, Y., Kikukawa, T., Mizuguchi, M., Kawano, K. (2014). Interaction between tachyplesin I, an antimicrobial peptide derived from horseshoe crab, and lipopolysaccharide. *Biochimica et Biophysica Acta (BBA) - Proteins and Proteomics*, *1844*(3), 527–534. doi:10.1016/j.bbapap.2013.12.017

[133] Lamaziere, A., Burlina, F., Wolf, C., Chassaing, G., Trugnan, G., Ayala-Sanmartin, J. 2007. Non-metabolic membrane tubulation and permeability induced by bioactive peptides. *Plos One, 2(2),* 201.

[134] Lawyer, C., Pai, S., Watabe, M., Borgia, P., Mashimo, T., Eagleton, L. and Watabe K. (1996) Antimicrobial activity of a 13 amino acid trytophan-rich peptide derived from a puative porcine precursor protein of a novel family of antibacterial peptides. *FEBS Letters, 90,* 95–98.

[135] Lee, D. Y., Huang, C. M., Nakatsuji, T., Thiboutat, D., Kang, S. A., Monestier, M. & Gallo, R. L. (2009). Histone H4 is a major component of the antimicrobial action of human sebocytes. *Journal of Investigative Dermatology*, *129,* 2489–2496.

[136] Lee, H. S., Park, C. B., Kim, J. M., Jang, S. a, Park, I. Y., Kim, M. S., Kim, S. C. (2008). Mechanism of anticancer activity of buforin IIb, a histone H2A-derived peptide. *Cancer Letters*, *271*(1), 47–55. doi:10.1016/j.canlet.2008.05.041

[137] Lee, J., Wan, K., & Mohd-adnan, A. (2012). Molecular characterization of hepcidin in the Asian seabass (Lates calcarifer) provides insights into its role in innate immune response. *Aquaculture*, *330-333*, 8–14. doi:10.1016/j.aquaculture.2011.12.001

[138] Leung, L.K., Wang, T.T.Y. (1999). Differential effects of chemotherapeutic agents on the Bcl-2/Bax apoptosis pathway in human breast cancer cell line MCF-7. *Breast Cancer Research and Treatment, 55,* 73-83.

[139] Li, C., Blencke, H. M., Smith, L. C., Karp, M. T. and Stensva, K. (2010). Two recombinant peptides, Sp Strongylocins 1 and 2, from *Strongylocentrotus purpuratus,* show antimicrobial activity against Gram-positive and Gram-negative bacteria. *Developmental and Comparative Immunology*, *34,* 286–292.

[140] Li, C., Haug, T., Styrvold, O. B., Jorgensen, T. O. and Stensvag, K. (2008a). Strongylocins, novel antimicrobial peptides from the green sea urchin, *Strongylocentrotus droebachiensis. Developmental and Comparative Immunology*, *32,* 1430–1440.

[141] Li C., Zhao J., Song L., Mu C., Zhang H., Gai, Y. (2008b). Molecular cloning, genomic organization and functional analysis of an anti-lipopolysaccharide factor from Chinese mitten crab *Eriocheir sinensis*. *Developmental and Comparative Immunology, 32,* 784-94

[142] Li, C., Song, L., Zhao, J., Zhu, L., & Zou, H. (2007). Preliminary study on a potential antibacterial peptide derived from histone H2A in hemocytes of scallop *Chlamys farreri. Fish and Shellfish Immunology*, *22*, 663–672. doi:10.1016/j.fsi.2006.08.013.

[143] Li, F., Wang, L., Qiu, L., Zhang, H., Gai, Y., & Song, L. (2012). A double WAP domain-containing protein from Chinese mitten crab *Eriocheir sinensis* with antimicrobial activities against Gram-negative bacteria and yeast. *Developmental and Comparative Immunology*, *36*(1), 183–90. doi:10.1016/j.dci.2011.07.003

[144] Li, S., Guo, S., Li, F., & Xiang, J. (2014). Characterization and function analysis of an anti-lipopolysaccharide factor (ALF) from the Chinese shrimp *Fenneropenaeus chinensis*. *Developmental and Comparative Immunology*, *46*(2), 349–355. doi:10.1016/j.dci.2014.05.013

[145] Li, Y. (2011). Recombinant production of antimicrobial peptides in Escherichia coli : A review. *Protein Expression and Purification*, *80*(2), 260–267. doi:10.1016/j.pep.2011.08.001

[146] Li, Y. F. and Chen, Z. X. (2008). RAPD: a database of recombinantly-produced antimicrobial peptides. *FEMS Microbiology Letters, 289,* 126–129.

[147] Lin, M. C., Lin, S. B., Chen, J. C., Hui, C.-F., & Chen, J.-Y. (2010). Shrimp anti-lipopolysaccharide factor peptide enhances the antitumor activity of cisplatin in vitro and inhibits HeLa cells growth in nude mice. *Peptides*, *31*(6), 1019–25. doi:10.1016/j.peptides.2010.02.023

[148] Lin, M. C., Pan, C. Y., Hui, C. F., Chen, J.-Y., & Wu, J.-L. (2013). Shrimp anti-lipopolysaccharide factor (SALF), an antimicrobial peptide, inhibits proinflammatory cytokine expressions through the MAPK and NF-κB pathways in LPS-induced HeLa cells. *Peptides*, *40*, 42–8. doi:10.1016/j.peptides.2012.11.010

[149] Lindholm, P., Goransson, U., Johansson, S., Claeson, P., Gullbo, J., Larsson, R., Bohlin, L., Backlund, A. (2002). Cyclotides: a novel type of cytotoxic agents. *Molecular Cancer Therapeutics,1*, 365-369.

[150] Liu, F. S., Liu, Y. C., Li, F. H., Dong, B., Xiang, J. H. (2005). Molecular cloning and expression profile of putative antilipopolysaccharide factor in Chinese shrimp (*Fenneropenaeus chinensis*). *Marine Biotechnology, 7,* 600–608.

[151] Liu, H., Chen, R., Zhang, Q., Wang, Q., Li, C., Peng, H., Wang, K. (2012). Characterization of two isoforms of antiliopolysacchride factors (Sp-ALFs) from the mud crab *Scylla paramamosain. Fish & Shellfish Immunology*, *33*(1), 1–10. doi:10.1016/j.fsi.2012.03.014

[152] Liu, H., Jiravanichpaisal, P., So, I., Cerenius, L., & So, K. (2006). Antilipopolysaccharide Factor Interferes with White Spot Syndrome Virus Replication In Vitro and In Vivo in the Crayfish *Pacifastacus leniusculus*, *80*(21), 10365–10371. doi:10.1128/JVI.01101-06

[153] Liu, J., & Lin, A. (2005). Role of JNK activation in apoptosis: a double-edged sword. *Cell Research*, *15*(1), 36–42. doi:10.1038/sj.cr.7290262

[154] Liu, N., Zhang, R.-R., Fan, Z.-X., Zhao, X.-F., Wang, X.-W., & Wang, J.-X. (2016). Characterization of a type-I crustin with broad-spectrum antimicrobial activity from red swamp crayfish *Procambarus clarkii*. *Developmental & Comparative Immunology*, *61*, 145–153. doi:10.1016/j.dci.2016.03.025

[155] Liu, Y., Cui, Z., Li, X., Song, C., Li, Q., & Wang, S. (2012). Molecular cloning, expression pattern and antimicrobial activity of a new isoform of anti-lipopolysaccharide factor from the swimming crab *Portunus trituberculatus*. *Fish & Shellfish Immunology*, *33*(1), 85–91. doi:10.1016/j.fsi.2012.04.004

[156] Liu, Y., Cui, Z., Luan, W., Song, C., Nie, Q., Wang, S. (2011). Three isoforms of anti- lipopolysaccharide factor identified from eyestalk cDNA library of swimming crab *Portunus trituberculatus, Fish and Shellfish Immunology*, *30,* 583-591.

[157] Livak, K. J., & Schmittgen, T. D. (2001). Analysis of Relative Gene Expression Data Using Real- Time Quantitative PCR and the 2 ‫ ؏‬C T Method. *Methods*, *25*, 402–408. doi:10.1006/meth.2001.1262

[158] Lu, K. Y., Sung, H. J., Liu, C. L., Sung, H. H. (2009). Differentially enhanced gene expression in hemocytes from *Macrobrachium rosenbergii* challenged *in vivo* with lipopolysaccharide. *Journal of Invertebrate Pathology, 100,* 9–15.

[159] Malmsten, M., Davoudi, M., Walse, B., Rydengård, V., Pasupuleti, M., Mörgelin, M. (2007). Antimicrobial peptides derived from growth factors. *Growth Factors*, *25(1),* 60–70

[160] Maltseva, A. L., Aleshina, G. M., Kokryakov, V. N., Krasnodembsky, E. G. & Ovchinnikova, T. V. (2004). New antimicrobial peptides from coelomocytes of sea star *Asterias rubens* L. *Vestnik Sankt-Peterburgskogo Universiteta, Seriya 3, Biologiya,* 4, 101-108.

[161] Matsuzaki, K. (1998). Magainins as paradigm for the mode of action of pore forming polypeptides. *Biochimica et Biophysica Acta, 1376*, 391–400.

[162] Matsuzaki, K. (1999). Why and how are peptide-lipid interactions utilized for self-defense? Magainins and tachyplesins as archetypes. *Biochimica et Biophysica Acta, 1462,* 1-10.

[163] McGwire, B.S., Olson, C.L., Tack, B.F., Engman, D.M. (2003). Killing of african trypanosomes by antimicrobial peptides. *Journal of Infectious Diseases, 188,* 146–152.

[164] Michaut, L., Fehlbaum, P., Moniatte, M., Van Dorsselaer, A., Reichhart, J. M. and Bulet, P (1996) Determination of the disulphide array of the first inducible antifungal pep- tide from insects: drosomycin from *Drosophila melanogaster*. *FEBS Letters*, *395*, 6–10.

[165] Miyasaki, K.T. & Lehrer, R.I. (1998). β-Sheet antibiotic peptides as potential dental therapeutics. *International Journal of Antimicrobial Agents*, *9,* 269-280.

[166] Montero T., Vallespi, M. G., Garay, H., Reyes, O., Aran, M. J. (2003) A Limulus anti-LPS factor-derived peptide modulates cytokine gene expression and promotes resolution of bacterial acute infection in mice, *International Immunopharmacology*, *3,* 247- 256.

[167] Mu, C., Zheng, P., Zhao, J., Wang, L., Zhang, H., Qiu, L., Song, L. (2010). Molecular characterization and expression of a crustin-like gene from Chinese mitten crab, *Eriocheir sinensis*. *Developmental and Comparative Immunology*, *34*(7), 734–40. doi:10.1016/j.dci.2010.02.001

[168] Nagoshi, H., Inagawa, H., Morii, K., Harada, H., Kohchi, C., Nishizawa, T., Soma, G.-I. (2006). Cloning and characterization of a LPS-regulatory gene having an LPS binding domain in kuruma prawn *Marsupenaeus japonicus*. *Molecular Immunology*, *43*(13), 2061–9. doi:10.1016/j.molimm.2005.12.009

[169] Nam, B. H., Moon, J. Y., Kim, Y. O., Kong, H. J., Kim, W. J., Lee, S. J. & Kim, K. K. (2010). Multiple β-defensin isoforms identified in early developmental stages of the teleost *Paralichthys olivaceus*. *Fish and Shellfish Immunology, 28,* 267–274.

[170] Narayana, J. L. and Chen, J. Y. (2015). Antimicrobial peptides: Possible anti-infective agents. *Peptides, 72*, 88–94.

[171] Nguyen, L. T., Haney, E. F. & Vogel, H. J. (2011). The expanding scope of antimicrobial peptide structures and their modes of action. *Trends in Biotechnology, 29*, 464–472.

[172] Ohashi, K., Niwa, M., Nakamura, T., Morita, T., & Iwanaga, S. (1984). Anti-LPS factor in the horseshoe crab, *Tachypleus tridentatus* Its hemolytic activity on the red blood cell sensitized with lipopolysaccharide. *FEBS*, *176*(1), 3–6.

[173] Onuma, Y., Satake, M., Ukena, T., Roux, J., Chanteau, S., Rasolofonirina, N., Ratsimaloto, M., Naoki, H., Yasumoto, T., (1999). Identification of putative palytoxin as the cause of clupeotoxism. *Toxicon*, *37*, 55–65.

[174] Oren, Z., Shai, Y. (1998). Mode of action of linear amphipathic alpha-helical antimicrobial peptides. *Biopolymers, 47*, 451–463.

[175] Otvos, L., Jr., Rogers, I. O., M. E., Consolvo, P. J., Condie, B. A., Lovas, S., Bulet, P. and Blaszczyk-Thurin, M. (2000). Interaction between heat shock proteins and antimicrobial peptides. *Biochemistry, 39,* 14150-14159.

[176] Pal, T., Abraham, B., Sonnevend, A., Jumaa, P. and Conlon, J. M. (2006) Brevinin-1BYa: a naturally occurring peptide from frog skin with broad-spectrum antibacterial and antifungal properties. *International Journal of Antimicrobial Agents, 27,* 525–529.

[177] Pan, C., Chao, T., Chen, J., Chen, J., Liu, W., Lin, C., & Kuo, C. (2007). Shrimp (*Penaeus monodon*) anti-lipopolysaccharide factor reduces the lethality of Pseudomonas aeruginosa sepsis in mice. *International Immunopharmacology*, *7*, 687–700. doi:10.1016/j.intimp.2007.01.006

[178] Pan, C., Chen, J., Lin, T., & Lin, C. (2009). Peptides In vitro activities of three synthetic peptides derived from epinecidin-1 and an anti-lipopolysaccharide factor against *Propionibacterium acnes, Candida albicans*, and *Trichomonas vaginalis*, *Peptides, 30*, 1058–1068. doi:10.1016/j.peptides.2009.02.006

[179] Pan, C., Chow, T., Yu, C., Yu, C., Chen, J., & Chen, J. (2010). Peptides Antimicrobial peptides of an anti-lipopolysaccharide factor, epinecidin-1, and hepcidin reduce the lethality of *Riemerella anatipestifer* sepsis in ducks. *Peptides*, *31*(5), 806–815. doi:10.1016/j.peptides.2010.01.013

[180] Papo, N. & Shai, Y. (2005). Host defense peptides as new weapons in cancer treatment, *Cellular and Molecular Life Sciences, 62,* 784–790.

[181] Parachin, N. S., Mulder, K. C., Américo, A., Viana, B., Dias, S. C., & Franco, O. L. (2012). Peptides Expression systems for heterologous production of antimicrobial peptides. *Peptides*, *38*(2), 446–456. doi:10.1016/j.peptides.2012.09.020

[182] Park, C. B., Kim, H. S., & Kim, S. C. (1998a). Mechanism of action of the antimicrobial peptide buforin II: buforin II kills microorganisms by penetrating the cell membrane and inhibiting cellular functions. *Biochemical and Biophysical Research Communications*, *244*(1), 253–7. doi:10.1006/bbrc.1998.8159

[183] Park, I. Y., Park, C. B., Kim, M. S., & Kim, S. C. (1998b). Parasin I, an antimicrobial peptide derived from histone H2A in the catfish, *Parasilurus asotus*. *FEBS Letters, 437*(3), 258-262.

[184] Park, C. B., Kim, M. S., Kim, S. C. (1996). A novel antimicrobial peptide from *Bufo bufo gargarizans*, *Biochemical and Biophysical Research Communications*, *218,* 408-413.

[185] Park, C. B., Yi, K. S., Matsuzaki, K., Kim, M. S. & Kim, S. C. (2000). Structure-activity analysis of buforin II, a histone H2A-derived antimicrobial peptide: the proline hinge is responsible for the cell-penetrating ability of buforin II. *Proceedings of the National Academy of Sciences of the United States of America*, *97*(15), 8245-8250.

[186] Park, I. Y., Cho, J. H. & Kim, K. S. (2004). Helix stability confers salt resistance upon helical antimicrobial peptides. *The Journal of Biological Chemistry*, *279*, 13896–901.

[187] Park, J. M., Jung, J. E. and Lee, B. J. (1994) Antimicrobial peptides from the skin of a Korean frog, *Rana rugosa*, *Biochemistry and Biophysical Research Communications, 205***,** 948–954

[188] Park, Y., Jang, S. H., Lee, D. G. & Hahm, K. S. (2004). Antinematodal effect of antimicrobial peptide, pmap-23, isolated from porcine myeloid against caenorhabditis elegans. *Journal of Peptide Science, 10*, 304–311.

[189] Parseghian, M.H. & Luhrs, K.A. (2006). Beyond the walls of the nucleus: the role of histones in cellular signaling and innate immunity, *Biochemistry and Cell Biology, 84,* 589-604.

[190] Pasupuleti. M., Schmidtchen, A., Malmsten, M. (2012). Antimicrobial peptides: key components of the innate immune system. *Critical Reviews in Biotechnology, 32*, 143–71

[191] Patat, S., Carnegie, R. B., Kingsbury, C., Gross, P. S. & Chapman, R. (2004). Antimicrobial activity of histones from hemocytes of the Pacific white shrimp. *European Journal of Biochemistry, 271*, 4825-4833.

[192] Patrzykat, A., Zhang, L., Mendoza, V., Iwama, G. & Hancock, R. (2001). Synergy of histone-derived peptides of coho salmon with lysozyme and flounder pleurocidin. *Antimicrobial Agents Chemotherapy, 45,* 1337–1342.

[193] Pedersen, G. M., Gildberg, A., Steiro, K., Olsen, R. L. (2003). Histone-like proteins from Atlantic cod milt: stimulatory effect on Atlantic salmon leucocytes in vivo and in vitro, *Comparative Biochemistry and Physiology - Part B Biochemistry and Molecular Biology, 134*, 407-416.

[194] Pisuttharachai, D., Yasuike, M., Aono, H., Yano, Y., Murakami, K., Kondo, H., Aoki, T., Hirono, I. (2009). Characterization of two isoforms of Japanese spiny lobster *Panulirus japonicas* defensin cDNA. *Developmental and Comparative Immunology*, *33,* 434-438.

[195] Ponprateep, S., Tharntada, S., Somboonwiwat, K., & Tassanakajon, A. (2012). Gene silencing reveals a crucial role for anti-lipopolysaccharide factors from Penaeus monodon in the protection against microbial infections. *Fish & Shellfish Immunology*, *32*(1), 26–34. doi:10.1016/j.fsi.2011.10.010

[196] Pouny, Y., Rapaport, D., Mor, A., Nicolas, P. & Shai, Y. (1992). Interaction of antimicrobial dermaseptin and its fluorescently labeled analogues with phospholipid membranes. *Biochemistry, 31(49),* 12416-12423.

[197] Pushpanathan, M., Rajendhran, J., Jayashree, S., Sundarakrishnan, B., Jayachandran, S. and Gunasekaran, P. (2012). Identification of a novel antifungal peptide with chitin-binding property from marine metagenome. *Protein and Peptide Letters*, *19*, 1289–1296.

[198] Razavi, G.S.E. & Allen, T. (2014). Emerging Role of Interleukins in Cancer Treatment. *Immunome Research*, *1*(2), 1–21. doi:10.4172/1745-7580.S2.006

[199] Reichhart, R., Zeppezauer, M. & Jornvall, H. (1985). Preparations of homeostatic thymus hormone consist predominantly of histones 2A and 2B and suggest additional histone functions, *Proceedings of the National Academy of Sciences of the United States of America*, *82,* 4871-4875.

[200] Relf, J. M., Chisholm, J. R. S., Kemp, G. D., Smith, V. J., (1999). Purification and charac- terisation of a cysteine-rich 11.5 kDa antibacterial protein from the granular haemocytes of the shore crab, *Carcinus maenas*. *European Journal of Biochemistry*, *264,* 350–357.

[201] Ren, J., Gao, H., Tang, M., Gu, J., Xia, P., & Xiao, G. (2010). Lipopolysaccharide (LPS) detoxification of analogue peptides derived from limulus anti-LPS factor. *Peptides*, *31*(10), 1853–9. doi:10.1016/ j.peptides.2010.07.004

[202] Ren, J.D., Gu, J.-S., Gao, H.F., Xia, P.Y., & Xiao, G.X. (2008). A synthetic cyclic peptide derived from Limulus anti-lipopolysaccharide factor neutralizes endotoxin *in vitro* and *in vivo*. *International Immunopharmacology*, *8*(6), 775–81. doi:10.1016/j.intimp.2008.01.015

[203] Ren, Q., Zhang, Z., Li, X.C., Jie, D., Hui, K.M., Zhang, C.Y., Wang, W. (2012). Three different anti-lipopolysaccharide factors identified from giant freshwater prawn, *Macrobrachium rosenbergii. Fish and Shellfish Immunology, 33*, 766-774.

[204] Richards, R. C., O'Neil, D. B., Thibault, P. & Ewart, K. V. (2001). Histone H1: an antimicrobial protein of Atlantic salmon (*Salmo salar*). *Biochemical and Biophysical Research Communications* 284, 549–555.

[205] Ried, C., Wahl, C., Miethke, T., Wellnhofer, G., Landgraf, C., Schneider, M. J. (1996). High affinity endotoxin-binding and neutralizing peptides based on the crystal structure of recombinant Limulus anti-lipopolysaccharide factor. *The Journal of Biological Chemistry*, *271,* 28120–7.

[206] Risso, A., Braidot, E., Sordano, M. C., Vianello, A., Macrì, F. & Skerlavaj, B. (2002). BMAP- 28, an antibiotic peptide of innate immunity, induces cell death through opening of the mitochondrial permeability transition pore. *Molecular and Cellular Biology, 22,* 1926–35.

[207] Robinette, D., Wada, S., Arroll, T., Levy, M. G., Miller, W. L. & Noga, E. J. (1998). Antimicrobial activity in the skin of the channel catfish, *Ictalurus punctatus*: characterization of broad-spectrum histone-like antimicrobial proteins. *Cell and Molecular Life Sciences. 54,* 467–475.

[208] Rogozhin, E. A., Oshchepkova, Y. I., Odintsova, T. I., Khadeeva, N. V., Veshkurova, O. N., Egorov, T. A., Grishin, E. V. & Salikhov, S. I. (2011) Novel antifungal defensins from *Nigella sativa* L. seeds. *Plant Physiology and Biochemistry, 49,* 131–137.

[209] Rolland, J. L., Abdelouahab, M., Dupont, J., Lefevre, F., Bachère, E., & Romestand, B. (2010). Stylicins, a new family of antimicrobial peptides from the Pacific blue shrimp *Litopenaeus stylirostris*. *Molecular Immunology*, *47*, 1269–1277. doi:10.1016/j.molimm.2009.12.007

[210] Rosa, R. D., & Barracco, M. A. (2010). Antimicrobial peptides in crustaceans. *Invertebrate Survival Journal*, *7*, 262–284.

[211] Rosa, R. D., Vergnes, A., de Lorgeril, J., Goncalves, P., Perazzolo, L. M., Sauné, L. & Destoumieux-Garzón, D. (2013). Functional divergence in shrimp anti-lipopolysaccharide factors (ALFs): from recognition of cell wall components to antimicrobial activity. *PloS One*, *8*(7), e67937. doi:10.1371/journal.pone.0067937

[212] Rosa, R. D., Stoco, P. H., Barracco, M. A. (2008). Cloning and characterisation of cDNA sequences encoding for anti-lipopolysaccharide factors ALFs in Brazilian palaemonid and penaeid shrimps. *Fish & Shellfish Immunology*, *25,* 693–696.

[213] Rose, F. R., Bailey, K., Keyte, J.W., Chan, W.C., Greenwood, D., Mahida, Y.R. (1998). Potential role of epithelial cell-derived histone H1 proteins in innate antimicrobial defense in the human gastrointestinal tract, *Infection and Immunity, 66,* 3255-3263.

[214] Saito, A., Ueda, K., Imamura, M., Atsumi, S. & Tabunoki, H. (2005). Purification and cDNA cloning of a cecropin from the longicorn beetle, *Acalolepta luxuriosa* B. *Comparative Biochemistry and Physiology Part B: Biochemistry and Molecular Biology, 142,* 317–323.

[215] Samad, A., Sultana, Y. & Aqil, M. (2007). Liposomal drug delivery systems: An update review. *Current Drug Delivery, 4,* 297–305.

[216] Sathyan, N., Philip, R., Chaithanya, E. R., Anil Kumar, P. R., & Antony, S. P. (2012a). Identification of a histone derived, putative antimicrobial peptide Himanturin from round whip ray *Himantura pastinacoides* and its phylogenetic significance. *Results in Immunology*, *2*, 120–124. doi:10.1016/j.rinim.2012.06.001

[217] Sathyan, N., Philip, R., Chaithanya, E. R., & Anil Kumar, P. R. (2012b). Identification and Molecular Characterization of Molluskin, a Histone-H2A-Derived Antimicrobial Peptide from Molluscs. *ISRN Molecular Biology*, *2012*(2012), 1–6. doi:10.5402/2012/219656

[218] Sathyan, N., Philip, R., Chaithanya, E. R., Anil Kumar, P. R., Sanjeevan, V. N., & Singh, I. S. B. (2013). Characterization of Histone H2A Derived Antimicrobial Peptides, Harriottins, from Sicklefin Chimaera *Neoharriotta pinnata* (Schnakenbeck, 1931) and Its Evolutionary Divergence with respect to CO1 and Histone H2A. *ISRN Molecular Biology*, *2013*, 1–10. doi:10.1155/2013/930216

[219] Schnapp, D., Kemp, G.D. & Smith, V.J. (1996). Purification and characterization of a proline-rich antibacterial peptide, with sequence similarity to bactenecin-7, from the haemocytes of the shore crab, *Carcinus maenas*. *European Journal of Biochemistry, 2403,* 532-539.

[220] Schwede, T., Kopp, J., Guex, N. & Peitsch, M.C. (2003). SWISS-MODEL: an automated protein homology-modeling server. *Nucleic Acids Research*, *31*, 3381-3385.

[221] Scudiero, D.A., Shoemaker, R.H., Paull, K.D., Monks, A., Tierney, S., Nofziger, T.H., Currens, M.J., Seniff, D., Boyd, M.R. (1988). Evaluation of a soluble tetrazolium/formazan assay for cell growth and drug sensitivity in culture using human and other tumor cell lines. *Cancer Research*, *48,* 4827-4833.

[222] Seo, J. K., Stephenson, J. & Noga, E. J. (2011). Multiple antibacterial histone H2B proteins are expressed in tissues of American oyster. *Comparative Biochemistry and Physiology Part B ,158*, 223–9.

[223] Seo, J. K., Stephenson, J., Crawford, J. M., Stone, K. L. & Noga, E. J. (2010). American oyster, *Crassostrea virginica,* expresses a potent antibacterial histone H2B protein. *Marine Biotechnology, 12,* 543–51

[224] Seo, M. D., Won, H. S., Kim, J. H., Mishig-Ochir, T., and Lee, B.J. (2012). Antimicrobial peptides for therapeutic applications: a review. *Molecules* 17, 12276–12286. doi: 10.3390/molecules171012276

[225] Shai, Y. (2002). Mode of action of membrane active antimicrobial peptides. *Peptide Science, 66,* 236–248.

[226] Silphaduang, U., Colorni, A., & Noga, E. J. (2006). Evidence for widespread distribution of piscidin antimicrobial peptides in teleost fish. *Diseases of Aquatic Organisms 72(3),* 241-252.

[227] Silva, N. C., Sarmento, B. and Pintado, M. (2013) The importance of antimicrobial peptides and their potential for therapeutic use in ophthalmology. *International Journal of Antimicrobial Agents, 41*, 5–10.

[228] Smith, V. J., Fernandes, J. M. O., Kemp, G. D., & Hauton, C. (2008). Crustins: enigmatic WAP domain-containing antibacterial proteins from crustaceans. *Developmental and Comparative Immunology*, *32*(7), 758–72. doi:10.1016/j.dci.2007.12.002

[229] Smith, V.J., Desbois, A.P., Dyrynda, E.A. (2010). Conventional and unconventional antimicrobials from fish, marine invertebrates and micro-algae. *Marine Drugs, 8*, 1213–1262.

[230] Söderhäll, K., Cerenius, L. (1992). Crustacean immunity. *Annual Review of Fish Diseases*, *Volume 2*, 3–23.

[231] Somboonwiwat, K., Bachere, E., Rimphanitchayakit, V., Tassanakajon, A. (2008). Localization of anti-lipopolysaccharide factor (ALF Pm 3) in tissues of the black tiger shrimp, *Penaeus monodon,* and characterization of its binding properties. *Developmental and Comparative Immunology*, *32*, 1170–1176. doi:10.1016/j.dci.2008.03.008

[232] Somboonwiwat, K., Marcos, M., Tassanakajon, A., Klinbunga, S., Aumelas, A., Romestand, B., Bachère, E. (2005). Recombinant expression and anti-microbial activity of anti-lipopolysaccharide factor (ALF) from the black tiger shrimp *Penaeus monodon. Developmental and Comparative Immunology*, *29*(10), 841–51. doi:10.1016/j.dci.2005.02.004

[233] Sook, Y., Min, J., Yup, I., Jo, B., Jang, S. A., Kim, K. (2008). Structure-activity relations of parasin I, a histone H2A-derived antimicrobial peptide. *Peptides, 29,* 1102-1108.

[234] Sperstad, S.V., Haug, T., Vasskog, T. & Stensvag, K., (2009a). Hyastatin, a glycine erich multi-domain antimicrobial peptide isolated from the spider crab (*Hyas araneus*) hemocytes. *Molecular Immunology,* 46, 2604–2612.

[235] Sperstad, S. V., Haug, T., Paulsen, V., Rode, T. M., Strandskog, G., Solem, S. T. & Stensvåg, K. (2009b). Characterization of crustins from the hemocytes of the spider crab, Hyas araneus, and the red king crab, *Paralithodes camtschaticus. Developmental and Comparative Immunology*, *33*(4), 583–91. doi:10.1016/j.dci.2008.10.010

[236] Sruthy, K. S., Chaithanya, E. R., Sathyan, N., Nair, A., Antony, S. P., Bright Singh, I. S., & Philip, R. (2015). Molecular Characterization and Phylogenetic Analysis of Novel Isoform of Anti-lipopolysaccharide Factor from the Mantis Shrimp, *Miyakea nepa. Probiotics and Antimicrobial Proteins*. doi:10.1007/s12602-015-9198-2

[237] Stensvag, K., Haug, T., Sperstad, S. V, Rekdal, O., Indrevoll, B., & Styrvold, O. B. (2008). Arasin 1, a proline-arginine-rich antimicrobial peptide isolated from the spider crab, *Hyas araneus*. *Developmental and Comparative Immunology*, *32*(3), 275–85. doi:10.1016/j.dci.2007.06.002

[238] Stewart, E. J. & Aslund, F. (1998). Disulfide bond formation in the Escherichia coli cytoplasm: an in vivo role reversal for the thioredoxins. *The EMBO Journal, 17(19),* 5543–5550

[239] Stoss, T.D., Nickell, M.D., Hardin, D., Derby, C., Mc Clintock, T.S. (2003). Inducible transcript expressed by reactive epithelial cells at sites of olfactory sensory neuron proliferation. *Journal of Neurobiology, 58*, 355-368.

[240] Subbalakshmi, C. & Sitaram, N. (1998). Mechanism of antimicrobial action of indolicidin. *FEMS Microbiology Letters, 160,* 91–96.

[241] Subramanian, S., Ross, N. W., Mackinnon, S. L. (2008). Comparison of the biochemical com- position of normal epidermal mucus and extruded slime of hagfish (*Myxine glutinosa* L.). *Fish & Shellfish Immunology, 25,* 625–32

[242] Sun C, Xu WT, Zhang HW, Dong LP, Zhang T, Zhao XF, & Wang JX (2011). An anti-lipopolysaccharide factor from red swamp crayfish, *Procambarus clarkii,* exhibited antimicrobial activities in vitro and in vivo *Fish & Shellfish Immunology*, *30*(1): 295–303. doi:10.1016/j.fsi.2010.10.022

[243] Sun, C., Du, X., Xu, W., Zhang, H., Zhao, X., & Wang, J. (2010). Fish & Shellfish Immunology Molecular cloning and characterization of three crustins from the Chinese white shrimp, *Fenneropenaeus chinensis*. *Fish and Shellfish Immunology*, *28*(4), 517–524. doi:10.1016 /j.fsi.2009.12.001

[244] Sun, W., Wan, W., Zhu, S., Wang, S., Wang, S., Wen, X., Li, S. (2015). Characterization of a novel anti-lipopolysaccharide factor isoform (SpALF5) in mud crab, *Scylla paramamosain. Molecular Immunology*, *64*(2), 262–275. doi:10.1016/j.molimm.2014.12.006

[245] Supungul, P., Klinbunga, S., Pichyangkura, R., Hirono, I., Aoki, T., Tassanakajon, A. (2004). Antimicrobial peptides discovered in the black tiger shrimp *Penaeus monodon* using the EST approach. *Diseases of Aquatic Organisms*, 61, 123–135.

[246] Supungul, P., Klinbunga, S., Pichyangkura, R., Jitrapakdee, S., Hirono, I., Aoki, T., Tassanakajon, A. (2002). Identification of immune-related genes in hemocytes of black tiger shrimp *Penaeus monodon*. *Marine Biotechnology*, *4,* 487-494.

[247] Supungul, P., Tang, S., Maneeruttanarungroj, C., Rimphanitchayakit, V., Hirono, I., Aoki, T., & Tassanakajon, A. (2008). Cloning, expression and antimicrobial activity of crustinPm1, a major isoform of crustin, from the black tiger shrimp *Penaeus monodon*. *Developmental and Comparative Immunology*, *32*(1), 61–70. doi:10.1016/j.dci.2007.04.004

[248] Suthianthong, P., Donpudsa, S., Supungul, P., & Tassanakajon, A. (2012). The N-terminal glycine-rich and cysteine-rich regions are essential for antimicrobial activity of crustinPm1 from the black tiger shrimp *Penaeus monodon*. *Fish and Shellfish Immunology*, *33*(4), 977–983. doi:10.1016/j.fsi.2012.08.010

[249] Svensson, S. L., Pasupuleti, M., Walse, B., Malmsten, M., Mörgelin, M., Sjögren, C. (2010). Midkine and pleiotrophin have bactericidal properties: preserved antibacterial activity in a family of heparin-binding growth factors during evolution. *The Journal of Biological Chemistry, 285(21),* 16105–15.

[250] Tagai C, Morita S, Shiraishi T, Miyaji K, Iwamuro S. (2011). Antimicrobial properties of arginine- and lysine-rich histones and involvement of bacterial outer membrane protease T in their differential mode of actions. *Peptides, 32,* 2003–9.

[251] Tamamura, H., Kuroda, M., Masuda, M. (1993). A comparative study of the solution structures of tachyplesin I and a novel anti-HIV syn- thetic peptide. T 22 ([tyr 5,12, lys 7]-polyphemusin ii), determined by nuclear magnetic resonance. *Biochimica et Biophysica Acta (BBA) - Proteins and Proteomics*, *1163,* 209–16.

[252] Tanaka, S., Nakamura, T., Morita, T., Iwanaga, S. (1982). Limulus anti-LPS factor: an anticoagulant which inhibits the endotoxin mediated activation of limulus coagulation system. *Biochemical and Biophysical Research Communications*, *105,* 717–723

[253] Tang T., Li L., Sun L., Bu J., Xie S., Liu F. (2014). Functional analysis of *Fenneropenaeus chinensis* anti-lipopolysaccharide factor promoter regulated by lipopolysaccharide and (1, 3)-β-D-glucan. *Fish & Shellfish Immunology*, *38(2),* 348–353. doi:10.1016/j.fsi.2014.03.026

[254] Tassanakajon, A., Amparyup, P., Somboonwiwat, K., Supungul, P. (2010). Cationic antimicrobial peptides in penaeid shrimp. *Marine Biotechnology*, *12,* 487-505.

[255] Tharntada, S., Somboonwiwat, K., Rimphanitchayakit, V., Tassanakajon, A., (2008). Anti- lipopolysaccharide factors from the black tiger shrimp, Penaeus monodon, are encoded by two genomic loci. *Fish & Shellfish Immunology*, *24*, 46–54.

[256] Thatcher, T. H. & Gorovsky, M. A. (1994). Phylogenetic analysis of the core histones H2A, H2B, H3 and H4. *Nucleic Acids Research, 22,* 174-179.

[257] Tossi, A., Sandri, L. & Giangaspero, A. (2000). Amphipathic, alpha-helical antimicrobial peptides. *Biopolymers*, *55*(1), 4-30.

[258] Tossi, A., Sandri, L. (2002). Molecular diversity in gene-encoded, cationic antimicrobial polypeptides. *Current Pharmaceutical Design, 8*, 743–761.'

[259] Uyterhoeven, E. T., Butler, C. H., Ko, D., & Elmore, D. E. (2008). Investigating the nucleic acid interactions and antimicrobial mechanism of buforin II. *FEBS Letters*, *582*(12), 1715–1718. doi:10.1016/j.febslet. 2008.04.036

[260] Vallespi, M. G., Glaria, L. A., Reyes, O., Garay, H. E., Ferrero, J., & Aran, M. J. (2000). A Limulus Antilipopolysaccharide Factor-Derived Peptide Exhibits a New Immunological Activity with Potential Applicability in Infectious Diseases. *Clinical Diagnosis Laboratory Immunology*, *7*(4), 669–675.

[261] Vallespi, M.G., Alvarez-Obregón, J.C., Rodriguez-Alonso, I., Montero, T., Garay, H., Reyes, O. (2003). A Limulus anti-LPS factor-derived peptide modulates cytokine gene expression and promotes resolution of bacterial acute infection in mice. *International Immunopharmacology, 3*, 247–256.

[262] van't Hof W, Veerman EC, Helmerhorst EJ, Amerongen AV. (2001) Antimicrobial peptides: properties and applicability. *The Jounal of Biological Chemistry, 382(4)*, 597-619.

[263] Vargas-Albores, F., Yepiz-Plascencia, G., Jiménez-Vega, F., & Ávila-Villa, A. (2004). Structural and functional differences of *Litopenaeus vannamei* crustins. *Comparative Biochemistry and Physiology Part B: Biochemistry and Molecular Biology*, *138*(4), 415–422. doi:10.1016/j.cbpc.2004.05.007

[264] Vatanavicharn, T., Supungul, P., Puanglarp, N., Yingvilasprasert, W., Tassanakajon, A. (2009). Genomic structure, expression pattern and functional characterization of crustinPm5, a unique isoform of crustin from *Penaeus monodon*. *Comparative Biochemistry and Physiology - Part B, 153*, 244–252.

[265] Wachinger, M., Kleinschmidt, A., Winder, D., von Pechmann, N., Ludvigsen, A., Neumann, M., Holle, R., Salmons, B., Erfle, V. and Brack-Werner, R. (1998). Antimicrobial peptides melittin and cecropininhibit replication of human immunodeficiency virus 1 by suppressing viral gene expression. *Journal of General Virology*, *79,* 731–740.

[266] Wang, K., Huang, W., Yang, M., Chen, H., Bo, J., Li, S., Wang, G., (2007). A male-specific expression gene, encodes a novel anionic antimicrobial peptide, scygonadin, in *Scylla serrata*. *Molecular Immunology,* 44, 1961–1968.

[267] Wang, X., Zhang, L. (2009). Physicochemical properties and antitumor activities for sulfated derivatives of lentinan. *Carbohydrate Research, 344,* 2209-2216.

[268] Wang, Y., Tang, T., Gu, J., Li, X., Yang, X., Gao, X., Wang, J. (2015). Identification of five anti-lipopolysaccharide factors in oriental river prawn, *Macrobrachium nipponense*. *Fish and Shellfish Immunology*, *46*(2), 252–260. doi:10.1016/j.fsi.2015.07.003

[269] Whang, Y.E., Yuan, X.J., Liu, Y., Majumder, S., Lewis, T.D. (2004). Regulation of sensitivity to RAIL by the PTEN tumor suppressor. *Vitamins and Hormones, 67*, 409-426.

[270] Williams, M. J. & Primavera, J. H. (2001). Choosing tropical portunid species for culture, domestication and stock enhancement in the Indo-Pacific. *Asian Fisheries Science, 14,* 121 - 142.

[271] Wu, M., Maier, E., Benz, R., Hancock, R.E. (1999). Mechanism of interaction of different classes of cationic antimicrobial peptides with planar bilayers and with the cytoplasmic membrane of *Escherichia coli*. *Biochemistry, 38,* 7235–7242.

[272] Wyrick, J. J. & Parra, M. A. (2009). The role of histone H2A and H2B post-translational modifications in transcription: A genomic perspective. *Biochemical and Biophysical Research Communications, 1789,* 37–44

[273] Xu, T., Levitz, S. M., Diamond, R. D. and Oppenheim, F. G. (1991) Anticandidal activity of major human salivary histatins. *Infection and Immunity, 59,* 2549–2954.

[274] Yang Y, Boze H, Chemardin P, Padilla A, Moulin G, Tassanakajon A. (2009). NMR structure of rALF-Pm3, an anti-lipopolysaccharide factor from shrimp: model of the possible lipid A-binding site. *Biopolymers, 91,* 207-20.

[275] Yang, H., Li, S., Li, F., & Xiang, J. (2016b). Structure and bioactivity of a modified peptide derived from the LPS-binding domain of an anti-lipopolysaccharide factor (ALF) of shrimp. *Marine Drugs*, *14*(5). doi:10.3390/md14050096

[276] Yang, H., Li, S., Li, F., Lv, X., & Xiang, J. (2015). Recombinant expression and functional analysis of an isoform of anti-lipopolysaccharide factors (FcALF5) from Chinese shrimp *Fenneropenaeus chinensis. Developmental and Comparative Immunology*, *53*(1), 47–54. doi:10.1016/j.dci.2015.06.015

[277] Yang, H., Li, S., Li, F., Yu, K., Yang, F., & Xiang, J. (2016a). Recombinant Expression of a Modified Shrimp Anti-Lipopolysaccharide Factor Gene in *Pichia pastoris* GS115 and Its Characteristic Analysis. *Marine Drugs*, *14*(8), 152. doi:10.3390/md14080152

[278] Yang, Y., Boze, H., Chemardin, P., Padilla, A., Moulin, G., Tassanakajon, A., (2009). NMR structure of rALF-Pm3, an anti-lipopolysaccharide factor from shrimp: model of the possible lipid A-binding site. *Biopolymers* 91, 207–220.

[279] Yeaman, M. R. and Yount, N. Y. (2003) Mechanisms of antimicrobial peptide action and resistance. *Pharmacology Reviews* 55, 27–55.

[280] Yedery, R. D., & Reddy, K. V. R. (2009). Identification, cloning, characterization and recombinant expression of an anti-lipopolysaccharide factor from the hemocytes of Indian mud crab, *Scylla serrata. Fish & Shellfish Immunology*, *27*(2), 275–84. doi:10.1016/j.fsi.2009.05.009

[281] Yi, G. S., Park, C. B., Kim, S. C., & Cheong, C. (1996). Solution structure of an antimicrobial peptide buforin II. *FEBS Letters, 398(1),* 87–90. doi:10.1016/S0014-5793(96)01193-3

[282] Yonezawa, A., Kuwahara, J., Fujii, N., Sugiura, Y. (1992). Binding of tachyplesin I to DNA revealed by footprinting analysis: significant contribution of secondary structure to DNA binding and implication for biological action, *Biochemistry, 31,* 2998–3004.

[283] Yount, N. Y., Bayer, A. S., Xiong, Y. Q. & Yeaman, M. R. (2006). Advances in antimicrobial peptide immunobiology. *Biopolymers, 84,* 435-458.

[284] Yu, A., Shi, Y., Wang, Q., Immunology, S., & Y-h, S. (2015). Characterisation of a novel Type I crustin involved in antibacterial responses in the red claw crayfish, *Cherax quadricarinatus. Fish & Shellfish Immunology,* doi:10.1016/j.fsi.2015.11.019.

[285] Zasloff, M. (1987). Magainins, a class of antimicrobial peptides from *Xenopus* skin: isolation, characterization of two active forms, and partial cDNA sequence of a precursor. *Proceedings of the National Academy of Sciences of the U S A, 84,* 5449-5453.

[286] Zasloff, M. (2001). The Commercial Development of the Antimicrobial Peptide Pexiganan. *In:* K. Lohner (Ed.): Development of Novel Antimicrobial Agents: Emerging Strategies, Horizon Scientific Press, Wymondham, UK, pp. 261–270.

[287] Zhang, J., Li, F., Wang, Z., & Xiang, J. (2007). Cloning and recombinant expression of a crustin-like gene from Chinese shrimp, *Fenneropenaeus chinensis. Journal of Biotechnology, 127(4),* 605–14. *doi*:10.1016/j.jbiotec. 2006.08.013

[288] Zhang, K., Lu, Q., Zhang, Q., Hu, X. (2004). Regulation of activities of nk cells and cd4 expression in t cells by human hnp-1, -2, and -3. Biochemical and *Biophysical Research Communications, 323,* 437–444.

[289] Zhang, Y., Wang, L., Wang, L., Yang, J., Gai, Y., Qiu, L., & Song, L. (2010). The second anti-lipopolysaccharide factor (EsALF-2) with antimicrobial activity from *Eriocheir sinensis. Developmental and Comparative Immunology*, *34*(9), 945–52. doi:10.1016/j.dci.2010.04.002

[290] Zhu, L., Lan, J.-F., Huang, Y.-Q., Zhang, C., Zhou, J.-F., Fang, W.-H., Li, X.-C. (2014). SpALF4: a newly identified anti-lipopolysaccharide factor from the mud crab *Scylla paramamosain* with broad spectrum antimicrobial activity. *Fish & Shellfish Immunology*, *36*(1), 172–80. doi:10.1016/j.fsi.2013.10.023.

GenBank Submissions

[1] GenBank accession number **KM034808. Sruthy, K. S.,** Nair, A., Chaithanya, E.R., Sathyan, N., Antony, S.P., Bright Singh, I.S. and Philip,R (2014), Miyakea nepa cytochrome oxidase subunit I gene, partial cds; mitochondrial.

[2] GenBank accession number **KJ995817. Sruthy, K. S.,** Nair, A., Bright Singh, I.S. and Philip, R. (2014), *Miyakea nepa* anti-lipopolysaccharide factor-like mRNA, complete sequence.

[3] GenBank accession number **KP688577**. **Sruthy, K. S.,** Nair, A., Bright Singh, I.S. and Philip, R. (2015), *Charybdis feriatus* anti-lipopolysaccharide factor mRNA, complete cds.

[4] GenBank accession number **KT224347**. **Sruthy, K. S.,** Nair, A., Bright Singh, I.S. and Philip, R. (2015), *Charybdis feriatus* anti-lipopolysaccharide factor-like mRNA, partial sequence.

[5] GenBank accession number **KY126319. Sruthy, K. S.,** Nair, A., Bright Singh, I.S. and Philip, R. (2016), *Fenneropenaeus indicus* Histone H2A mRNA partial sequence.

[6] GenBank accession number **KX622789. Sruthy, K. S.,** Nair, A., Bright Singh, I.S. and Philip, R. (2016), *Fenneropenaeus indicus* Crustin like mRNA, complete sequence.

.....ꕥ.....

List of Publications

[1] **Sruthy K. S**., Aishwarya Nair, Sherine Sonia Cubelio, I. S. Bright Singh, Rosamma Philip. Molecular Characterization and Phylogenetic Analysis of an Antilipopolysaccharide Factor from the Crucifix Crab, *Charybdis feriatus*, Open access Animal Physiology, 2015: 7, 149-156.

[2] **Sruthy K. S.**, Chaithanya E. R., Naveen Sathyan, Aishwarya Nair, Swapna P. Antony, I. S. Bright Singh, Rosamma Philip. Molecular Characterization and Phylogenetic Analysis of Novel Isoform of Anti-Lipopolysaccharide Factor from the Mantis Shrimp, *Miyakea nepa*. Probiotics and Antimicrobial Proteins, Published Online 18th July, 2015. DOI 10.1007/s12602-015-9198-2

[3] **Sruthy K. S**., Chaithanya E. R., Naveen Sathyan, Anilkumar P. R., Bright Singh, Rosamma Philip. Isolation, Purification and Characterization of Antimicrobial Peptides from Indian Ruff, *Psenopsis cyanea* (Alcock, 1890). International Journal of Research in Biological Sciences, 2015; 5(1): 1-6.

[4] Naveen Sathyan, Chaithanya E.R., Anil Kumar P.R., **Sruthy K. S.,** Rosamma Philip. Genetic divergence and phylogenetic analysis based on cytochrome c oxidase subunit-1 sequence of enope squid *Abralia andamanica* (Goodrich 1896) inhabiting Andaman Sea. International Journal of Research in Marine Sciences, 2014, 3(2): 30-36.

[5] Naveen Sathyan, Chaithanya E.R., Anil Kumar P.R., **Sruthy K. S.,** Rosamma Philip. Comparison of the antimicrobial potential of the crude peptides from various groups of marine mollusks. International Journal of Research in Marine Sciences, 2014, 3(2): 16-22.